



**UNIVERSITY OF SOUTH WALES**  
**FACULTY OF COMPUTING AND ENGINEERING SCIENCES**  
*MASTER OF SCIENCE WILDLIFE AND CONSERVATION MANAGEMENT*

---

**ZELIA ROMANO**  
Student number: 30060558

**INFLUENCE OF ENVIRONMENTAL FACTORS ON THE MOVEMENT  
PATTERNS OF AFRICAN ELEPHANTS IN THE SELATI GAME RESERVE,  
SOUTH AFRICA.**

Supervisors: Dr ANTHONY CARAVAGGI  
Dr EMMA HIGGINS

September 2023

*This work was carried out in part fulfilment of the requirements for the award of degree  
of Master of Science in Wildlife and Conservation Management.*

## CONTENTS

<b>1</b>	<b>INTRODUCTION.....</b>	<b>1</b>
1.1	<i>Animal movements .....</i>	<i>1</i>
1.2	<i>Statistical modelling on movement data .....</i>	<i>3</i>
1.3	<i>African Elephant (Loxodonta africana).....</i>	<i>5</i>
1.3.1	<i>Taxonomy, distribution, and biology.....</i>	<i>5</i>
1.3.2	<i>Ecological role and impact on the ecosystem .....</i>	<i>6</i>
1.3.3	<i>Habitat selection, home range, and diet .....</i>	<i>7</i>
1.3.4	<i>Social hierarchy and reproductive behaviour.....</i>	<i>9</i>
1.3.5	<i>Movement patterns and environmental drivers.....</i>	<i>10</i>
1.3.6	<i>Changes in spatial behaviour within fenced reserves.....</i>	<i>12</i>
1.4	<i>Hypotheses, Aims and Objectives.....</i>	<i>13</i>
<b>2</b>	<b>METHOD.....</b>	<b>14</b>
2.1	<i>Study location.....</i>	<i>14</i>
2.2	<i>GPS Collar Data collection .....</i>	<i>18</i>
2.3	<i>Data preparation for covariates and Remote Sensing Data .....</i>	<i>19</i>
2.4	<i>Hidden Markov Model (HMM).....</i>	<i>20</i>
2.5	<i>Data processing and fitting HMM.....</i>	<i>21</i>
<b>3</b>	<b>RESULTS .....</b>	<b>25</b>

3.1	<i>Elza</i> .....	25
3.2	<i>Jean</i> .....	58
4	<b>DISCUSSION</b> .....	83
4.1	<i>Terrain roughness</i> .....	85
4.2	<i>Distance to nearest road/path</i> .....	86
4.3	<i>Distance to nearest water source</i> .....	87
4.4	<i>NDVI</i> .....	89
5	<b>CONCLUSION AND RECOMMENDATIONS</b> .....	91
6	<b>REFERENCES</b> .....	93
7	<b>APPENDIX I</b> .....	127
8	<b>APPENDIX II</b> .....	133
9	<b>APPENDIX III</b> .....	142
10	<b>APPENDIX IV</b> .....	144

## LIST OF FIGURES

<b>Figure 1.</b> Location map of Selati Game Reserve. Created with QGIS Desktop by Zelia Romano.....	15
<b>Figure 2.</b> Distribution of the three different bioregions inside SGR (Mucina and Rutherford, 2006).....	17
<b>Figure 3.</b> Structure of dependency in Hidden Markov Model (Michelot et al., 2016). ...	21
<b>Figure 4.</b> Graphic overview of step lengths and turning angles calculation (Michelot et al., 2023). ....	21
<b>Figure 5.</b> Graph showing transition probabilities under the influence of terrain roughness as a covariate in June, between state 1 and 2 (1→2), state 1 and 3 (1→3), state 2 and 1 (2→1), state 2 and 3 (2→3), state 3 and 1 (3→1), and state 3 and 2 (3→2). The graph also shows persistence probabilities in state 1 (1→1), state 2 (2→2) and in state 3 (3→3)....	30
<b>Figure 6.</b> Graph showing transition probabilities under the influence of distance to nearest road/path as a covariate in June, between state 1 and 2 (1→2), state 1 and 3 (1→3), state 2 and 1 (2→1), state 2 and 3 (2→3), state 3 and 1 (3→1), and state 3 and 2 (3→2). The graph also shows persistence probabilities in state 1 (1→1), state 2 (2→2) and in state 3 (3→3). ....	30
<b>Figure 7.</b> Graph showing transition probabilities under the influence of distance to nearest water source as a covariate in June, between state 1 and 2 (1→2), state 1 and 3 (1→3), state 2 and 1 (2→1), state 2 and 3 (2→3), state 3 and 1 (3→1), and state 3 and 2 (3→2). The graph also shows persistence probabilities in state 1 (1→1), state 2 (2→2) and in state 3 (3→3).....	31
<b>Figure 8.</b> Graph showing transition probabilities under the influence of NDVI as a covariate in June, between state 1 and 2 (1→2), state 1 and 3 (1→3), state 2 and 1 (2→1), state 2 and 3 (2→3), state 3 and 1 (3→1), and state 3 and 2 (3→2). The graph also shows persistence probabilities in state 1 (1→1), state 2 (2→2) and in state 3 (3→3).....	31
<b>Figure 9.</b> Graph showing transition probabilities under the influence of terrain roughness as a covariate in July, between state 1 and 2 (1→2), state 1 and 3 (1→3), state 2 and 1 (2→1), state 2 and 3 (2→3), state 3 and 1 (3→1), and state 3 and 2 (3→2). The graph also shows persistence probabilities in state 1 (1→1), state 2 (2→2) and in state 3 (3→3)....	33
<b>Figure 10.</b> Graph showing transition probabilities under the influence of distance to nearest road/path as a covariate in July, between state 1 and 2 (1→2), state 1 and 3 (1→3),	



state 2 and 1 ( $2 \rightarrow 1$ ), state 2 and 3 ( $2 \rightarrow 3$ ), state 3 and 1 ( $3 \rightarrow 1$ ), and state 3 and 2 ( $3 \rightarrow 2$ ). The graph also shows persistence probabilities in state 1 ( $1 \rightarrow 1$ ), state 2 ( $2 \rightarrow 2$ ) and in state 3 ( $3 \rightarrow 3$ )..... 33

**Figure 11.** Graph showing transition probabilities under the influence of distance to nearest water source as a covariate in July, between state 1 and 2 ( $1 \rightarrow 2$ ), state 1 and 3 ( $1 \rightarrow 3$ ), state 2 and 1 ( $2 \rightarrow 1$ ), state 2 and 3 ( $2 \rightarrow 3$ ), state 3 and 1 ( $3 \rightarrow 1$ ), and state 3 and 2 ( $3 \rightarrow 2$ ). The graph also shows persistence probabilities in state 1 ( $1 \rightarrow 1$ ), state 2 ( $2 \rightarrow 2$ ) and in state 3 ( $3 \rightarrow 3$ )..... 34

**Figure 12.** Graph showing transition probabilities under the influence of NDVI as a covariate in July, between state 1 and 2 ( $1 \rightarrow 2$ ), state 1 and 3 ( $1 \rightarrow 3$ ), state 2 and 1 ( $2 \rightarrow 1$ ), state 2 and 3 ( $2 \rightarrow 3$ ), state 3 and 1 ( $3 \rightarrow 1$ ), and state 3 and 2 ( $3 \rightarrow 2$ ). The graph also shows persistence probabilities in state 1 ( $1 \rightarrow 1$ ), state 2 ( $2 \rightarrow 2$ ) and in state 3 ( $3 \rightarrow 3$ )..... 34

**Figure 13.** Graph showing transition probabilities under the influence of terrain roughness as a covariate in August, between state 1 and 2 ( $1 \rightarrow 2$ ), state 1 and 3 ( $1 \rightarrow 3$ ), state 2 and 1 ( $2 \rightarrow 1$ ), state 2 and 3 ( $2 \rightarrow 3$ ), state 3 and 1 ( $3 \rightarrow 1$ ), and state 3 and 2 ( $3 \rightarrow 2$ ). The graph also shows persistence probabilities in state 1 ( $1 \rightarrow 1$ ), state 2 ( $2 \rightarrow 2$ ) and in state 3 ( $3 \rightarrow 3$ )... 36

**Figure 14.** Graph showing transition probabilities under the influence of distance to nearest road/path as a covariate in August, between state 1 and 2 ( $1 \rightarrow 2$ ), state 1 and 3 ( $1 \rightarrow 3$ ), state 2 and 1 ( $2 \rightarrow 1$ ), state 2 and 3 ( $2 \rightarrow 3$ ), state 3 and 1 ( $3 \rightarrow 1$ ), and state 3 and 2 ( $3 \rightarrow 2$ ). The graph also shows persistence probabilities in state 1 ( $1 \rightarrow 1$ ), state 2 ( $2 \rightarrow 2$ ) and in state 3 ( $3 \rightarrow 3$ ). ..... 36

**Figure 15.** Graph showing transition probabilities under the influence of distance to nearest water source as a covariate in August, between state 1 and 2 ( $1 \rightarrow 2$ ), state 1 and 3 ( $1 \rightarrow 3$ ), state 2 and 1 ( $2 \rightarrow 1$ ), state 2 and 3 ( $2 \rightarrow 3$ ), state 3 and 1 ( $3 \rightarrow 1$ ), and state 3 and 2 ( $3 \rightarrow 2$ ). The graph also shows persistence probabilities in state 1 ( $1 \rightarrow 1$ ), state 2 ( $2 \rightarrow 2$ ) and in state 3 ( $3 \rightarrow 3$ ). ..... 37

**Figure 16.** Graph showing transition probabilities under the influence of NDVI as a covariate in August, between state 1 and 2 ( $1 \rightarrow 2$ ), state 1 and 3 ( $1 \rightarrow 3$ ), state 2 and 1 ( $2 \rightarrow 1$ ), state 2 and 3 ( $2 \rightarrow 3$ ), state 3 and 1 ( $3 \rightarrow 1$ ), and state 3 and 2 ( $3 \rightarrow 2$ ). The graph also shows persistence probabilities in state 1 ( $1 \rightarrow 1$ ), state 2 ( $2 \rightarrow 2$ ) and in state 3 ( $3 \rightarrow 3$ )..... 37

**Figure 17.** Graph showing transition probabilities under the influence of terrain roughness as a covariate in September, between state 1 and 2 ( $1 \rightarrow 2$ ), state 1 and 3 ( $1 \rightarrow 3$ ), state 2 and 1 ( $2 \rightarrow 1$ ), state 2 and 3 ( $2 \rightarrow 3$ ), state 3 and 1 ( $3 \rightarrow 1$ ), and state 3 and 2 ( $3 \rightarrow 2$ ). The graph

also shows persistence probabilities in state 1 ( $1 \rightarrow 1$ ), state 2 ( $2 \rightarrow 2$ ) and in state 3 ( $3 \rightarrow 3$ ).

..... 39

**Figure 18.** Graph showing transition probabilities under the influence of distance to nearest road/path as a covariate in September, between state 1 and 2 ( $1 \rightarrow 2$ ), state 1 and 3 ( $1 \rightarrow 3$ ), state 2 and 1 ( $2 \rightarrow 1$ ), state 2 and 3 ( $2 \rightarrow 3$ ), state 3 and 1 ( $3 \rightarrow 1$ ), and state 3 and 2 ( $3 \rightarrow 2$ ). The graph also shows persistence probabilities in state 1 ( $1 \rightarrow 1$ ), state 2 ( $2 \rightarrow 2$ ) and in state 3 ( $3 \rightarrow 3$ ). .... 39

**Figure 19.** Graph showing transition probabilities under the influence of distance to nearest water source as a covariate in September, between state 1 and 2 ( $1 \rightarrow 2$ ), state 1 and 3 ( $1 \rightarrow 3$ ), state 2 and 1 ( $2 \rightarrow 1$ ), state 2 and 3 ( $2 \rightarrow 3$ ), state 3 and 1 ( $3 \rightarrow 1$ ), and state 3 and 2 ( $3 \rightarrow 2$ ). The graph also shows persistence probabilities in state 1 ( $1 \rightarrow 1$ ), state 2 ( $2 \rightarrow 2$ ) and in state 3 ( $3 \rightarrow 3$ ). .... 40

**Figure 20.** Graph showing transition probabilities under the influence of NDVI as a covariate in September, between state 1 and 2 ( $1 \rightarrow 2$ ), state 1 and 3 ( $1 \rightarrow 3$ ), state 2 and 1 ( $2 \rightarrow 1$ ), state 2 and 3 ( $2 \rightarrow 3$ ), state 3 and 1 ( $3 \rightarrow 1$ ), and state 3 and 2 ( $3 \rightarrow 2$ ). The graph also shows persistence probabilities in state 1 ( $1 \rightarrow 1$ ), state 2 ( $2 \rightarrow 2$ ) and in state 3 ( $3 \rightarrow 3$ ). ... 40

**Figure 21.** Graph showing transition probabilities under the influence of terrain roughness as a covariate in October, between state 1 and 2 ( $1 \rightarrow 2$ ), state 1 and 3 ( $1 \rightarrow 3$ ), state 2 and 1 ( $2 \rightarrow 1$ ), state 2 and 3 ( $2 \rightarrow 3$ ), state 3 and 1 ( $3 \rightarrow 1$ ), and state 3 and 2 ( $3 \rightarrow 2$ ). The graph also shows persistence probabilities in state 1 ( $1 \rightarrow 1$ ), state 2 ( $2 \rightarrow 2$ ) and in state 3 ( $3 \rightarrow 3$ ). ... 42

**Figure 22.** Graph showing transition probabilities under the influence of distance to nearest road/path as a covariate in October, between state 1 and 2 ( $1 \rightarrow 2$ ), state 1 and 3 ( $1 \rightarrow 3$ ), state 2 and 1 ( $2 \rightarrow 1$ ), state 2 and 3 ( $2 \rightarrow 3$ ), state 3 and 1 ( $3 \rightarrow 1$ ), and state 3 and 2 ( $3 \rightarrow 2$ ). The graph also shows persistence probabilities in state 1 ( $1 \rightarrow 1$ ), state 2 ( $2 \rightarrow 2$ ) and in state 3 ( $3 \rightarrow 3$ ). .... 42

**Figure 23.** Graph showing transition probabilities under the influence of distance to nearest water source as a covariate in October, between state 1 and 2 ( $1 \rightarrow 2$ ), state 1 and 3 ( $1 \rightarrow 3$ ), state 2 and 1 ( $2 \rightarrow 1$ ), state 2 and 3 ( $2 \rightarrow 3$ ), state 3 and 1 ( $3 \rightarrow 1$ ), and state 3 and 2 ( $3 \rightarrow 2$ ). The graph also shows persistence probabilities in state 1 ( $1 \rightarrow 1$ ), state 2 ( $2 \rightarrow 2$ ) and in state 3 ( $3 \rightarrow 3$ ). .... 43

**Figure 24.** Graph showing transition probabilities under the influence of NDVI as a covariate in October, between state 1 and 2 ( $1 \rightarrow 2$ ), state 1 and 3 ( $1 \rightarrow 3$ ), state 2 and 1 ( $2 \rightarrow 1$ ), state 2 and 3 ( $2 \rightarrow 3$ ), state 3 and 1 ( $3 \rightarrow 1$ ), and state 3 and 2 ( $3 \rightarrow 2$ ). The graph also shows persistence probabilities in state 1 ( $1 \rightarrow 1$ ), state 2 ( $2 \rightarrow 2$ ) and in state 3 ( $3 \rightarrow 3$ ). ... 43

**Figure 25.** Graph showing transition probabilities under the influence of terrain roughness as a covariate in November, between state 1 and 2 ( $1 \rightarrow 2$ ), state 1 and 3 ( $1 \rightarrow 3$ ), state 2 and 1 ( $2 \rightarrow 1$ ), state 2 and 3 ( $2 \rightarrow 3$ ), state 3 and 1 ( $3 \rightarrow 1$ ), and state 3 and 2 ( $3 \rightarrow 2$ ). The graph also shows persistence probabilities in state 1 ( $1 \rightarrow 1$ ), state 2 ( $2 \rightarrow 2$ ) and in state 3 ( $3 \rightarrow 3$ ).

..... 46

**Figure 26.** Graph showing transition probabilities under the influence of terrain roughness as a covariate in December, between state 1 and 2 ( $1 \rightarrow 2$ ), state 1 and 3 ( $1 \rightarrow 3$ ), state 2 and 1 ( $2 \rightarrow 1$ ), state 2 and 3 ( $2 \rightarrow 3$ ), state 3 and 1 ( $3 \rightarrow 1$ ), and state 3 and 2 ( $3 \rightarrow 2$ ). The graph also shows persistence probabilities in state 1 ( $1 \rightarrow 1$ ), state 2 ( $2 \rightarrow 2$ ) and in state 3 ( $3 \rightarrow 3$ ).

..... 46

**Figure 27.** Graph showing transition probabilities under the influence of distance to nearest road/path as a covariate in November, between state 1 and 2 ( $1 \rightarrow 2$ ), state 1 and 3 ( $1 \rightarrow 3$ ), state 2 and 1 ( $2 \rightarrow 1$ ), state 2 and 3 ( $2 \rightarrow 3$ ), state 3 and 1 ( $3 \rightarrow 1$ ), and state 3 and 2 ( $3 \rightarrow 2$ ). The graph also shows persistence probabilities in state 1 ( $1 \rightarrow 1$ ), state 2 ( $2 \rightarrow 2$ ) and in state 3 ( $3 \rightarrow 3$ ).

..... 47

**Figure 28.** Graph showing transition probabilities under the influence of distance to nearest road/path as a covariate in December, between state 1 and 2 ( $1 \rightarrow 2$ ), state 1 and 3 ( $1 \rightarrow 3$ ), state 2 and 1 ( $2 \rightarrow 1$ ), state 2 and 3 ( $2 \rightarrow 3$ ), state 3 and 1 ( $3 \rightarrow 1$ ), and state 3 and 2 ( $3 \rightarrow 2$ ). The graph also shows persistence probabilities in state 1 ( $1 \rightarrow 1$ ), state 2 ( $2 \rightarrow 2$ ) and in state 3 ( $3 \rightarrow 3$ ).

..... 47

**Figure 29.** Graph showing transition probabilities under the influence of distance to nearest water source as a covariate in November, between state 1 and 2 ( $1 \rightarrow 2$ ), state 1 and 3 ( $1 \rightarrow 3$ ), state 2 and 1 ( $2 \rightarrow 1$ ), state 2 and 3 ( $2 \rightarrow 3$ ), state 3 and 1 ( $3 \rightarrow 1$ ), and state 3 and 2 ( $3 \rightarrow 2$ ). The graph also shows persistence probabilities in state 1 ( $1 \rightarrow 1$ ), state 2 ( $2 \rightarrow 2$ ) and in state 3 ( $3 \rightarrow 3$ ).

..... 48

**Figure 30.** Graph showing transition probabilities under the influence of distance to nearest water source as a covariate in December, between state 1 and 2 ( $1 \rightarrow 2$ ), state 1 and 3 ( $1 \rightarrow 3$ ), state 2 and 1 ( $2 \rightarrow 1$ ), state 2 and 3 ( $2 \rightarrow 3$ ), state 3 and 1 ( $3 \rightarrow 1$ ), and state 3 and 2 ( $3 \rightarrow 2$ ). The graph also shows persistence probabilities in state 1 ( $1 \rightarrow 1$ ), state 2 ( $2 \rightarrow 2$ ) and in state 3 ( $3 \rightarrow 3$ ).

..... 48

**Figure 31.** Graph showing transition probabilities under the influence of NDVI as a covariate in November, between state 1 and 2 ( $1 \rightarrow 2$ ), state 1 and 3 ( $1 \rightarrow 3$ ), state 2 and 1 ( $2 \rightarrow 1$ ), state 2 and 3 ( $2 \rightarrow 3$ ), state 3 and 1 ( $3 \rightarrow 1$ ), and state 3 and 2 ( $3 \rightarrow 2$ ). The graph also shows persistence probabilities in state 1 ( $1 \rightarrow 1$ ), state 2 ( $2 \rightarrow 2$ ) and in state 3 ( $3 \rightarrow 3$ )...

..... 49

<b>Figure 32.</b> Graph showing transition probabilities under the influence of NDVI as a covariate in December, between state 1 and 2 (1→2), state 1 and 3 (1→3), state 2 and 1 (2→1), state 2 and 3 (2→3), state 3 and 1 (3→1), and state 3 and 2 (3→2). The graph also shows persistence probabilities in state 1 (1→1), state 2 (2→2) and in state 3 (3→3)....	49
<b>Figure 33.</b> Graph showing transition probabilities under the influence of terrain roughness as a covariate for the 7-month period (June to December), between state 1 and 2 (1→2), state 1 and 3 (1→3), state 2 and 1 (2→1), state 2 and 3 (2→3), state 3 and 1 (3→1), and state 3 and 2 (3→2). The graph also shows persistence probabilities in state 1 (1→1), state 2 (2→2) and in state 3 (3→3). .....	51
<b>Figure 34.</b> Graph showing transition probabilities under the influence of distance to nearest road/path as a covariate for the 7-month period (June to December), between state 1 and 2 (1→2), state 1 and 3 (1→3), state 2 and 1 (2→1), state 2 and 3 (2→3), state 3 and 1 (3→1), and state 3 and 2 (3→2). The graph also shows persistence probabilities in state 1 (1→1), state 2 (2→2) and in state 3 (3→3). .....	51
<b>Figure 35.</b> Graph showing transition probabilities under the influence of distance to nearest water source as a covariate for the 7-month period (June to December), between state 1 and 2 (1→2), state 1 and 3 (1→3), state 2 and 1 (2→1), state 2 and 3 (2→3), state 3 and 1 (3→1), and state 3 and 2 (3→2). The graph also shows persistence probabilities in state 1 (1→1), state 2 (2→2) and in state 3 (3→3).....	52
<b>Figure 36.</b> Graph showing transition probabilities under the influence of NDVI as a covariate for the 7-month period (June to December), between state 1 and 2 (1→2), state 1 and 3 (1→3), state 2 and 1 (2→1), state 2 and 3 (2→3), state 3 and 1 (3→1), and state 3 and 2 (3→2). The graph also shows persistence probabilities in state 1 (1→1), state 2 (2→2) and in state 3 (3→3). .....	52
<b>Figure 37.</b> Graph showing stationary state probabilities for each covariate in June. ....	54
<b>Figure 38.</b> Graph showing stationary state probabilities for each covariate in July. ....	54
<b>Figure 39.</b> Graph showing stationary state probabilities for each covariate in August. ..	55
<b>Figure 40.</b> Graph showing stationary state probabilities for each covariate in September. ....	55
<b>Figure 41.</b> Graph showing stationary state probabilities for each covariate in October. .	56
<b>Figure 42.</b> Graph showing stationary state probabilities for each covariate in November. ....	56
<b>Figure 43.</b> Graph showing stationary state probabilities for each covariate in December. ....	57

<b>Figure 44.</b> Graph showing stationary state probabilities for each covariate combining all the months.....	57
<b>Figure 45.</b> Graph showing transition probabilities under the influence of terrain roughness as a covariate in June, between state 1 and 2 (1→2), state 1 and 3 (1→3), state 2 and 1 (2→1), state 2 and 3 (2→3), state 3 and 1 (3→1), and state 3 and 2 (3→2). The graph also shows persistence probabilities in state 1 (1→1), state 2 (2→2) and in state 3 (3→3)....	62
<b>Figure 46.</b> Graph showing transition probabilities under the influence of distance to nearest road/path as a covariate in June, between state 1 and 2 (1→2), state 1 and 3 (1→3), state 2 and 1 (2→1), state 2 and 3 (2→3), state 3 and 1 (3→1), and state 3 and 2 (3→2). The graph also shows persistence probabilities in state 1 (1→1), state 2 (2→2) and in state 3 (3→3).....	62
<b>Figure 47.</b> Graph showing transition probabilities under the influence of distance to nearest water source as a covariate in June, between state 1 and 2 (1→2), state 1 and 3 (1→3), state 2 and 1 (2→1), state 2 and 3 (2→3), state 3 and 1 (3→1), and state 3 and 2 (3→2). The graph also shows persistence probabilities in state 1 (1→1), state 2 (2→2) and in state 3 (3→3). .....	63
<b>Figure 48.</b> Graph showing transition probabilities under the influence of NDVI as a covariate in June, between state 1 and 2 (1→2), state 1 and 3 (1→3), state 2 and 1 (2→1), state 2 and 3 (2→3), state 3 and 1 (3→1), and state 3 and 2 (3→2). The graph also shows persistence probabilities in state 1 (1→1), state 2 (2→2) and in state 3 (3→3).....	63
<b>Figure 49.</b> Graph showing transition probabilities under the influence of terrain roughness as a covariate in August, between state 1 and 2 (1→2), state 1 and 3 (1→3), state 2 and 1 (2→1), state 2 and 3 (2→3), state 3 and 1 (3→1), and state 3 and 2 (3→2). The graph also shows persistence probabilities in state 1 (1→1), state 2 (2→2) and in state 3 (3→3)....	65
<b>Figure 50.</b> Graph showing transition probabilities under the influence of distance to nearest road/path as a covariate in August, between state 1 and 2 (1→2), state 1 and 3 (1→3), state 2 and 1 (2→1), state 2 and 3 (2→3), state 3 and 1 (3→1), and state 3 and 2 (3→2). The graph also shows persistence probabilities in state 1 (1→1), state 2 (2→2) and in state 3 (3→3). .....	65
<b>Figure 51.</b> Graph showing transition probabilities under the influence of distance to nearest water source as a covariate in August, between state 1 and 2 (1→2), state 1 and 3 (1→3), state 2 and 1 (2→1), state 2 and 3 (2→3), state 3 and 1 (3→1), and state 3 and 2 (3→2). The graph also shows persistence probabilities in state 1 (1→1), state 2 (2→2) and in state 3 (3→3). .....	66

**Figure 52.** Graph showing transition probabilities under the influence of NDVI as a covariate in August, between state 1 and 2 ( $1 \rightarrow 2$ ), state 1 and 3 ( $1 \rightarrow 3$ ), state 2 and 1 ( $2 \rightarrow 1$ ), state 2 and 3 ( $2 \rightarrow 3$ ), state 3 and 1 ( $3 \rightarrow 1$ ), and state 3 and 2 ( $3 \rightarrow 2$ ). The graph also shows persistence probabilities in state 1 ( $1 \rightarrow 1$ ), state 2 ( $2 \rightarrow 2$ ) and in state 3 ( $3 \rightarrow 3$ ). ..... 66

**Figure 53.** Graph showing transition probabilities under the influence of terrain roughness as a covariate in September, between state 1 and 2 ( $1 \rightarrow 2$ ), state 1 and 3 ( $1 \rightarrow 3$ ), state 2 and 1 ( $2 \rightarrow 1$ ), state 2 and 3 ( $2 \rightarrow 3$ ), state 3 and 1 ( $3 \rightarrow 1$ ), and state 3 and 2 ( $3 \rightarrow 2$ ). The graph also shows persistence probabilities in state 1 ( $1 \rightarrow 1$ ), state 2 ( $2 \rightarrow 2$ ) and in state 3 ( $3 \rightarrow 3$ ). ..... 68

**Figure 54.** Graph showing transition probabilities under the influence of distance to nearest road/path as a covariate in September, between state 1 and 2 ( $1 \rightarrow 2$ ), state 1 and 3 ( $1 \rightarrow 3$ ), state 2 and 1 ( $2 \rightarrow 1$ ), state 2 and 3 ( $2 \rightarrow 3$ ), state 3 and 1 ( $3 \rightarrow 1$ ), and state 3 and 2 ( $3 \rightarrow 2$ ). The graph also shows persistence probabilities in state 1 ( $1 \rightarrow 1$ ), state 2 ( $2 \rightarrow 2$ ) and in state 3 ( $3 \rightarrow 3$ ). ..... 68

**Figure 55.** Graph showing transition probabilities under the influence of distance to nearest water source as a covariate in September, between state 1 and 2 ( $1 \rightarrow 2$ ), state 1 and 3 ( $1 \rightarrow 3$ ), state 2 and 1 ( $2 \rightarrow 1$ ), state 2 and 3 ( $2 \rightarrow 3$ ), state 3 and 1 ( $3 \rightarrow 1$ ), and state 3 and 2 ( $3 \rightarrow 2$ ). The graph also shows persistence probabilities in state 1 ( $1 \rightarrow 1$ ), state 2 ( $2 \rightarrow 2$ ) and in state 3 ( $3 \rightarrow 3$ ). ..... 69

**Figure 56.** Graph showing transition probabilities under the influence of NDVI as a covariate in September, between state 1 and 2 ( $1 \rightarrow 2$ ), state 1 and 3 ( $1 \rightarrow 3$ ), state 2 and 1 ( $2 \rightarrow 1$ ), state 2 and 3 ( $2 \rightarrow 3$ ), state 3 and 1 ( $3 \rightarrow 1$ ), and state 3 and 2 ( $3 \rightarrow 2$ ). The graph also shows persistence probabilities in state 1 ( $1 \rightarrow 1$ ), state 2 ( $2 \rightarrow 2$ ) and in state 3 ( $3 \rightarrow 3$ ). ... 69

**Figure 57.** Graph showing transition probabilities under the influence of terrain roughness as a covariate in October, between state 1 and 2 ( $1 \rightarrow 2$ ), state 1 and 3 ( $1 \rightarrow 3$ ), state 2 and 1 ( $2 \rightarrow 1$ ), state 2 and 3 ( $2 \rightarrow 3$ ), state 3 and 1 ( $3 \rightarrow 1$ ), and state 3 and 2 ( $3 \rightarrow 2$ ). The graph also shows persistence probabilities in state 1 ( $1 \rightarrow 1$ ), state 2 ( $2 \rightarrow 2$ ) and in state 3 ( $3 \rightarrow 3$ ). ... 71

**Figure 58.** Graph showing transition probabilities under the influence of distance to nearest road/path as a covariate in October, between state 1 and 2 ( $1 \rightarrow 2$ ), state 1 and 3 ( $1 \rightarrow 3$ ), state 2 and 1 ( $2 \rightarrow 1$ ), state 2 and 3 ( $2 \rightarrow 3$ ), state 3 and 1 ( $3 \rightarrow 1$ ), and state 3 and 2 ( $3 \rightarrow 2$ ). The graph also shows persistence probabilities in state 1 ( $1 \rightarrow 1$ ), state 2 ( $2 \rightarrow 2$ ) and in state 3 ( $3 \rightarrow 3$ ). ..... 71

**Figure 59.** Graph showing transition probabilities under the influence of distance to nearest water source as a covariate in October, between state 1 and 2 ( $1 \rightarrow 2$ ), state 1 and 3

(1→3), state 2 and 1 (2→1), state 2 and 3 (2→3), state 3 and 1 (3→1), and state 3 and 2 (3→2). The graph also shows persistence probabilities in state 1 (1→1), state 2 (2→2) and in state 3 (3→3). ..... 72

**Figure 60.** Graph showing transition probabilities under the influence of NDVI as a covariate in October, between state 1 and 2 (1→2), state 1 and 3 (1→3), state 2 and 1 (2→1), state 2 and 3 (2→3), state 3 and 1 (3→1), and state 3 and 2 (3→2). The graph also shows persistence probabilities in state 1 (1→1), state 2 (2→2) and in state 3 (3→3)... 72

**Figure 61.** Graph showing transition probabilities under the influence of terrain roughness as a covariate in December, between state 1 and 2 (1→2), state 1 and 3 (1→3), state 2 and 1 (2→1), state 2 and 3 (2→3), state 3 and 1 (3→1), and state 3 and 2 (3→2). The graph also shows persistence probabilities in state 1 (1→1), state 2 (2→2) and in state 3 (3→3). ..... 74

**Figure 62.** Graph showing transition probabilities under the influence of distance to nearest road/path as a covariate in December, between state 1 and 2 (1→2), state 1 and 3 (1→3), state 2 and 1 (2→1), state 2 and 3 (2→3), state 3 and 1 (3→1), and state 3 and 2 (3→2). The graph also shows persistence probabilities in state 1 (1→1), state 2 (2→2) and in state 3 (3→3). ..... 74

**Figure 63.** Graph showing transition probabilities under the influence of distance to nearest water source as a covariate in December, between state 1 and 2 (1→2), state 1 and 3 (1→3), state 2 and 1 (2→1), state 2 and 3 (2→3), state 3 and 1 (3→1), and state 3 and 2 (3→2). The graph also shows persistence probabilities in state 1 (1→1), state 2 (2→2) and in state 3 (3→3). ..... 75

**Figure 64.** Graph showing transition probabilities under the influence of NDVI as a covariate in December, between state 1 and 2 (1→2), state 1 and 3 (1→3), state 2 and 1 (2→1), state 2 and 3 (2→3), state 3 and 1 (3→1), and state 3 and 2 (3→2). The graph also shows persistence probabilities in state 1 (1→1), state 2 (2→2) and in state 3 (3→3)... 75

**Figure 65.** Graph showing transition probabilities under the influence of terrain roughness as a covariate for the 7-month period (June to December), between state 1 and 2 (1→2), state 1 and 3 (1→3), state 2 and 1 (2→1), state 2 and 3 (2→3), state 3 and 1 (3→1), and state 3 and 2 (3→2). The graph also shows persistence probabilities in state 1 (1→1), state 2 (2→2) and in state 3 (3→3). ..... 77

**Figure 66.** Graph showing transition probabilities under the influence of distance to nearest road/path as a covariate for the 7-month period (June to December), between state 1 and 2 (1→2), state 1 and 3 (1→3), state 2 and 1 (2→1), state 2 and 3 (2→3), state 3 and

1 ( $3 \rightarrow 1$ ), and state 3 and 2 ( $3 \rightarrow 2$ ). The graph also shows persistence probabilities in state 1 ( $1 \rightarrow 1$ ), state 2 ( $2 \rightarrow 2$ ) and in state 3 ( $3 \rightarrow 3$ ). .....	77
<b>Figure 67.</b> Graph showing transition probabilities under the influence of distance to nearest water source as a covariate for the 7-month period (June to December), between state 1 and 2 ( $1 \rightarrow 2$ ), state 1 and 3 ( $1 \rightarrow 3$ ), state 2 and 1 ( $2 \rightarrow 1$ ), state 2 and 3 ( $2 \rightarrow 3$ ), state 3 and 1 ( $3 \rightarrow 1$ ), and state 3 and 2 ( $3 \rightarrow 2$ ). The graph also shows persistence probabilities in state 1 ( $1 \rightarrow 1$ ), state 2 ( $2 \rightarrow 2$ ) and in state 3 ( $3 \rightarrow 3$ ). .....	78
<b>Figure 68.</b> Graph showing transition probabilities under the influence of NDVI as a covariate for the 7-month period (June to December), between state 1 and 2 ( $1 \rightarrow 2$ ), state 1 and 3 ( $1 \rightarrow 3$ ), state 2 and 1 ( $2 \rightarrow 1$ ), state 2 and 3 ( $2 \rightarrow 3$ ), state 3 and 1 ( $3 \rightarrow 1$ ), and state 3 and 2 ( $3 \rightarrow 2$ ). The graph also shows persistence probabilities in state 1 ( $1 \rightarrow 1$ ), state 2 ( $2 \rightarrow 2$ ) and in state 3 ( $3 \rightarrow 3$ ). .....	78
<b>Figure 69.</b> Graph showing stationary state probabilities for each covariate in June. ....	80
<b>Figure 70.</b> Graph showing stationary state probabilities for each covariate in August. ..	80
<b>Figure 71.</b> Graph showing stationary state probabilities for each covariate in September. ....	81
<b>Figure 72.</b> Graph showing stationary state probabilities for each covariate in October. .	81
<b>Figure 73.</b> Graph showing stationary state probabilities for each covariate in December. ....	82
<b>Figure 74.</b> Graph showing stationary state probabilities for each covariate combining all the months. ....	82



## LIST OF TABLES

<b>Table 1.</b> Missing detections of GPS fixes for each analysed month per matriarch. Additionally, the total number of GPS points divided per month and matriarch. ....	19
<b>Table 2.</b> Step length parameters showing the mean (expressed in km) and standard deviation (SD) for each month and for all the months combined (last row). The step length mean corresponds to the average distance covered in a single step for each state. ....	26
<b>Table 3.</b> The turning angle parameters, showing the mean and the concentration for each month and for all the months combined (last row). The turning angle mean corresponds to the average angle performed in a single step for each state. ....	27
<b>Table 4.</b> Percentage of time spent for each state obtained with the Viterbi algorithm, included in the Viterbi function of the moveHMM package. It provides the most probable sequence of states that generated the observation, based on the fitted model. ....	28
<b>Table 5.</b> Regression coefficients for the transition probabilities referred to the month of June. The table shows the probability of transition between state 1 and 2 (1→2), state 1 and 3 (1→3), state 2 and 1 (2→1), state 2 and 3 (2→3), state 3 and 1 (3→1), and state 3 and 2 (3→2). The first row indicates the baseline probability of transition when all the covariates are set to zero. From the second to the fifth row, 4 different covariates and their influence on the transition probabilities are shown. ....	29
<b>Table 6.</b> Regression coefficients for the transition probabilities referred to the month of July. The table shows the probability of transition between state 1 and 2 (1→2), state 1 and 3 (1→3), state 2 and 1 (2→1), state 2 and 3 (2→3), state 3 and 1 (3→1), and state 3 and 2 (3→2). The first row indicates the baseline probability of transition when all the covariates are set to zero. From the second to the fifth row, 4 different covariates and their influence on the transition probabilities are shown. ....	32
<b>Table 7.</b> Regression coefficients for the transition probabilities referred to the month of August. The table shows the probability of transition between state 1 and 2 (1→2), state 1 and 3 (1→3), state 2 and 1 (2→1), state 2 and 3 (2→3), state 3 and 1 (3→1), and state 3 and 2 (3→2). The first row indicates the baseline probability of transition when all the covariates are set to zero. From the second to the fifth row, 4 different covariates and their influence on the transition probabilities are shown. ....	35
<b>Table 8.</b> Regression coefficients for the transition probabilities referred to the month of September. The table shows the probability of transition between state 1 and 2 (1→2), state	

1 and 3 (1→3), state 2 and 1 (2→1), state 2 and 3 (2→3), state 3 and 1 (3→1), and state 3 and 2 (3→2). The first row indicates the baseline probability of transition when all the covariates are set to zero. From the second to the fifth row, 4 different covariates and their influence on the transition probabilities are shown. ....	38
<b>Table 9.</b> Regression coefficients for the transition probabilities referred to the month of October. The table shows the probability of transition between state 1 and 2 (1→2), state 1 and 3 (1→3), state 2 and 1 (2→1), state 2 and 3 (2→3), state 3 and 1 (3→1), and state 3 and 2 (3→2). The first row indicates the baseline probability of transition when all the covariates are set to zero. From the second to the fifth row, 4 different covariates and their influence on the transition probabilities are shown. ....	41
<b>Table 10.</b> Regression coefficients for the transition probabilities referred to the month of November. The table shows the probability of transition between state 1 and 2 (1→2), state 1 and 3 (1→3), state 2 and 1 (2→1), state 2 and 3 (2→3), state 3 and 1 (3→1), and state 3 and 2 (3→2). The first row indicates the baseline probability of transition when all the covariates are set to zero. From the second to the fifth row, 4 different covariates and their influence on the transition probabilities are shown. ....	44
<b>Table 11.</b> Regression coefficients for the transition probabilities referred to the month of December. The table shows the probability of transition between state 1 and 2 (1→2), state 1 and 3 (1→3), state 2 and 1 (2→1), state 2 and 3 (2→3), state 3 and 1 (3→1), and state 3 and 2 (3→2). The first row indicates the baseline probability of transition when all the covariates are set to zero. From the second to the fifth row, 4 different covariates and their influence on the transition probabilities are shown. ....	45
<b>Table 12.</b> Regression coefficients for the transition probabilities referred to the month from June to December combined as a whole. The table shows the probability of transition between state 1 and 2 (1→2), state 1 and 3 (1→3), state 2 and 1 (2→1), state 2 and 3 (2→3), state 3 and 1 (3→1), and state 3 and 2 (3→2). The first row indicates the baseline probability of transition when all the covariates are set to zero. From the second to the fifth row, 4 different covariates and their influence on the transition probabilities are shown.	50
<b>Table 13.</b> Step length parameters showing the mean (expressed in km) and standard deviation (SD) for each month and for all the months combined (last row). The step length mean corresponds to the average distance covered in a single step for each state. ....	58
<b>Table 14.</b> The turning angle parameters, showing the mean and the concentration for each month and for all the months combined (last row). The turning angle mean corresponds to the average angle performed in a single step for each state.....	59

<b>Table 15.</b> Percentage of time spent for each state obtained with the Viterbi algorithm, included in the Viterbi function of the moveHMM package. It provides the most probable sequence of states that generated the observation, based on the fitted model. ....	60
<b>Table 16.</b> Regression coefficients for the transition probabilities referred to the month of June. The table shows the probability of transition between state 1 and 2 (1→2), state 1 and 3 (1→3), state 2 and 1 (2→1), state 2 and 3 (2→3), state 3 and 1 (3→1), and state 3 and 2 (3→2). The first row indicates the baseline probability of transition when all the covariates are set to zero. From the second to the fifth row, 4 different covariates and their influence on the transition probabilities are shown. ....	61
<b>Table 17.</b> Regression coefficients for the transition probabilities referred to the month of August. The table shows the probability of transition between state 1 and 2 (1→2), state 1 and 3 (1→3), state 2 and 1 (2→1), state 2 and 3 (2→3), state 3 and 1 (3→1), and state 3 and 2 (3→2). The first row indicates the baseline probability of transition when all the covariates are set to zero. From the second to the fifth row, 4 different covariates and their influence on the transition probabilities are shown. ....	64
<b>Table 18.</b> Regression coefficients for the transition probabilities referred to the month of September. The table shows the probability of transition between state 1 and 2 (1→2), state 1 and 3 (1→3), state 2 and 1 (2→1), state 2 and 3 (2→3), state 3 and 1 (3→1), and state 3 and 2 (3→2). The first row indicates the baseline probability of transition when all the covariates are set to zero. From the second to the fifth row, 4 different covariates and their influence on the transition probabilities are shown. ....	67
<b>Table 19.</b> Regression coefficients for the transition probabilities referred to the month of October. The table shows the probability of transition between state 1 and 2 (1→2), state 1 and 3 (1→3), state 2 and 1 (2→1), state 2 and 3 (2→3), state 3 and 1 (3→1), and state 3 and 2 (3→2). The first row indicates the baseline probability of transition when all the covariates are set to zero. From the second to the fifth row, 4 different covariates and their influence on the transition probabilities are shown. ....	70
<b>Table 20.</b> Regression coefficients for the transition probabilities referred to the month of December. The table shows the probability of transition between state 1 and 2 (1→2), state 1 and 3 (1→3), state 2 and 1 (2→1), state 2 and 3 (2→3), state 3 and 1 (3→1), and state 3 and 2 (3→2). The first row indicates the baseline probability of transition when all the covariates are set to zero. From the second to the fifth row, 4 different covariates and their influence on the transition probabilities are shown. ....	73

**Table 21.** Regression coefficients for the transition probabilities referred to the month from June to December combined as a whole. The table shows the probability of transition between state 1 and 2 ( $1 \rightarrow 2$ ), state 1 and 3 ( $1 \rightarrow 3$ ), state 2 and 1 ( $2 \rightarrow 1$ ), state 2 and 3 ( $2 \rightarrow 3$ ), state 3 and 1 ( $3 \rightarrow 1$ ), and state 3 and 2 ( $3 \rightarrow 2$ ). The first row indicates the baseline probability of transition when all the covariates are set to zero. From the second to the fifth row, 4 different covariates and their influence on the transition probabilities are shown.<sup>76</sup>

## ABSTRACT

Animal movement patterns are influenced by a combination of internal and external drivers that interact synergistically and ultimately drive animals' behaviour. Examining the factors behind these influences and their role in guiding animals' choices is crucial for comprehending movement patterns. Exploring the spatial ecology of African savanna elephants (*Loxodonta africana*) provides vital information, particularly within the context of a fenced reserve in South Africa, that is important for the effective and efficient management and conservation of both the species and its habitat. In pursuit of this objective, Hidden Markov Models (HMMs) and hourly Global Positioning System fixes were used to distinguish movements of two matriarchs within the Selati Game Reserve (SGR) into three distinct states. Subsequently, the analysis of the influence of four environmental variables (terrain roughness, distance to nearest road/path, distance to nearest water source, and NDVI) on the probability of persistence in, and transition to, a particular state between June 2022 and December 2022 was conducted. The results showed that all the different covariates consistently influenced elephant movements. Particularly, when the terrain was rougher, matriarchs tended to switch to state 1. Moreover, they showed to use the road network to navigate the landscape faster during the dry season, and to exploit roadside vegetation during the wet season. Additionally, persistence in state 3, the farthest from water sources, was found with direct and accurate movement patterns. Finally, matriarchs consistently occurred in state 1, when NDVI values were highest, and in state 3, when NDVI values were lowest. More in-depth analyses can be carried out to assess whether these results are confirmed on a larger scale, for example over subsequent years. Thus, this study has provided vital information for improving conservation management of elephant within fenced reserves, where their proper management is crucial for the well-being of the entire ecosystem.

**Keywords:** movement ecology; African elephant; fenced reserve; external drivers; HMMs; South Africa.

## ACKNOWLEDGEMENT

I extend my heartfelt gratitude to my supervisor, Dr Anthony Caravaggi, for his unwavering support and invaluable guidance during the course of my study. I deeply appreciate the significant time and effort he invested in coordinating this complex multi-state project, without which it would have been an insurmountable task. Dr Caravaggi's trust in granting me autonomy in my research endeavours, while maintaining consistent communication and offering prompt feedback and assistance, even during the geographic separation of the last two months of our work, is something I will always be grateful for. His mentorship has been instrumental in my academic and personal development, and I genuinely cherish it. Throughout our shared journey, he consistently encouraged me to achieve increasingly ambitious goals. His constant and genuine belief in my potential and capabilities served as a guiding light during moments when challenges seemed insuperable. Meeting Dr Anthony Caravaggi during my studies has been an incredible stroke of luck, and I will always remember his enthusiastic support for my ideas and even the smallest of my accomplishments.

I wish to express my sincere appreciation to Dr Emma Higgins, my co-supervisor, whose invaluable assistance proved indispensable when both Dr Anthony Caravaggi and I faced challenges in navigating essential aspects of the project. I not only gained significant knowledge from her but also found her to be a remarkable person who fostered a collaborative atmosphere throughout the project.

I want to convey my deepest gratitude to Steve Seager, Madeline Siegel, and Matthias Niederer, the dedicated managers and field guides of the Selati Game Reserve. Finding the right words to express how truly blessed I feel to have met all of you and to have had the privilege of working alongside you is a challenge. Your unwavering passion and tireless efforts, not just in recent years but throughout your collective history, have been the cornerstone of everything we have achieved. From day one, you believed in me, despite knowing very little about me, and steadfastly supported me throughout the project, offering invaluable assistance whenever I required it. My gratitude towards you will forever fall short; you've turned one of my greatest dreams into a reality.

Thank must be given to the University of South Wales as a whole, as well as to all my fellow students in my master's program and every lecturer who collectively made this journey an unforgettable one. It has been filled with incredible experiences, opportunities for learning, true friendships, and steady support. Being an international student comes with its challenges, but thanks to all of you, I always felt like I was at home, even if it was a bit colder and rainier than what I was used to. In particular, I want to express special thanks to my closest friends, Van, Hannah, Ozzy, Craig, Ricky, Carys, and Nick. Without your presence, my experience would have undoubtedly lacked the descriptors "great and memorable." Additionally, I wish to convey my deepest appreciation to Dr Gareth Powell, Dr Amelia Grass, and Niamh Breslin for their invaluable contributions to my academic journey.

Gratitude must be given to my family, who have consistently supported my dreams and decisions, even when it meant leaving my country. Life has blessed me with two brothers, Armando and Luigi, who have been unceasing sources of support and serenity, especially during the most difficult moments.

I want to express my genuine thanks to my lifelong friend, Maria Rosaria, who has known me since we were six years old. She has witnessed my growth, transformation, and the choices I have made along my journey. When I first expressed my desire to pursue further studies abroad, she never uttered a single negative word. Despite our diverse preferences and life paths, she has always encouraged me to follow my passions, even if it meant physical distance between us. I hold a deep sense of appreciation for her, especially over the past year, as she was there for me during my darkest moments and guided me back towards the light. We often liken ourselves to the moon and the sun due to our stark differences in almost everything. Yet, to me, she is also a star, a constant point of reference to help me find my way whenever I need it.

My thanks also go to my friends, Marika, Mirella, and Elisa. We have known each other since the first day of our bachelor's degree and, even though our paths went in different directions very early on, we have always found time to enjoy each other's presence. I don't know how to express how pure and true our friendship is. You have always supported all my life choices as if they were your own.

Finally, I want to dedicate the most profound thanks to the love of my life, Simone. You are my everything and this entire experience would have been absolutely unimaginable without you by my side. You make me happier every single day, and you have made even the most stressful and tiring days of this trip magical. We have spent nearly nine months living together day by day, and thanks to you, it has been the best nine months of my life, simply because we were together. The hardest part of the last year was being apart for two months. Although we've had longer separations in the past, not seeing each other for two months after nearly a year of sharing every moment together, after all the happy and deeply sad events we had experienced together, was the most painful experience I've ever endured. At the same time, I knew it was the most important moment of our lives, and I wholeheartedly supported your journey to South Africa to pursue your greatest dream. Witnessing your boundless happiness every day as you pursued your passion was the most fulfilling feeling I've ever known. During the past year you have had to face the most difficult times of your entire life, yet you never gave up. Your strength is admirable, your love and dedication for what you do are the purest things I have ever seen in my life. From the depth of my heart, I can only love you endlessly.



# 1 INTRODUCTION

## 1.1 *Animal movements*

The field of movement ecology aims to understand why organisms move through space following certain patterns and the possible constraints that condition them (Patterson *et al.*, 2017). Animal movement patterns inherently involve internal and external drivers, which interact synergistically, thus impacting animal choices (Mckellar *et al.*, 2015). Therefore, the study of these movement patterns allows ecologists to identify the spatio-temporal distribution of the species analysed, as well as the influencing factors of their movement patterns between different environments (Birkett *et al.*, 2012). Despite the growing importance of animal movement studies in ecology and conservation biology, due to considerable interest in this topic over the past decades, research has commenced to emphasise animal movements in a quantitative manner only in the last decade (Mckellar *et al.*, 2015).

Both marine and terrestrial animals move to optimize their chances of survival and reproductive success, ultimately leading to their physical growth and overall fitness (Whoriskey *et al.*, 2017). Furthermore, animal movements offer advantages by potentially reducing competition within a species and facilitating the discovery of new or improved resources (Bowler *et al.*, 2005). Consequently, risk scenarios might thus be avoided and the probability of finding new mates enhanced (Vogel *et al.*, 2020). Additionally, understanding movement patterns concerning different habitats can aid in discovering the motivations behind the choice of a specific habitat (Nathan *et al.*, 2008). For instance, several papers have found that in richer and more varied landscapes, large herbivores show slower movements and more frequent turning behaviour, whereas, in areas with less forage value, they turn less and show faster pacing patterns (Venter *et al.*, 2015; Fryxell *et al.*, 2008; Senft *et al.*, 1987). This change in movement pattern may indicate that forage availability influences the spatial behaviour of the animals (Vogel *et al.*, 2020). In this regard, it has been demonstrated that spatial variations in animal movement patterns are the result of the non-homogeneous distribution of vital resources, including habitat type, water resources and high-value foraging areas (De Knecht *et al.*, 2007; Apps *et al.*, 2001). Furthermore, movements are also influenced by variations in time, i.e., the seasonal or annual periods when essential resources are accessible to the animals themselves. In turn,

abiotic factors, such as rainfall and temperature, influence the seasonal availability of the resources (Birkett *et al.*, 2012). As evidence, the latter has been widely ascertained for mountain caribou (Apps *et al.*, 2001), as well as for large African herbivores (de Knegt *et al.*, 2007).

Animal movements play a crucial role in maintaining key ecosystem processes, including also seed and natural fertiliser dispersal (Doughty *et al.*, 2013; Guimaraes *et al.*, 2008). In turn, such ecosystem processes contribute to ecosystem health and steadiness (Gravel *et al.*, 2016), as well as enhancing biodiversity (Berti *et al.*, 2023). Despite this, movements also carry a significant energy expenditure and an increased risk of mortality. Fahrig (2007) found a certain association between fast, linear movements and the crossing of risky habitats. This has been to some extent confirmed by several authors who have found an increase in stepping speeds in landscapes with high anthropogenic presence (Karelus *et al.*, 2017; Stillfried *et al.*, 2017; Wang *et al.*, 2017). Human-occupied landscapes influence animal movements, as although they occasionally have high foraging areas, they are still avoided by wildlife given the increased risk of mortality or conflict (Vogel *et al.*, 2020).

Movement is at the core of individual biology and the decisions made are reflected in the movements that are performed, with both direct and indirect repercussions on various levels (Beirne *et al.*, 2021). At the individual level, the movement patterns exhibited by individuals directly determine their fitness, as their capacity for self-sufficiency, survival, and mating depend on them (Kays *et al.*, 2015; Owen-Smith *et al.*, 2010). At the population level, the movement trends of one population can affect those of other populations, modifying possible future interactions (Spiegel *et al.*, 2017; Morales *et al.*, 2010). At the ecosystem level, the movement choices of animals play an important role in the mobilisation of dispersed nutrients in the ecosystem, as well as regulating the degree of impact of the individual within the ecosystem it inhabits (Earl and Zollner, 2017). In light of the above, the conservation not only of a focal species but also of the entire ecosystem, of which it is a part, is highly dependent on understanding and learning about how animals move, the motivations behind the choices that govern these movements, and the consequences of such choices (Beirne *et al.*, 2021). The pervasive recognition of the vital role of the identification of such patterns and the variation they entail is increasingly supported by high-performance tracking technologies (Beirne *et al.*, 2021; Birkett *et al.*, 2012). Such GPS devices have allowed a quantitative collection of fine-scale animal movements data (Kays *et al.*, 2015; Cagnacci *et al.*, 2010;), fostering the emergence of

increasingly up-to-date, accurate and precise statistical models capable of correctly analysing this type of data (Hooten et al., 2017).

## ***1.2 Statistical modelling on movement data***

A significant number of papers on statistical modelling of animal movement have been concerned with the insight-based attempt to distinguish between time series of movement in different behavioural states through the application of state-switching modelling (Michelot *et al.*, 2023). The main explanation for this common choice is that displacement patterns are a reflection of animal behaviour, which in turn is a product of the individual's reaction to physiological impulses and the ecosystem (Whoriskey *et al.*, 2017). Therefore, the identification of these hidden drivers of animal movement (a.k.a. behavioural states) is necessary to further the knowledge of how and why animals decide to exploit available areas (Whoriskey *et al.*, 2017). As evidence, in the last 20 years, different research has classified displacement routes into distinct states, on the basis of individual motivations; among these papers, the following is the most exhaustive: Morales *et al.* (2004) distinguished encamped and exploratory states of elk individuals (*Cervus elaphus*); Pomerleau *et al.* (2011) classified bowhead whales (*Balaena mysticetus*) movement patterns as transient and resident; Franke *et al.* (2004) described three different states, namely bedding, feeding and relocating, in woodland caribou (*Rangifer tarandus*); and Bagniewska *et al.* (2013) determined three distinct dive states in the semi-aquatic American mink (*Neovison vison*). Through the analysis of such behavioural states, it is possible to comprehend how animals utilise resources within the ecosystem (Fryxell *et al.*, 2008; Forester *et al.*, 2007) and, to a greater extent, to investigate population dynamics (Morales *et al.*, 2010). The identification of these characteristics, especially in endangered species, can be a crucial tool in the service of conservation decision-makers (Anadón *et al.*, 2012; Pomerleau *et al.*, 2011; Lusseau, 2003). Moreover, with regard to migrating animal populations, it is critical to determine their movement patterns in space and time and the factors that drive them, when the objective is their conservation and management (Schick *et al.*, 2008; Berger, 2004; Thirgood *et al.*, 2004). A lack of knowledge of these dynamics can pose a risk to animal safety and, indirectly, can lead to an intensification of human-wildlife conflicts (Harris *et al.*, 2009; Bolger *et al.*, 2008).

Refinements in location devices have enabled data to be recorded on fine spatial and temporal scales. Thus, such high-precision data can be combined with external variables, for instance, environmental and topographical covariates, providing meaningful information on how extrinsic factors affect movement behaviour (see Langrock *et al.*, 2014; Patterson *et al.*, 2009; Morales *et al.*, 2004). As a result, numerous works have determined the fine-scale movement behaviour of large mammalian species, including elk (Fryxell *et al.*, 2008), moose (*Alces alces*) (Demarchi, 2003), caribou (Apps *et al.*, 2001) and African elephant (*Loxodonta africana*) (Wittemyer *et al.*, 2008; Cushman *et al.*, 2005). Many of these fine-scale movement studies define different behavioural states between seasons and consider multiple time scales (e.g., days, weeks, months). The authors often analyse seasonal patterns using meteorological proxies, which generally include temperature and precipitation.

Statistical modelling for partitioning movement patterns into distinct unobserved states has generally been developed and adapted using more generalist State-Space Models (SSMs) (Jonsen *et al.*, 2013; Patterson *et al.*, 2008; Schick *et al.*, 2008; Jonsen *et al.*, 2005) or Hidden Markov Models (HMMs) (Langrock *et al.*, 2012; Patterson *et al.*, 2009; Holzmann *et al.*, 2006; Morales *et al.*, 2004), usually assuming a discrete or continuous time structure (Blackwell, 2003). HMMs have been applied for studying movement patterns of a variety of animals, including marine animals, such as tunas (Patterson *et al.*, 2009) and white sharks (Towner *et al.*, 2016), birds, in particular, woodpeckers (Mckellar *et al.*, 2015), insects, with a study on fruit flies (Holzmann *et al.*, 2006), and mammals, including caribous (Franke *et al.*, 2004), and panthers (van de Kerk *et al.*, 2015).

### 1.3 African Elephant (*Loxodonta africana*)

#### 1.3.1 Taxonomy, distribution, and biology

---

Belonging to the class *Mammalia* and order *Proboscidea*, the elephant is classified within the family *Elephantidae*, of which only two genus have extant species: the genera *Loxodonta* and *Elephas* (Shoshani and Tassy, 2004). The latter is represented only by the species of the Asian elephant (*Elephas maximum*), which in turn comprises three subspecies (Shoshani *et al.*, 2001). Two species belongs to the genus *Loxodonta*, the African savanna elephant (*Loxodonta africana*, Blumenbach, 1797) and the African forest elephant (*Loxodonta cyclotis*, Matschie, 1900) (Grubb *et al.*, 2000). From this point forward, this study exclusively pertains to the African savanna elephant, which will be referred to as the African elephant or simply as ‘elephant’.

Once characterised by a large-scale homogeneous presence across the African continent, the African elephant is currently distributed across a highly fragmented and discontinuous landscape (Shaffer *et al.*, 2019). Despite this, it is still present in 37 countries in sub-Saharan Africa, with a total population estimated at between 550,000 and 700,000 individuals (Shaffer *et al.*, 2019). According to the latest IUCN report, of all 37 countries, southern Africa has the largest number of elephants of all four regions. East Africa is in second place, followed by Central Africa and West Africa, with the lowest number of individuals per region (Thouless *et al.*, 2016). Due to high habitat loss and fragmentation, elephant’s current range is 3.3 million km<sup>2</sup>, which is only 22% of the African continent (Campos-Arceiz and Blake, 2011; Blanc *et al.*, 2007).

The African elephant is one of the most dominant animals across the Sub-Saharan African countries. It is the largest extant terrestrial species, where adult males reach a body weight of about six tonnes and adult females between two and three tonnes (Laursen and Bekoff, 1978). African elephants are long-lived animals, which can attain the age of 65. However, the average longevity in their natural environment is estimated at 24 and 41 years for males and females, respectively (Moss, 2001). Elephants exhibit allometric growth between the sexes: females grow until the age of 30, after which they show an abrupt slowdown in growth rate (Hanks, 1972), while males continue to grow beyond the age of 45 (Poole *et al.*, 2011). Furthermore, females are already sexually mature at around nine years old, recording an average age of successful procreation in nature of around 14 years

(Moss, 2001). In contrast, although males reach sexual maturity at 11 years old, they do not manage to compete with more mature males in their natural environment until their 20s, thus becoming truly reproductive no earlier than that age (Poole *et al.*, 2011; Slotow *et al.*, 2000).

### *1.3.2 Ecological role and impact on the ecosystem*

---

African elephants are keystone species and ecological engineers of African savanna ecosystems (Haynes, 2012; Western, 1989) given their disproportionate effect on ecosystem structure and functionalities (Chibeya *et al.*, 2021; Ripple *et al.*, 2015; Kohi *et al.*, 2011; Estes *et al.*, 2011). Additionally, elephants play a crucial role in the dispersal of seeds across the different habitats within their range (Campos-Arceiz and Blake, 2011). Dudley (2000) estimated a dispersal rate of 2054 seeds per square kilometres per day, and Campos-Arceiz and Blake (2011) reported an improvement in the germination stage in seeds dispersed by elephants. They are also recognised as an umbrella species, which means they have a significant impact on other species in the same ecosystem (Gross and Heinsohn, 2023). Their movement and foraging activities foster biodiversity at the environmental and faunal levels (Thompson *et al.*, 2022; Shaffer *et al.*, 2019). As evidence, long-term studies in savanna ecosystems have demonstrated the key role of elephants in reshaping landscapes through damage to canopies, saplings, and shrubs (Fritz, 2017; Coverdale *et al.*, 2016; Kohi *et al.*, 2011).

As one of the most influential species in African landscapes (de Beer *et al.*, 2006), its impact on vegetation radically alters the plant composition (Guldemonnd *et al.*, 2017; Baxter and Getz, 2008; Baxter and Getz, 2005; Augustine and McNaughton, 2004; Eckhardt *et al.*, 2001), however, if not properly balanced in space and time, it can be detrimental to the recovery and survival of plant species (Chui, 2021; Jacobs and Biggs, 2002; Lombard *et al.*, 2001). Notwithstanding, the impact of this alteration on the savanna habitat is a debated topic, as the literature reports contrasting outcomes (Howes *et al.*, 2020). Several studies have highlighted how elephants can effectively induce irreversible damage to trees and riparian habitats, where they repeatedly impact over time, thus impeding natural regeneration (Cook and Henley, 2019; Teren *et al.*, 2018; Guldemonnd

and Van Aarde, 2007; Dublin, 2003; Owen-Smith, 1988; Mwalyosi, 1987). Furthermore, this phenomenon is exacerbated when the number of elephants exceeds the maximum carrying capacity of the ecosystem (Thouless *et al.*, 2016; Coverdale *et al.*, 2016; Landman and Kerley, 2014; Wittemyer *et al.*, 2013). However, Stevens *et al.* (2016) suggested that the heterogeneity of savanna ecosystems can counteract the possible negative elephants' impact, which thus becomes a contributor to the preservation of the optimal state of the savanna. Similarly, the effect on species richness is still not entirely clear. Guldmond *et al.* (2017) stated that the disturbance of elephants on the landscape can generate new niches that can be populated by other species, which in turn leads to an increase in biodiversity. Conversely, in Amboseli National Park, two antelope species (bushbuck *Tragelaphus scriptus* and lesser kudu *Tragelaphus imberbis*) have disappeared precisely because of the damage caused by elephants to the ecosystem (Howes *et al.*, 2020; Cummings *et al.*, 1997). Likewise, within the same park, other mammal species (giraffe *Giraffa camelopardalis*, gerenuk *Litocranius walleri*, and baboon *Papio ursinus*) have diminished in total abundance due to elephant-induced habitat changes (Whyte, 2001). Nevertheless, a study conducted in 2011 revealed that meso-browser, including impalas, showed a preference to feed in areas highly impacted by elephants (Valeix *et al.*, 2011), whilst Nasser *et al.* (2011) determined an increase in diversity and abundance of herpetofauna in habitats with a high degree of elephant disturbance. A systematic review of studies on elephant impact concluded that elephants certainly have a significant effect on vegetation, but with no evident knock-on effect on the other species with which they coexist (Guldmond *et al.*, 2017).

### *1.3.3 Habitat selection, home range, and diet*

---

Elephants are capable of living in a wide variety of environments, given their adaptability to large differences in altitude, which allows them to occupy areas from sea level to mountain altitudes (c.a. 1200 metres above sea level), as well as their ability to persist in multiple habitat types, from desert to tropical forest (Jiang *et al.*, 2020; Laws, 1970). It is widely documented that elephant herds expand their range during the wet period of summer compared to the winter season, during which they confine themselves to areas with high proximity to water sources (Lindeque and Lindeque 1991; Ottichilo 1986;

Norton-Griffiths 1975; Jarman 1972; but see also Shannon *et al.*, 2006). However, Shannon *et al.* (2006) pointed out that in an environment of food scarcity during the dry season, the elephant herd's habitat selection may increase in size compared to the wet season, thus widening their home range to increase the likelihood of food availability. When food resources are in abundance, elephants exhibit less accuracy in habitat selection (William *et al.*, 2018; Mabilile *et al.*, 2012). Given the high availability and variety of food, they mix multiple food types to obtain a wide nutritional spectrum rather than mere energy intake (Codron *et al.*, 2012). In the opposite scenario - during a period of food scarcity - they specifically select a habitat with a secure food provision, preferring quantity over quality (Tsalyuk *et al.*, 2019; Young *et al.*, 2009a). Chui (2021) showed that elephants select habitats according to seasonal ecological changes and plant production regimes. However, habitat selection also depends on the choices of the individual, where personal traits such as memory, personality and social behaviour are the main driving factors (Hertel *et al.*, 2020; Webber and Vander Wal, 2018; Polansky *et al.*, 2015; Dingemanse *et al.*, 2010; Wittemyer *et al.*, 2007). Therefore, individual heterogeneity plays an equally important role in habitat selection and use (Chui, 2021).

Due to their elevated alimentary tolerance (Chui, 2021), elephants are classified as mixed feeders, which means they can alternate feeding behaviour between seasons depending on which type of food is most abundant (Chibeya *et al.*, 2021). According to recent studies, they seem to mainly browse during the dry season and graze during the wet season (Kos *et al.*, 2012). Consequently, depending on the season, between 60% and 95% of their diet consists of grasses (Archie *et al.*, 2006a). When feeding on trees or shrubs, they generally choose species with high nutrient levels (Holdo, 2003), avoiding plants with defence strategies such as high presence of tannin polyphenols (Sheil and Salim, 2006). Likewise, they tend to choose trees with large canopies in order to maximise the energy gain per plant (Howes *et al.*, 2020), debarking the larger branches and toppling the smaller ones (Thompson *et al.*, 2022; Ssali *et al.*, 2013; Ihwagi *et al.*, 2012; Boundja and Midgley, 2010).



### 1.3.4 Social hierarchy and reproductive behaviour

---

The social hierarchy of African elephants is one of the most complex among mammal species. Genetic studies have shown that groups of elephants are matrilineally related, which means that their social organisation is driven by kinship bonds between female elephants (Archie *et al.*, 2006b). Indeed, females represent the core of elephant society, maintaining ties with other female individuals throughout their lives (Schulte and LaDue, 2021; Schuttler *et al.*, 2014; Fishlock and Lee, 2013; Wittemyer and Getz, 2007; Moss and Poole, 1983). In the organisation within these groups of females, the older ones play the dominant role over the younger ones, establishing a clear hierarchy in the group, creating fission-fusion types of society (de Silva and Wittemyer, 2012; Wittemyer and Getz, 2007; Archie *et al.*, 2006b; Wittemyer *et al.*, 2005). Each herd has its matriarch, who will fulfil her role until her death. However, when competition between adult females occurs, it leads to the separation of one of them from the original herd, together with other herd members, who will assume the role of matriarch for the new group (Chui, 2021; Wittemyer *et al.*, 2005). Despite this, the matriarchs still have kinship ties, so they will likely fuse again, forming a two-herd bond group (Archie *et al.*, 2006b; Wittemyer *et al.*, 2005).

Contrastingly, males move away from their native herds around the age of 14 (Lee *et al.*, 2011), commencing to migrate between solitary groups of young males only, or with non-natal herds of females, alternately (Chui, 2021; Chiyo *et al.*, 2014; Lee *et al.*, 2011). Male and female individuals are normally spatially segregated, except for the breeding season, when females are in oestrus and males are in 'musth', i.e., a highly reproductive period when the aggressiveness level increases considerably (Schulte and LaDue, 2021; Rasmussen *et al.*, 1996; Poole, 1987; Poole *et al.*, 1984).

However, while musth happens on a regular basis, albeit temporally staggered among males, females are only in oestrus for a couple of weeks with a gap of 4-5 years (Brown, 2014; Moss and Lee, 2011; Freeman *et al.*, 2009). Furthermore, the gestation period is approximately 22 months (Chui, 2021). Therefore, the latter, combined with the physiological interval between two fertile periods, results in a low reproductive rate (Chui, 2021). Adult males in musth could represent a social advantage for young males. They move, in fact, between different female herds, representing an opportunity for young males to separate from their parental groups. The possibility of learning ecological and social skills from males in musth (Chiyo *et al.*, 2012; Slotow *et al.*, 2000) may represent one of

the main factors in the dispersal of young males from their natal herds (Chui, 2021). Once displaced, the young males' associations with adult elephants modify their socio-behavioural knowledge, a crucial step in the transition to adulthood (Murphy *et al.*, 2020; Lee *et al.*, 2011; Evans and Harris, 2008). Despite these interactions, young males are likely to bond with other elephants of the same age to engage in activities, such as sparring, in order to assess their strength to be ready to establish dominance in their future adulthood (Chiyo *et al.*, 2011; Evans and Harris, 2008).

Therefore, although the social structure of females is stronger, as their hierarchical organisation is crucial for their fitness and survival and for the transfer of eco-social knowledge across generations, the social organisation of males is also influenced by several factors, such as age, kinship, reproductive status and dominant behaviour, which are the main drivers of their social bonds (Goldenberg *et al.*, 2014; Chiyo *et al.*, 2011; O'Connell-Rodwell *et al.*, 2011).

### *1.3.5 Movement patterns and environmental drivers*

---

African elephants are physiologically predisposed to travel long distances (Birkett *et al.*, 2012). Their movement patterns are extremely complex in time and space, as well as highly influenced by seasons (Young *et al.*, 2009a; Young *et al.*, 2009b; de Beer and van Aarde, 2008; Leggett, 2006; Cushman *et al.*, 2005; Douglas-Hamilton *et al.*, 2005); therefore, they are highly variable depending on the scale applied (Birkett *et al.*, 2012; Owen-Smith, 2002; Senft *et al.*, 1987): fine-scale movement patterns may involve periods of one hour, while prolonged periods on larger scales may include weekly, monthly, seasonal, annual and interannual movement patterns (Fryxell *et al.*, 2008; Senft *et al.*, 1987). When elephant populations flourish, it is essential to know their movement behaviour and how they use the habitat in the long term in order to pursue appropriate management (Loarie *et al.*, 2009). External factors, such as the presence of artificial water sources and fences, can have an impact on elephant populations' growth rate and movement behaviour (Loarie *et al.*, 2009). Additionally, a diversified environment results in a non-homogeneous allocation of resources, including habitats, foraging areas, and water (de Knegt *et al.*, 2007; Apps *et al.*, 2001). However, each resource is available to the individual according to its own timeframe, which may depend on the seasons, abiotic factors, or the presence/absence of

other environmental resources (Birkett *et al.*, 2012). In African savanna ecosystems, food availability is linked to seasonal variations, therefore elephants adapt to these changes by modifying their displacement patterns throughout the seasons (Birkett *et al.*, 2012; Fryxell *et al.*, 2008). Hence, the presence and distribution of environmental resources influence the seasonal ranges of elephants. In turn, these highlight which factors are limiting and how demographic variables are affected. Therefore, these dynamics and their drivers are crucial to answering the question of how elephant herds can be limited (Shannon *et al.*, 2006).

It has been pointed out that the movement patterns of elephants are influenced by the type of vegetation, as high-density areas, e.g., clusters of trees, are favoured by these pachyderms because of the higher levels of fibre and nutrients they can gain compared to savanna grasses (Vogel *et al.*, 2020; Ludwig *et al.*, 2008). However, despite the high dietary value of some areas, the energetic costs of travelling, in terms of duration and danger, to reach the habitat may reduce its desirability (Vogel *et al.*, 2020). Local ecology and risk components may in fact represent additional environmental factors influencing the spatial behaviour of elephants (Mramba *et al.*, 2019; Goldenberg *et al.*, 2018; Wittemyer *et al.*, 2017; Shannon *et al.*, 2010; Shannon *et al.*, 2008). Furthermore, when elephants have to choose their route, they are notorious for preferring well-known and well-trodden paths or corridors (Songhurst *et al.*, 2016; Von Gerhardt *et al.*, 2014; Jachowski *et al.*, 2013; Guerbois *et al.*, 2012; Gerhardt-Weber, 2011). Lastly, water is one of the main environmental drivers influencing the movement patterns of elephants, also affecting their use of space (de Beer and van Aarde, 2008; Leggett, 2006; Stokke and du Toit, 2002). Elephants are reliant on water as they have a great turnover, due to water loss through dermal and respiratory evaporation when environmental temperatures are elevated (Purdon and Van Aarde, 2017). Moreover, elephants heavily depend on practices associated with water use, such as mud bathing, swimming, and splashing to thermoregulate themselves (Mole *et al.*, 2016; Dunkin *et al.*, 2013). Thus, it is becoming evident that the combined availability of food and water, are key driving factors in elephant movement patterns and habitat use; therefore, knowledge of how these factors influence elephant ecology and behaviour is critical for conservation (Bohrer *et al.*, 2014).

### 1.3.6 Changes in spatial behaviour within fenced reserves

---

At the present time, 84% of African elephants are found within Protected Areas (PAs) (Gross and Heinsohn, 2023). Particularly, South Africa has been a pioneer in the development of fenced reserves aimed at protecting wildlife (e.g., Slotow, 2012; Gusset *et al.*, 2008; Grant *et al.*, 2008; Hayward *et al.*, 2007). Elephants were removed from most of the South African lands by 1900 (Whyte *et al.*, 1999). When reintroduction programs commenced to become successful, large numbers of elephants were relocated within private reserves, i.e., closed systems where the presence of fences restricted any kind of migration (Slotow *et al.*, 2005). One of the main reasons for creating a fenced reserve is the conservation of the species, ensuring an environment protected from external dangers (Slotow, 2012). Despite this, PAs have often recorded elevated elephant mortality, due to illegal killing within the reserve, such as poaching or subsistence hunting (Chase *et al.*, 2016; Woodroffe *et al.*, 2014). Nevertheless, an increasing number of fenced reserves are experiencing an overpopulation of elephants (Gross and Heinsohn, 2023; Selier *et al.*, 2018), which greatly affects the maintenance of balanced ecosystems (Gross and Heinsohn, 2023). PAs often host other threatened species, therefore the ecosystem imbalance created by elephant surplus may have an indirect impact on the survival of these species (Wall *et al.*, 2013). However, in unfenced areas, the steady decline of elephants is similarly leading to ecological dysfunction of the ecosystem, compromising inter-species and environmental dynamics (Gross and Heinsohn, 2023).

Spatial confinement of elephants within fenced reserves may exaggerate their impact on habitat (Thompson *et al.*, 2022; Baxter and Getz, 2005; Hoare, 1999; Laws, 1970). The presence of fences can lead to a decrease in seasonal movements and, therefore, a concentration of foraging impacts in selected areas (Guldmond and Van Aarde, 2008; Lombard *et al.*, 2001; Cummings *et al.*, 1997). Therefore, in fenced reserves the likelihood for elephants to repeatedly use the same patches of vegetation increases, due to limited dispersal possibilities across the landscape in relation to food supply (Thompson *et al.*, 2022; Howes *et al.*, 2020; de Boer *et al.*, 2015; Mackey *et al.*, 2006; Slotow *et al.*, 2005). Furthermore, the fence line may itself pose a problem, as Loarie *et al.* (2009) showed how it sometimes induced elephants to group against it. Additionally, movement patterns are also affected by proximity to fences, with articles showing an increase in habitat use as distance from the fences increases (see e.g., Thompson *et al.*, 2022; Vanak *et al.*, 2010).

### ***1.4 Hypotheses, Aims and Objectives***

Through the use of hourly GPS fixes, this research aimed to explore the movement patterns of two matriarchs within a fenced reserve in South Africa over a 7-month period. Utilising Hidden Markov Models (HMMs), the study's objective was to determine the most suitable multi-state model for the two matriarchs. This aimed to evaluate their baseline movement patterns and variations in behavioural states, both on a monthly scale and over a combined period of seven months. Afterward, the study proceeded to assess the influence of four distinct extrinsic factors: terrain roughness, distance to the nearest road/path, distance to the nearest water source, and NDVI. This evaluation aimed to determine whether these factors played a pivotal role in shaping the movement patterns of the two matriarchs and to what degree. All four predictor variables were examined independently to assess their direct influence on elephant movements. By explicitly testing their influence on a monthly and collective scale, the aim of the study was to clarify the extent to which movement patterns depend on such covariates, providing a better understanding of the elephants' choices and preferences that drove their movement within the reserve. Thus, in turn, this research aimed to provide information of critical importance for the successful and effective management of the species and, consequently, the entire ecosystem.

## 2 METHOD

### 2.1 *Study location*

Selati Game Reserve (SGR) is located in South Africa, specifically in Limpopo Province, north of the Olifants River (23°54'S - 24°06'S, and 30°36'E - 30°55'E) (Fig.1). The SGR was founded in 1993 when several private landowners joined together 16 properties, with the aim of safeguarding and supporting wildlife and plants richness of the site (Siegel, 2023; Peel and Martindale, 2020). Being surrounded by electrified fences, the SGR is an enclosed reserve, covering a total area of 258 km<sup>2</sup> (Selati Game Reserve, 2017). To the northwest of the reserve lies the Gravelotte Emerald Mine. Along the western border is the town of Gravelotte, while near the eastern border, the community managed Marakapula Reserve is based. This latter reserve serves as a barrier between the SGR and the Namakgale rural area, as well as between Abelana and Balule Private Nature Reserve (Comley, 2019; Peel and Martindale, 2020). The SGR is bordered by other protected lands to the south, specifically Makalali-Pidwa and Karongwe Reserves, while to the north by community livestock farms. The entire reserve is located within the Ba-Phalaborwa Local Municipality, which is part of Mopani District Municipality of Limpopo Province (Peel and Martindale, 2020). At the present time, the reserve is based on low-impact ecotourism (Siegel, 2023) and authorised low-impact hunting, which partially supports the reserve at the economic level (Peel and Martindale, 2020).

The SGR is characterised by hot summers and warm-to-cold winters. The reserve experiences about 500 mm of precipitation per year (Kottek et al., 2006; Peel and Martindale, 2020). Evapotranspiration rates have occasionally exceeded rainfall, causing a strong impact on plants (Peel and Martindale, 2020). Precipitation is mainly concentrated between October and March, reaching the maximum amount of mm per month between December and January (Fig.) (Comley, 2019).

The scarcity and inconsistency of rainfall are characteristic features of semi-arid savanna ecosystems. In this context, only two seasons characterise the area over the course of the year: a five-month hot and wet season (November-March) and a cold and dry season between May and September, with April and October as transition periods between the two seasons (Peel and Martindale, 2020). During the summer, temperatures vary between 18°C and 45°C, whereas in the winter, they range from 8°C to 23°C. The average highest

monthly temperature typically reaches around 40°C, while the lowest mean minimum temperature hovers around 0°C (Peel and Martindale, 2020).

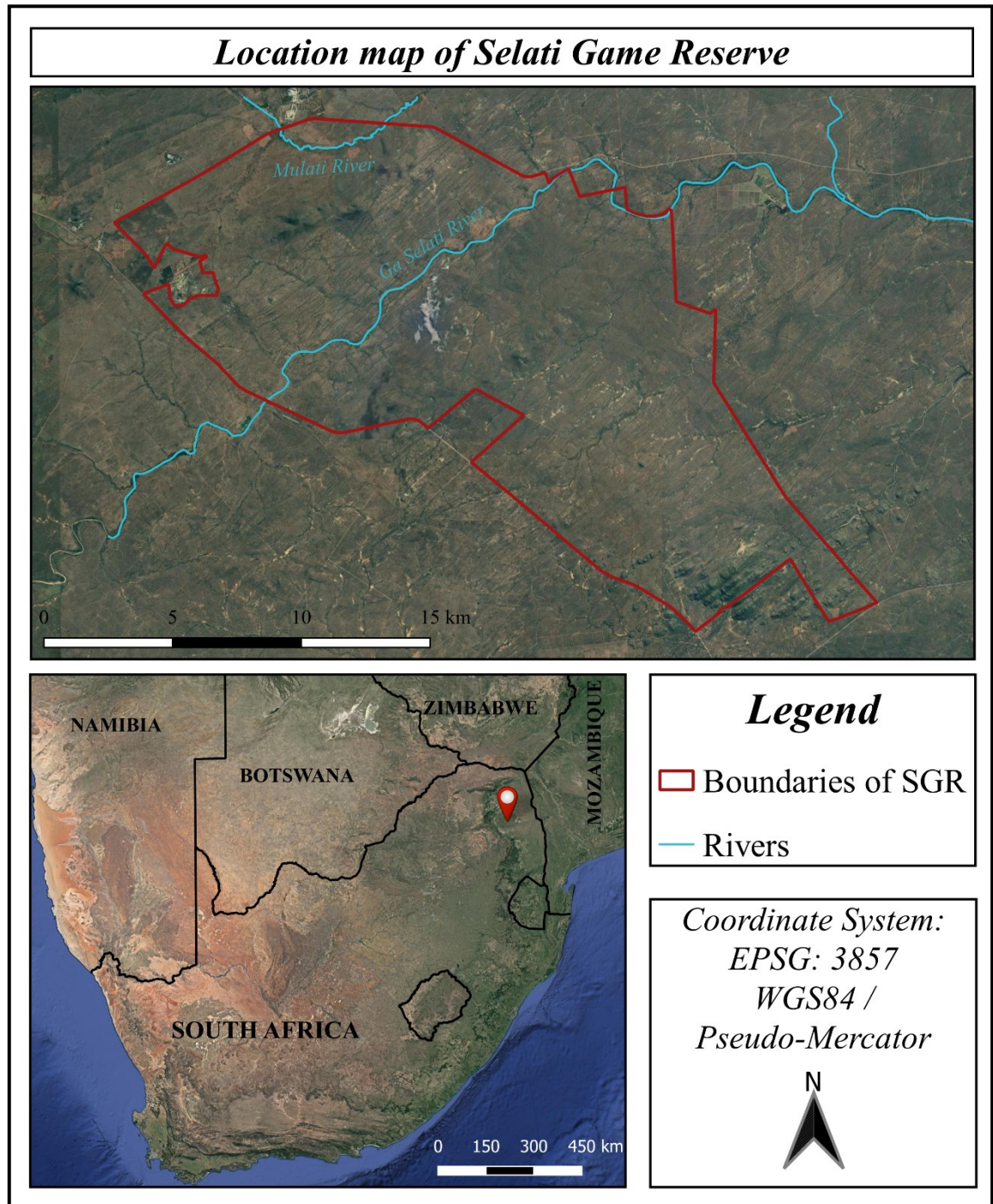


**Figure 1.** Location map of Selati Game Reserve. Created with QGIS Desktop by Zelia Romano.

The SGR is at an elevation averaging 530 m above sea level (a.s.l.), reaching 778 m a.s.l. in the southernmost part of the reserve, with the Ga-Mashishimale Hills. The Selati River flows through the reserve from west to northeast, and along with other drainage streams, flows as a tributary into the Olifants River, partly creating the Greater Olifants River Basin (Peel and Martindale, 2020).

Within the SGR boundaries, multiple water points are present for wildlife, scattered throughout the reserve (Fig.). These include 38 seasonal pans, 22 artificial water sources, 7 reservoirs and at least 10 boreholes, of which only about half are active. The seasonal pans are designed so that rainwater runoff flows into them, however supplementary water can come from surrounding boreholes as well. In the section of the Selati River that lies within the reserve, six dams were built in the past: currently only three are still intact (Comley, 2019; Siegel, 2023).

The SGR is entirely within the South African Savanna Biome, including three different bioregions within its boundaries (Rutherford *et al.*, 2006) (Fig.2):

- i) The Phalaborwa-Timbavati Mopaneveld bioregion, which covers 61% of the reserve, fully dominate the central areas of the reserve. It covers an area with a wide variation in elevation, ranging from 300 m to 600 a.s.l. It is dominated by red bushwillow (*Combretum apiculatum*), silver cluster-leaf (*Terminalia sericea*) and mopane (*Colophospermum mopane*) (Rutherford *et al.*, 2006), across mopane forests, mixed mopane-bushwillow forests and mixed mopane-bushwillow-*Acacia spp.* forests (Peel and Martindale, 2020). The abundance of termite mounds scattered throughout the bioregion is another distinctive feature of the area (Mucina and Rutherford, 2006).
- ii) The Granite Lowveld bioregion represents only the 33% of the SGR, and it is mainly distributed in the northern and southern areas. It extends over a wide range of elevations, particularly between 250 and 700 m a.s.l., resulting in major changes in soil composition throughout this elevation range. Ancient granites and Makhutswi gneiss, which represent the bedrock geology, form sandy soils at higher elevations and clay soils in lower areas (Rutherford *et al.*, 2006). The bioregion is represented by scattered shrubland and low, fairly dense forests in the sandy areas, where three main species dominated, namely silver cluster-leaf, large-fruited bushwillow (*Combretum zeyheri*) and red bushwillow (Mucina and Rutherford, 2006). In contrast, in dense and open savanna areas, knob thorn (*Senegalia nigrescens*), sicklebush (*Dichrostachys cinerea*) and



brandy bush (*Grewia bicolor*) dominate (Mucina and Rutherford, 2006). Red bushwillow veld, mixed red bushwillow-marula (*Sclerocarya birrea*) veld, and silver cluster-leaf veld are found within this bioregion (Mucina and Rutherford, 2006).

- iii) The Gravelotte Rocky Bushveld bioregion constitutes only the mountainous zones, scattered at west and east of the reserve, with a total cover of about 6%. It lies between 450 and 950 m a.s.l. and is characterised by open deciduous and semi-deciduous woodlands on rocky areas and isolated hill that stands above well-developed plains (Mucina and Rutherford, 2006). Indeed, rocky soils differentiate this bioregion from the others, generally shallow with rocky outcrops and slopes all around the woodlands. The main tree species typical of this bioregion are African teak (*Pterocarpus angolensis*), hook-thorn (*Senegalia caffra*), bushveld candelabra (*Euphorbia cooperi*) and red bushwillow (Comley, 2019).

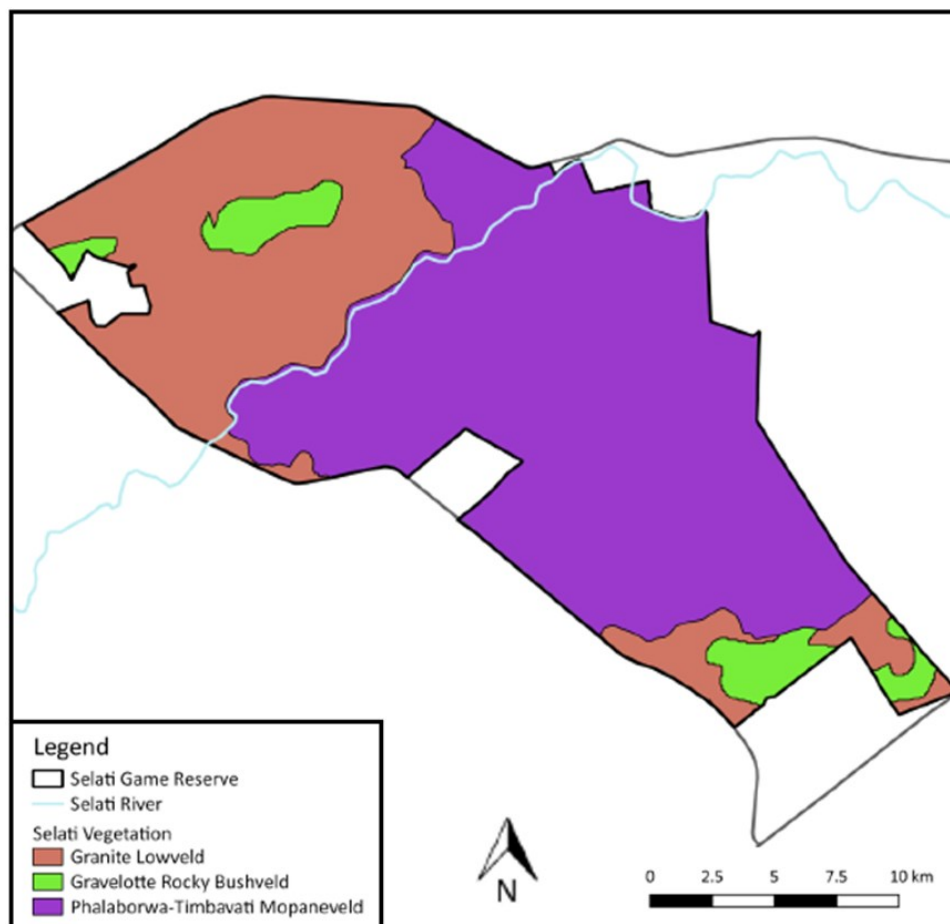


**Figure 2.** Distribution of the three different bioregions inside SGR (Mucina and Rutherford, 2006).

## 2.2 GPS Collar Data collection

In 2022, two matriarchs, Elza and Jean (Appendix I), were collared with the Long Range (LoRa) collar devices in the Selati Game Reserve in June. These types of collars enabled GPS positions to be acquired on an hourly basis. Therefore, to study the movements of each matriarch, and thus also those of their herds, GPS-fixes were used from the day the collar was fitted - which is the 1<sup>st</sup> of June for Elza, and the 8<sup>th</sup> of June for Jean - until 31<sup>st</sup> December 2022, the end date for both the matriarchs studied. Throughout the reserve, three gateways were installed in order to have total signal reception coverage of the collars (Seager, 2023). The LoRa collars are a type of tracking device that use LoRaWAN (Long Range Wide Area Network) technology to monitor and collect data about elephant movements (Meenakshi *et al.*, 2022). The collar collects data from the GPS receiver and sensors installed inside it. This data includes the elephant's coordinates, movement patterns, speed, and environmental conditions. The LoRa technology allows the collar to transmit the collected data over long distances using low-power, wide-area networks (Meenakshi *et al.*, 2022). Subsequently, gateways located within the reserve pick up the transmitted data from the collar. Finally, the received data is sent to an Amazon Web Service Stack (AWS Stack) and then to ArcGis Online, where it is stored (Seager, 2023).

The LoRa collars involved in this study have a spatial accuracy of 5 metres and a temporal error between 0 and 2 minutes every hour, i.e., a GPS fix is recorded every 60-62 minutes (Seager, 2023). GPS reception problems resulted in missing position data. These were imputed using a customised R function that interpolated values for intervals greater than 65 minutes. In the 7-month period analysed in this study, LoRa collars recorded 2.18% and 1.67% missing data from Elza and Jean respectively, ensuring reasonable completeness (Table 1).

**Table 1.** Missing detections of GPS fixes for each analysed month per matriarch. Additionally, the total number of GPS points divided per month and matriarch.

GPS fixes				
	<i>Elza</i>		<i>Jean</i>	
	<i>Missing detections</i>	<i>Total records</i>	<i>Missing detections</i>	<i>Total records</i>
June	6	711	6	542
July	5	742	2	743
August	71	742	63	740
September	14	720	4	719
October	7	743	5	743
November	4	718	3	719
December	5	742	3	742

### ***2.3 Data preparation for covariates and Remote Sensing Data***

The model built to analyse each matriarch movement pattern included four covariates: terrain roughness, distance to nearest road/path, distance to nearest water source, and NDVI.

Selati Game Reserve shared essential shapefiles to carry out this project, particularly concerning the distribution of all the main and secondary gravel roads (see Appendix II), and the location of all water sources within the reserve, both natural and artificial (see Appendix II). The water points were then divided into seasonal and perennial, so that during the dry season only the active ones were applied. The distance from each GPS fix to the nearest water source and road was calculated in R for both matriarchs. Terrain roughness and elevation of the entire reserve were calculated using ‘terra’ and

‘elevatr’ packages, respectively (Hijmans *et al.*, 2023; Hollister *et al.*, 2023). Even though previous research pointed out that elevation could indirectly influence preferences by having an effect on the other covariates (Asner *et al.*, 2016; Berti *et al.*, 2022; Chibeya *et al.*, 2021; Ngene *et al.*, 2009; Taher *et al.*, 2021; Talukdar *et al.*, 2020), the elevation variable was excluded because the best performing model did not include elevation. Instead, terrain roughness was included as a covariate since it was in the best approximating model.

The Normalized Difference Vegetation Index (NDVI) was calculated to be added as another covariate in order to assess habitat preferences. The satellite images used to calculate the NDVI value were downloaded from Planet (<https://www.planet.com/>). Their spatial resolution is 3 metres per pixel. One image per month was downloaded, choosing a date close to the middle of that month and having a cloud cover below 5%. The chosen image was used as representative of the entire month to which it referred (details of all satellite tiles use are given in Appendix III). The NDVI calculation was performed separately for each month on QGIS Desktop (version 3.30.1 “s-Hertogenbosch”), using the raster calculator tool. Only the near-infrared (NIR) and red (RED) bands were utilized as input for the calculation, following the formula  $NDVI = \frac{NIR - RED}{NIR + RED}$ . The NDVI value obtained from the satellite image for a particular month was consistently applied to every day within that same month (see Appendix II).

## 2.4 *Hidden Markov Model (HMM)*

Elephant movement patterns were statistically analysed through a Hidden Markov Model (HMM). HMM is a state-space models that outline animal behaviours as a series of states delineated by both movement parameters and transition probabilities between states (Jonsen *et al.*, 2005; McClintock *et al.*, 2020). In detail, it consists of two dependent parts: a set of observations  $Z_1; \dots; Z_T$  and a sequence of unobservable states  $S_1; \dots; S_T$  (Fig.3). The latter take on values between  $\{1, \dots, N\}$ , respecting the Markov first-order finite-state Markov chain (Langrock *et al.*, 2012). Therefore, at any time  $t$ , the execution of  $Z_t$  is assumed to have been extracted from one of  $N$  constituent distributions, determined in turn by the value of the state at time  $t$ . In this study, the unobservable states are represented by the different behavioural states (Michelot *et al.*, 2016).

The HMM was adapted to this study using the R package moveHMM, which applies HMMs and associated tools for modelling animal movement (see Michelot *et al.*, 2023). The package was employed to pre-process the data for analysis, to fit HMM to the data and to diagnose fitted models (Michelot *et al.*, 2023).

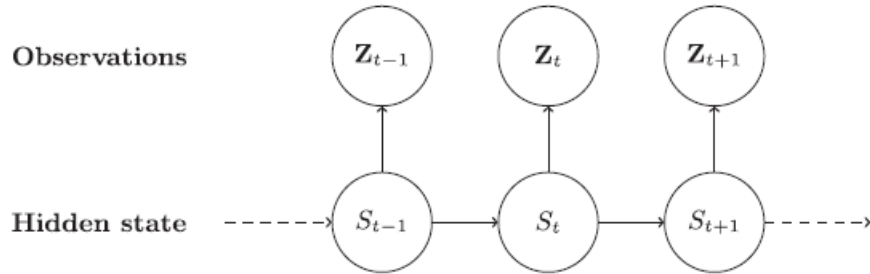


**Figure 3.** Structure of dependency in Hidden Markov Model (Michelot *et al.*, 2016).

## 2.5 Data processing and fitting HMM

The HMM procedure for modelling animal movements concerns a bivariate time series with  $z_t = (l_t, \phi_t)$ , where  $l_t$  is the step length, i.e., the Euclidean distance between two subsequent GPS fixes  $(x_t, y_t)$  and  $(x_{t+1}, y_{t+1})$ , and  $\phi_t$  is the turning angle, i.e. the change in direction in the intervals  $[t-1, t]$  and  $[t, t+1]$  of the analysed animal (Fig.4) (Patterson *et al.*, 2017). Therefore, for being able to fit an HMM using moveHMM, the series of step lengths (meters) and turning angles (radians) were calculated through the prepData function from the GPS fixes.

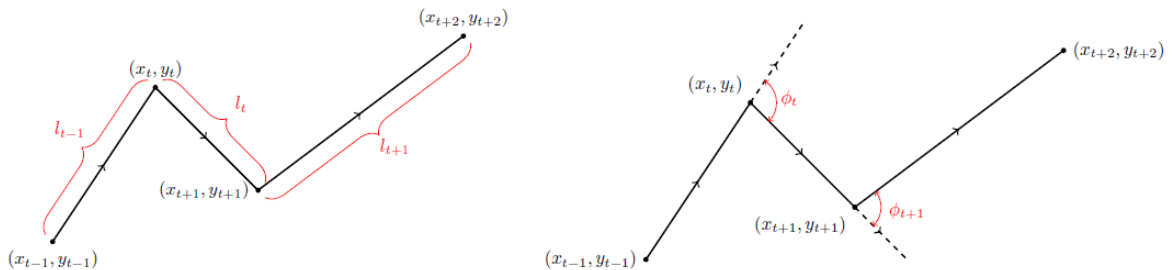


**Figure 4.** Graphic overview of step lengths and turning angles calculation (Michelot *et al.*, 2023).

Step lengths were modelled with a Gamma ( $\Gamma$ ) distribution, dependent on two initial parameters: the step mean ( $\mu$ ) and the step standard deviation ( $\sigma$ ). Turning angles were modelled with a Von Mises ( $VM$ ) distribution, dependent on two initial parameters: the angle-mean and the concentration of the distribution around the mean ( $k$ ). At a given time, these parameters are governed by the unobserved state corresponding to that fix (Michelot *et al.*, 2023).

The number of states (i.e., behavioural categories) must be entered, along with their state transition probabilities. Likewise, the initial parameters exemplifying the state-dependent distributions, must be stated. As Michelot *et al.* (2016) stressed, these choices are fundamental as the starting values influence the algorithm governing the function for the maximum likelihood estimation (MLE). Furthermore, the choice can influence the outputs of the HMM, since a different estimate of the starting parameters depends on the number of states chosen, thus a change in the parameters can lead to different fitted estimations (Berti *et al.*, 2023). Therefore, if the starting parameters and the number of states are inadequately selected, this affects the fitting of the HMM.

To overcome these possible biases, several trials were conducted in order to find the most suitable number of behavioural states for this study. In particular, a two-state model and a three-state model were adapted as a trial. Both the graphical outputs and the analysis through the Akaike Information Criterion (AIC) confirmed a better fit of the three-state model for the specific case of this research. In addition, this is in line with the findings of Taylor *et al.* (2020), who found that the three-state model was the best fit when analysing elephant movements. Once the number of behavioural states was defined, a function was created to generate random initial parameter values for each state of the HMM's step model ( $\mu$  and  $\sigma$ ) and angle model (angleMean and  $k$ ). These values were generated within specified ranges, following the methodology explained by Berti *et al.* (2023). Specifically, the initial parameters were ranged between the 10%-90% quantiles of the movement values obtained from the GPS fixes; since the chosen model was three-state, this interval of quantiles' was split into three sub-intervals, one for each state, as follows:  $U(q_{10\%}, q_{40\%})$ ,  $U(q_{40\%}, q_{70\%})$ ,  $U(q_{70\%}, q_{90\%})$ , respectively (Berti *et al.*, 2023). The function was set on 100 iterations for which the HMM were fitted with different initial parameter values for each state. Subsequently, the model with the lowest negative log-likelihood was chosen as the best-fitted three-state HMM model, thus its parameters were used for all the matriarchs.

Once the starting parameters were set, the model calculated the regression coefficients for the transition probabilities. These coefficients returned an estimate of the probability of transition from one state to the other, based on the values of the predictor variables (Michelot *et al.*, 2023). Additionally, the stationary state probabilities were also performed by the model. They comprised the long-term probabilities of occurring in each state at different values of the covariate (Michelot *et al.*, 2023).

Pseudo-residuals - also called quantile residuals - were applied to assess the correctness and accuracy of the chosen fitted HMM. If the model has analysed the data correctly, the pseudo-residuals must have an approximately normal distribution. Therefore, a deviation from a standard normal distribution suggests a lack of fit of the HMM (Michelot *et al.*, 2023; Michelot *et al.*, 2016). The sequence of behavioural states of the unobserved Markov chain was also decoded to analyse more in depth the state-switching process, using the Viterbi algorithm. The latter provides the most probable succession of states that generated the observation (Michelot *et al.*, 2023; Michelot *et al.*, 2016). Therefore, the Viterbi function was applied to estimate the percentage of time spent in each state. Additionally, the state probabilities, i.e., the probability of occurrence of each state in the model for each GPS time point, given the fitted model, were calculated with a function already present in the moveHMM package. For an HMM with N states and a series of GPS fixes recorded following a succession in time of length T, the function used generates a matrix T x N, where in each row is given the probability that the Markov chain was in each of the N states at the time of row T (Michelot *et al.*, 2023). The state with the greatest likelihood found with the latter function may not correspond with the state in the most likely sequence calculated by the Viterbi algorithm. The reason lies in the different type of execution between the two functions, which can be described as 'local decoding' and 'global decoding', respectively (Michelot *et al.*, 2023).

The modelling was created to analyse the matriarchs' movement patterns with the influence of four covariates on a monthly scale. In addition, matriarchs' movement patterns were also evaluated by combining all months together, in order to gain an overall understanding. The maximum period analysed for a single elephant was seven months (1<sup>st</sup> of June to 31<sup>st</sup> of December), of which five months (June to October) were classified as the 'dry season' and the last two (November and December) as the 'wet season', based on the weather conditions of that year, combined with empirical evidence recorded by the reserve managers. Based on the AIC evaluation, the best HMMs model identified three distinct states in all individuals. These states can be classified into broad categories of

behaviour: state 1, represented by the short steps, was mainly characterised by slower movements without a specific direction; state 3, represented by the long steps, was the fastest state with a specific direction traced throughout; finally, state 2, represented by the medium steps, had characteristics intermediate between the other two states, i.e., a cadenced speed of movement with both non-directed and directed directions.

During the analysis of Jean's movement patterns, two months, July and November, were notably absent. This absence stemmed from a recurring error in the initial parameters, preventing the extraction of any meaningful results from the GPS data for these particular months. Nevertheless, both July and November were factored into the analysis of all months combined, contributing to the overall assessment.

For maps of monthly movement patterns, see Appendix IV.



### 3 RESULTS

A total of 10,066 GPS fixes (n) were analysed to study the movement patterns of two matriarchs, Elza (n = 5,118) and Jean (n = 4,948), within the Selati Game Reserve, between June and December 2022.

#### ***3.1 Elza***

The step length means for each state fluctuated in a month-scale analysis: state 1 had a minimum of 55 metres c.a. (in June) and a maximum of 102 metres c.a. (in October); state 2 ranged from a minimum of 157 metres c.a. (in October) and a maximum of 369 metres c.a. (in December); state 3 exhibited a minimum of 754 metres c.a. (in September) and a maximum of 1129 metres c.a. (in December). Overall, on a 7-month period, the step length means were 61.5, 272, and 994 meters, for states 1,2, and 3 respectively. Fluctuations were also recorded for the standard deviation (SD) of the step length, as well as for the mean and concentration of the turning angle (see Table 2 and 3).

**Table 2.** Step length parameters showing the mean (expressed in km) and standard deviation (SD) for each month and for all the months combined (last row). The step length mean corresponds to the average distance covered in a single step for each state.

Step length parameters						
	<i>Mean</i>			<i>SD</i>		
	<i>State 1</i>	<i>State 2</i>	<i>State 3</i>	<i>State 1</i>	<i>State 2</i>	<i>State 3</i>
June	0.055	0.310	1.077	0.055	0.221	0.543
July	0.066	0.270	0.953	0.064	0.160	0.533
August	0.074	0.222	0.857	0.071	0.104	0.579
September	0.063	0.182	0.754	0.063	0.127	0.511
October	0.102	0.157	1.001	0.125	0.131	0.710
November	0.066	0.305	0.983	0.061	0.182	0.404
December	0.079	0.369	1.129	0.077	0.201	0.430
<b>June- December</b>	<b>0.061</b>	<b>0.272</b>	<b>0.994</b>	<b>0.058</b>	<b>0.166</b>	<b>0.556</b>

**Table 3.** The turning angle parameters, showing the mean and the concentration for each month and for all the months combined (last row). The turning angle mean corresponds to the average angle performed in a single step for each state.

Turning angle parameters						
	<i>Mean</i>			<i>Concentration</i>		
	<i>State 1</i>	<i>State 2</i>	<i>State 3</i>	<i>State 1</i>	<i>State 2</i>	<i>State 3</i>
June	0.300	0.012	-0.147	0.541	1.165	2.279
July	-0.029	0.070	-0.030	0.627	1.619	1.551
August	0.205	0.027	0.052	0.721	1.872	1.737
September	0.501	-0.028	0.044	0.267	2.212	1.867
October	-2.692	0.095	0.054	0.889	1.416	2.101
November	-0.030	-0.027	0.076	0.239	1.123	2.051
December	0.414	-0.097	-0.024	0.663	1.231	2.157
<b>June- December</b>	<b>0.178</b>	<b>0.021</b>	<b>-0.015</b>	<b>0.484</b>	<b>1.407</b>	<b>1.824</b>

A clear difference was found in the time spent in state 3 (long step) between the dry and wet seasons, with an average for all dry months of around 35% of the total time spent walking long distances, in contrast to only 14.5% during the wet months (Table 4). In particular, in November, the first month after the dry season, there is a peak in the percentage of time spent in state 1 (short step), with a value of 41% (Table 4).

**Table 4.** Percentage of time spent for each state obtained with the Viterbi algorithm, included in the Viterbi function of the moveHMM package. It provides the most probable sequence of states that generated the observation, based on the fitted model.

Percentage of time spent on each state			
	<i>State 1</i>	<i>State 2</i>	<i>State 3</i>
June	0.319	0.462	0.217
July	0.364	0.426	0.215
August	0.318	0.384	0.402
September	0.267	0.361	0.390
October	0.131	0.588	0.289
November	0.413	0.476	0.116
December	0.312	0.508	0.185
<b>June- December</b>	<b>0.319</b>	<b>0.462</b>	<b>0.217</b>

In June (Table 5, Fig. 5-8), when all covariates are set to zero, the baseline probability of transitioning from state 1 to state 2 ( $1 \rightarrow 2$ ) was +0.71. Under the influence of the NDVI variable, this probability became -3.09, indicating that an increase in the value of this predictor variable was associated with a decrease in the odds of the event occurring. Conversely, the baseline probability of moving from state 1 to state 3 ( $1 \rightarrow 3$ ) and from state 2 to state 1 ( $2 \rightarrow 1$ ) exhibited considerable negative values (-15.50 and -5.15, respectively). In contrast, when the influence of distance to the water source was considered, the  $1 \rightarrow 3$  probability suggested a positive relationship between the predictor and the outcome (+1.26). This indicated that as the distance from a water source increased, the  $1 \rightarrow 3$  switching probability increased as well. Similarly, when considering the influence of NDVI, the probability of  $2 \rightarrow 1$  transitioning was positively affected, with a value of +6.49. This implied that in greener areas, there was a greater probability of transitioning to state

1. Fig. 5-8 also showed the probability of persistence in a state due to the influence of each covariate: for example, the rougher the terrain, the more likely Elza was to persist in state 1 (Fig.5); just as the lower the roughness value, the higher the probability of persistence in state 3 (Fig.5); furthermore, the higher the NDVI value, the lower the probability of persistence in states 2 and 3 (Fig.8).

**Table 5.** Regression coefficients for the transition probabilities referred to the month of June. The table shows the probability of transition between state 1 and 2 ( $1 \rightarrow 2$ ), state 1 and 3 ( $1 \rightarrow 3$ ), state 2 and 1 ( $2 \rightarrow 1$ ), state 2 and 3 ( $2 \rightarrow 3$ ), state 3 and 1 ( $3 \rightarrow 1$ ), and state 3 and 2 ( $3 \rightarrow 2$ ). The first row indicates the baseline probability of transition when all the covariates are set to zero. From the second to the fifth row, 4 different covariates and their influence on the transition probabilities are shown.

	Regression coefficients for the transition probabilities						June
	$1 \rightarrow 2$	$1 \rightarrow 3$	$2 \rightarrow 1$	$2 \rightarrow 3$	$3 \rightarrow 1$	$3 \rightarrow 2$	
Intercept	0.711	-15.504	-5.159	-0.706	-12.022	-2.608	
Terrain roughness	-0.375	1.1585	0.241	0.371	0.413	0.824	
Min. road/path distance	0.072	-1.311	0.162	0.146	0.902	0.554	
Min. water source distance	0.188	1.264	0.009	0.212	0.029	-0.116	
NDVI	-3.090	-8.245	6.497	-2.212	-5.608	3.705	

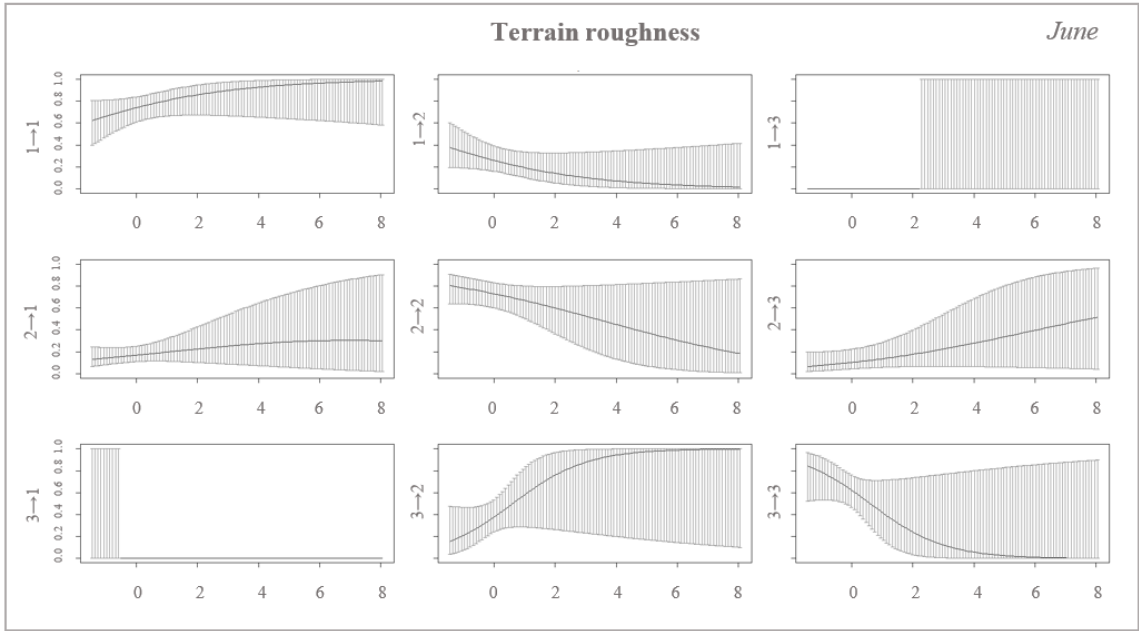


**Figure 5.** Graph showing transition probabilities under the influence of terrain roughness as a covariate in June, between state 1 and 2 ( $1 \rightarrow 2$ ), state 1 and 3 ( $1 \rightarrow 3$ ), state 2 and 1 ( $2 \rightarrow 1$ ), state 2 and 3 ( $2 \rightarrow 3$ ), state 3 and 1 ( $3 \rightarrow 1$ ), and state 3 and 2 ( $3 \rightarrow 2$ ). The graph also shows persistence probabilities in state 1 ( $1 \rightarrow 1$ ), state 2 ( $2 \rightarrow 2$ ) and in state 3 ( $3 \rightarrow 3$ ).

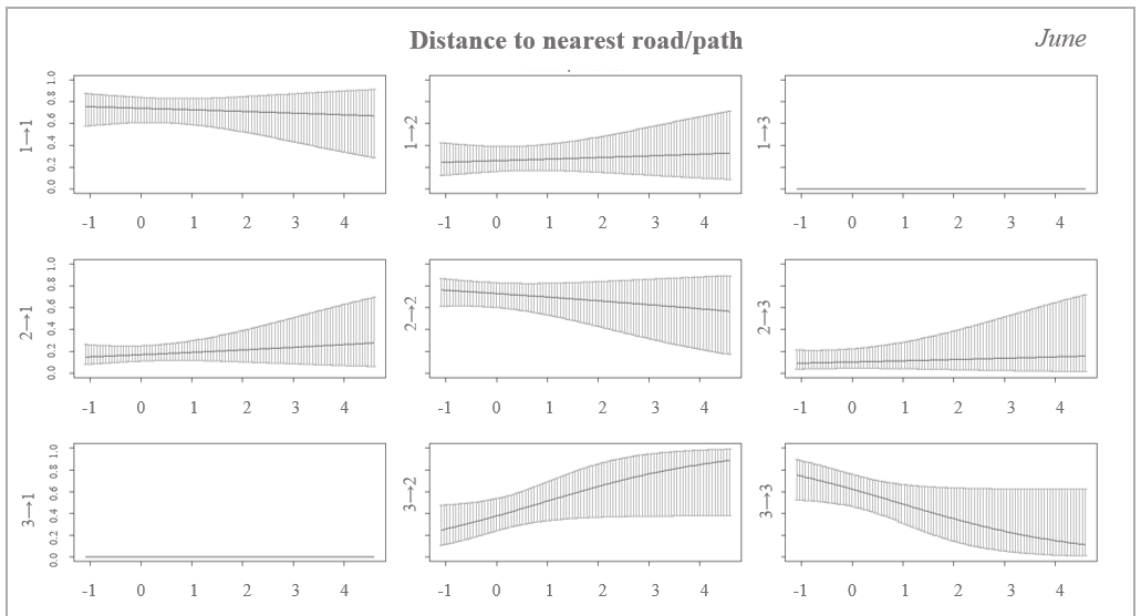


**Figure 6.** Graph showing transition probabilities under the influence of distance to nearest road/path as a covariate in June, between state 1 and 2 ( $1 \rightarrow 2$ ), state 1 and 3 ( $1 \rightarrow 3$ ), state 2 and 1 ( $2 \rightarrow 1$ ), state 2 and 3 ( $2 \rightarrow 3$ ), state 3 and 1 ( $3 \rightarrow 1$ ), and state 3 and 2 ( $3 \rightarrow 2$ ). The graph also shows persistence probabilities in state 1 ( $1 \rightarrow 1$ ), state 2 ( $2 \rightarrow 2$ ) and in state 3 ( $3 \rightarrow 3$ ).

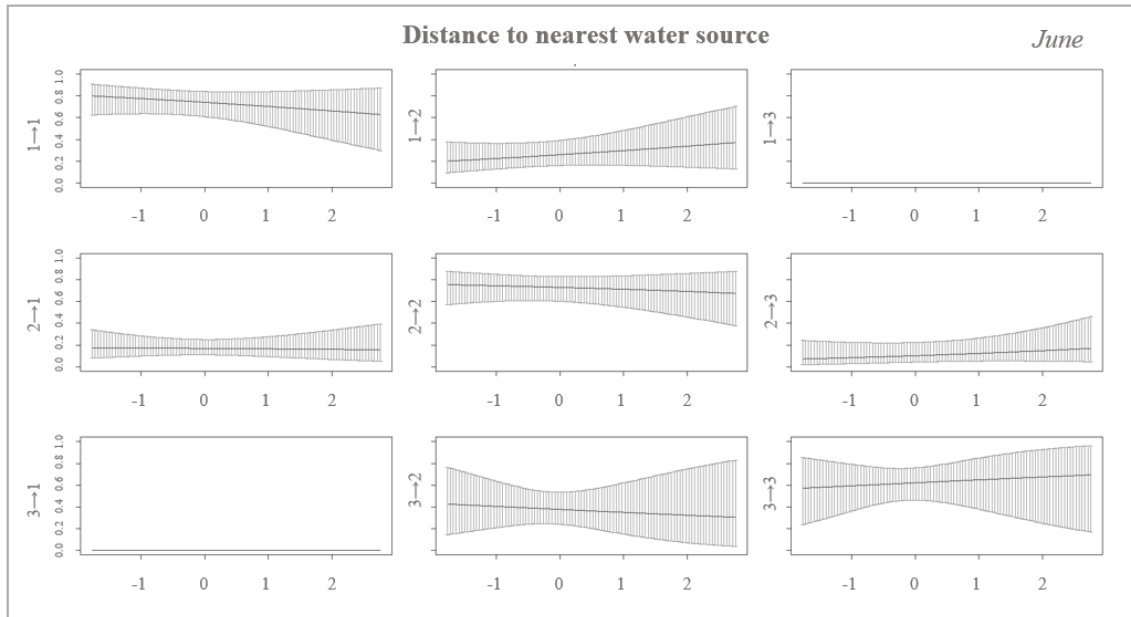


**Figure 7.** Graph showing transition probabilities under the influence of distance to nearest water source as a covariate in June, between state 1 and 2 ( $1 \rightarrow 2$ ), state 1 and 3 ( $1 \rightarrow 3$ ), state 2 and 1 ( $2 \rightarrow 1$ ), state 2 and 3 ( $2 \rightarrow 3$ ), state 3 and 1 ( $3 \rightarrow 1$ ), and state 3 and 2 ( $3 \rightarrow 2$ ). The graph also shows persistence probabilities in state 1 ( $1 \rightarrow 1$ ), state 2 ( $2 \rightarrow 2$ ) and in state 3 ( $3 \rightarrow 3$ ).

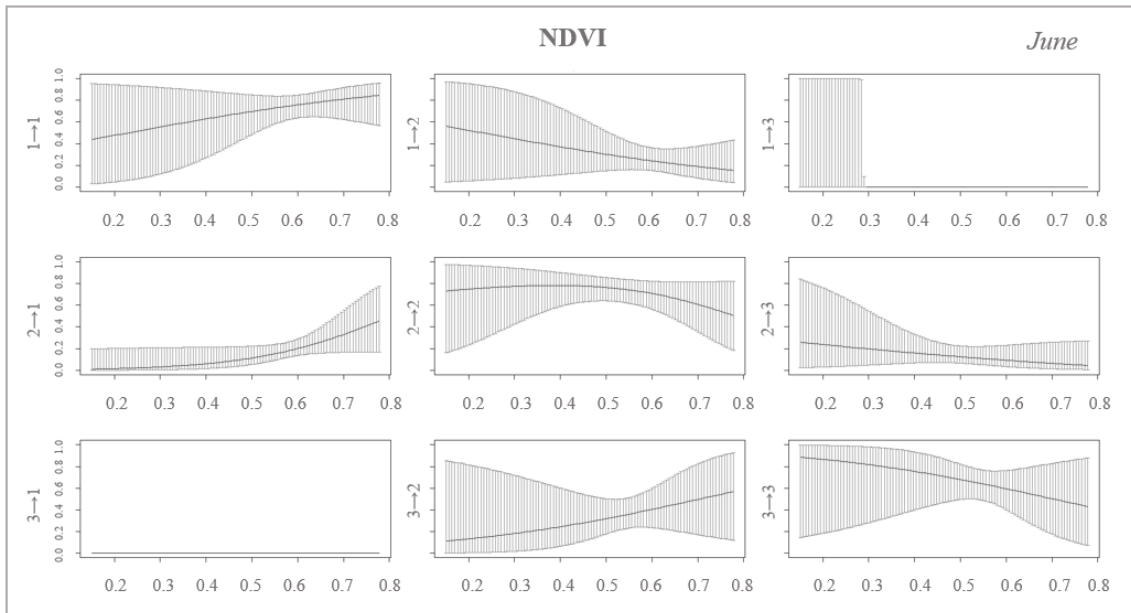


**Figure 8.** Graph showing transition probabilities under the influence of NDVI as a covariate in June, between state 1 and 2 ( $1 \rightarrow 2$ ), state 1 and 3 ( $1 \rightarrow 3$ ), state 2 and 1 ( $2 \rightarrow 1$ ), state 2 and 3 ( $2 \rightarrow 3$ ), state 3 and 1 ( $3 \rightarrow 1$ ), and state 3 and 2 ( $3 \rightarrow 2$ ). The graph also shows persistence probabilities in state 1 ( $1 \rightarrow 1$ ), state 2 ( $2 \rightarrow 2$ ) and in state 3 ( $3 \rightarrow 3$ ).

In July (Table 6, Fig. 9-12), Elza presented a tendency to move into state 1 as the terrain was rougher ( $3 \rightarrow 1 = +0.93$ ), into state 2 as the distance to the nearest road/path increased ( $3 \rightarrow 2 = +0.80$ ), and into state 3 as the furthest from water sources ( $1 \rightarrow 3 = +0.21$  and  $2 \rightarrow 3 = +0.29$ ). Under the influence of the NDVI, the  $2 \rightarrow 1$  transition showed a slightly negative value (-0.89); however, a substantially positive value was recorded for the  $3 \rightarrow 1$  switching probability (+9.68), which meant that a large NDVI value promoted the transition. A high probability of persistence in state 3 was indicated at the shortest distance from the road/path (Fig. 10).

**Table 6.** Regression coefficients for the transition probabilities referred to the month of July. The table shows the probability of transition between state 1 and 2 ( $1 \rightarrow 2$ ), state 1 and 3 ( $1 \rightarrow 3$ ), state 2 and 1 ( $2 \rightarrow 1$ ), state 2 and 3 ( $2 \rightarrow 3$ ), state 3 and 1 ( $3 \rightarrow 1$ ), and state 3 and 2 ( $3 \rightarrow 2$ ). The first row indicates the baseline probability of transition when all the covariates are set to zero. From the second to the fifth row, 4 different covariates and their influence on the transition probabilities are shown.

	Regression coefficients for the transition probabilities						July
	$1 \rightarrow 2$	$1 \rightarrow 3$	$2 \rightarrow 1$	$2 \rightarrow 3$	$3 \rightarrow 1$	$3 \rightarrow 2$	
Intercept	0.193	-12.159	-0.920	-0.548	-13.793	-0.570	
Terrain roughness	-0.416	-1.215	-0.038	-0.064	0.931	0.999	
Min. road/path distance	-0.135	-0.577	-0.048	-0.517	-1.975	0.805	
Min. water source distance	-0.077	0.213	-0.160	0.298	-3.568	0.083	
NDVI	-2.946	-5.539	-0.893	-1.904	9.684	-0.258	



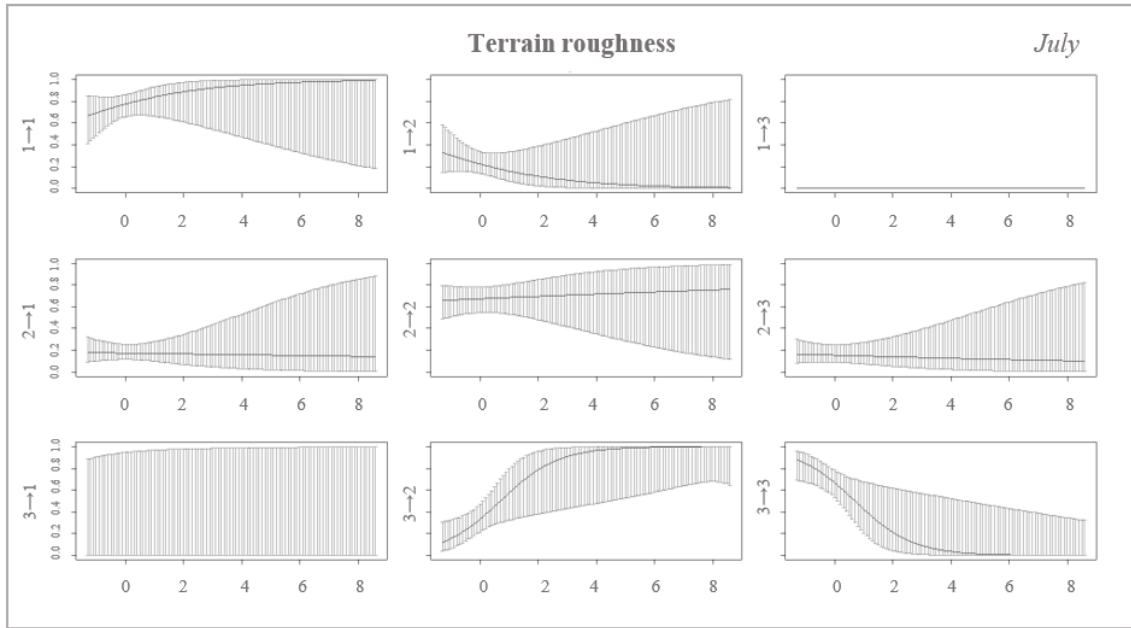


**Figure 9.** Graph showing transition probabilities under the influence of terrain roughness as a covariate in July, between state 1 and 2 ( $1 \rightarrow 2$ ), state 1 and 3 ( $1 \rightarrow 3$ ), state 2 and 1 ( $2 \rightarrow 1$ ), state 2 and 3 ( $2 \rightarrow 3$ ), state 3 and 1 ( $3 \rightarrow 1$ ), and state 3 and 2 ( $3 \rightarrow 2$ ). The graph also shows persistence probabilities in state 1 ( $1 \rightarrow 1$ ), state 2 ( $2 \rightarrow 2$ ) and in state 3 ( $3 \rightarrow 3$ ).

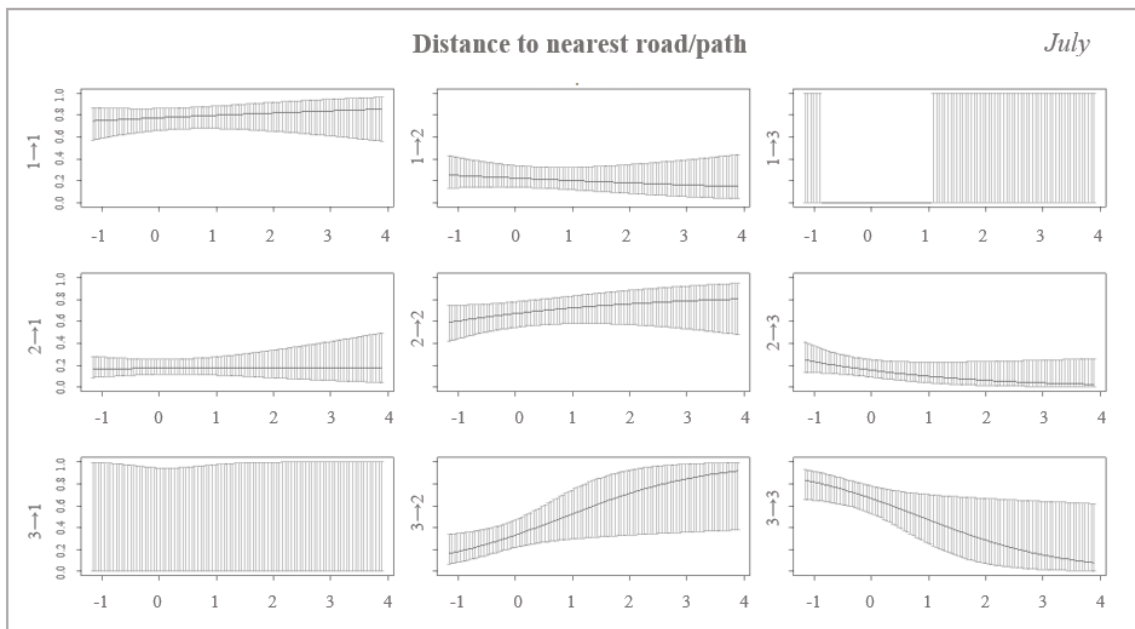


**Figure 10.** Graph showing transition probabilities under the influence of distance to nearest road/path as a covariate in July, between state 1 and 2 ( $1 \rightarrow 2$ ), state 1 and 3 ( $1 \rightarrow 3$ ), state 2 and 1 ( $2 \rightarrow 1$ ), state 2 and 3 ( $2 \rightarrow 3$ ), state 3 and 1 ( $3 \rightarrow 1$ ), and state 3 and 2 ( $3 \rightarrow 2$ ). The graph also shows persistence probabilities in state 1 ( $1 \rightarrow 1$ ), state 2 ( $2 \rightarrow 2$ ) and in state 3 ( $3 \rightarrow 3$ ).

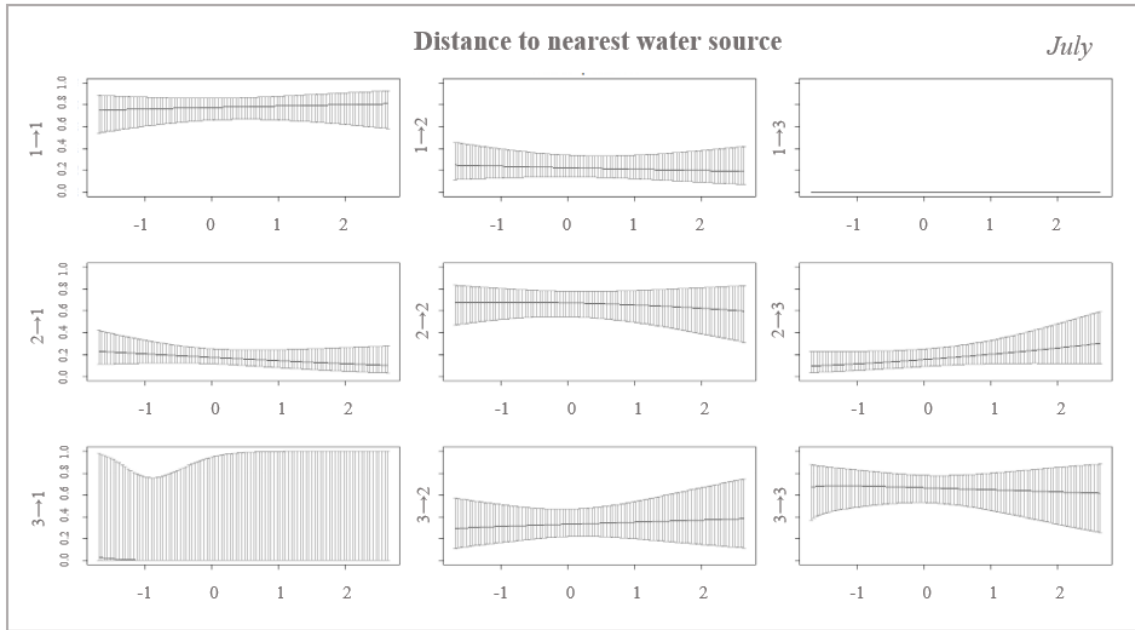


**Figure 11.** Graph showing transition probabilities under the influence of distance to nearest water source as a covariate in July, between state 1 and 2 ( $1 \rightarrow 2$ ), state 1 and 3 ( $1 \rightarrow 3$ ), state 2 and 1 ( $2 \rightarrow 1$ ), state 2 and 3 ( $2 \rightarrow 3$ ), state 3 and 1 ( $3 \rightarrow 1$ ), and state 3 and 2 ( $3 \rightarrow 2$ ). The graph also shows persistence probabilities in state 1 ( $1 \rightarrow 1$ ), state 2 ( $2 \rightarrow 2$ ) and in state 3 ( $3 \rightarrow 3$ ).

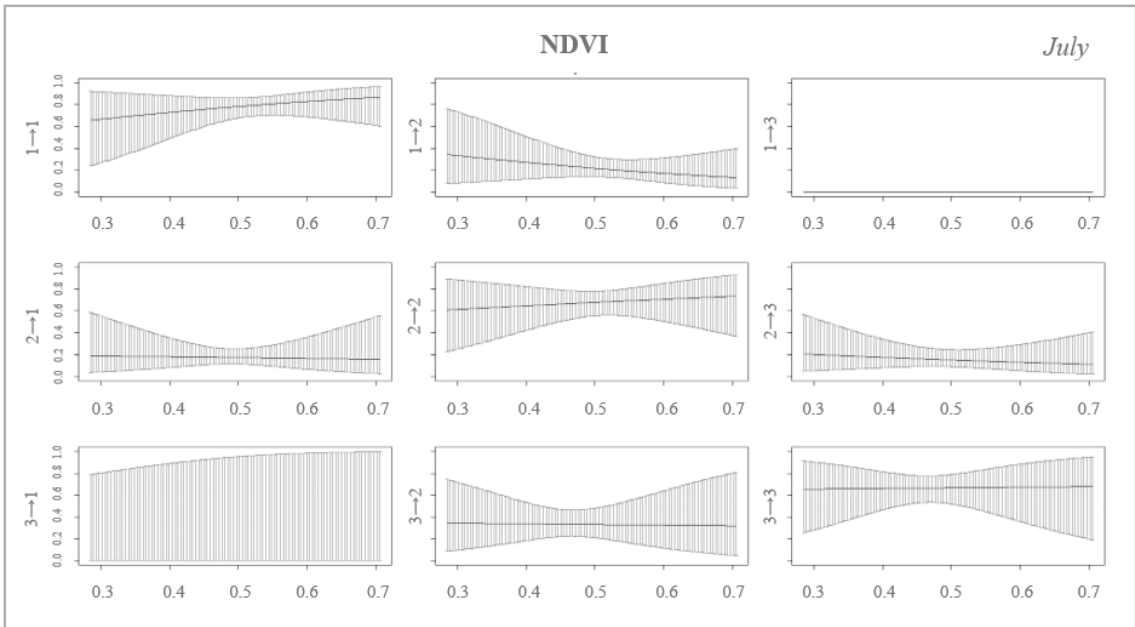


**Figure 12.** Graph showing transition probabilities under the influence of NDVI as a covariate in July, between state 1 and 2 ( $1 \rightarrow 2$ ), state 1 and 3 ( $1 \rightarrow 3$ ), state 2 and 1 ( $2 \rightarrow 1$ ), state 2 and 3 ( $2 \rightarrow 3$ ), state 3 and 1 ( $3 \rightarrow 1$ ), and state 3 and 2 ( $3 \rightarrow 2$ ). The graph also shows persistence probabilities in state 1 ( $1 \rightarrow 1$ ), state 2 ( $2 \rightarrow 2$ ) and in state 3 ( $3 \rightarrow 3$ ).

In August (Table 7, Fig. 13-16), when the road predictive variable was set, Elza recorded both positive and negative values, although all very close to zero. In contrast, during the same month, strongly positive values were observed for  $2 \rightarrow 1$  and  $3 \rightarrow 2$  transition probabilities (+11.94 and +20.03, respectively) as the NDVI value increased (Table 7). Additionally, when it was far from the road, Elza was less likely to persist in state 2 (Fig.14); furthermore, it stayed in state 1 when it was closer to the water (Fig.15). Under the influence of the NDVI variable, Elza was likely to be found in state 3 at a low NDVI value (Fig.16).

**Table 7.** Regression coefficients for the transition probabilities referred to the month of August. The table shows the probability of transition between state 1 and 2 ( $1 \rightarrow 2$ ), state 1 and 3 ( $1 \rightarrow 3$ ), state 2 and 1 ( $2 \rightarrow 1$ ), state 2 and 3 ( $2 \rightarrow 3$ ), state 3 and 1 ( $3 \rightarrow 1$ ), and state 3 and 2 ( $3 \rightarrow 2$ ). The first row indicates the baseline probability of transition when all the covariates are set to zero. From the second to the fifth row, 4 different covariates and their influence on the transition probabilities are shown.

	Regression coefficients for the transition probabilities					August
	$1 \rightarrow 2$	$1 \rightarrow 3$	$2 \rightarrow 1$	$2 \rightarrow 3$	$3 \rightarrow 1$	$3 \rightarrow 2$
Intercept	-0.638	-3.041	-5.672	-0.306	-5.344	-9.230
Terrain roughness	-0.284	-0.203	-0.254	0.347	0.271	-0.045
Min. road/path distance	-0.198	-0.189	-0.141	0.366	0.106	0.160
Min. water source distance	0.114	0.404	-0.206	0.015	0.613	-1.868
NDVI	-2.904	3.072	11.948	-4.643	8.069	20.032

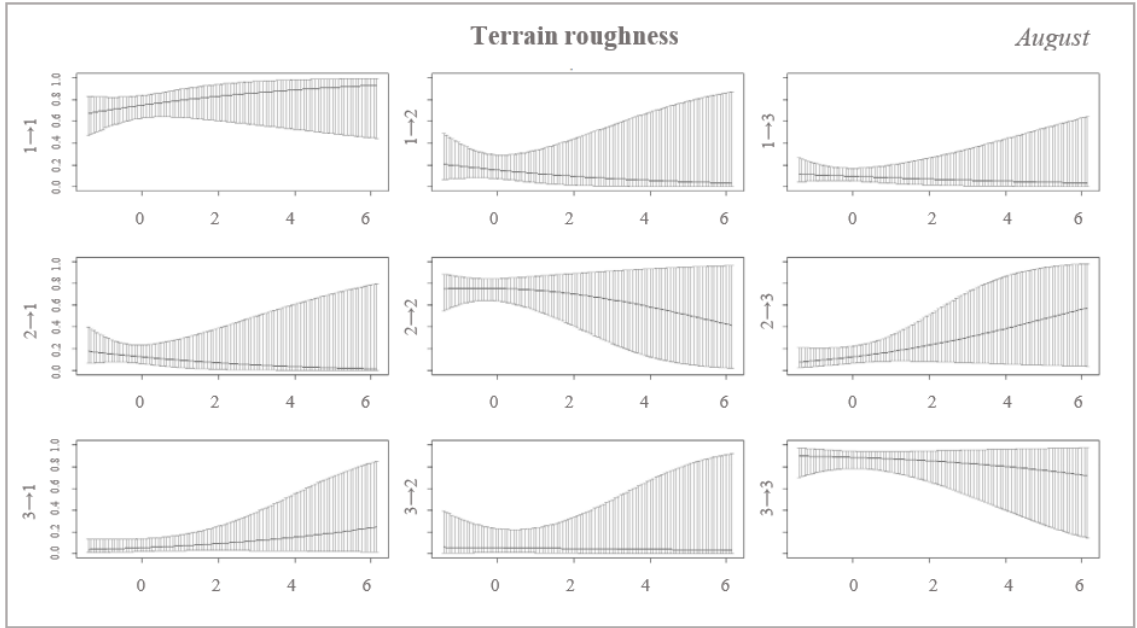


**Figure 13.** Graph showing transition probabilities under the influence of terrain roughness as a covariate in August, between state 1 and 2 ( $1 \rightarrow 2$ ), state 1 and 3 ( $1 \rightarrow 3$ ), state 2 and 1 ( $2 \rightarrow 1$ ), state 2 and 3 ( $2 \rightarrow 3$ ), state 3 and 1 ( $3 \rightarrow 1$ ), and state 3 and 2 ( $3 \rightarrow 2$ ). The graph also shows persistence probabilities in state 1 ( $1 \rightarrow 1$ ), state 2 ( $2 \rightarrow 2$ ) and in state 3 ( $3 \rightarrow 3$ ).

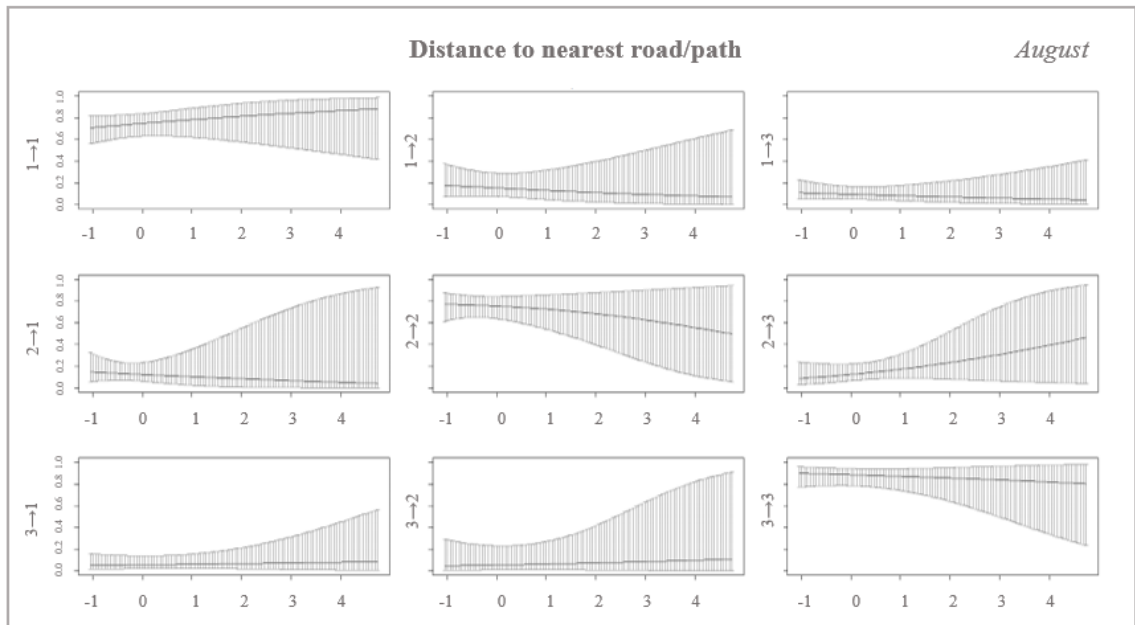


**Figure 14.** Graph showing transition probabilities under the influence of distance to nearest road/path as a covariate in August, between state 1 and 2 ( $1 \rightarrow 2$ ), state 1 and 3 ( $1 \rightarrow 3$ ), state 2 and 1 ( $2 \rightarrow 1$ ), state 2 and 3 ( $2 \rightarrow 3$ ), state 3 and 1 ( $3 \rightarrow 1$ ), and state 3 and 2 ( $3 \rightarrow 2$ ). The graph also shows persistence probabilities in state 1 ( $1 \rightarrow 1$ ), state 2 ( $2 \rightarrow 2$ ) and in state 3 ( $3 \rightarrow 3$ ).

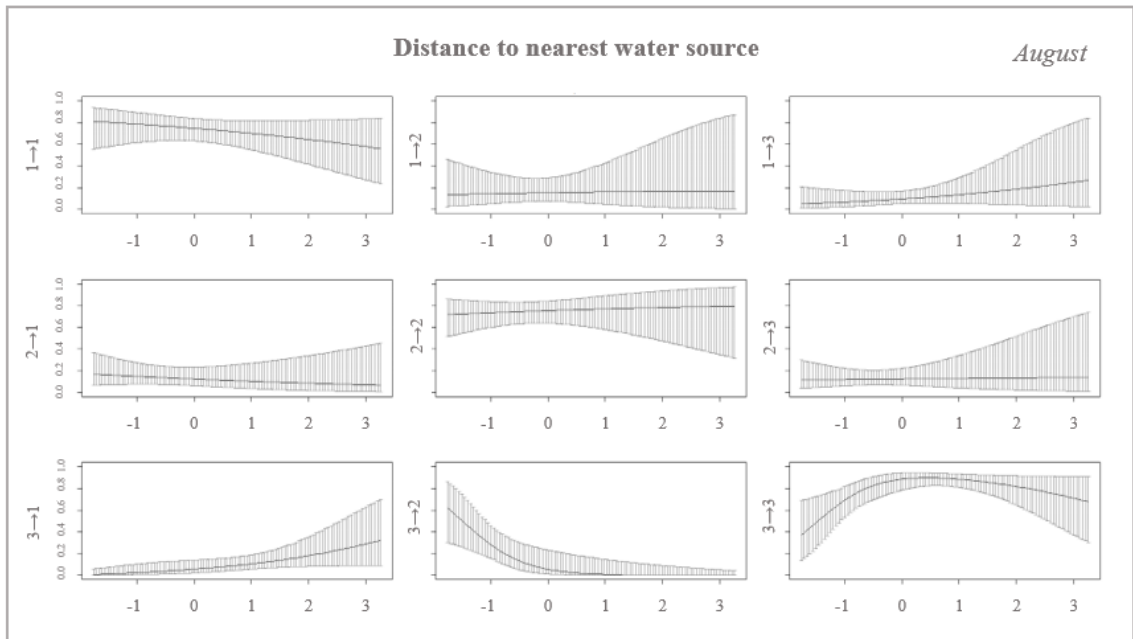


**Figure 15.** Graph showing transition probabilities under the influence of distance to nearest water source as a covariate in August, between state 1 and 2 ( $1 \rightarrow 2$ ), state 1 and 3 ( $1 \rightarrow 3$ ), state 2 and 1 ( $2 \rightarrow 1$ ), state 2 and 3 ( $2 \rightarrow 3$ ), state 3 and 1 ( $3 \rightarrow 1$ ), and state 3 and 2 ( $3 \rightarrow 2$ ). The graph also shows persistence probabilities in state 1 ( $1 \rightarrow 1$ ), state 2 ( $2 \rightarrow 2$ ) and in state 3 ( $3 \rightarrow 3$ ).

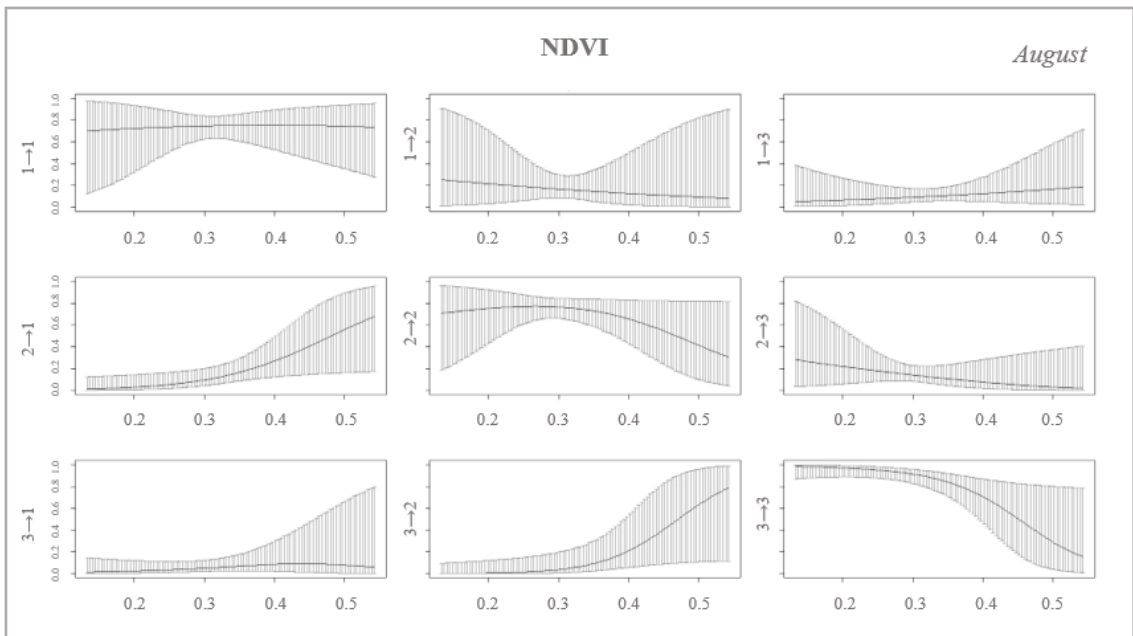


**Figure 16.** Graph showing transition probabilities under the influence of NDVI as a covariate in August, between state 1 and 2 ( $1 \rightarrow 2$ ), state 1 and 3 ( $1 \rightarrow 3$ ), state 2 and 1 ( $2 \rightarrow 1$ ), state 2 and 3 ( $2 \rightarrow 3$ ), state 3 and 1 ( $3 \rightarrow 1$ ), and state 3 and 2 ( $3 \rightarrow 2$ ). The graph also shows persistence probabilities in state 1 ( $1 \rightarrow 1$ ), state 2 ( $2 \rightarrow 2$ ) and in state 3 ( $3 \rightarrow 3$ ).

September (Table 8, Fig.13-16) showed extremely high values of  $2 \rightarrow 1$  (+31.50) under the influence of the NDVI (Fig.16). In support of the latter result, Elza persisted in state 2 when at the lowest NDVI values (Fig.16). Regarding the distance from the road, the  $3 \rightarrow 1$  transition was significantly inhibited (-6.00) as the distance from the nearest road increased (Table 8). As evidence, persistence in state 1 was more likely to occur as close to the road as possible (Fig.14). When setting the terrain roughness as a covariate, the  $3 \rightarrow 1$  transition was promoted as the roughness increased (+1.73). Persistence in state 2 was more likely to occur near water sources.

**Table 8.** Regression coefficients for the transition probabilities referred to the month of September. The table shows the probability of transition between state 1 and 2 ( $1 \rightarrow 2$ ), state 1 and 3 ( $1 \rightarrow 3$ ), state 2 and 1 ( $2 \rightarrow 1$ ), state 2 and 3 ( $2 \rightarrow 3$ ), state 3 and 1 ( $3 \rightarrow 1$ ), and state 3 and 2 ( $3 \rightarrow 2$ ). The first row indicates the baseline probability of transition when all the covariates are set to zero. From the second to the fifth row, 4 different covariates and their influence on the transition probabilities are shown.

	Regression coefficients for the transition probabilities						September
	$1 \rightarrow 2$	$1 \rightarrow 3$	$2 \rightarrow 1$	$2 \rightarrow 3$	$3 \rightarrow 1$	$3 \rightarrow 2$	
Intercept	17.761	2.451	-11.419	-2.966	-24.425	-4.667	
Terrain roughness	-0.250	0.053	0.076	0.133	1.736	-0.272	
Min. road/path distance	-2.294	0.129	-0.486	0.052	-6.008	-0.117	
Min. water source distance	0.196	0.125	0.535	0.635	0.318	-0.158	
NDVI	-63.557	-9.996	31.507	2.559	-6.257	10.131	

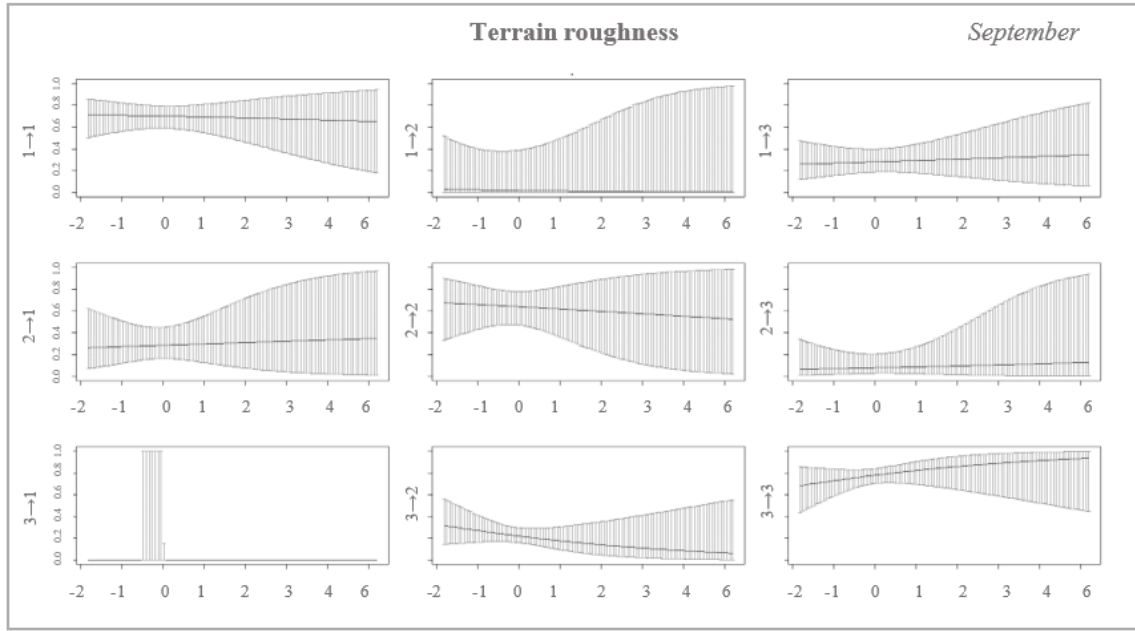


**Figure 17.** Graph showing transition probabilities under the influence of terrain roughness as a covariate in September, between state 1 and 2 ( $1 \rightarrow 2$ ), state 1 and 3 ( $1 \rightarrow 3$ ), state 2 and 1 ( $2 \rightarrow 1$ ), state 2 and 3 ( $2 \rightarrow 3$ ), state 3 and 1 ( $3 \rightarrow 1$ ), and state 3 and 2 ( $3 \rightarrow 2$ ). The graph also shows persistence probabilities in state 1 ( $1 \rightarrow 1$ ), state 2 ( $2 \rightarrow 2$ ) and in state 3 ( $3 \rightarrow 3$ ).

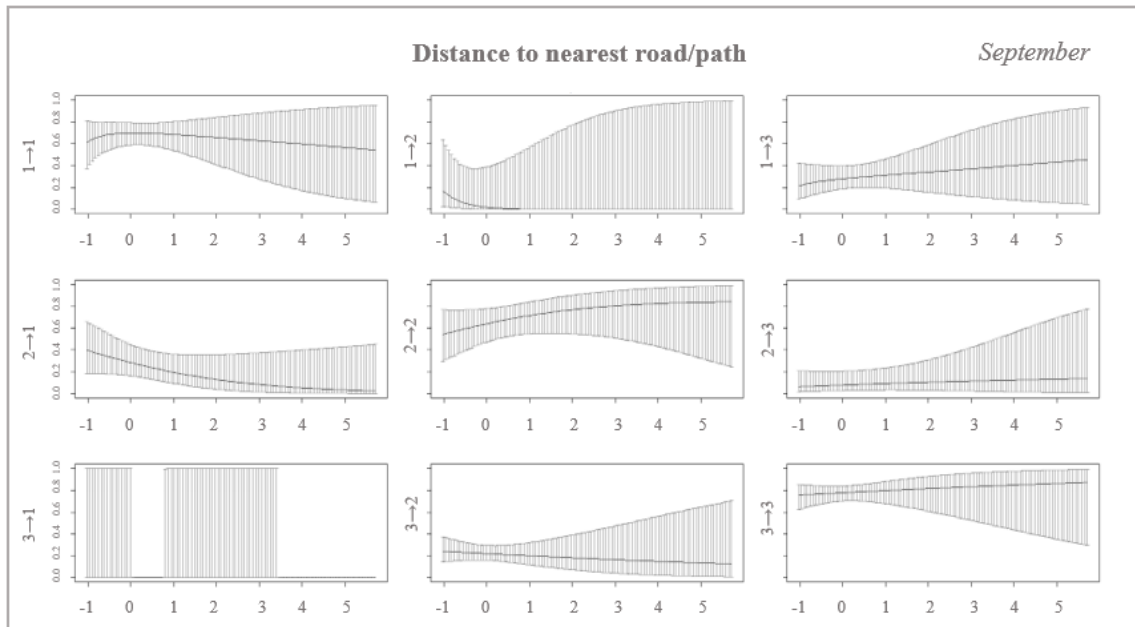


**Figure 18.** Graph showing transition probabilities under the influence of distance to nearest road/path as a covariate in September, between state 1 and 2 ( $1 \rightarrow 2$ ), state 1 and 3 ( $1 \rightarrow 3$ ), state 2 and 1 ( $2 \rightarrow 1$ ), state 2 and 3 ( $2 \rightarrow 3$ ), state 3 and 1 ( $3 \rightarrow 1$ ), and state 3 and 2 ( $3 \rightarrow 2$ ). The graph also shows persistence probabilities in state 1 ( $1 \rightarrow 1$ ), state 2 ( $2 \rightarrow 2$ ) and in state 3 ( $3 \rightarrow 3$ ).

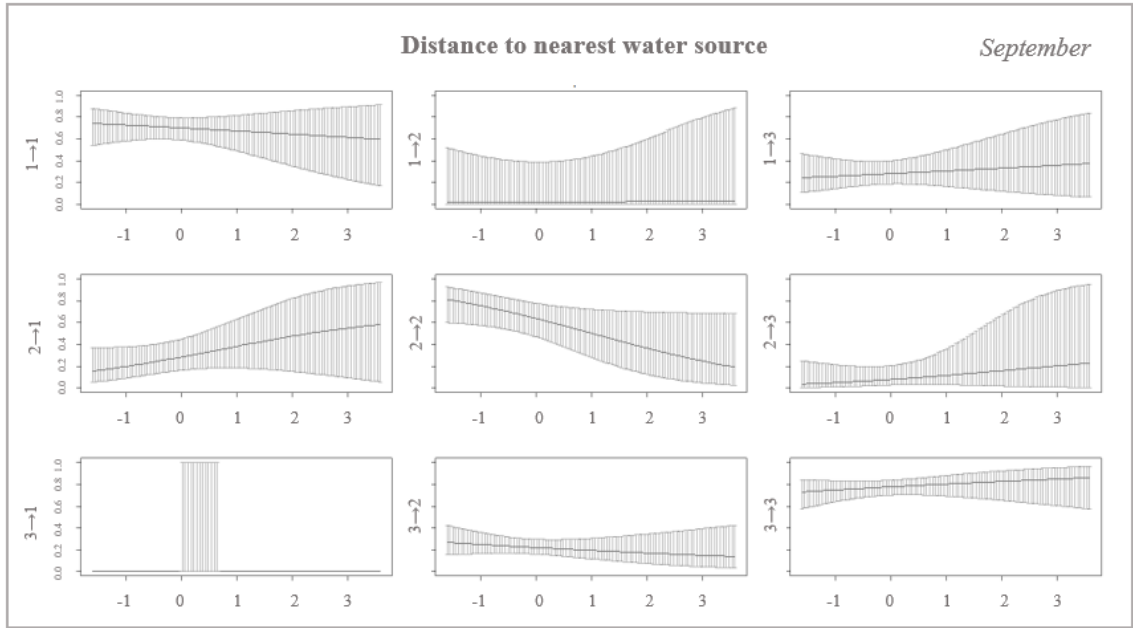


**Figure 19.** Graph showing transition probabilities under the influence of distance to nearest water source as a covariate in September, between state 1 and 2 ( $1 \rightarrow 2$ ), state 1 and 3 ( $1 \rightarrow 3$ ), state 2 and 1 ( $2 \rightarrow 1$ ), state 2 and 3 ( $2 \rightarrow 3$ ), state 3 and 1 ( $3 \rightarrow 1$ ), and state 3 and 2 ( $3 \rightarrow 2$ ). The graph also shows persistence probabilities in state 1 ( $1 \rightarrow 1$ ), state 2 ( $2 \rightarrow 2$ ) and in state 3 ( $3 \rightarrow 3$ ).

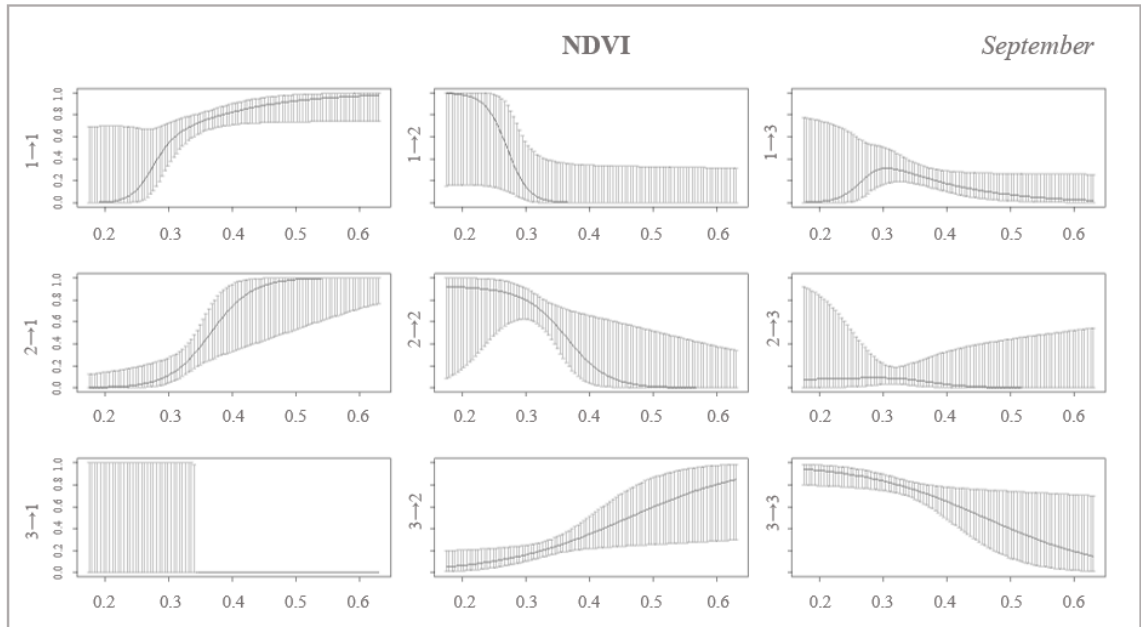


**Figure 20.** Graph showing transition probabilities under the influence of NDVI as a covariate in September, between state 1 and 2 ( $1 \rightarrow 2$ ), state 1 and 3 ( $1 \rightarrow 3$ ), state 2 and 1 ( $2 \rightarrow 1$ ), state 2 and 3 ( $2 \rightarrow 3$ ), state 3 and 1 ( $3 \rightarrow 1$ ), and state 3 and 2 ( $3 \rightarrow 2$ ). The graph also shows persistence probabilities in state 1 ( $1 \rightarrow 1$ ), state 2 ( $2 \rightarrow 2$ ) and in state 3 ( $3 \rightarrow 3$ ).



In October (Table 9, Fig.21-24), when NDVI or distance from the road were set as covariates (Fig.22,24), Elza was more likely to be in state 1 (+33.56) as the former increased and the latter at a minimum value. Contrastingly, this month recorded an opposite trend in transition probabilities when terrain roughness was set as a covariate, showing a high probability of persisting in state 1 at the lowest value of roughness (Table 9, Fig.21). Regarding the predictor variable of distance to the nearest water source, the  $1 \rightarrow 2$  switching probability was more probable to occur near the water (Fig.23).

**Table 9.** Regression coefficients for the transition probabilities referred to the month of October. The table shows the probability of transition between state 1 and 2 ( $1 \rightarrow 2$ ), state 1 and 3 ( $1 \rightarrow 3$ ), state 2 and 1 ( $2 \rightarrow 1$ ), state 2 and 3 ( $2 \rightarrow 3$ ), state 3 and 1 ( $3 \rightarrow 1$ ), and state 3 and 2 ( $3 \rightarrow 2$ ). The first row indicates the baseline probability of transition when all the covariates are set to zero. From the second to the fifth row, 4 different covariates and their influence on the transition probabilities are shown.

	Regression coefficients for the transition probabilities					October
	$1 \rightarrow 2$	$1 \rightarrow 3$	$2 \rightarrow 1$	$2 \rightarrow 3$	$3 \rightarrow 1$	$3 \rightarrow 2$
Intercept	0.195	12.604	-3.924	-3.712	-12.971	-9.022
Terrain roughness	3.458	-1.751	0.359	-0.350	0.286	-0.159
Min. road/path distance	-0.636	2.494	-1.537	-0.363	-0.051	-0.313
Min. water source distance	-4.016	-0.166	-0.962	0.127	-0.330	-0.239
NDVI	-13.550	-45.985	0.534	4.238	33.561	23.391

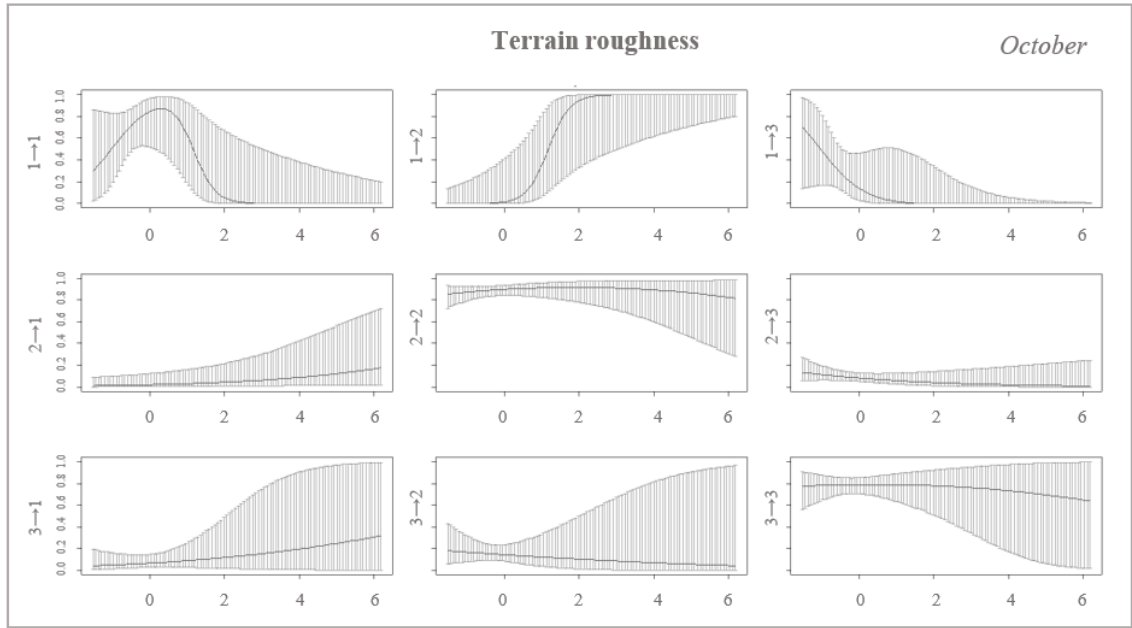


**Figure 21.** Graph showing transition probabilities under the influence of terrain roughness as a covariate in October, between state 1 and 2 ( $1 \rightarrow 2$ ), state 1 and 3 ( $1 \rightarrow 3$ ), state 2 and 1 ( $2 \rightarrow 1$ ), state 2 and 3 ( $2 \rightarrow 3$ ), state 3 and 1 ( $3 \rightarrow 1$ ), and state 3 and 2 ( $3 \rightarrow 2$ ). The graph also shows persistence probabilities in state 1 ( $1 \rightarrow 1$ ), state 2 ( $2 \rightarrow 2$ ) and in state 3 ( $3 \rightarrow 3$ ).

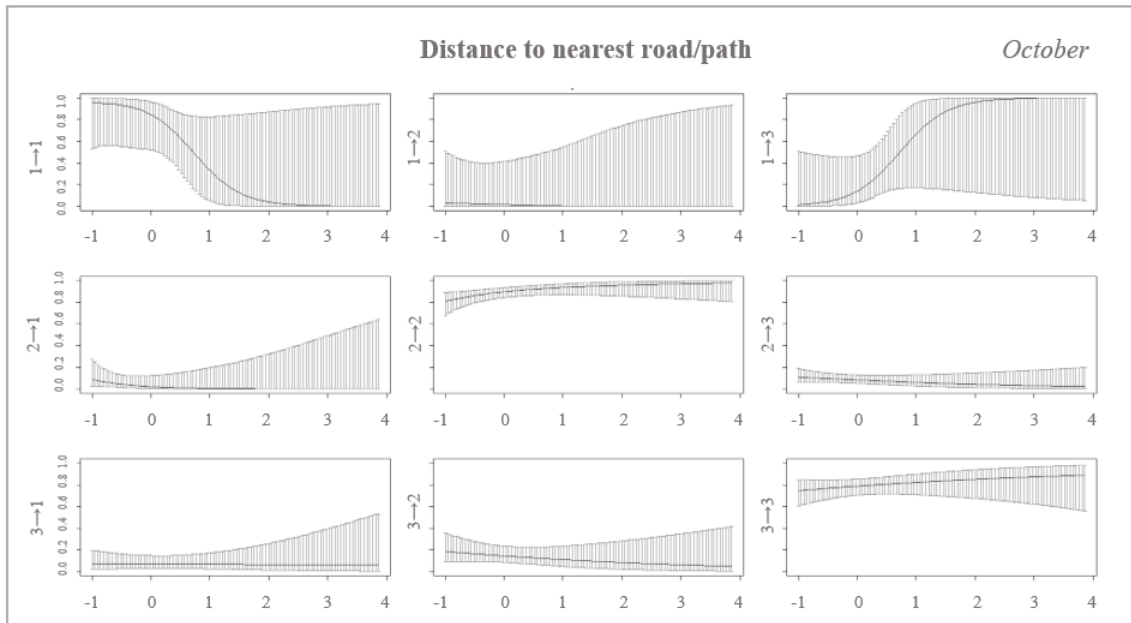


**Figure 22.** Graph showing transition probabilities under the influence of distance to nearest road/path as a covariate in October, between state 1 and 2 ( $1 \rightarrow 2$ ), state 1 and 3 ( $1 \rightarrow 3$ ), state 2 and 1 ( $2 \rightarrow 1$ ), state 2 and 3 ( $2 \rightarrow 3$ ), state 3 and 1 ( $3 \rightarrow 1$ ), and state 3 and 2 ( $3 \rightarrow 2$ ). The graph also shows persistence probabilities in state 1 ( $1 \rightarrow 1$ ), state 2 ( $2 \rightarrow 2$ ) and in state 3 ( $3 \rightarrow 3$ ).

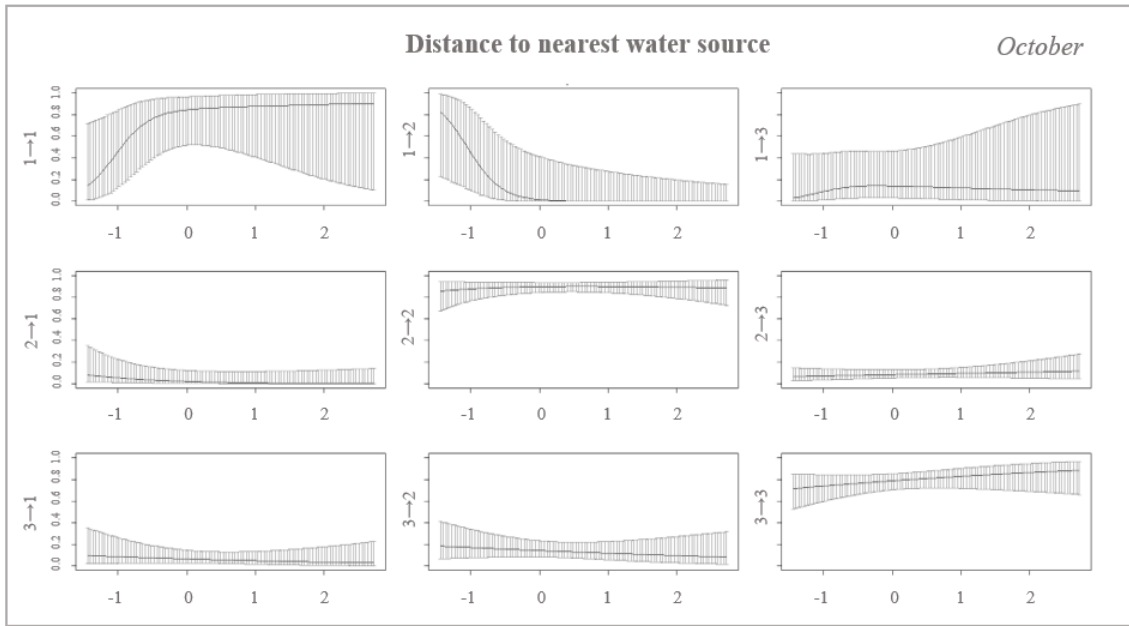


**Figure 23.** Graph showing transition probabilities under the influence of distance to nearest water source as a covariate in October, between state 1 and 2 ( $1 \rightarrow 2$ ), state 1 and 3 ( $1 \rightarrow 3$ ), state 2 and 1 ( $2 \rightarrow 1$ ), state 2 and 3 ( $2 \rightarrow 3$ ), state 3 and 1 ( $3 \rightarrow 1$ ), and state 3 and 2 ( $3 \rightarrow 2$ ). The graph also shows persistence probabilities in state 1 ( $1 \rightarrow 1$ ), state 2 ( $2 \rightarrow 2$ ) and in state 3 ( $3 \rightarrow 3$ ).

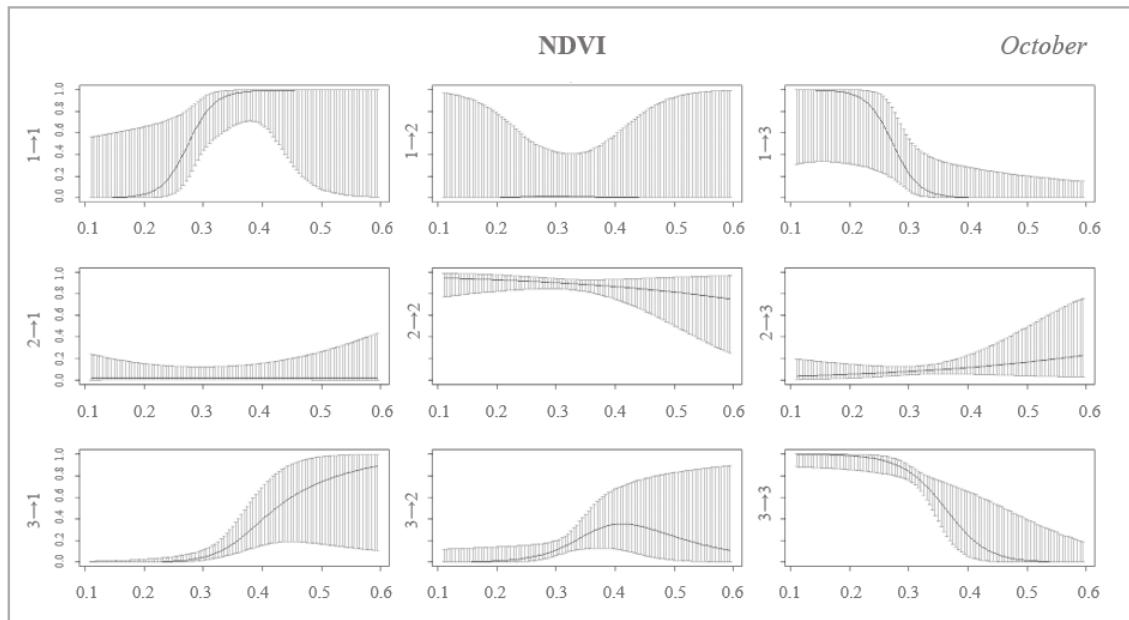


**Figure 24.** Graph showing transition probabilities under the influence of NDVI as a covariate in October, between state 1 and 2 ( $1 \rightarrow 2$ ), state 1 and 3 ( $1 \rightarrow 3$ ), state 2 and 1 ( $2 \rightarrow 1$ ), state 2 and 3 ( $2 \rightarrow 3$ ), state 3 and 1 ( $3 \rightarrow 1$ ), and state 3 and 2 ( $3 \rightarrow 2$ ). The graph also shows persistence probabilities in state 1 ( $1 \rightarrow 1$ ), state 2 ( $2 \rightarrow 2$ ) and in state 3 ( $3 \rightarrow 3$ ).

Between November and December, the only two months belonging to the wet season, the results of the transition probabilities followed almost the same patterns for both (Table 10-11, Fig.25-32): a high probability of remaining in state 2 as the terrain was rougher (Fig.25-26); an elevated likelihood of persisting in states 1 and 2 near water and switch into state 3 when the distance from it increased (Fig.29-30); a higher probability of staying in state 3 at a lower NDVI value, moving to state 2, and then to state 1, as the greenness increased (Fig.31-32); and a discrete likelihood of remaining in state 2 when distant from road (Fig.27-28).

**Table 10.** Regression coefficients for the transition probabilities referred to the month of November. The table shows the probability of transition between state 1 and 2 (1→2), state 1 and 3 (1→3), state 2 and 1 (2→1), state 2 and 3 (2→3), state 3 and 1 (3→1), and state 3 and 2 (3→2). The first row indicates the baseline probability of transition when all the covariates are set to zero. From the second to the fifth row, 4 different covariates and their influence on the transition probabilities are shown.

	Regression coefficients for the transition probabilities						November
	1→2	1→3	2→1	2→3	3→1	3→2	
Intercept	-1.722	-37.559	-8.057	-2.799	-27.154	-4.848	
Terrain roughness	-0.172	-1.745	-0.118	-1.512	-10.641	-0.110	
Min. road/path distance	0.125	3.618	-0.125	0.202	0.625	0.339	
Min. water source distance	-0.082	-0.650	-0.090	0.399	-7.341	-0.694	
NDVI	0.562	-20.944	11.299	0.904	-9.960	8.594	

**Table 11.** Regression coefficients for the transition probabilities referred to the month of December. The table shows the probability of transition between state 1 and 2 ( $1 \rightarrow 2$ ), state 1 and 3 ( $1 \rightarrow 3$ ), state 2 and 1 ( $2 \rightarrow 1$ ), state 2 and 3 ( $2 \rightarrow 3$ ), state 3 and 1 ( $3 \rightarrow 1$ ), and state 3 and 2 ( $3 \rightarrow 2$ ). The first row indicates the baseline probability of transition when all the covariates are set to zero. From the second to the fifth row, 4 different covariates and their influence on the transition probabilities are shown.

	Regression coefficients for the transition probabilities						December
	$1 \rightarrow 2$	$1 \rightarrow 3$	$2 \rightarrow 1$	$2 \rightarrow 3$	$3 \rightarrow 1$	$3 \rightarrow 2$	
Intercept	2.388	14.848	-1.833	-2.405	-481.931	-2.087	
Terrain roughness	0.375	-797.052	0.071	-0.317	-40.518	0.301	
Min. road/path distance	-0.165	-122.262	-0.082	0.039	10.639	0.009	
Min. water source distance	0.011	-241.173	0.142	0.753	-40.660	-0.117	
NDVI	-5.153	-2211.85	0.859	0.572	-291.208	2.015	

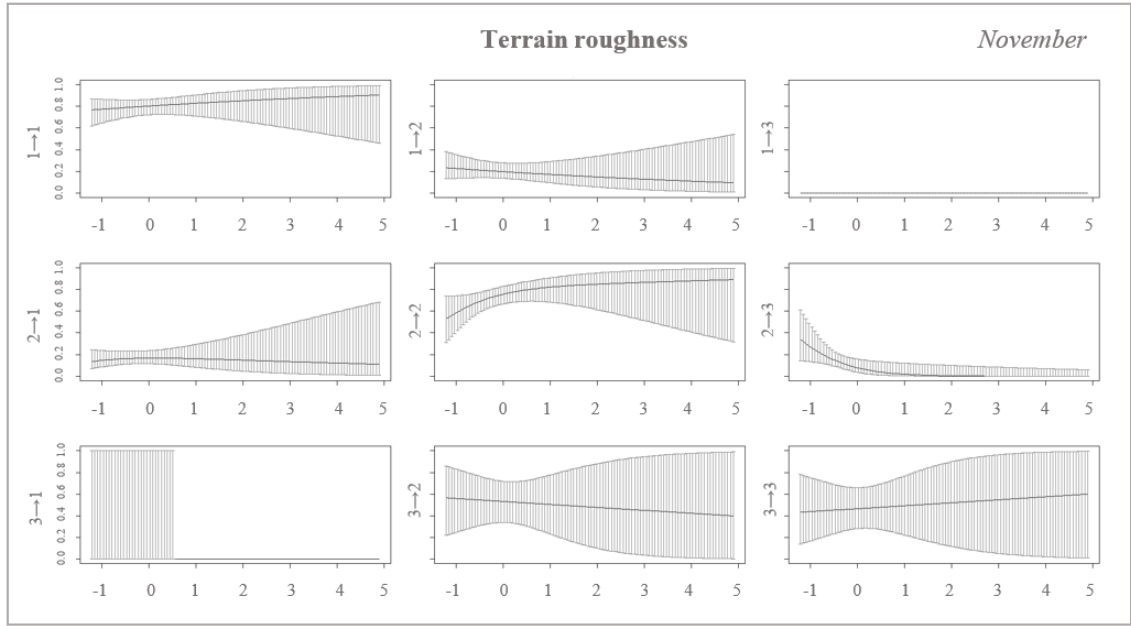


**Figure 25.** Graph showing transition probabilities under the influence of terrain roughness as a covariate in November, between state 1 and 2 ( $1 \rightarrow 2$ ), state 1 and 3 ( $1 \rightarrow 3$ ), state 2 and 1 ( $2 \rightarrow 1$ ), state 2 and 3 ( $2 \rightarrow 3$ ), state 3 and 1 ( $3 \rightarrow 1$ ), and state 3 and 2 ( $3 \rightarrow 2$ ). The graph also shows persistence probabilities in state 1 ( $1 \rightarrow 1$ ), state 2 ( $2 \rightarrow 2$ ) and in state 3 ( $3 \rightarrow 3$ ).

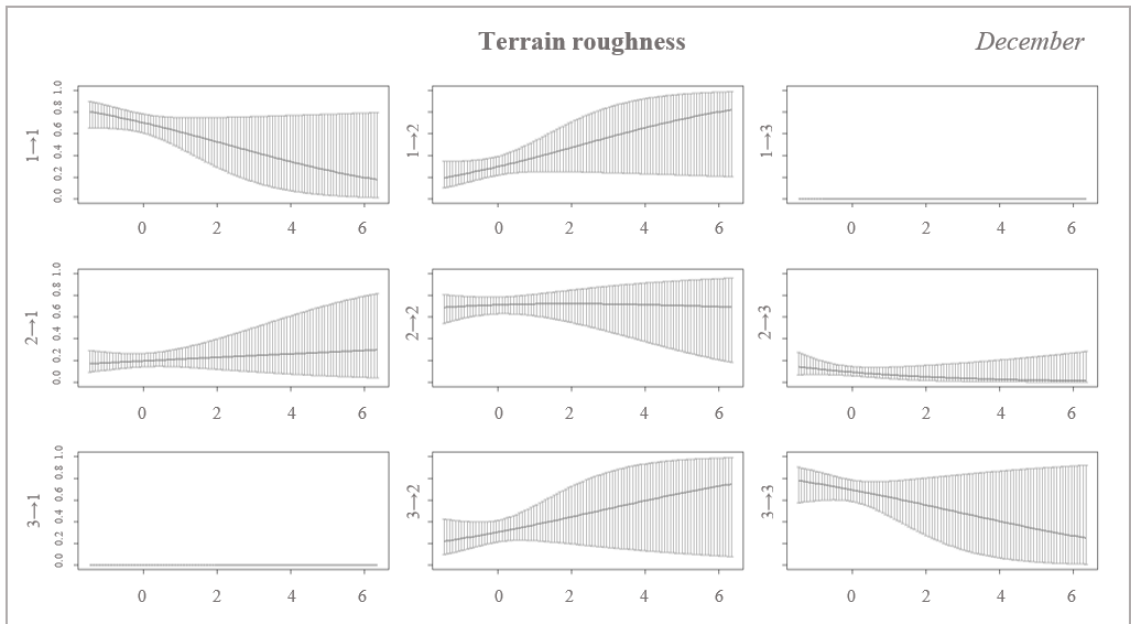


**Figure 26.** Graph showing transition probabilities under the influence of terrain roughness as a covariate in December, between state 1 and 2 ( $1 \rightarrow 2$ ), state 1 and 3 ( $1 \rightarrow 3$ ), state 2 and 1 ( $2 \rightarrow 1$ ), state 2 and 3 ( $2 \rightarrow 3$ ), state 3 and 1 ( $3 \rightarrow 1$ ), and state 3 and 2 ( $3 \rightarrow 2$ ). The graph also shows persistence probabilities in state 1 ( $1 \rightarrow 1$ ), state 2 ( $2 \rightarrow 2$ ) and in state 3 ( $3 \rightarrow 3$ ).

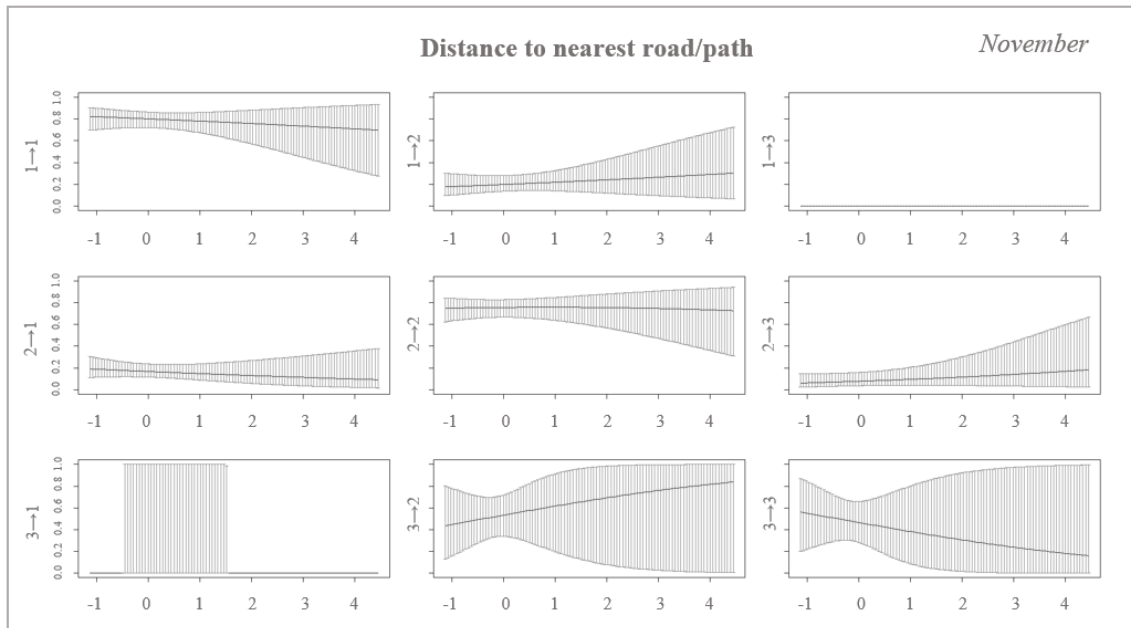


**Figure 27.** Graph showing transition probabilities under the influence of distance to nearest road/path as a covariate in November, between state 1 and 2 ( $1 \rightarrow 2$ ), state 1 and 3 ( $1 \rightarrow 3$ ), state 2 and 1 ( $2 \rightarrow 1$ ), state 2 and 3 ( $2 \rightarrow 3$ ), state 3 and 1 ( $3 \rightarrow 1$ ), and state 3 and 2 ( $3 \rightarrow 2$ ). The graph also shows persistence probabilities in state 1 ( $1 \rightarrow 1$ ), state 2 ( $2 \rightarrow 2$ ) and in state 3 ( $3 \rightarrow 3$ ).

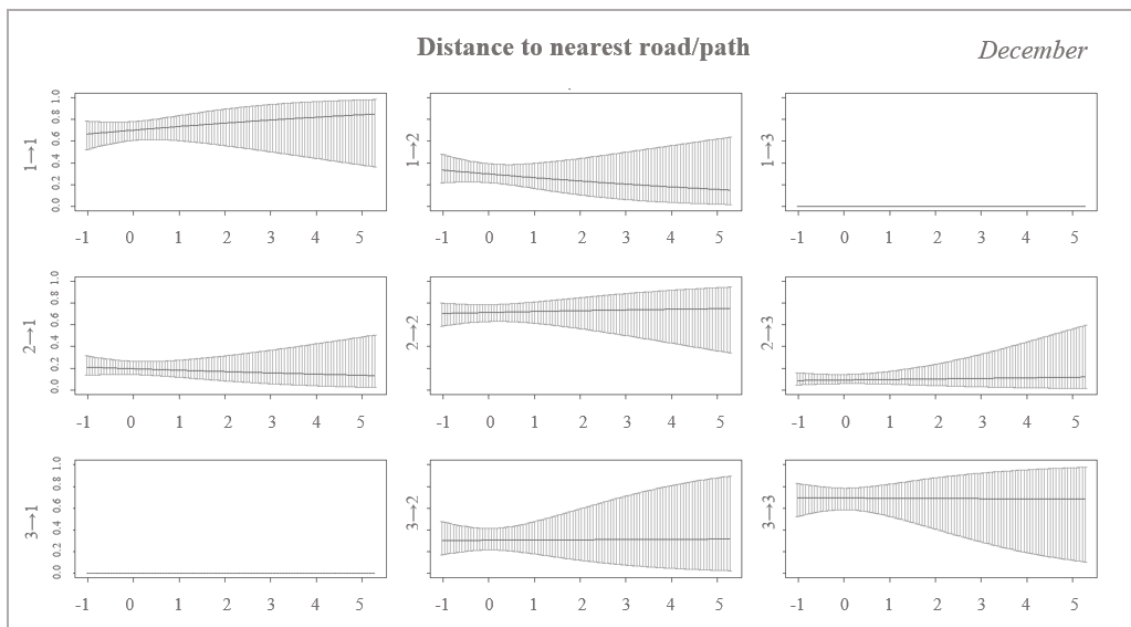


**Figure 28.** Graph showing transition probabilities under the influence of distance to nearest road/path as a covariate in December, between state 1 and 2 ( $1 \rightarrow 2$ ), state 1 and 3 ( $1 \rightarrow 3$ ), state 2 and 1 ( $2 \rightarrow 1$ ), state 2 and 3 ( $2 \rightarrow 3$ ), state 3 and 1 ( $3 \rightarrow 1$ ), and state 3 and 2 ( $3 \rightarrow 2$ ). The graph also shows persistence probabilities in state 1 ( $1 \rightarrow 1$ ), state 2 ( $2 \rightarrow 2$ ) and in state 3 ( $3 \rightarrow 3$ ).

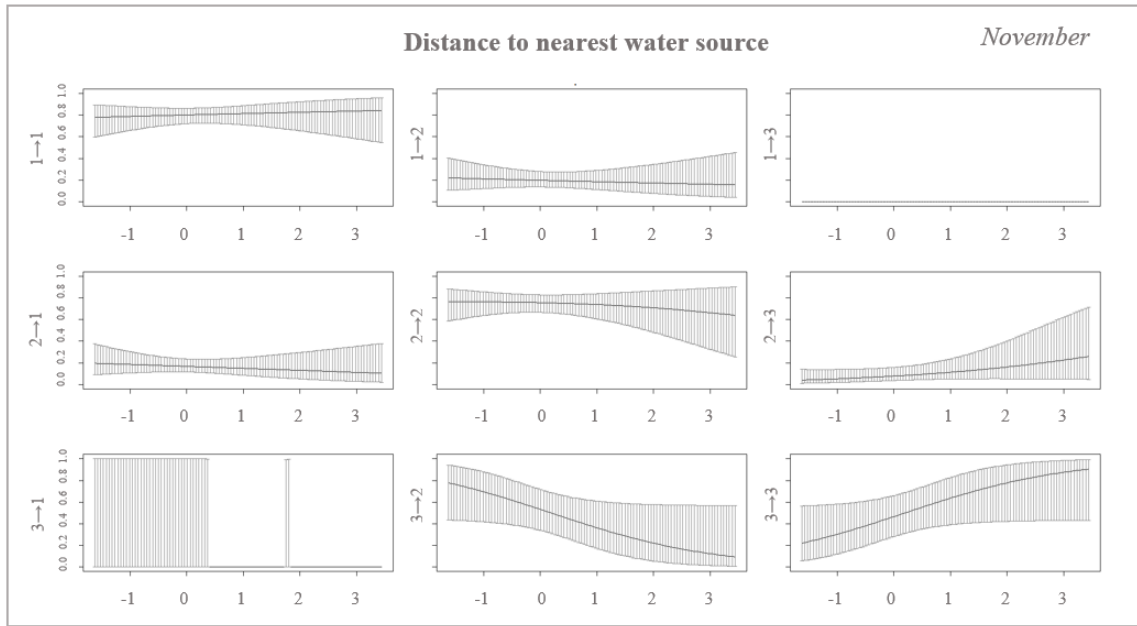


**Figure 29.** Graph showing transition probabilities under the influence of distance to nearest water source as a covariate in November, between state 1 and 2 ( $1 \rightarrow 2$ ), state 1 and 3 ( $1 \rightarrow 3$ ), state 2 and 1 ( $2 \rightarrow 1$ ), state 2 and 3 ( $2 \rightarrow 3$ ), state 3 and 1 ( $3 \rightarrow 1$ ), and state 3 and 2 ( $3 \rightarrow 2$ ). The graph also shows persistence probabilities in state 1 ( $1 \rightarrow 1$ ), state 2 ( $2 \rightarrow 2$ ) and in state 3 ( $3 \rightarrow 3$ ).

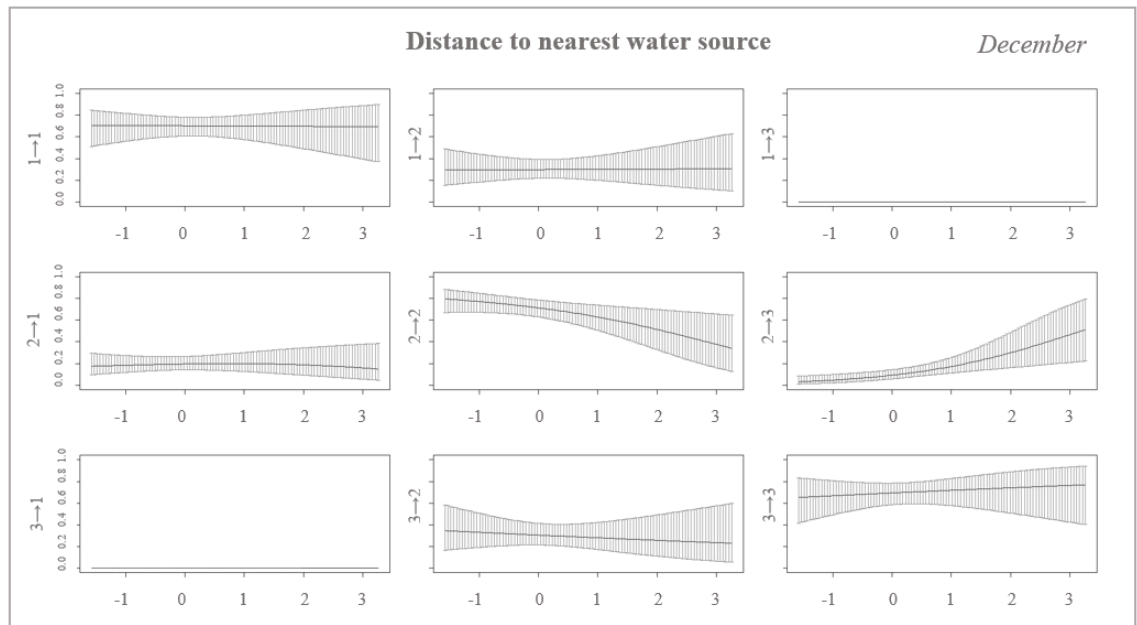


**Figure 30.** Graph showing transition probabilities under the influence of distance to nearest water source as a covariate in December, between state 1 and 2 ( $1 \rightarrow 2$ ), state 1 and 3 ( $1 \rightarrow 3$ ), state 2 and 1 ( $2 \rightarrow 1$ ), state 2 and 3 ( $2 \rightarrow 3$ ), state 3 and 1 ( $3 \rightarrow 1$ ), and state 3 and 2 ( $3 \rightarrow 2$ ). The graph also shows persistence probabilities in state 1 ( $1 \rightarrow 1$ ), state 2 ( $2 \rightarrow 2$ ) and in state 3 ( $3 \rightarrow 3$ ).



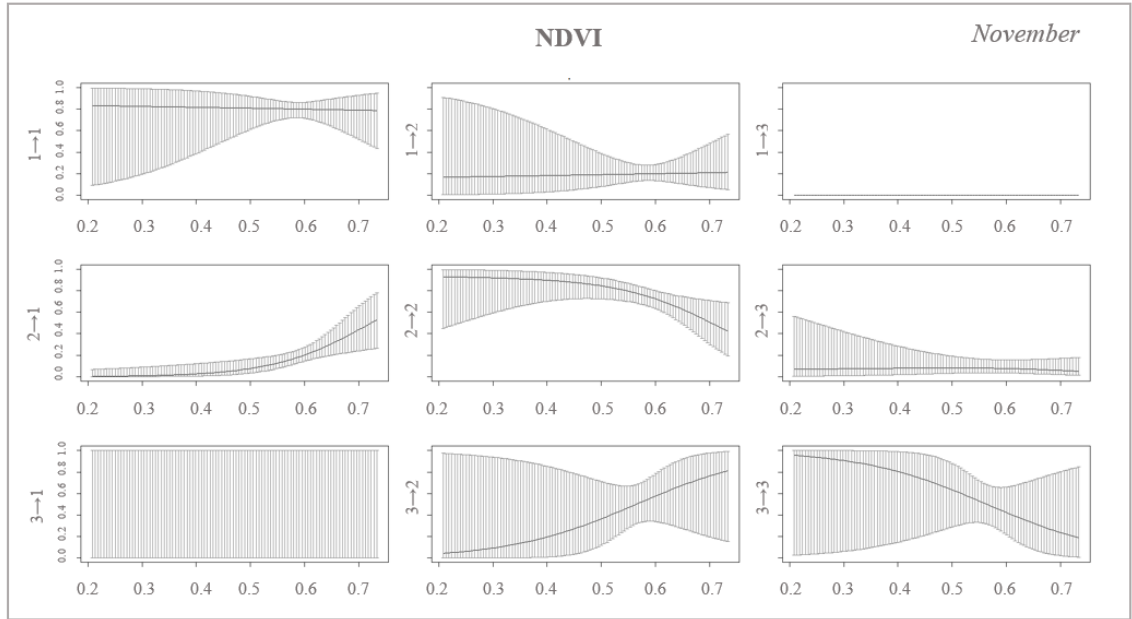


**Figure 31.** Graph showing transition probabilities under the influence of NDVI as a covariate in November, between state 1 and 2 ( $1 \rightarrow 2$ ), state 1 and 3 ( $1 \rightarrow 3$ ), state 2 and 1 ( $2 \rightarrow 1$ ), state 2 and 3 ( $2 \rightarrow 3$ ), state 3 and 1 ( $3 \rightarrow 1$ ), and state 3 and 2 ( $3 \rightarrow 2$ ). The graph also shows persistence probabilities in state 1 ( $1 \rightarrow 1$ ), state 2 ( $2 \rightarrow 2$ ) and in state 3 ( $3 \rightarrow 3$ ).

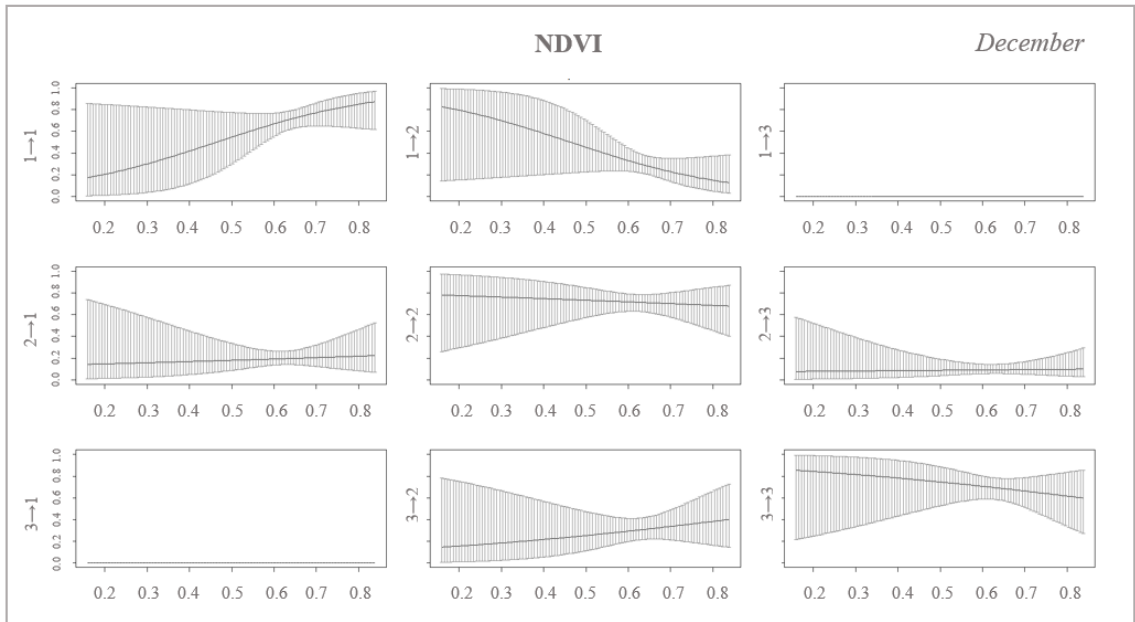


**Figure 32.** Graph showing transition probabilities under the influence of NDVI as a covariate in December, between state 1 and 2 ( $1 \rightarrow 2$ ), state 1 and 3 ( $1 \rightarrow 3$ ), state 2 and 1 ( $2 \rightarrow 1$ ), state 2 and 3 ( $2 \rightarrow 3$ ), state 3 and 1 ( $3 \rightarrow 1$ ), and state 3 and 2 ( $3 \rightarrow 2$ ). The graph also shows persistence probabilities in state 1 ( $1 \rightarrow 1$ ), state 2 ( $2 \rightarrow 2$ ) and in state 3 ( $3 \rightarrow 3$ ).

The transition probabilities of all 7 months combined followed the general trends shown month by month (Table 12, Fig.33-36): for example, the terrain roughness influenced the switching probabilities by promoting a transition to state 1 ( $2 \rightarrow 1 = +0.12$ ) and a persistence in that state as the roughness increased (Fig.33); or considering distance to the nearest water source, as the distance increased, the probability of persistence in state 2 diminished and the probability of  $2 \rightarrow 3$  transition increased (+0.40) (Fig.35).

**Table 12.** Regression coefficients for the transition probabilities referred to the month from June to December combined as a whole. The table shows the probability of transition between state 1 and 2 ( $1 \rightarrow 2$ ), state 1 and 3 ( $1 \rightarrow 3$ ), state 2 and 1 ( $2 \rightarrow 1$ ), state 2 and 3 ( $2 \rightarrow 3$ ), state 3 and 1 ( $3 \rightarrow 1$ ), and state 3 and 2 ( $3 \rightarrow 2$ ). The first row indicates the baseline probability of transition when all the covariates are set to zero. From the second to the fifth row, 4 different covariates and their influence on the transition probabilities are shown.

Regression coefficients for the transition probabilities <i>June-to-December</i>						
	$1 \rightarrow 2$	$1 \rightarrow 3$	$2 \rightarrow 1$	$2 \rightarrow 3$	$3 \rightarrow 1$	$3 \rightarrow 2$
Intercept	-1.334	-0.382	-1.612	-2.453	-5.588	-1.324
Terrain roughness	-0.150	-0.184	0.128	-0.080	-2.649	0.159
Min. road/path distance	0.028	0.132	-0.147	-0.093	0.494	-0.152
Min. water source distance	0.090	-0.320	0.098	0.404	0.486	-0.139
NDVI	0.243	-5.746	0.475	1.335	0.455	0.814

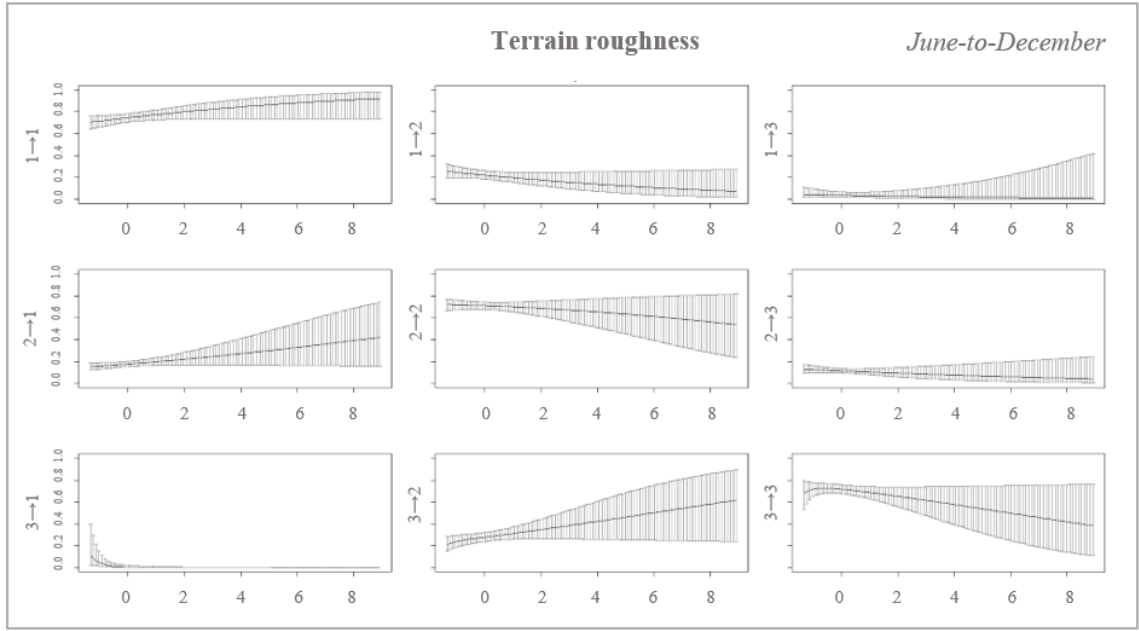


**Figure 33.** Graph showing transition probabilities under the influence of terrain roughness as a covariate for the 7-month period (June to December), between state 1 and 2 ( $1 \rightarrow 2$ ), state 1 and 3 ( $1 \rightarrow 3$ ), state 2 and 1 ( $2 \rightarrow 1$ ), state 2 and 3 ( $2 \rightarrow 3$ ), state 3 and 1 ( $3 \rightarrow 1$ ), and state 3 and 2 ( $3 \rightarrow 2$ ). The graph also shows persistence probabilities in state 1 ( $1 \rightarrow 1$ ), state 2 ( $2 \rightarrow 2$ ) and in state 3 ( $3 \rightarrow 3$ ).

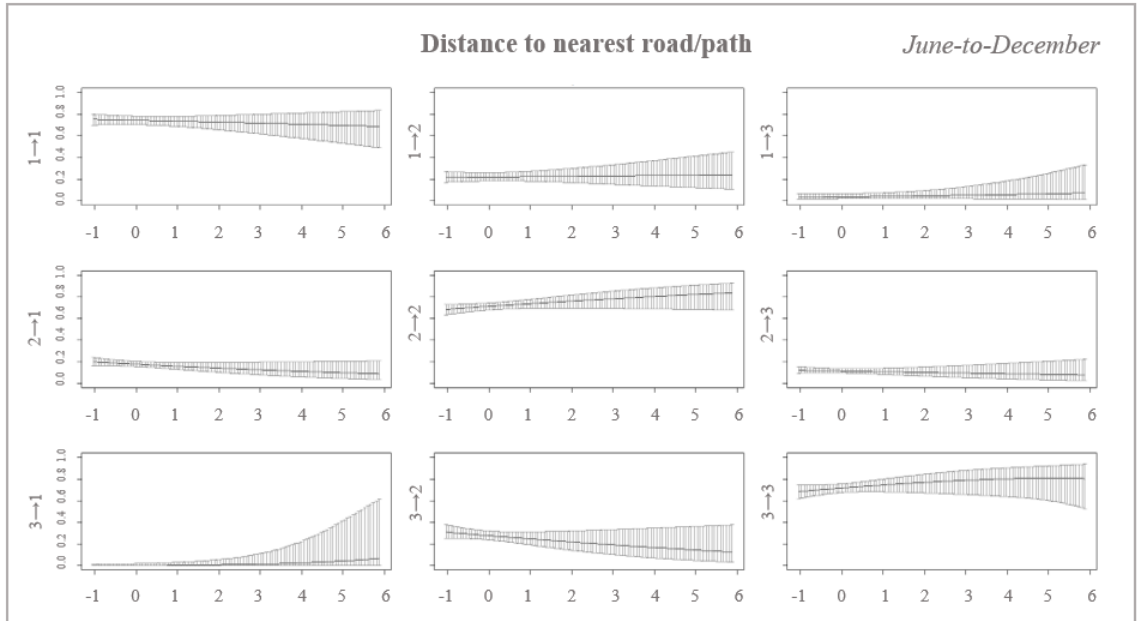


**Figure 34.** Graph showing transition probabilities under the influence of distance to nearest road/path as a covariate for the 7-month period (June to December), between state 1 and 2 ( $1 \rightarrow 2$ ), state 1 and 3 ( $1 \rightarrow 3$ ), state 2 and 1 ( $2 \rightarrow 1$ ), state 2 and 3 ( $2 \rightarrow 3$ ), state 3 and 1 ( $3 \rightarrow 1$ ), and state 3 and 2 ( $3 \rightarrow 2$ ). The graph also shows persistence probabilities in state 1 ( $1 \rightarrow 1$ ), state 2 ( $2 \rightarrow 2$ ) and in state 3 ( $3 \rightarrow 3$ ).

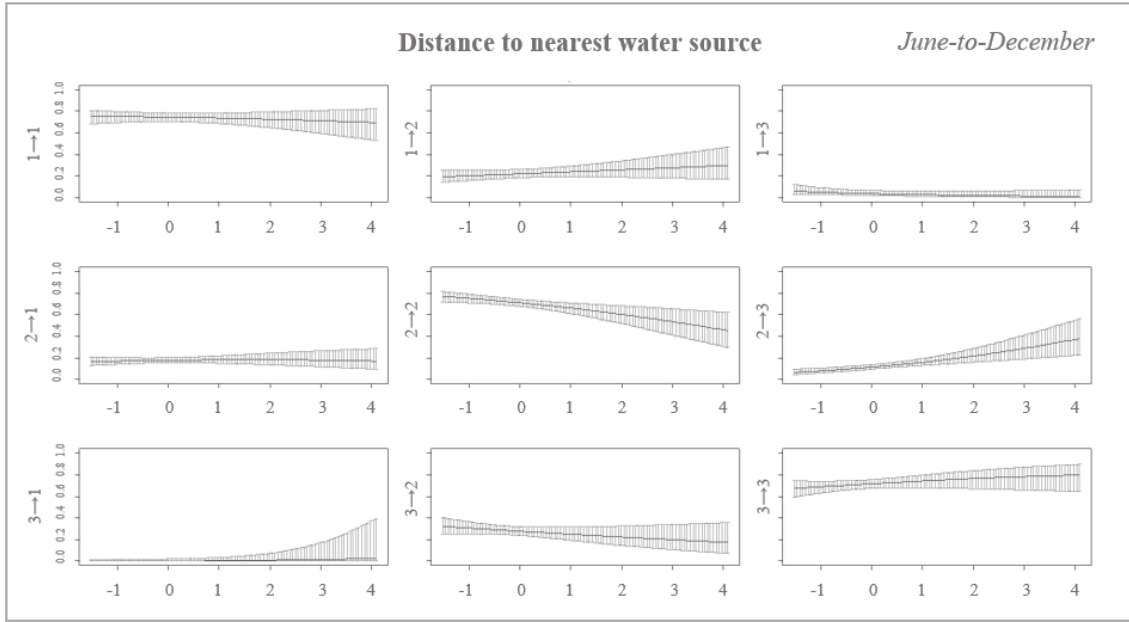


**Figure 35.** Graph showing transition probabilities under the influence of distance to nearest water source as a covariate for the 7-month period (June to December), between state 1 and 2 ( $1 \rightarrow 2$ ), state 1 and 3 ( $1 \rightarrow 3$ ), state 2 and 1 ( $2 \rightarrow 1$ ), state 2 and 3 ( $2 \rightarrow 3$ ), state 3 and 1 ( $3 \rightarrow 1$ ), and state 3 and 2 ( $3 \rightarrow 2$ ). The graph also shows persistence probabilities in state 1 ( $1 \rightarrow 1$ ), state 2 ( $2 \rightarrow 2$ ) and in state 3 ( $3 \rightarrow 3$ ).

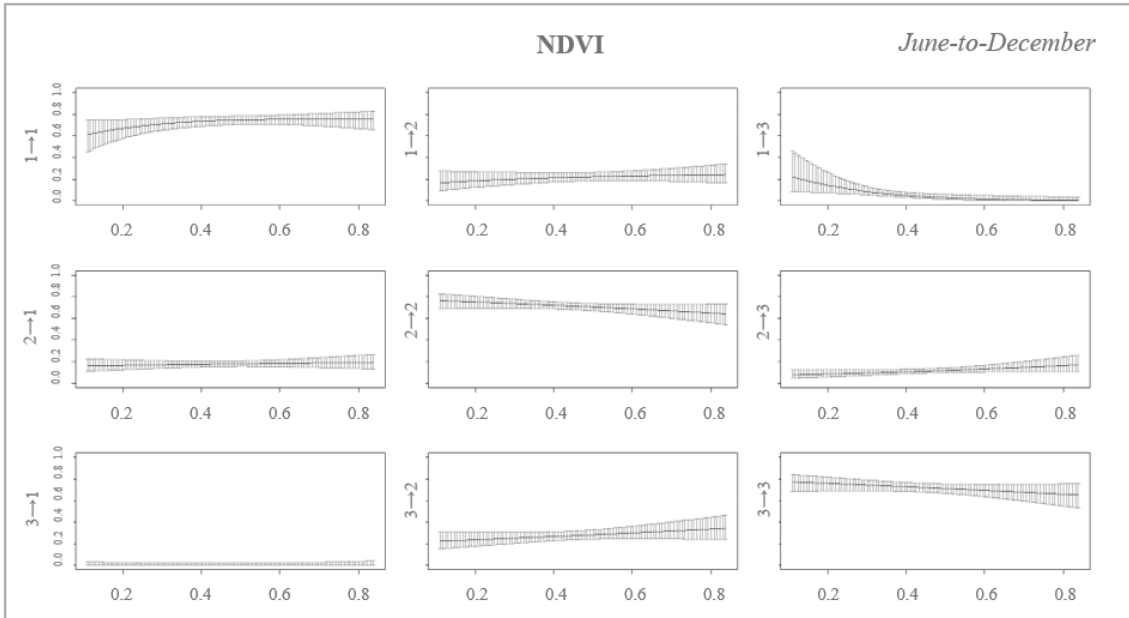


**Figure 36.** Graph showing transition probabilities under the influence of NDVI as a covariate for the 7-month period (June to December), between state 1 and 2 ( $1 \rightarrow 2$ ), state 1 and 3 ( $1 \rightarrow 3$ ), state 2 and 1 ( $2 \rightarrow 1$ ), state 2 and 3 ( $2 \rightarrow 3$ ), state 3 and 1 ( $3 \rightarrow 1$ ), and state 3 and 2 ( $3 \rightarrow 2$ ). The graph also shows persistence probabilities in state 1 ( $1 \rightarrow 1$ ), state 2 ( $2 \rightarrow 2$ ) and in state 3 ( $3 \rightarrow 3$ ).

The results regarding the stationary state probabilities were analysed covariate by covariate (Fig.37-44).

Considering the terrain roughness as covariate, across June, July, and August there was a clear prevalence of occurrence in state 1 at high roughness values (Fig.37-39). In September, the probability of being in state 3 increased with increasing the covariate value, while both state 1 and 2 had a low probability of occurrence at high roughness levels (Fig.40). In October, there was a marked predominance of state 2 at each value of terrain roughness (Fig.41). November and December, instead, registered the same probability of occurrence for the former, and higher odds of being in state 2 for the latter (Fig.42-43). Analysing the 7-month period as a whole, however, showed a strong prevalence of state 1 when the terrain was rougher (Fig.44).

When the distance to the nearest road/path was applied as a variable, in June there was a tendency to remain in state 2 regardless of the distance to the road, while there was a greater likelihood of persisting in state 3 when on the road (Fig.37). In July, a higher probability of being in states 2 and 1 was observed as distance increased, whereas state 3 was more likely at the shortest distance (Fig.38). In August and September, there was a net prevalence of state 3 among the different values of the covariate (Fig.39-40), whereas October showed a predominance of state 1 in the extreme proximity of the road, and of state 2 as the value of the covariate augmented (Fig.41). November and December showed similar patterns, with a preponderance of state 2 across the entire spectrum of covariate values (Fig.42-43). Overall, state 2 was the favourite under the influence of this covariate, with state 1 slightly more likely near the road (Fig.44).

Under the influence of distance from the nearest water source as a predictor variable, state 2 prevailed in June and July, regardless of the distance from the water (Fig.37-38). In August, September, and October, instead, state 2 was the most probable near the water source (with a substantial peak in October), while state 3 increased exponentially as distance from the water increased (Fig.39-41). A similar trend emerged between November and December, with state 1 following the same trend as state 2 with higher occurrence near the water point, but also with a greater likelihood of moving to state 3 once away from the water (Fig.42-43). The same trends as the latter were followed in the 7-month analysis (Fig.44).

With slightly different degrees of probability, when setting NDVI as a covariate, each month indicated a high persistence in state 1 at the highest values of the NDVI, and

a high probability of remaining in state 3 at the lowest values of the covariate, with the highest probability of being in state 2 at the mean values of NDVI (Fig.37-44).

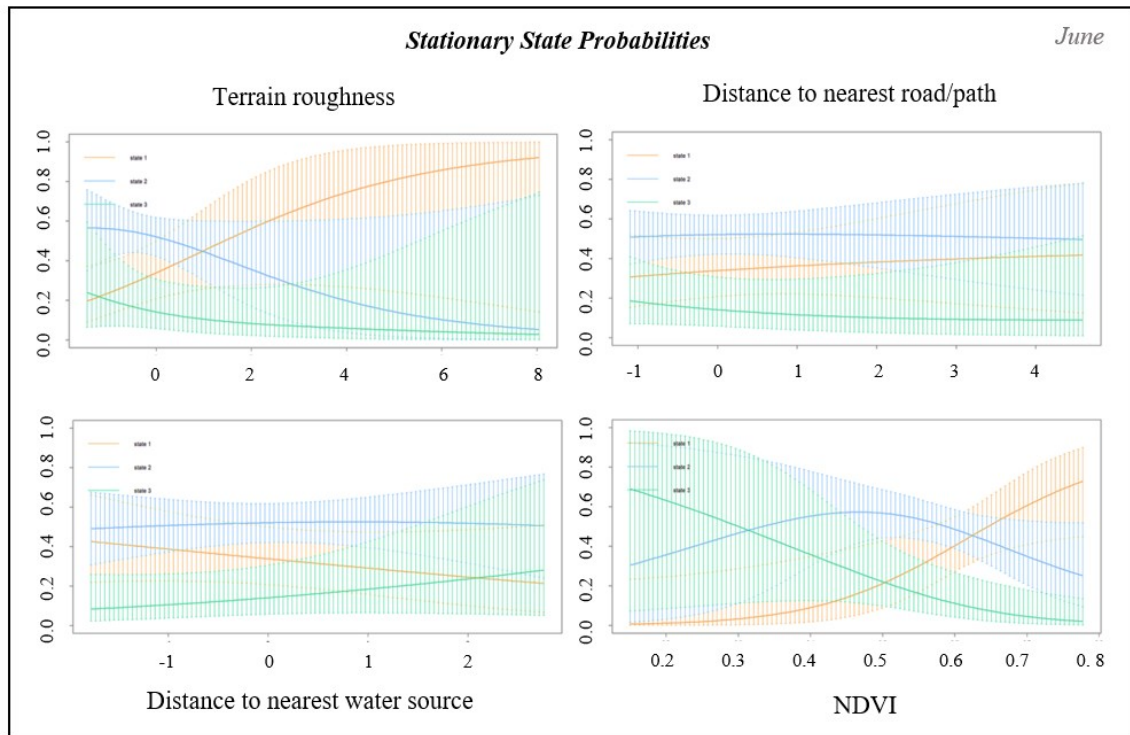


**Figure 37.** Graph showing stationary state probabilities for each covariate in June.

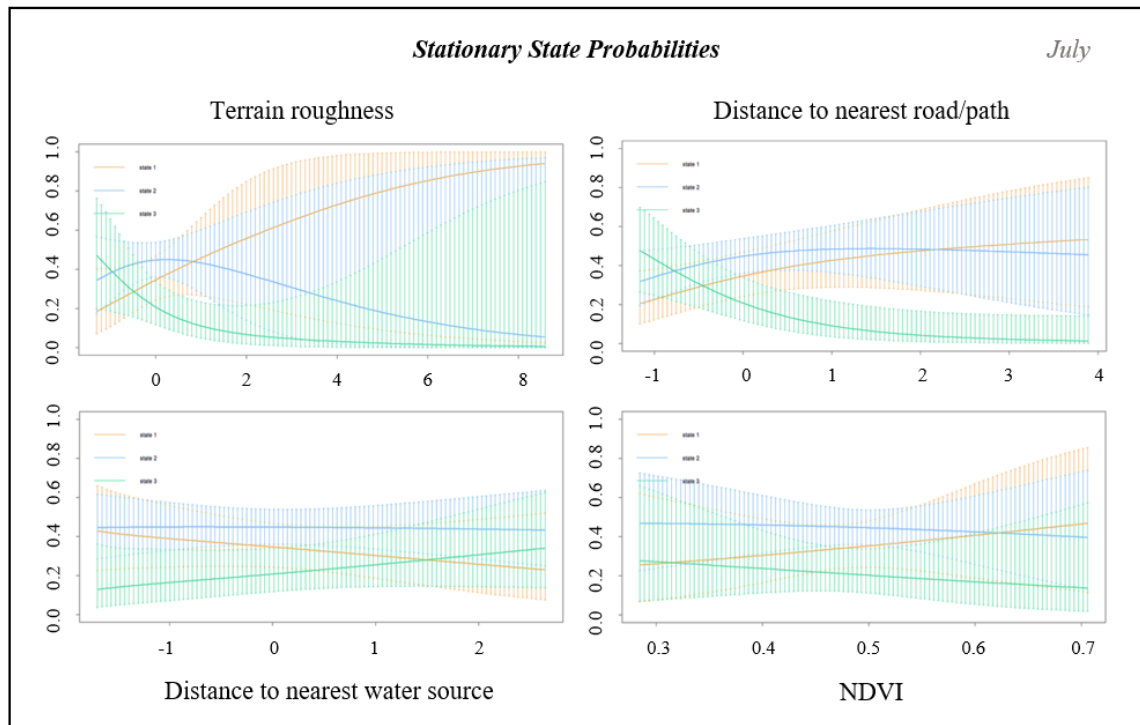


**Figure 38.** Graph showing stationary state probabilities for each covariate in July.

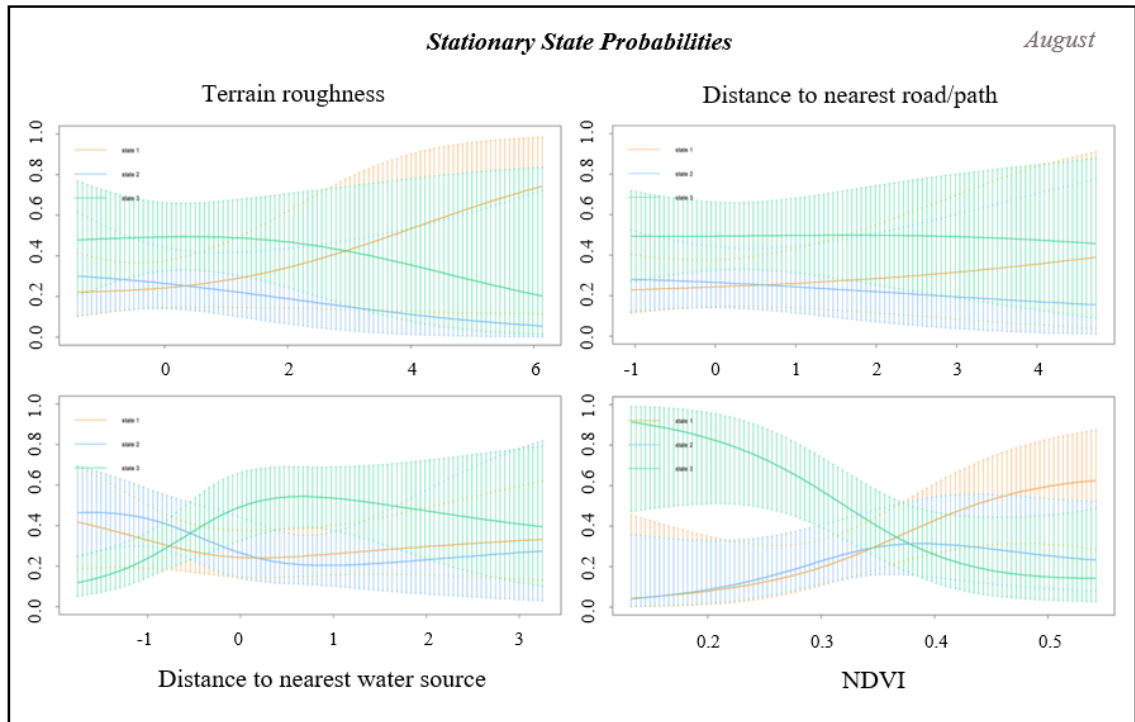


**Figure 39.** Graph showing stationary state probabilities for each covariate in August.

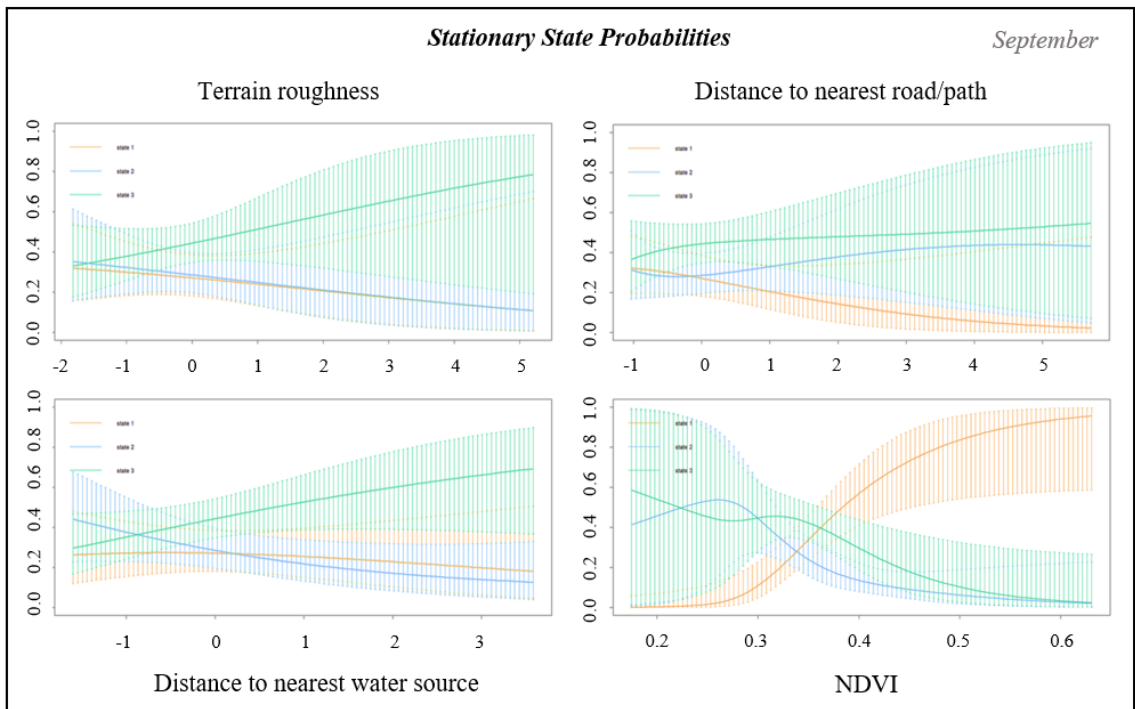


**Figure 40.** Graph showing stationary state probabilities for each covariate in September.

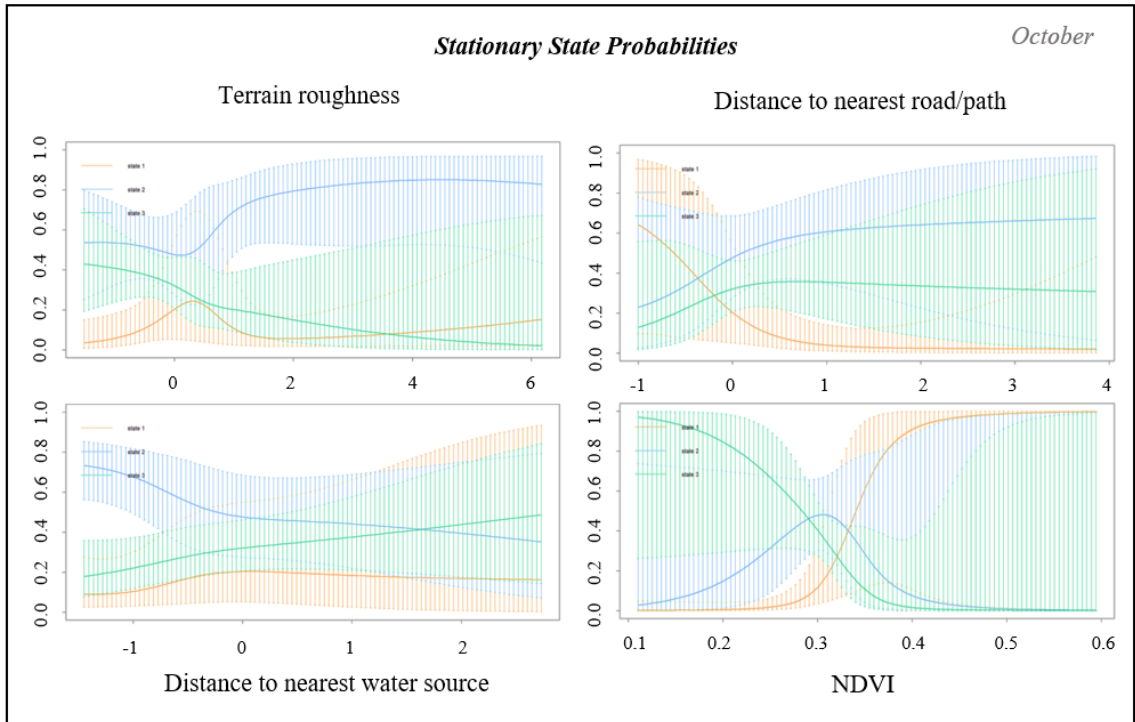


**Figure 41.** Graph showing stationary state probabilities for each covariate in October.

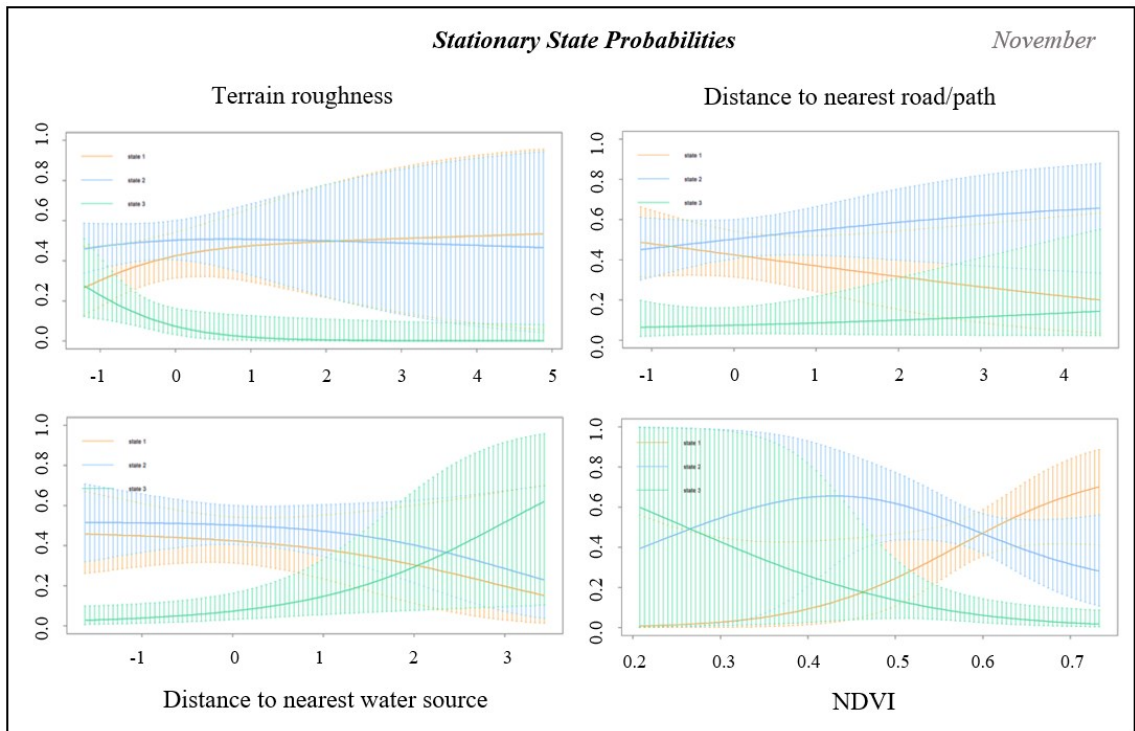


**Figure 42.** Graph showing stationary state probabilities for each covariate in November.



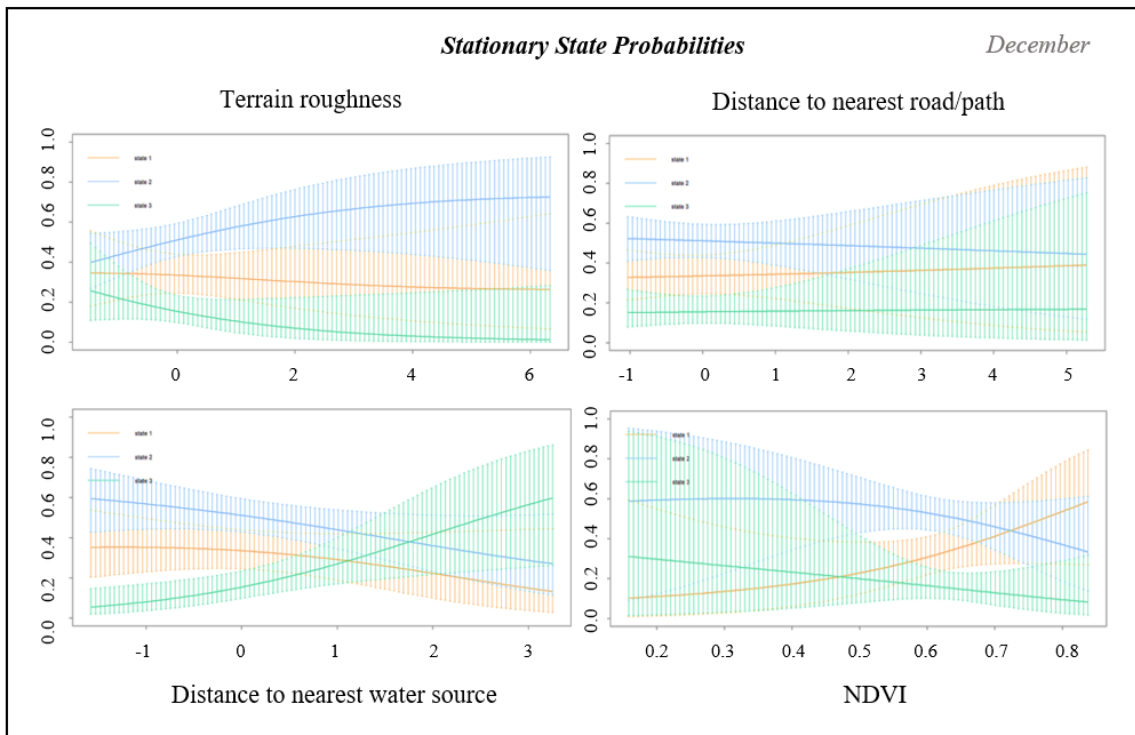


**Figure 43.** Graph showing stationary state probabilities for each covariate in December.

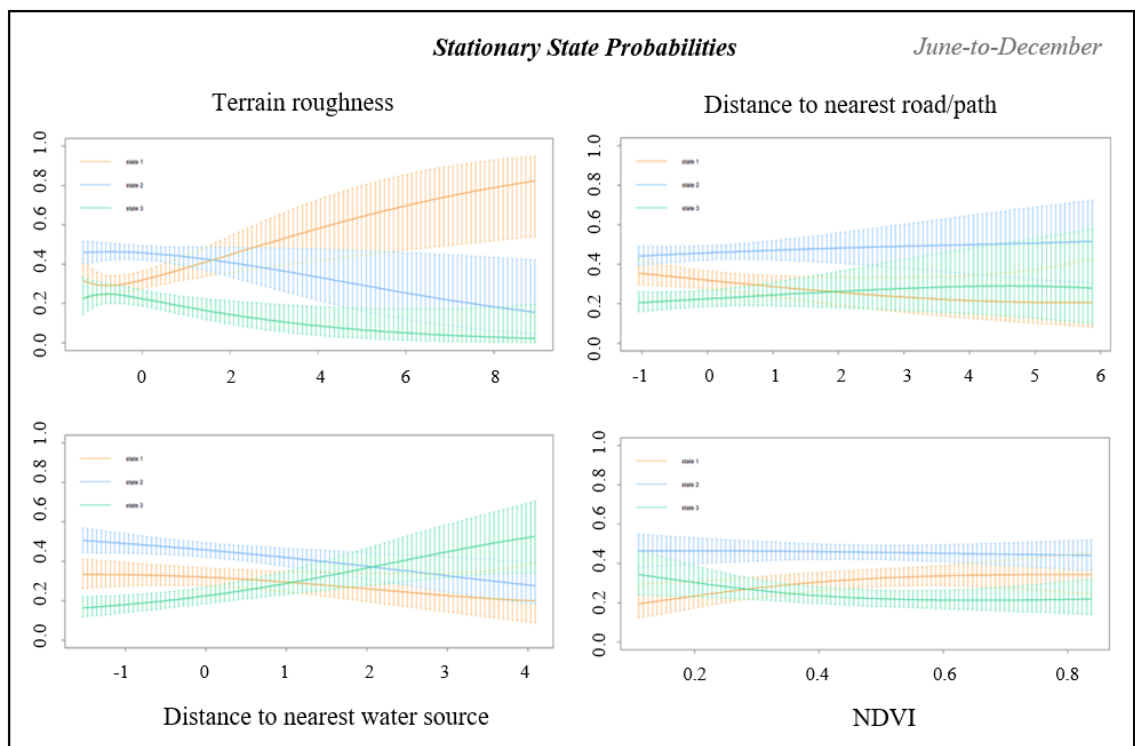


**Figure 44.** Graph showing stationary state probabilities for each covariate combining all the months.

### 3.2 Jean

The step length means for each state varied monthly over the 7 months analysed (Table 13). State 1 recorded a minimum of 68 metres in June and a maximum of 129 metres in December; state 2, presented a minimum and a maximum of 333 metres (in August) and 664 metres (in December), respectively; state 3 ranged between 842 metres (in December) as a minimum, and 1769 metres (in October) as a maximum. Taking the 7 months together, the step length mean is 50, 223, and 887 metres for states 1,2, and 3, respectively. The SD results followed the same fluctuation patterns as the mean. For greater accuracy of the model, the turning angle parameters, which include the mean and concentration, were also calculated (Table 14).

**Table 13.** Step length parameters showing the mean (expressed in km) and standard deviation (SD) for each month and for all the months combined (last row). The step length mean corresponds to the average distance covered in a single step for each state.

Step length parameters						
	<i>Mean</i>			<i>SD</i>		
	<i>State 1</i>	<i>State 2</i>	<i>State 3</i>	<i>State 1</i>	<i>State 2</i>	<i>State 3</i>
June	0.068	0.370	1.476	0.075	0.262	0.701
July	-	-	-	-	-	-
August	0.084	0.333	1.288	0.080	0.183	0.677
September	0.090	0.349	1.225	0.092	0.213	0.555
October	0.100	0.565	1.769	0.108	0.377	0.698
November	-	-	-	-	-	-
December	0.129	0.664	0.842	0.148	0.488	0.633
<b>June- December</b>	<b>0.050</b>	<b>0.223</b>	<b>0.887</b>	<b>0.056</b>	<b>0.146</b>	<b>0.580</b>

**Table 14.** The turning angle parameters, showing the mean and the concentration for each month and for all the months combined (last row). The turning angle mean corresponds to the average angle performed in a single step for each state.

Turning angle parameters						
	<i>Mean</i>			<i>Concentration</i>		
	<i>State 1</i>	<i>State 2</i>	<i>State 3</i>	<i>State 1</i>	<i>State 2</i>	<i>State 3</i>
June	0.042	-0.103	0.030	0.576	1.461	1.500
July	-	-	-	-	-	-
August	0.045	0.062	0.029	0.969	1.664	1.431
September	-0.108	0.133	-0.074	0.807	1.414	2.413
October	-0.070	0.042	-0.176	0.748	1.675	5.452
November	-	-	-	-	-	-
December	-0.324	-0.013	-0.048	0.374	1.213	7.032
<b>June- December</b>	<b>-0.243</b>	<b>0.045</b>	<b>-0.007</b>	<b>0.265</b>	<b>1.585</b>	<b>1.508</b>

Between June and October, the percentage of time spent in state 1 increasingly rose, reaching 51% occurrence in October, which also recorded the lowest percentage of time spent in state 3 (6%). In an analysis on a monthly scale, Jean recorded a high presence in state 2, with percentages ranging from 39% to 61%. Particularly, the wet season was characterised by elevated values of time spent in state 1 and 2. Considering collectively the months from June to December, Jean spent 42% of the time in state 2, 37% in state 3 and 20% in state 1 (Table 15).

**Table 15.** Percentage of time spent for each state obtained with the Viterbi algorithm, included in the Viterbi function of the moveHMM package. It provides the most probable sequence of states that generated the observation, based on the fitted model.

Percentage of time spent on each state			
	<i>State 1</i>	<i>State 2</i>	<i>State 3</i>
June	0.274	0.613	0.123
July	-	-	-
August	0.381	0.502	0.209
September	0.462	0.391	0.151
October	0.510	0.426	0.069
November	-	-	-
December	0.354	0.502	0.147
<b>June- December</b>	<b>0.201</b>	<b>0.428</b>	<b>0.369</b>

In June (Table 16, Fig.45-48), the baseline probability of  $1 \rightarrow 2$  transitioning was +1.23. When setting the terrain roughness as a predictor variable, the  $1 \rightarrow 2$  value became slightly negative (-0.22), whereas when considering  $2 \rightarrow 1$  transition, the probability was +0.22, indicating a tendency to remain in state 1 as roughness increased. As evidence, the probability of persistence in state 1 was higher when the terrain was rougher (Fig.45). Under the influence of NDVI as a covariate, a great negative transition probability was recorded for the  $2 \rightarrow 3$  transition (-5.29), whilst  $3 \rightarrow 1$  switching probability registered a value of +10.68. As proof, the persistence odds in state 1 increased with increasing NDVI value and, concurrently, switching probabilities of  $1 \rightarrow 2$  decreased (Fig.48). Considering the influence of the distance to the nearest water source, the  $3 \rightarrow 2$  probability was greater near the water, whereas  $3 \rightarrow 1$  probability was greater away from water points.

The regression coefficients for the  $1 \rightarrow 3$  transition were not taken into account for the analysis of this month's movements, as there was no correspondence in the graphs.

**Table 16.** Regression coefficients for the transition probabilities referred to the month of June. The table shows the probability of transition between state 1 and 2 ( $1 \rightarrow 2$ ), state 1 and 3 ( $1 \rightarrow 3$ ), state 2 and 1 ( $2 \rightarrow 1$ ), state 2 and 3 ( $2 \rightarrow 3$ ), state 3 and 1 ( $3 \rightarrow 1$ ), and state 3 and 2 ( $3 \rightarrow 2$ ). The first row indicates the baseline probability of transition when all the covariates are set to zero. From the second to the fifth row, 4 different covariates and their influence on the transition probabilities are shown.

	Regression coefficients for the transition probabilities						June
	$1 \rightarrow 2$	$1 \rightarrow 3$	$2 \rightarrow 1$	$2 \rightarrow 3$	$3 \rightarrow 1$	$3 \rightarrow 2$	
Intercept	1.238	-577.939	-4.768	0.426	-10.112	-2.011	
Terrain roughness	-0.222	82.068	0.222	0.285	-2.465	1.526	
Min. road/path distance	0.146	143.762	0.445	-0.059	-0.935	-0.151	
Min. water source distance	0.142	-462.273	-0.582	-0.100	2.481	-1.762	
NDVI	-3.632	-399.035	5.063	-5.292	10.618	1.354	

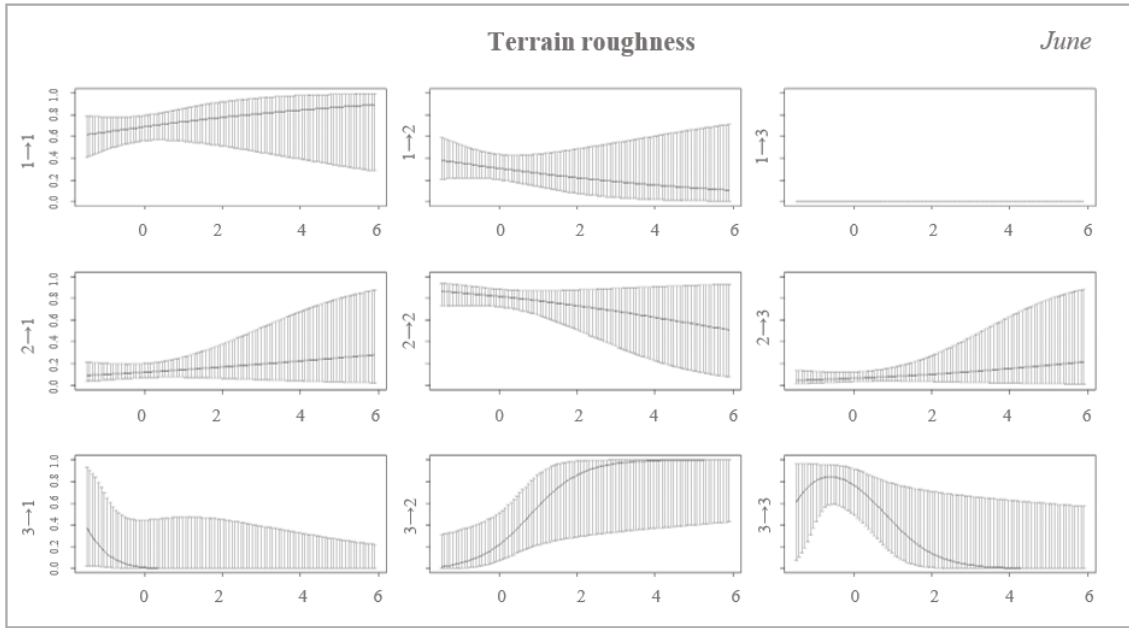


**Figure 45.** Graph showing transition probabilities under the influence of terrain roughness as a covariate in June, between state 1 and 2 ( $1 \rightarrow 2$ ), state 1 and 3 ( $1 \rightarrow 3$ ), state 2 and 1 ( $2 \rightarrow 1$ ), state 2 and 3 ( $2 \rightarrow 3$ ), state 3 and 1 ( $3 \rightarrow 1$ ), and state 3 and 2 ( $3 \rightarrow 2$ ). The graph also shows persistence probabilities in state 1 ( $1 \rightarrow 1$ ), state 2 ( $2 \rightarrow 2$ ) and in state 3 ( $3 \rightarrow 3$ ).

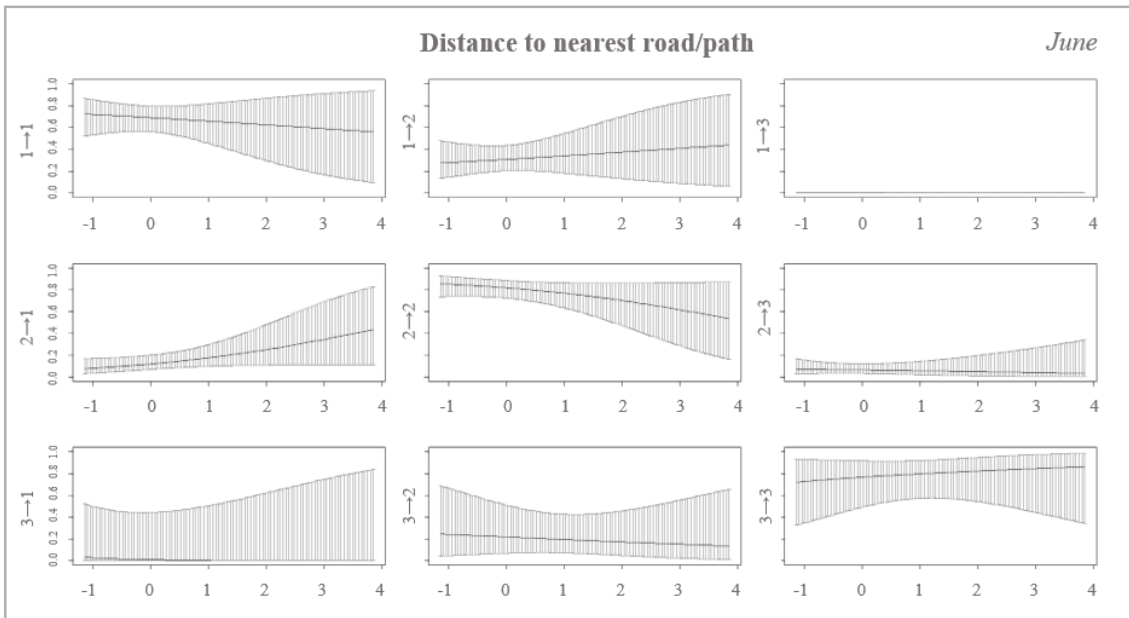


**Figure 46.** Graph showing transition probabilities under the influence of distance to nearest road/path as a covariate in June, between state 1 and 2 ( $1 \rightarrow 2$ ), state 1 and 3 ( $1 \rightarrow 3$ ), state 2 and 1 ( $2 \rightarrow 1$ ), state 2 and 3 ( $2 \rightarrow 3$ ), state 3 and 1 ( $3 \rightarrow 1$ ), and state 3 and 2 ( $3 \rightarrow 2$ ). The graph also shows persistence probabilities in state 1 ( $1 \rightarrow 1$ ), state 2 ( $2 \rightarrow 2$ ) and in state 3 ( $3 \rightarrow 3$ ).

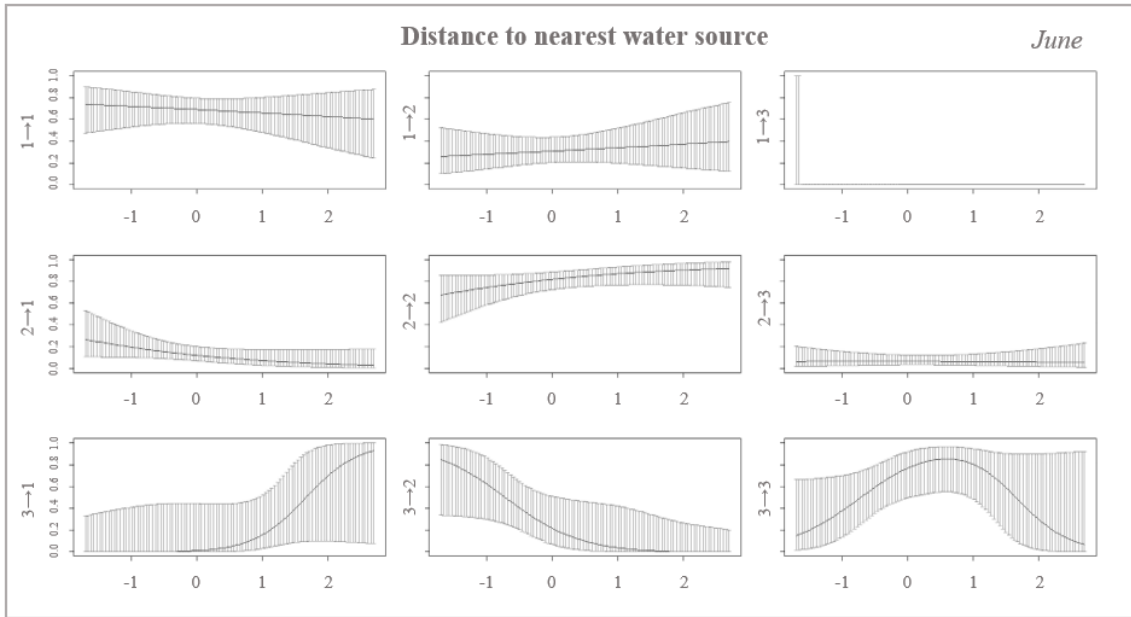


**Figure 47.** Graph showing transition probabilities under the influence of distance to nearest water source as a covariate in June, between state 1 and 2 ( $1 \rightarrow 2$ ), state 1 and 3 ( $1 \rightarrow 3$ ), state 2 and 1 ( $2 \rightarrow 1$ ), state 2 and 3 ( $2 \rightarrow 3$ ), state 3 and 1 ( $3 \rightarrow 1$ ), and state 3 and 2 ( $3 \rightarrow 2$ ). The graph also shows persistence probabilities in state 1 ( $1 \rightarrow 1$ ), state 2 ( $2 \rightarrow 2$ ) and in state 3 ( $3 \rightarrow 3$ ).

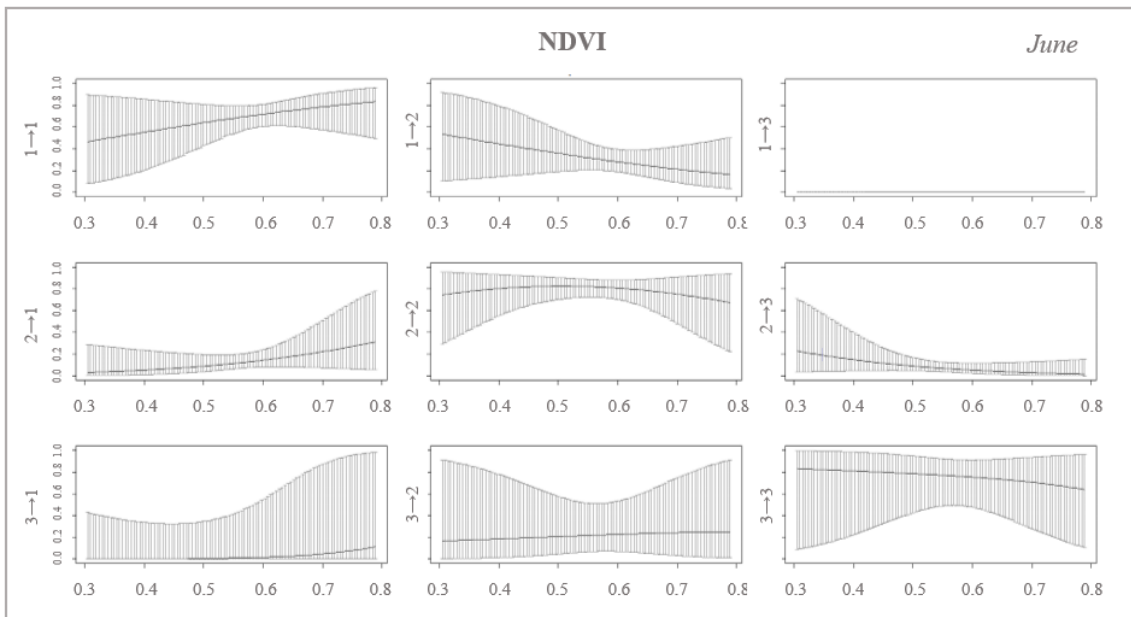


**Figure 48.** Graph showing transition probabilities under the influence of NDVI as a covariate in June, between state 1 and 2 ( $1 \rightarrow 2$ ), state 1 and 3 ( $1 \rightarrow 3$ ), state 2 and 1 ( $2 \rightarrow 1$ ), state 2 and 3 ( $2 \rightarrow 3$ ), state 3 and 1 ( $3 \rightarrow 1$ ), and state 3 and 2 ( $3 \rightarrow 2$ ). The graph also shows persistence probabilities in state 1 ( $1 \rightarrow 1$ ), state 2 ( $2 \rightarrow 2$ ) and in state 3 ( $3 \rightarrow 3$ ).

In August (Table 17, Fig.49-52), the NDVI had a great influence on transition probabilities, with a tendency to promote occurrence in state 1 as the covariate value increased ( $2 \rightarrow 1 = +10.98$ ). In support of this, as the NDVI value augmented, persistence in state 2 decreased remarkably, while persistence in state 1 increased (Fig.52). The distance to nearest road/path did not notably influence the transition probability, recording slightly positive value of  $2 \rightarrow 1$  and  $2 \rightarrow 3$  transition values as the distance augmented (+0.12 and +0.35 respectively), along with a persistence probability in state 2 that decreased as the distance to the road increased (Fig.50). Terrain roughness in this month presented a probability of  $2 \rightarrow 1$  switching when the terrain was rougher, followed by a decreasing value of persistence in state 2 when the roughness was greater (Fig.49).

**Table 17.** Regression coefficients for the transition probabilities referred to the month of August. The table shows the probability of transition between state 1 and 2 ( $1 \rightarrow 2$ ), state 1 and 3 ( $1 \rightarrow 3$ ), state 2 and 1 ( $2 \rightarrow 1$ ), state 2 and 3 ( $2 \rightarrow 3$ ), state 3 and 1 ( $3 \rightarrow 1$ ), and state 3 and 2 ( $3 \rightarrow 2$ ). The first row indicates the baseline probability of transition when all the covariates are set to zero. From the second to the fifth row, 4 different covariates and their influence on the transition probabilities are shown.

	Regression coefficients for the transition probabilities						August
	$1 \rightarrow 2$	$1 \rightarrow 3$	$2 \rightarrow 1$	$2 \rightarrow 3$	$3 \rightarrow 1$	$3 \rightarrow 2$	
Intercept	0.463	-332.935	-4.733	-5.846	-821.089	-2.169	
Terrain roughness	-0.235	-32.848	0.552	0.152	68.825	0.084	
Min. road/path distance	0.110	38.576	0.121	0.355	-477.328	-0.133	
Min. water source distance	-0.027	6.275	-0.303	-0.087	-124.250	0.041	
NDVI	-4.395	-103.113	10.983	13.098	463.953	4.159	



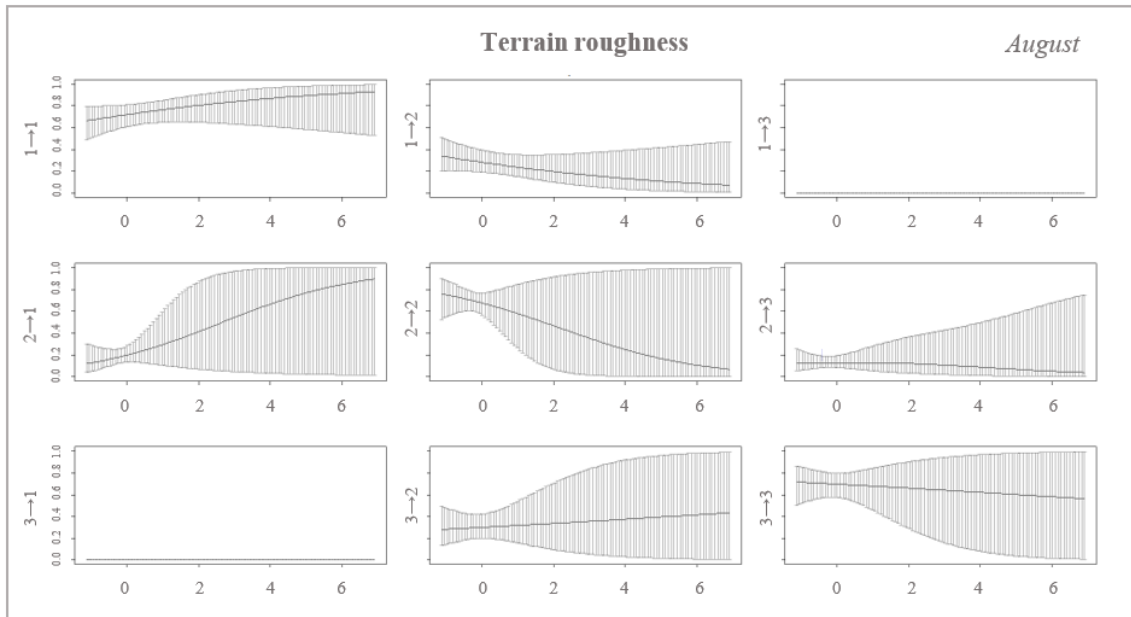


**Figure 49.** Graph showing transition probabilities under the influence of terrain roughness as a covariate in August, between state 1 and 2 ( $1 \rightarrow 2$ ), state 1 and 3 ( $1 \rightarrow 3$ ), state 2 and 1 ( $2 \rightarrow 1$ ), state 2 and 3 ( $2 \rightarrow 3$ ), state 3 and 1 ( $3 \rightarrow 1$ ), and state 3 and 2 ( $3 \rightarrow 2$ ). The graph also shows persistence probabilities in state 1 ( $1 \rightarrow 1$ ), state 2 ( $2 \rightarrow 2$ ) and in state 3 ( $3 \rightarrow 3$ ).

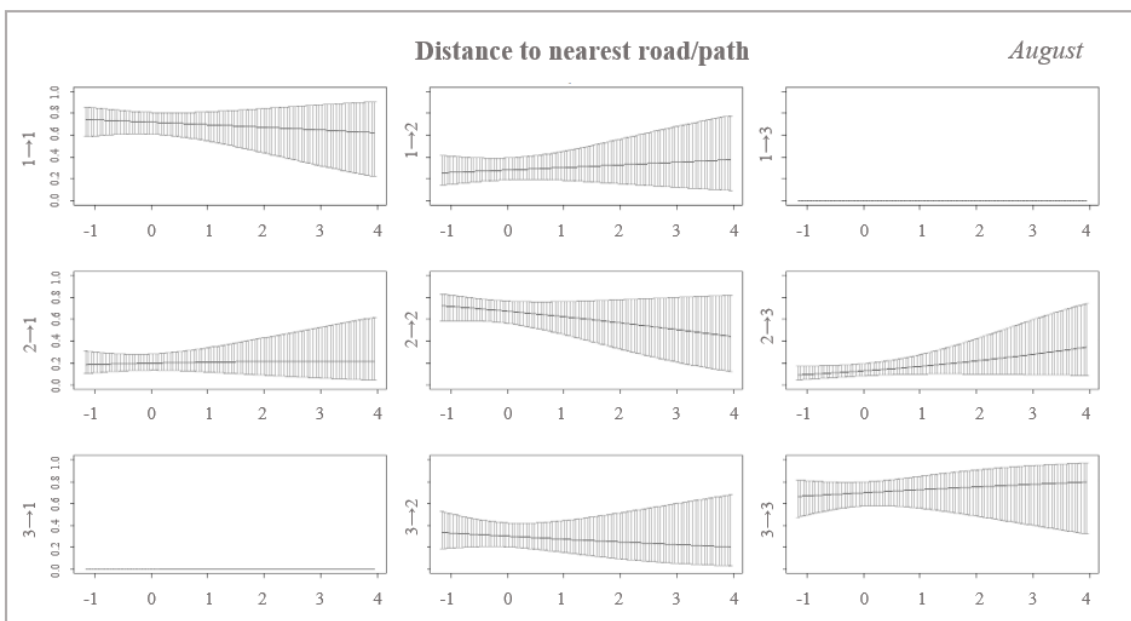


**Figure 50.** Graph showing transition probabilities under the influence of distance to nearest road/path as a covariate in August, between state 1 and 2 ( $1 \rightarrow 2$ ), state 1 and 3 ( $1 \rightarrow 3$ ), state 2 and 1 ( $2 \rightarrow 1$ ), state 2 and 3 ( $2 \rightarrow 3$ ), state 3 and 1 ( $3 \rightarrow 1$ ), and state 3 and 2 ( $3 \rightarrow 2$ ). The graph also shows persistence probabilities in state 1 ( $1 \rightarrow 1$ ), state 2 ( $2 \rightarrow 2$ ) and in state 3 ( $3 \rightarrow 3$ ).

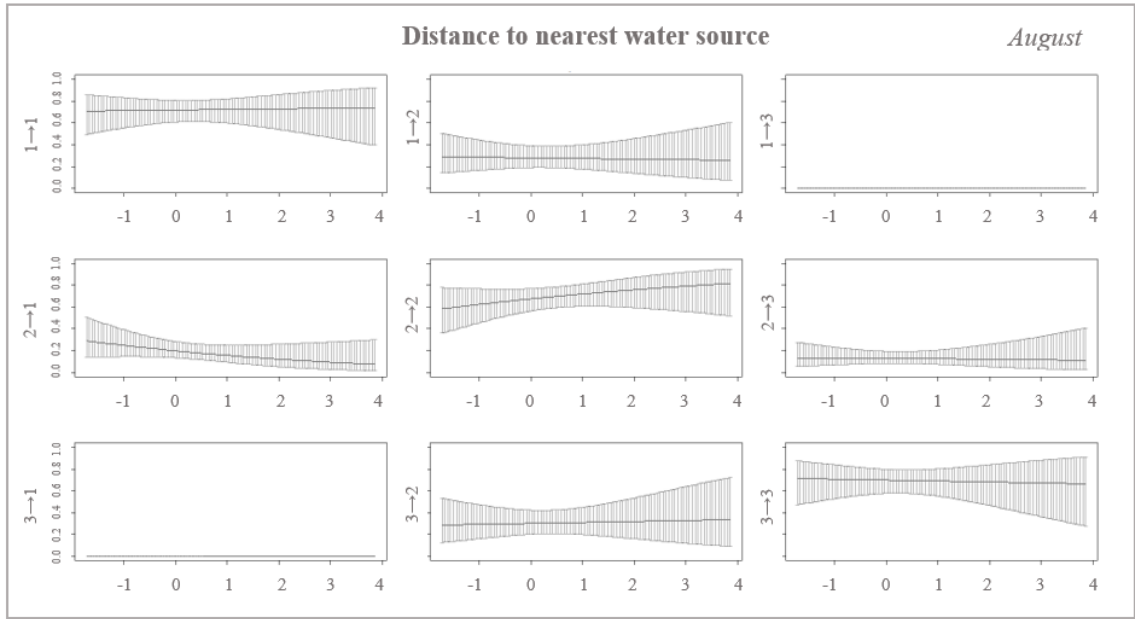


**Figure 51.** Graph showing transition probabilities under the influence of distance to nearest water source as a covariate in August, between state 1 and 2 ( $1 \rightarrow 2$ ), state 1 and 3 ( $1 \rightarrow 3$ ), state 2 and 1 ( $2 \rightarrow 1$ ), state 2 and 3 ( $2 \rightarrow 3$ ), state 3 and 1 ( $3 \rightarrow 1$ ), and state 3 and 2 ( $3 \rightarrow 2$ ). The graph also shows persistence probabilities in state 1 ( $1 \rightarrow 1$ ), state 2 ( $2 \rightarrow 2$ ) and in state 3 ( $3 \rightarrow 3$ ).

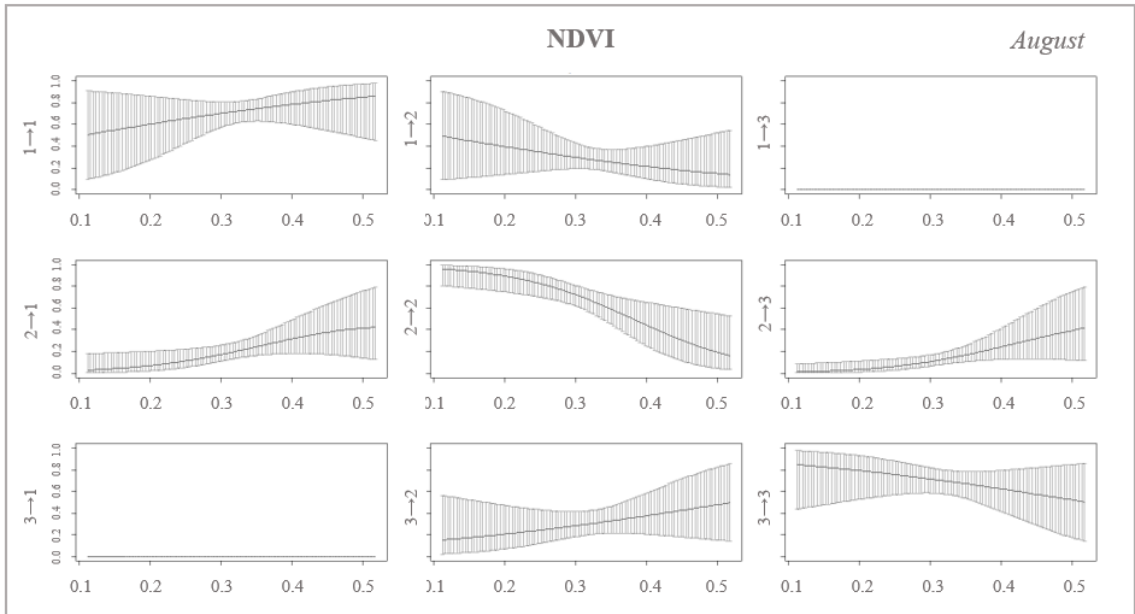


**Figure 52.** Graph showing transition probabilities under the influence of NDVI as a covariate in August, between state 1 and 2 ( $1 \rightarrow 2$ ), state 1 and 3 ( $1 \rightarrow 3$ ), state 2 and 1 ( $2 \rightarrow 1$ ), state 2 and 3 ( $2 \rightarrow 3$ ), state 3 and 1 ( $3 \rightarrow 1$ ), and state 3 and 2 ( $3 \rightarrow 2$ ). The graph also shows persistence probabilities in state 1 ( $1 \rightarrow 1$ ), state 2 ( $2 \rightarrow 2$ ) and in state 3 ( $3 \rightarrow 3$ ).

In September (Table 18, Fig.53-56), when the distance to the nearest road/path was set, persistence in state 3 was higher the further away from the road (Fig.54), as well as  $3 \rightarrow 2$  probability of occurrence was higher near the road and lower with the distance (-1.11). Therefore, the increase in distance from the road inhibited the likelihood of moving from state 3 to state 2. Regarding the influence of distance to the nearest water source, the probability of persisting in state 2 was higher near the water (Fig.55), while the  $2 \rightarrow 1$  increased with distance (+0.59). Considering the NDVI as a covariate, the probability of persisting in state 3 was null at the highest NDVI value (Fig.56). Furthermore,  $3 \rightarrow 1$  and  $2 \rightarrow 1$  probabilities were promoted as the NDVI values increased (+66.24 and +3.08, respectively).

**Table 18.** Regression coefficients for the transition probabilities referred to the month of September. The table shows the probability of transition between state 1 and 2 ( $1 \rightarrow 2$ ), state 1 and 3 ( $1 \rightarrow 3$ ), state 2 and 1 ( $2 \rightarrow 1$ ), state 2 and 3 ( $2 \rightarrow 3$ ), state 3 and 1 ( $3 \rightarrow 1$ ), and state 3 and 2 ( $3 \rightarrow 2$ ). The first row indicates the baseline probability of transition when all the covariates are set to zero. From the second to the fifth row, 4 different covariates and their influence on the transition probabilities are shown.

	Regression coefficients for the transition probabilities						September
	$1 \rightarrow 2$	$1 \rightarrow 3$	$2 \rightarrow 1$	$2 \rightarrow 3$	$3 \rightarrow 1$	$3 \rightarrow 2$	
Intercept	-1.466	-1452.85	-2.071	1.077	-26.902	-3.054	
Terrain roughness	-0.032	-694.761	0.275	0.152	0.236	-0.470	
Min. road/path distance	-0.350	282.184	-0.269	0.152	-1.398	-1.119	
Min. water source distance	0.086	437.579	0.595	0.528	1.396	-0.028	
NDVI	0.383	-1047.92	3.087	-7.719	66.247	8.161	

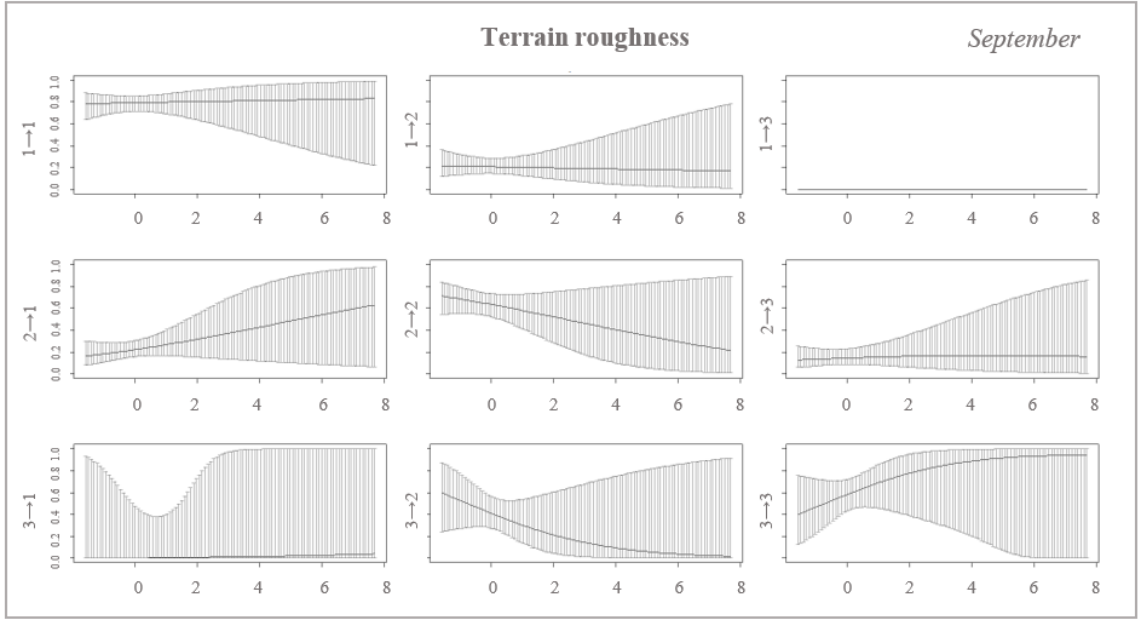


**Figure 53.** Graph showing transition probabilities under the influence of terrain roughness as a covariate in September, between state 1 and 2 ( $1 \rightarrow 2$ ), state 1 and 3 ( $1 \rightarrow 3$ ), state 2 and 1 ( $2 \rightarrow 1$ ), state 2 and 3 ( $2 \rightarrow 3$ ), state 3 and 1 ( $3 \rightarrow 1$ ), and state 3 and 2 ( $3 \rightarrow 2$ ). The graph also shows persistence probabilities in state 1 ( $1 \rightarrow 1$ ), state 2 ( $2 \rightarrow 2$ ) and in state 3 ( $3 \rightarrow 3$ ).

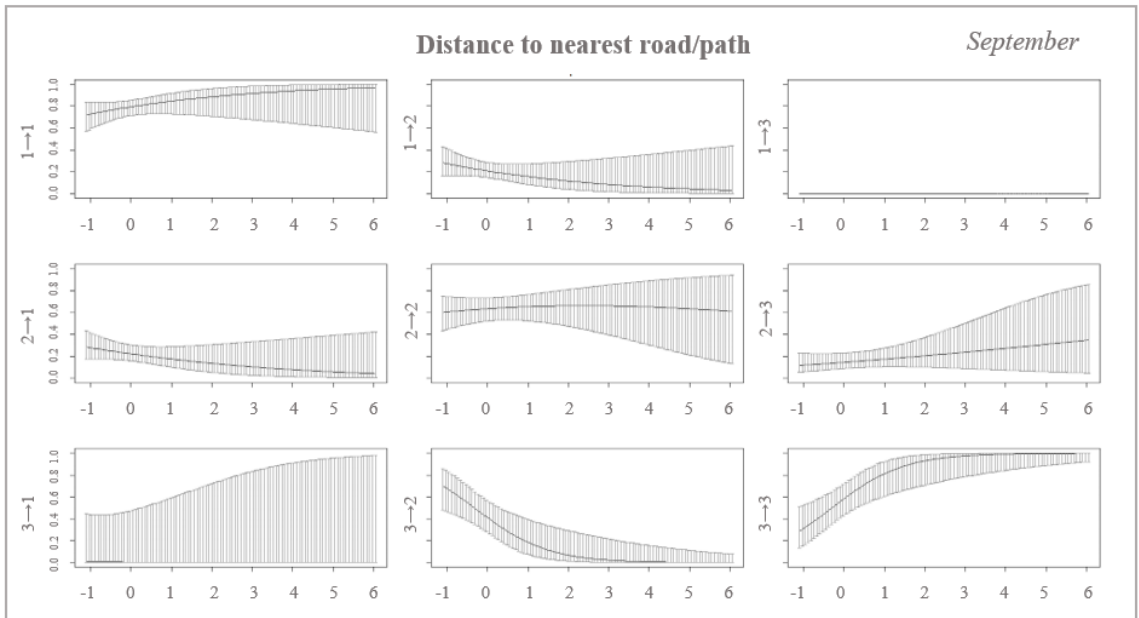


**Figure 54.** Graph showing transition probabilities under the influence of distance to nearest road/path as a covariate in September, between state 1 and 2 ( $1 \rightarrow 2$ ), state 1 and 3 ( $1 \rightarrow 3$ ), state 2 and 1 ( $2 \rightarrow 1$ ), state 2 and 3 ( $2 \rightarrow 3$ ), state 3 and 1 ( $3 \rightarrow 1$ ), and state 3 and 2 ( $3 \rightarrow 2$ ). The graph also shows persistence probabilities in state 1 ( $1 \rightarrow 1$ ), state 2 ( $2 \rightarrow 2$ ) and in state 3 ( $3 \rightarrow 3$ ).

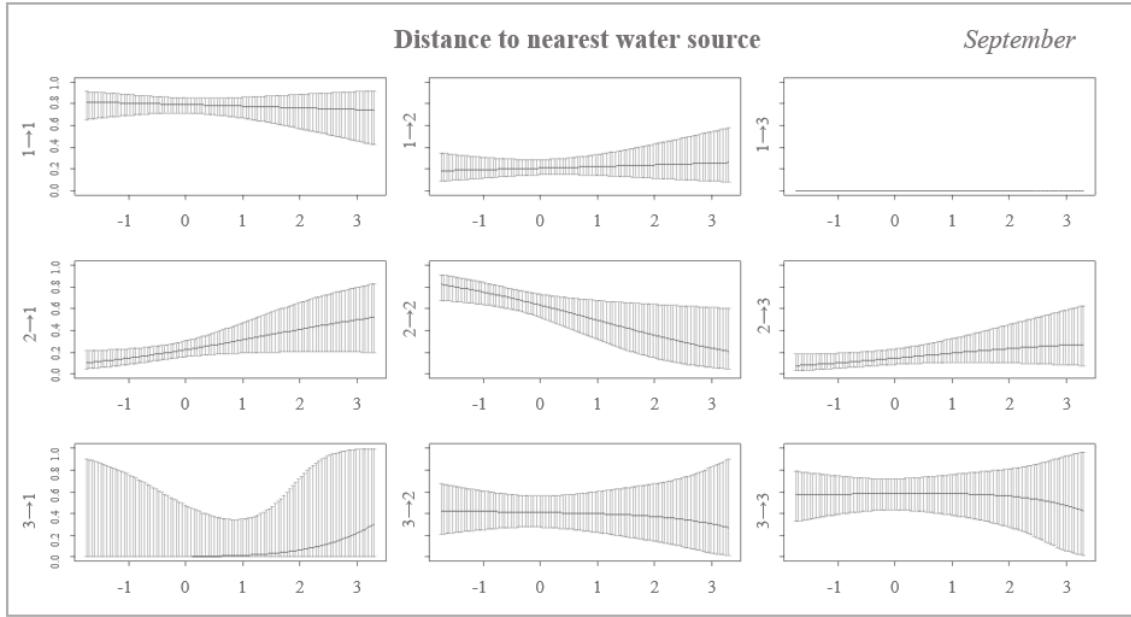


**Figure 55.** Graph showing transition probabilities under the influence of distance to nearest water source as a covariate in September, between state 1 and 2 ( $1 \rightarrow 2$ ), state 1 and 3 ( $1 \rightarrow 3$ ), state 2 and 1 ( $2 \rightarrow 1$ ), state 2 and 3 ( $2 \rightarrow 3$ ), state 3 and 1 ( $3 \rightarrow 1$ ), and state 3 and 2 ( $3 \rightarrow 2$ ). The graph also shows persistence probabilities in state 1 ( $1 \rightarrow 1$ ), state 2 ( $2 \rightarrow 2$ ) and in state 3 ( $3 \rightarrow 3$ ).

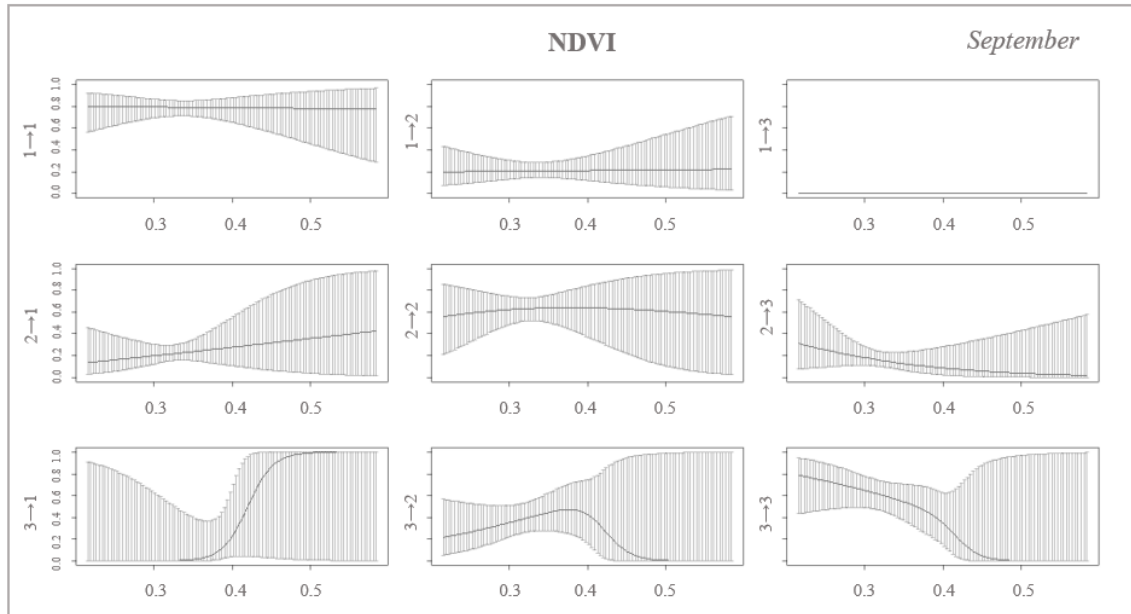


**Figure 56.** Graph showing transition probabilities under the influence of NDVI as a covariate in September, between state 1 and 2 ( $1 \rightarrow 2$ ), state 1 and 3 ( $1 \rightarrow 3$ ), state 2 and 1 ( $2 \rightarrow 1$ ), state 2 and 3 ( $2 \rightarrow 3$ ), state 3 and 1 ( $3 \rightarrow 1$ ), and state 3 and 2 ( $3 \rightarrow 2$ ). The graph also shows persistence probabilities in state 1 ( $1 \rightarrow 1$ ), state 2 ( $2 \rightarrow 2$ ) and in state 3 ( $3 \rightarrow 3$ ).

In October (Table 19, Fig.57-60) when setting the distance to the nearest road/path as a covariate, a persistence in state 1 was greater near the road, increasingly becoming prone to zero as moving away from the road (Fig.58). In support of this, when distance increased, the  $1 \rightarrow 2$  probability was promoted (+0.39) and the  $2 \rightarrow 1$  transition probability was inhibited (-0.22). When considering the influence of the distance to the water source, there was a tendency to transition to state 3 ( $1 \rightarrow 3 = 0.91$ ,  $2 \rightarrow 3 = 0.56$ ) as the distance from the water increased, which was also confirmed by the probability of persisting in state 3, which was higher the further away from the water (Fig.59). Under the influence of the NDVI, the probabilities to move from state 3 to state 2 and then to state 1 were the greatest ( $3 \rightarrow 2 = +65.08$  and  $2 \rightarrow 1 = +15.70$ ) (Fig.60). Persistence in state 1 was higher as the terrain was rougher (Fig.57).

**Table 19.** Regression coefficients for the transition probabilities referred to the month of October. The table shows the probability of transition between state 1 and 2 ( $1 \rightarrow 2$ ), state 1 and 3 ( $1 \rightarrow 3$ ), state 2 and 1 ( $2 \rightarrow 1$ ), state 2 and 3 ( $2 \rightarrow 3$ ), state 3 and 1 ( $3 \rightarrow 1$ ), and state 3 and 2 ( $3 \rightarrow 2$ ). The first row indicates the baseline probability of transition when all the covariates are set to zero. From the second to the fifth row, 4 different covariates and their influence on the transition probabilities are shown.

	Regression coefficients for the transition probabilities						October
	$1 \rightarrow 2$	$1 \rightarrow 3$	$2 \rightarrow 1$	$2 \rightarrow 3$	$3 \rightarrow 1$	$3 \rightarrow 2$	
Intercept	0.134	-9.979	-6.438	1.188	-0.212	-19.627	
Terrain roughness	-0.476	0.372	0.306	-0.522	-0.626	0.043	
Min. road/path distance	0.392	-4.882	-0.222	-0.055	0.108	-0.369	
Min. water source distance	0.023	0.918	0.124	0.566	0.047	-1.110	
NDVI	-4.771	3.236	15.707	-11.945	-3.544	65.083	

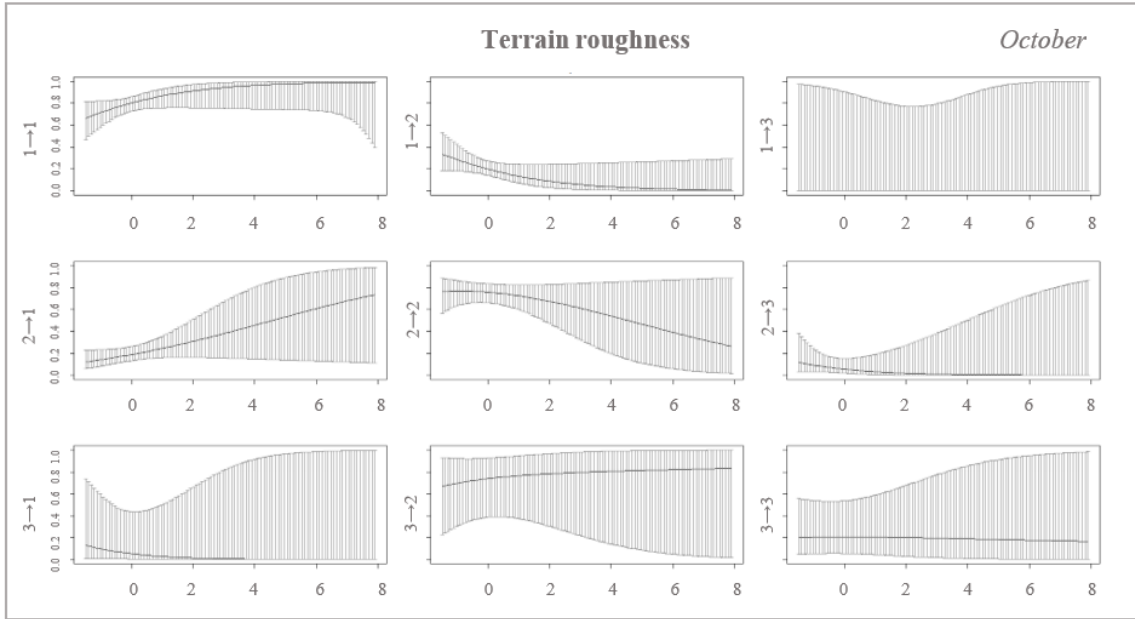


**Figure 57.** Graph showing transition probabilities under the influence of terrain roughness as a covariate in October, between state 1 and 2 ( $1 \rightarrow 2$ ), state 1 and 3 ( $1 \rightarrow 3$ ), state 2 and 1 ( $2 \rightarrow 1$ ), state 2 and 3 ( $2 \rightarrow 3$ ), state 3 and 1 ( $3 \rightarrow 1$ ), and state 3 and 2 ( $3 \rightarrow 2$ ). The graph also shows persistence probabilities in state 1 ( $1 \rightarrow 1$ ), state 2 ( $2 \rightarrow 2$ ) and in state 3 ( $3 \rightarrow 3$ ).

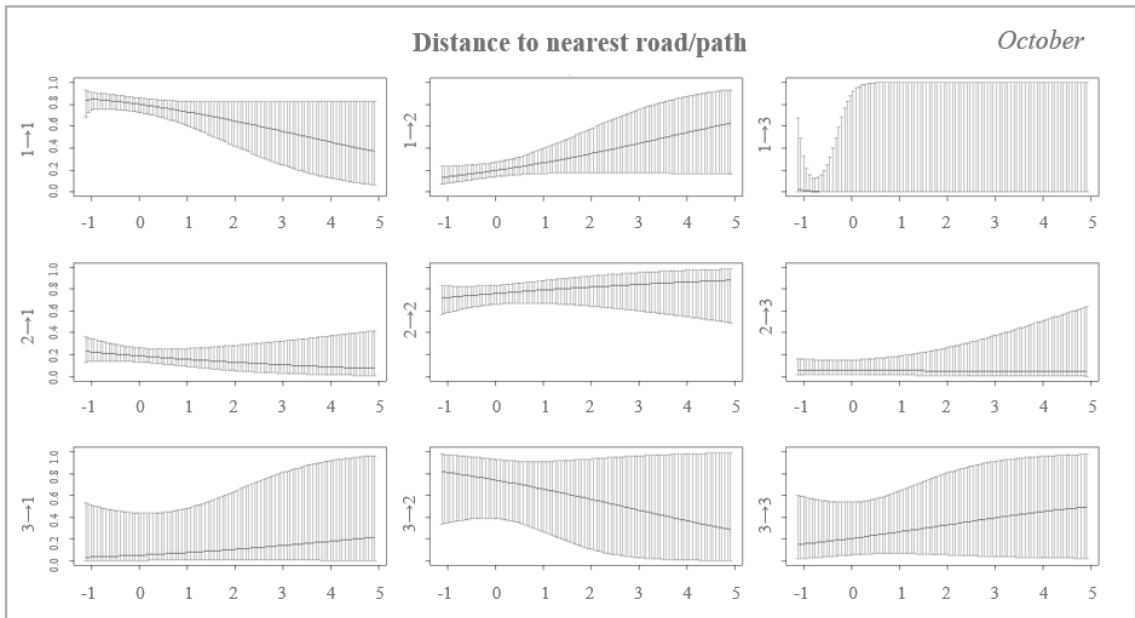


**Figure 58.** Graph showing transition probabilities under the influence of distance to nearest road/path as a covariate in October, between state 1 and 2 ( $1 \rightarrow 2$ ), state 1 and 3 ( $1 \rightarrow 3$ ), state 2 and 1 ( $2 \rightarrow 1$ ), state 2 and 3 ( $2 \rightarrow 3$ ), state 3 and 1 ( $3 \rightarrow 1$ ), and state 3 and 2 ( $3 \rightarrow 2$ ). The graph also shows persistence probabilities in state 1 ( $1 \rightarrow 1$ ), state 2 ( $2 \rightarrow 2$ ) and in state 3 ( $3 \rightarrow 3$ ).

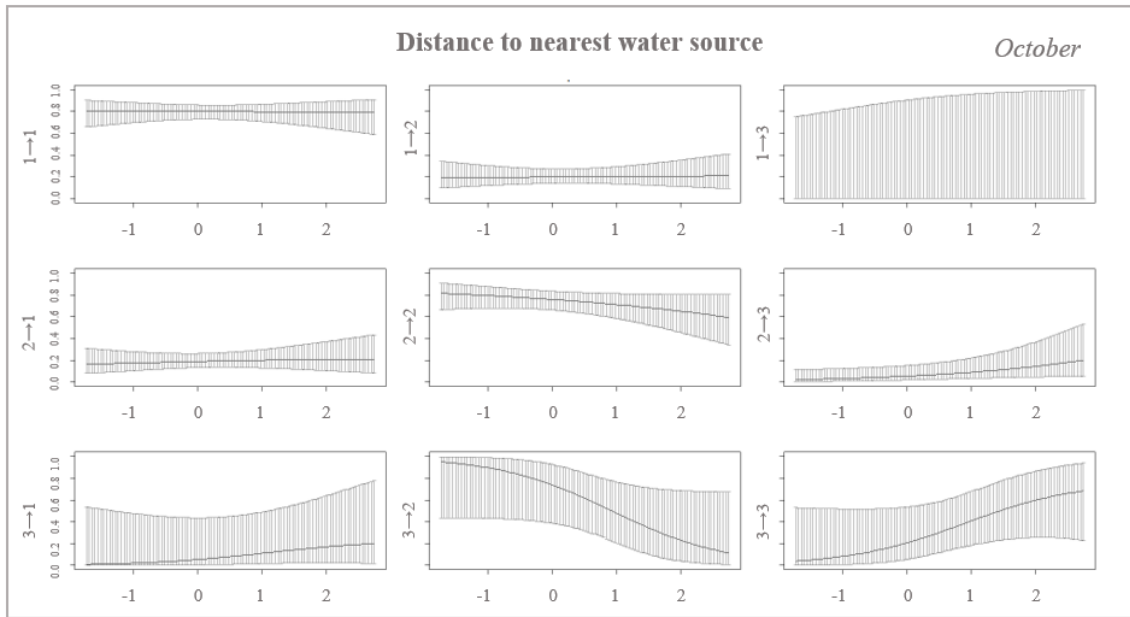


**Figure 59.** Graph showing transition probabilities under the influence of distance to nearest water source as a covariate in October, between state 1 and 2 ( $1 \rightarrow 2$ ), state 1 and 3 ( $1 \rightarrow 3$ ), state 2 and 1 ( $2 \rightarrow 1$ ), state 2 and 3 ( $2 \rightarrow 3$ ), state 3 and 1 ( $3 \rightarrow 1$ ), and state 3 and 2 ( $3 \rightarrow 2$ ). The graph also shows persistence probabilities in state 1 ( $1 \rightarrow 1$ ), state 2 ( $2 \rightarrow 2$ ) and in state 3 ( $3 \rightarrow 3$ ).

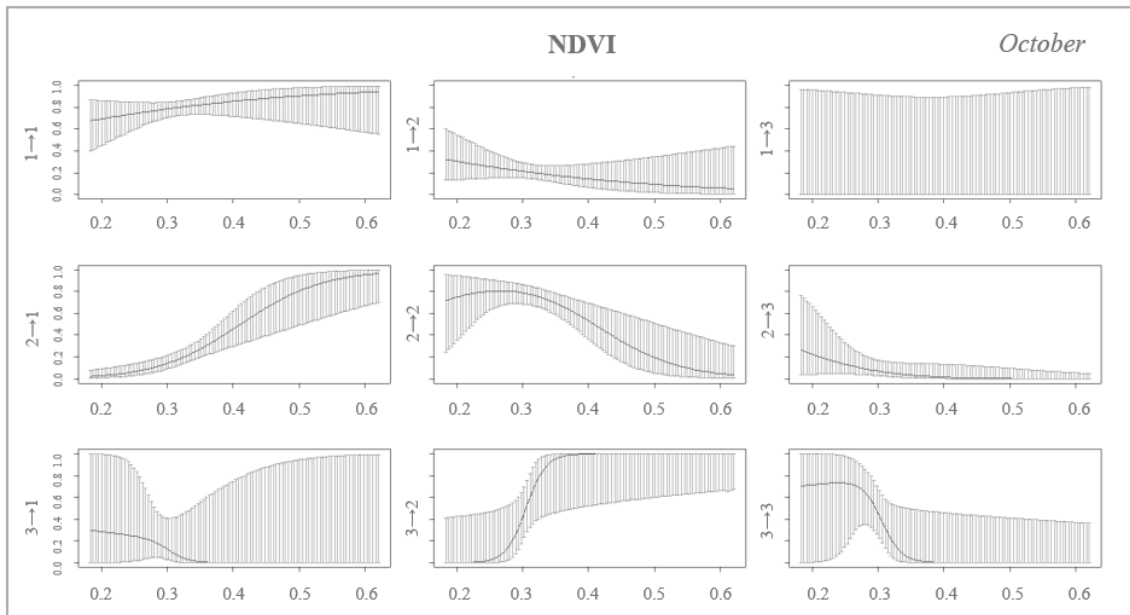


**Figure 60.** Graph showing transition probabilities under the influence of NDVI as a covariate in October, between state 1 and 2 ( $1 \rightarrow 2$ ), state 1 and 3 ( $1 \rightarrow 3$ ), state 2 and 1 ( $2 \rightarrow 1$ ), state 2 and 3 ( $2 \rightarrow 3$ ), state 3 and 1 ( $3 \rightarrow 1$ ), and state 3 and 2 ( $3 \rightarrow 2$ ). The graph also shows persistence probabilities in state 1 ( $1 \rightarrow 1$ ), state 2 ( $2 \rightarrow 2$ ) and in state 3 ( $3 \rightarrow 3$ ).



December (Table 20, Fig.61-64) recorded a high probability of persistence in state 2 in the vicinity of the water source (Fig.63), while as the distance increased, the 2→3 transition probability also increased (+1.23). Under the influence of NDVI as a covariate, an increasingly higher probability of switching to state 1 was showed when the NDVI value was higher (2→1= +28.02) (Fig.64). When considering distance to road, the probability of persisting in state 3 was more elevated when the distance increased, with a maximum peak at the greatest distance (Fig.62). Persistence in state 1 was higher as the rougher was the terrain.

**Table 20.** Regression coefficients for the transition probabilities referred to the month of December. The table shows the probability of transition between state 1 and 2 (1→2), state 1 and 3 (1→3), state 2 and 1 (2→1), state 2 and 3 (2→3), state 3 and 1 (3→1), and state 3 and 2 (3→2). The first row indicates the baseline probability of transition when all the covariates are set to zero. From the second to the fifth row, 4 different covariates and their influence on the transition probabilities are shown.

	Regression coefficients for the transition probabilities						December
	1→2	1→3	2→1	2→3	3→1	3→2	
Intercept	-3.446	-29.723	-22.761	0.471	1.213	-41.165	
Terrain roughness	-0.438	3.503	-2.136	0.342	-0.086	-0.400	
Min. road/path distance	-0.091	4.780	-0.397	-4.129	-0.927	-8.763	
Min. water source distance	0.278	0.831	0.060	1.238	0.108	2.140	
NDVI	3.446	-16.286	28.029	-6.504	-2.399	54.843	

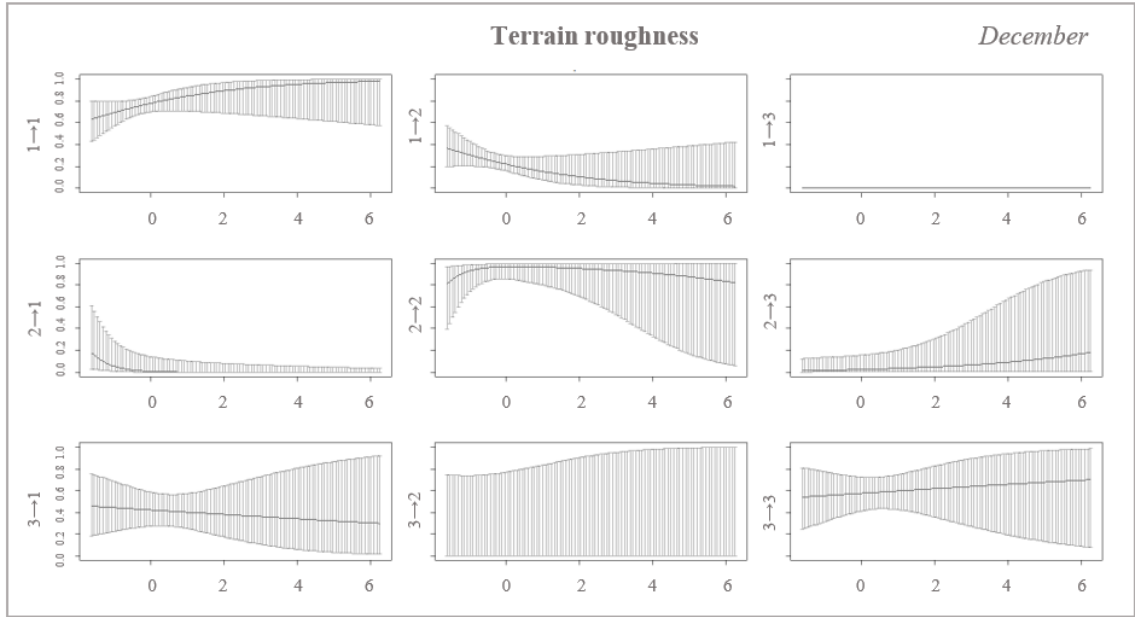


**Figure 61.** Graph showing transition probabilities under the influence of terrain roughness as a covariate in December, between state 1 and 2 ( $1 \rightarrow 2$ ), state 1 and 3 ( $1 \rightarrow 3$ ), state 2 and 1 ( $2 \rightarrow 1$ ), state 2 and 3 ( $2 \rightarrow 3$ ), state 3 and 1 ( $3 \rightarrow 1$ ), and state 3 and 2 ( $3 \rightarrow 2$ ). The graph also shows persistence probabilities in state 1 ( $1 \rightarrow 1$ ), state 2 ( $2 \rightarrow 2$ ) and in state 3 ( $3 \rightarrow 3$ ).

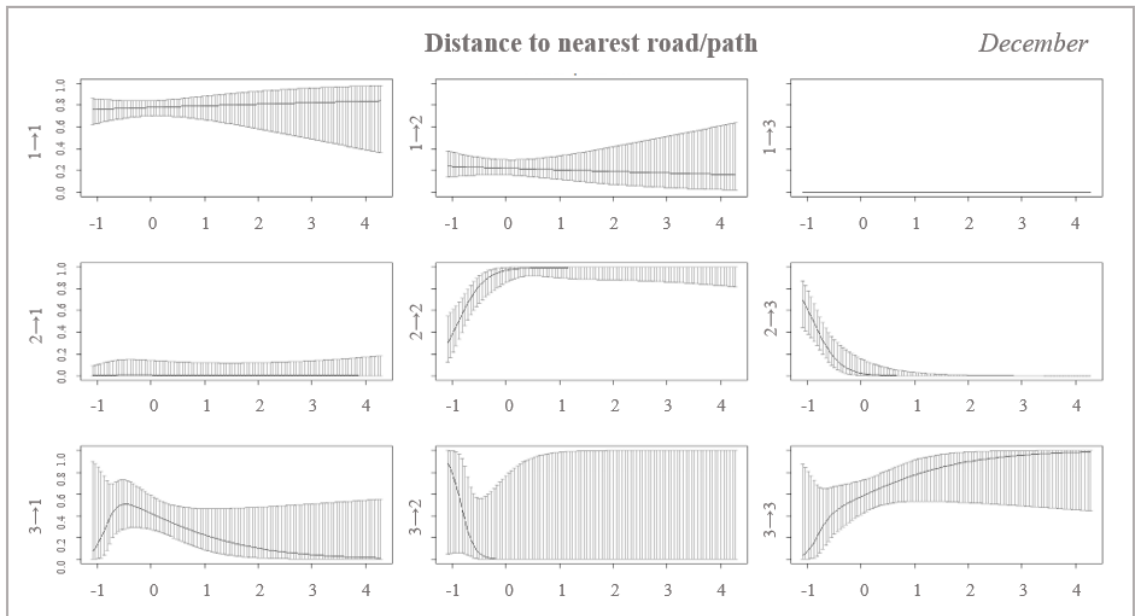


**Figure 62.** Graph showing transition probabilities under the influence of distance to nearest road/path as a covariate in December, between state 1 and 2 ( $1 \rightarrow 2$ ), state 1 and 3 ( $1 \rightarrow 3$ ), state 2 and 1 ( $2 \rightarrow 1$ ), state 2 and 3 ( $2 \rightarrow 3$ ), state 3 and 1 ( $3 \rightarrow 1$ ), and state 3 and 2 ( $3 \rightarrow 2$ ). The graph also shows persistence probabilities in state 1 ( $1 \rightarrow 1$ ), state 2 ( $2 \rightarrow 2$ ) and in state 3 ( $3 \rightarrow 3$ ).

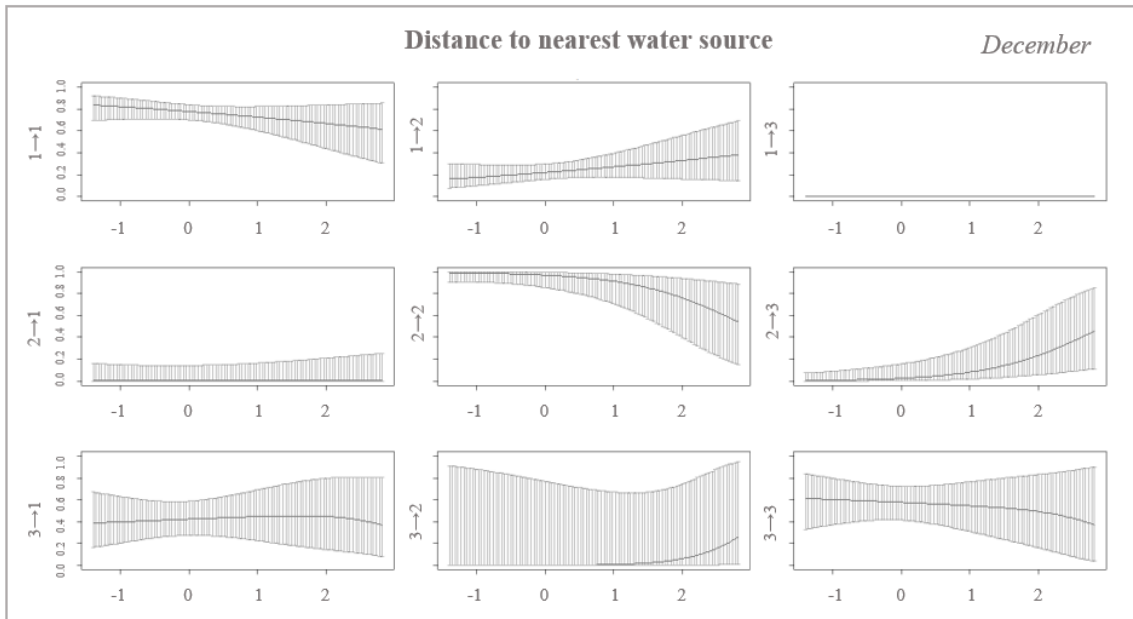


**Figure 63.** Graph showing transition probabilities under the influence of distance to nearest water source as a covariate in December, between state 1 and 2 ( $1 \rightarrow 2$ ), state 1 and 3 ( $1 \rightarrow 3$ ), state 2 and 1 ( $2 \rightarrow 1$ ), state 2 and 3 ( $2 \rightarrow 3$ ), state 3 and 1 ( $3 \rightarrow 1$ ), and state 3 and 2 ( $3 \rightarrow 2$ ). The graph also shows persistence probabilities in state 1 ( $1 \rightarrow 1$ ), state 2 ( $2 \rightarrow 2$ ) and in state 3 ( $3 \rightarrow 3$ ).

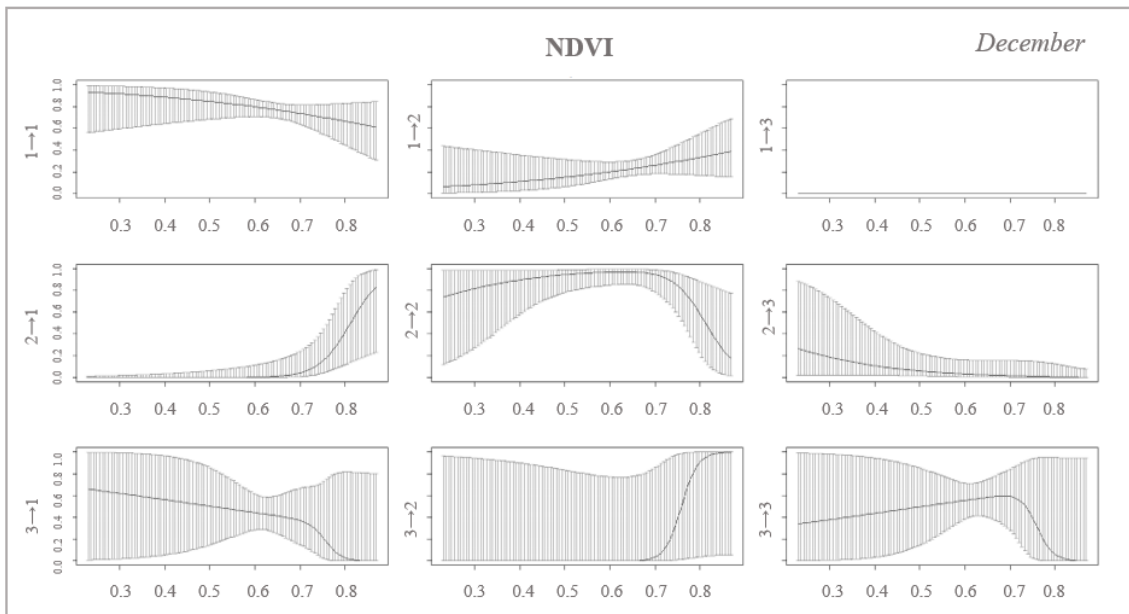


**Figure 64.** Graph showing transition probabilities under the influence of NDVI as a covariate in December, between state 1 and 2 ( $1 \rightarrow 2$ ), state 1 and 3 ( $1 \rightarrow 3$ ), state 2 and 1 ( $2 \rightarrow 1$ ), state 2 and 3 ( $2 \rightarrow 3$ ), state 3 and 1 ( $3 \rightarrow 1$ ), and state 3 and 2 ( $3 \rightarrow 2$ ). The graph also shows persistence probabilities in state 1 ( $1 \rightarrow 1$ ), state 2 ( $2 \rightarrow 2$ ) and in state 3 ( $3 \rightarrow 3$ ).

The overall analysis of transition probabilities considering all 7 months as a whole showed trends that mirrored the analysis on a monthly scale (Table 21, Fig.65-68): terrain roughness as a covariate influenced the transition probability by favouring the transition to state 1 the rougher the terrain was ( $3 \rightarrow 2 = +0.10$ ,  $2 \rightarrow 1 = +0.18$ , and  $1 \rightarrow 2 = -0.20$ ) (Fig.65); considering the distance to the nearest road/path as a predictor variable, the transition probabilities were in favour of moving to state 3 the further away from the road ( $1 \rightarrow 2 = +0.10$  and  $2 \rightarrow 3 = +0.24$ ) and persisting in such state at the greatest distance from the road (Fig.66); when distance from the water source was considered, a prevalence of occurrence in state 2 was recorded (Fig.67); when the NDVI was set as a covariate, state 1 was the most probable as the NDVI value increased ( $2 \rightarrow 1 = +1.47$  and  $3 \rightarrow 1 = +2.69$ ) (Fig.68).

**Table 21.** Regression coefficients for the transition probabilities referred to the month from June to December combined as a whole. The table shows the probability of transition between state 1 and 2 ( $1 \rightarrow 2$ ), state 1 and 3 ( $1 \rightarrow 3$ ), state 2 and 1 ( $2 \rightarrow 1$ ), state 2 and 3 ( $2 \rightarrow 3$ ), state 3 and 1 ( $3 \rightarrow 1$ ), and state 3 and 2 ( $3 \rightarrow 2$ ). The first row indicates the baseline probability of transition when all the covariates are set to zero. From the second to the fifth row, 4 different covariates and their influence on the transition probabilities are shown.

	Regression coefficients for the transition probabilities				June-to-December	
	$1 \rightarrow 2$	$1 \rightarrow 3$	$2 \rightarrow 1$	$2 \rightarrow 3$	$3 \rightarrow 1$	$3 \rightarrow 2$
Intercept	0.255	-2.420	-1.978	-2.566	-5.136	-1.608
Terrain roughness	-0.020	-0.575	0.180	0.036	-1.084	0.103
Min. road/path distance	0.103	0.032	0.079	0.241	-0.234	-0.151
Min. water source distance	-0.109	-0.071	0.050	0.266	0.367	-0.061
NDVI	-2.235	1.530	1.477	1.914	2.692	0.325

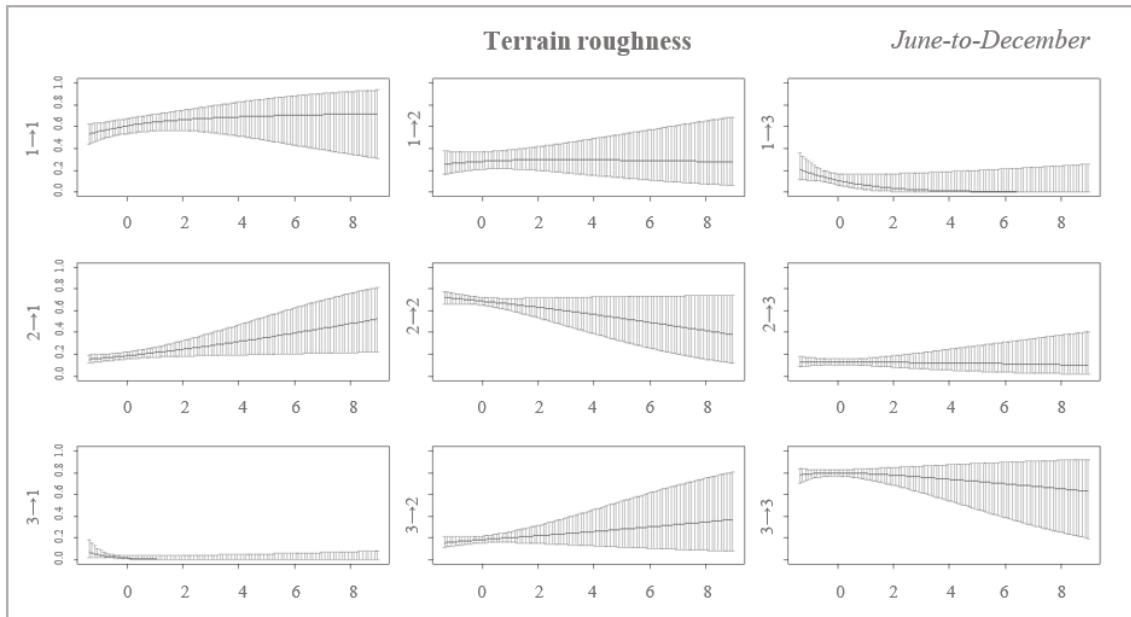


**Figure 65.** Graph showing transition probabilities under the influence of terrain roughness as a covariate for the 7-month period (June to December), between state 1 and 2 ( $1 \rightarrow 2$ ), state 1 and 3 ( $1 \rightarrow 3$ ), state 2 and 1 ( $2 \rightarrow 1$ ), state 2 and 3 ( $2 \rightarrow 3$ ), state 3 and 1 ( $3 \rightarrow 1$ ), and state 3 and 2 ( $3 \rightarrow 2$ ). The graph also shows persistence probabilities in state 1 ( $1 \rightarrow 1$ ), state 2 ( $2 \rightarrow 2$ ) and in state 3 ( $3 \rightarrow 3$ ).

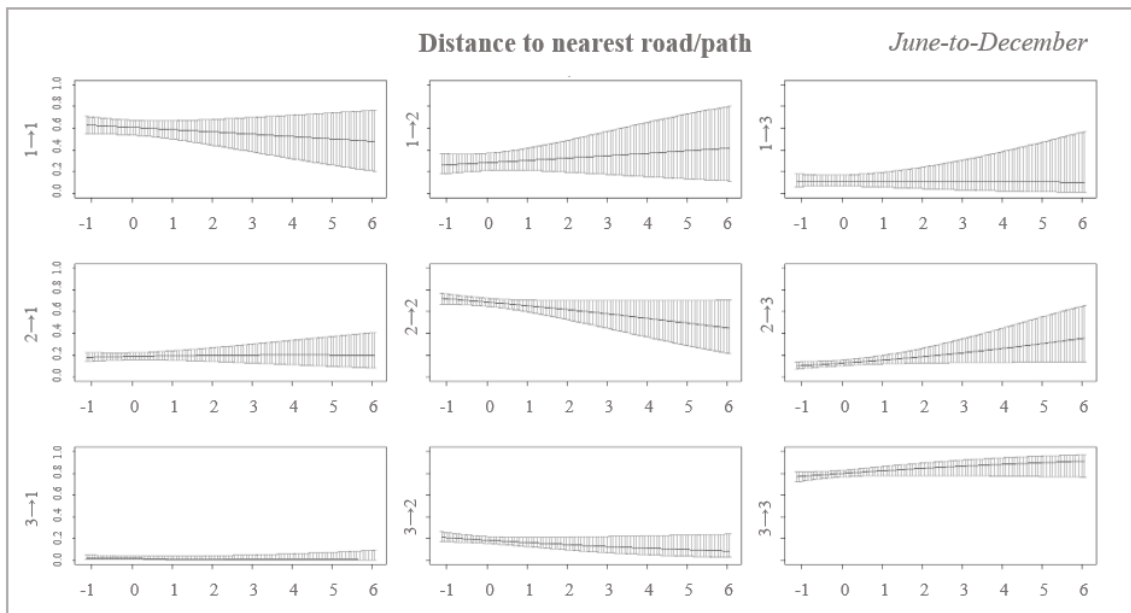


**Figure 66.** Graph showing transition probabilities under the influence of distance to nearest road/path as a covariate for the 7-month period (June to December), between state 1 and 2 ( $1 \rightarrow 2$ ), state 1 and 3 ( $1 \rightarrow 3$ ), state 2 and 1 ( $2 \rightarrow 1$ ), state 2 and 3 ( $2 \rightarrow 3$ ), state 3 and 1 ( $3 \rightarrow 1$ ), and state 3 and 2 ( $3 \rightarrow 2$ ). The graph also shows persistence probabilities in state 1 ( $1 \rightarrow 1$ ), state 2 ( $2 \rightarrow 2$ ) and in state 3 ( $3 \rightarrow 3$ ).

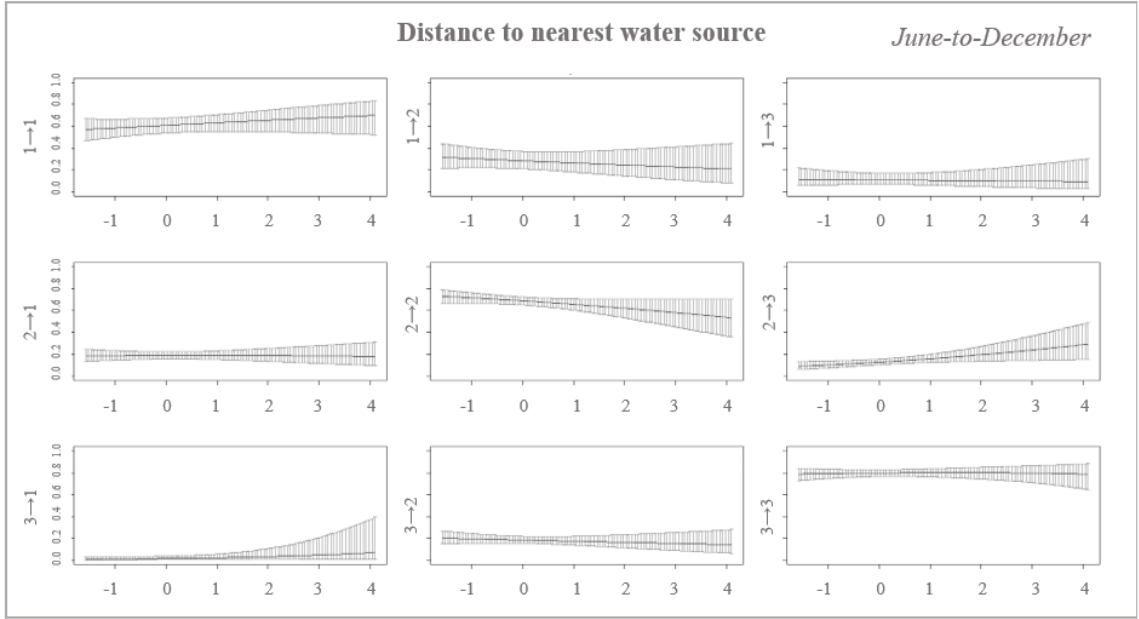


**Figure 67.** Graph showing transition probabilities under the influence of distance to nearest water source as a covariate for the 7-month period (June to December), between state 1 and 2 ( $1 \rightarrow 2$ ), state 1 and 3 ( $1 \rightarrow 3$ ), state 2 and 1 ( $2 \rightarrow 1$ ), state 2 and 3 ( $2 \rightarrow 3$ ), state 3 and 1 ( $3 \rightarrow 1$ ), and state 3 and 2 ( $3 \rightarrow 2$ ). The graph also shows persistence probabilities in state 1 ( $1 \rightarrow 1$ ), state 2 ( $2 \rightarrow 2$ ) and in state 3 ( $3 \rightarrow 3$ ).

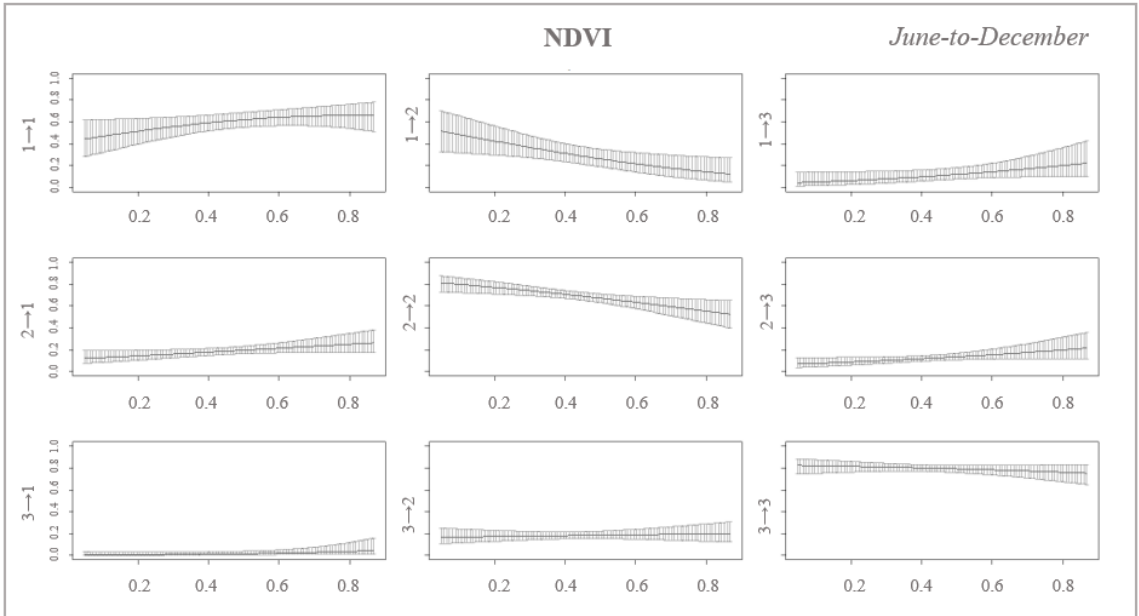


**Figure 68.** Graph showing transition probabilities under the influence of NDVI as a covariate for the 7-month period (June to December), between state 1 and 2 ( $1 \rightarrow 2$ ), state 1 and 3 ( $1 \rightarrow 3$ ), state 2 and 1 ( $2 \rightarrow 1$ ), state 2 and 3 ( $2 \rightarrow 3$ ), state 3 and 1 ( $3 \rightarrow 1$ ), and state 3 and 2 ( $3 \rightarrow 2$ ). The graph also shows persistence probabilities in state 1 ( $1 \rightarrow 1$ ), state 2 ( $2 \rightarrow 2$ ) and in state 3 ( $3 \rightarrow 3$ ).

The results regarding the stationary state probabilities were analysed covariate by covariate (Fig.69-74).

Considering the terrain roughness as a covariate, the stationary state probabilities reflected the same results across all the months analysed (Fig.69-73), with a higher probability of lying in state 1 as the roughness value increased and lying in state 2 at the lowest roughness value. This trend was also confirmed by the 7-month period analysis (Fig.74).

When setting the distance to the nearest road/path, the result differed between months. While June showed a stationary state probability of being in state 1 and 2 at the greatest distance from the road (Fig.69), August indicated a higher probability of staying in state 3 (Fig.70). In September, it was recorded an extremely high prevalence of state 3 as distance from the road augmented (Fig.71), while state 2 prevailed in October under the same conditions (Fig.72). The latter was also found in December (Fig.73), with a remarkably elevated probability. However, combining all months together, the occurrence in state 3 was the highest as distance from the road increased (Fig.74).

Under the influence of distance to the nearest water source as a predictor variable, in June at the nearest distance there was a higher probability of lying in state 1, whereas, at the maximum distance, state 2 was prevalent (Fig.69), as in August (Fig.70). September and October showed similar trends (Fig.71-72), with higher probabilities of lying in state 2 near water and state 1 far from water. December recorded a remarkably high value of being in state 2 in the proximity of water (Fig.73). However, although with very similar values between states, state 3 was the most likely when away from water (Fig.74).

The influence of the NDVI as a covariate was consistent across all the months. Even if with different grades of probability, lying in state 1 was the most probable at the highest values of NDVI throughout the analysed months (Fig.69-74).

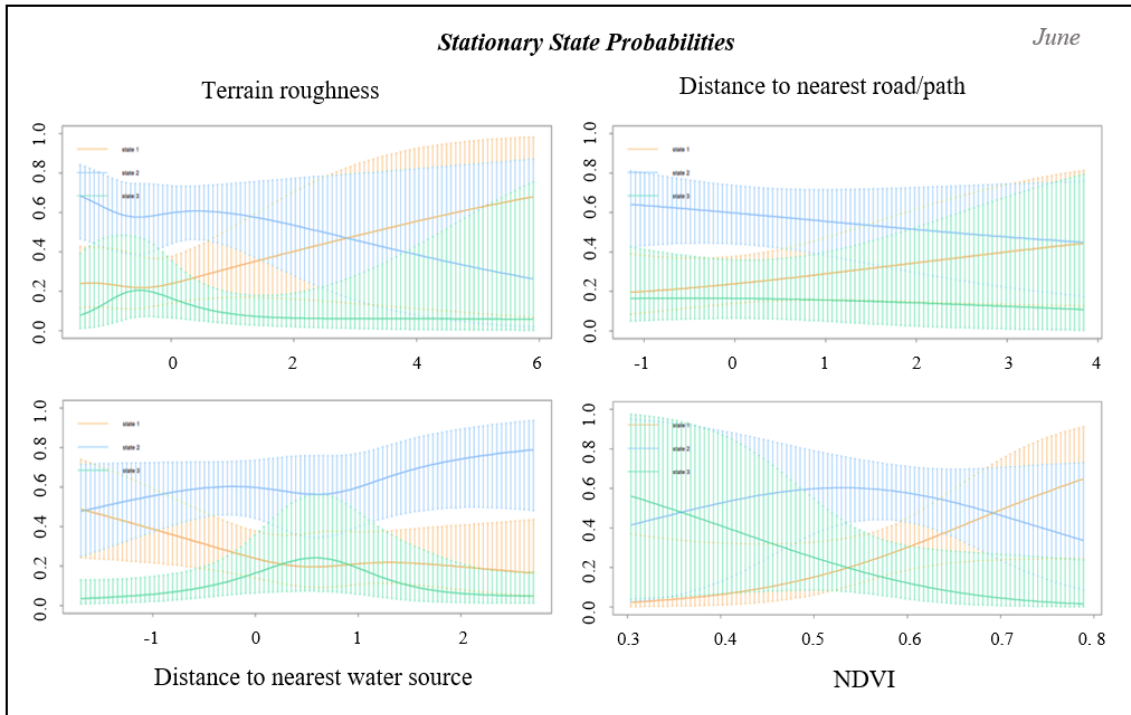


**Figure 69.** Graph showing stationary state probabilities for each covariate in June.

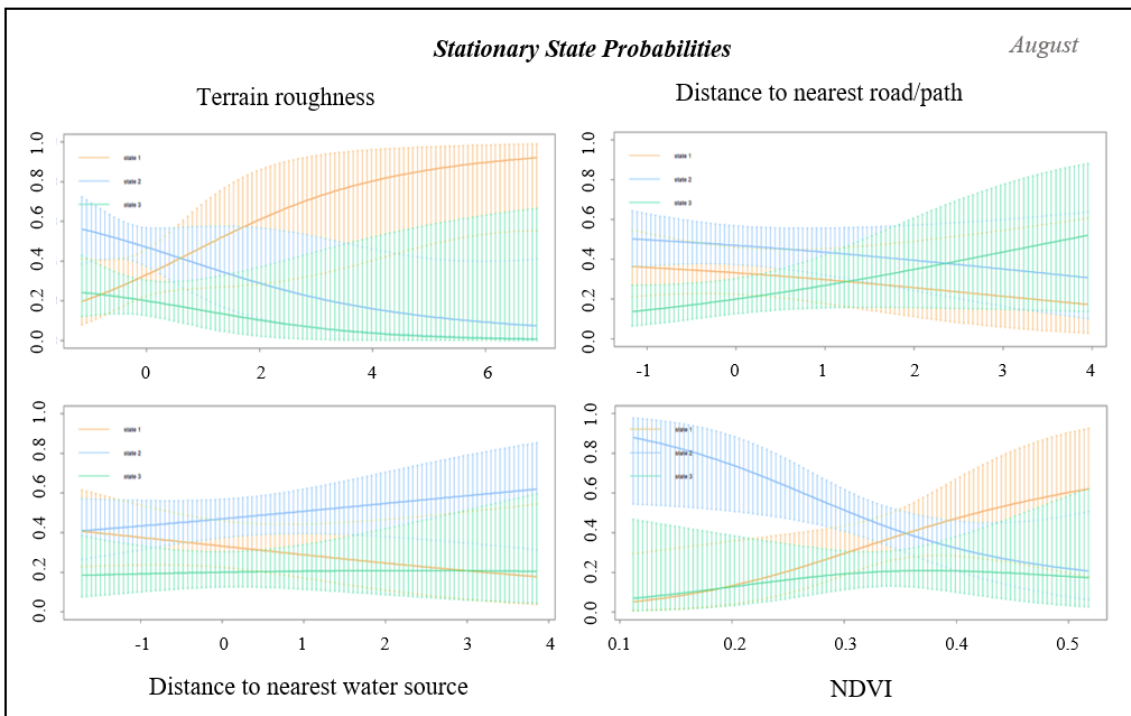


**Figure 70.** Graph showing stationary state probabilities for each covariate in August.



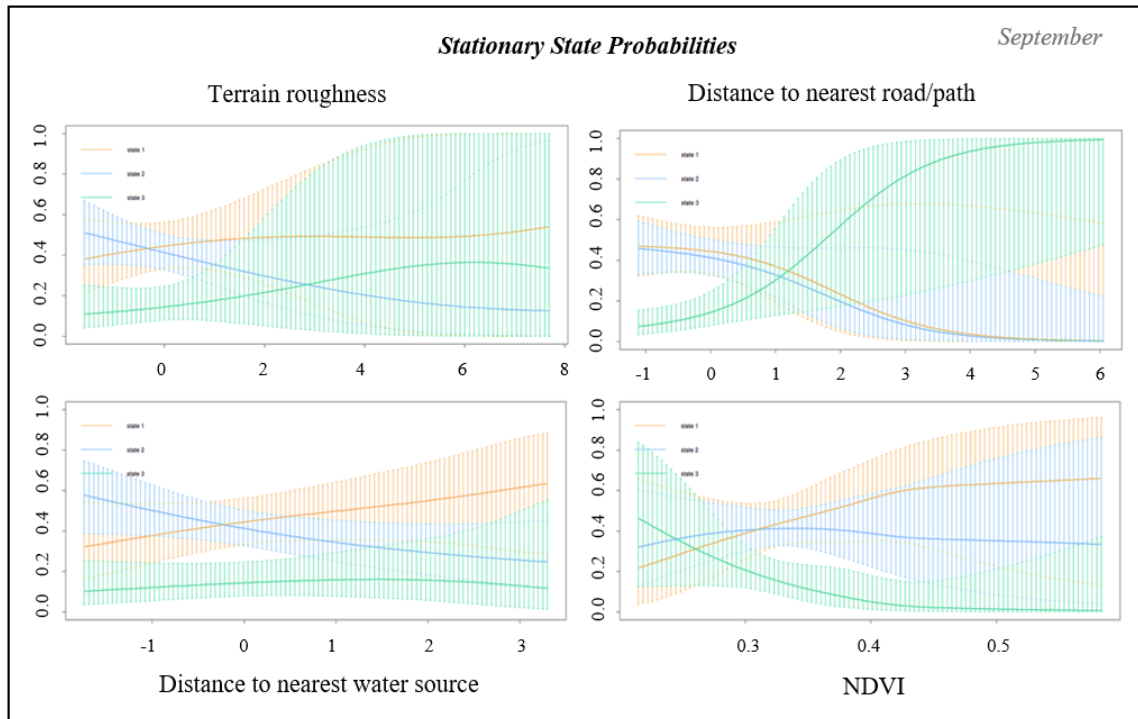


**Figure 71.** Graph showing stationary state probabilities for each covariate in September.

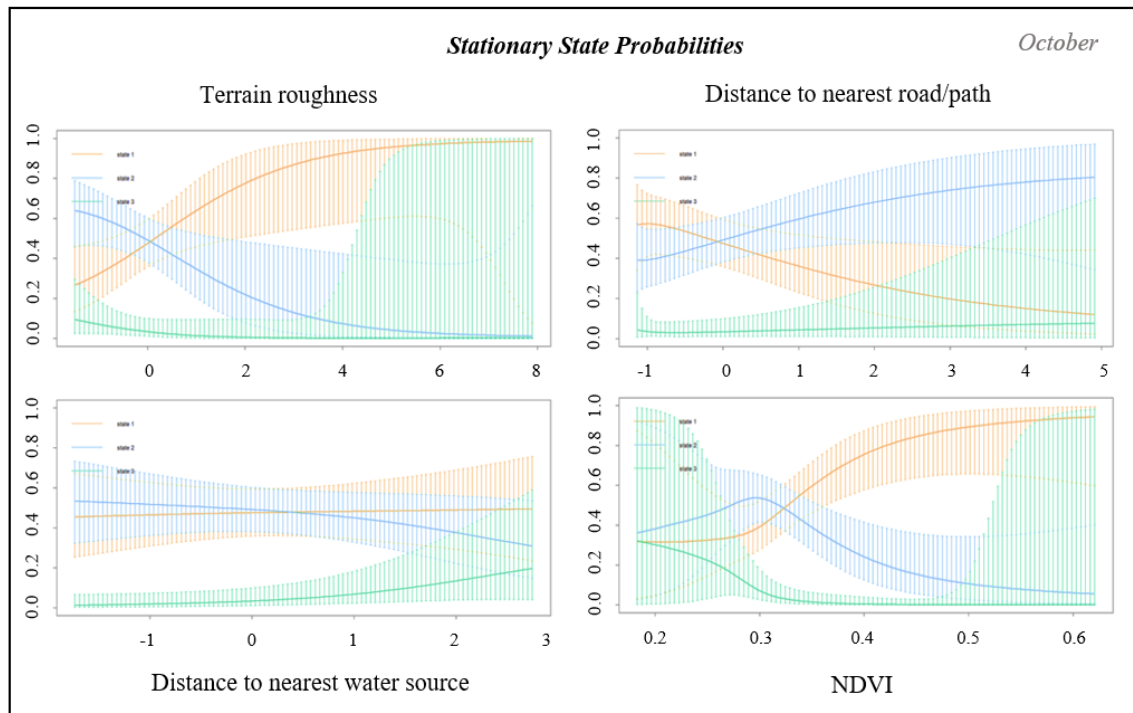


**Figure 72.** Graph showing stationary state probabilities for each covariate in October.

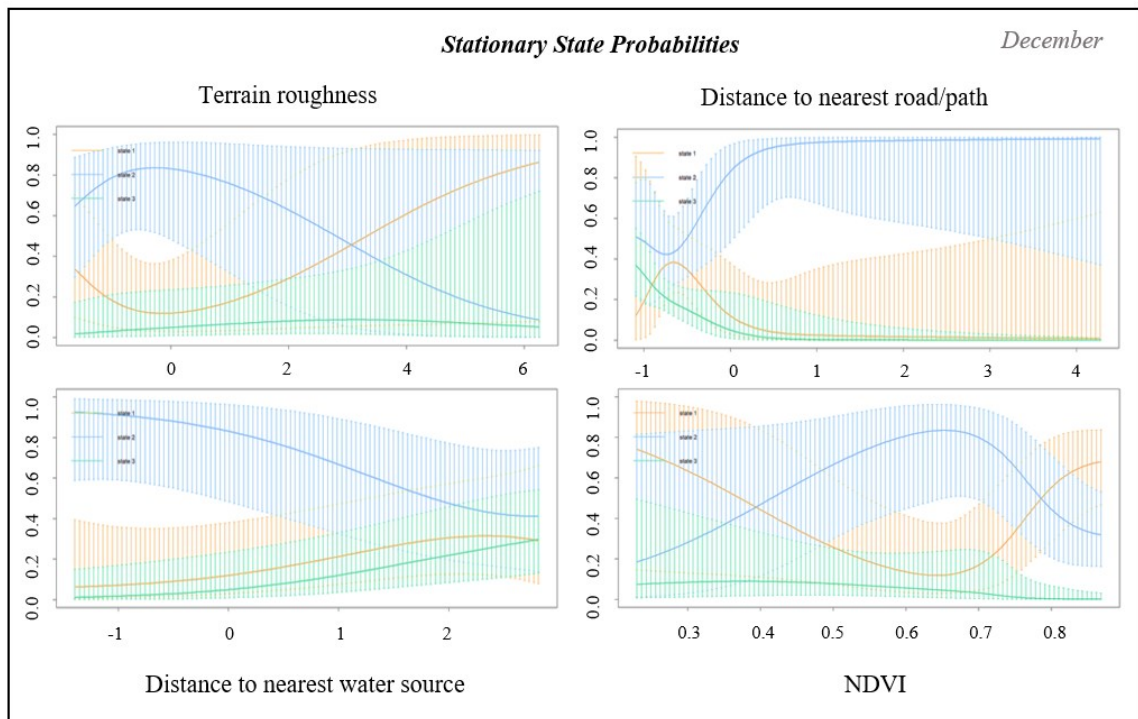


**Figure 73.** Graph showing stationary state probabilities for each covariate in December.

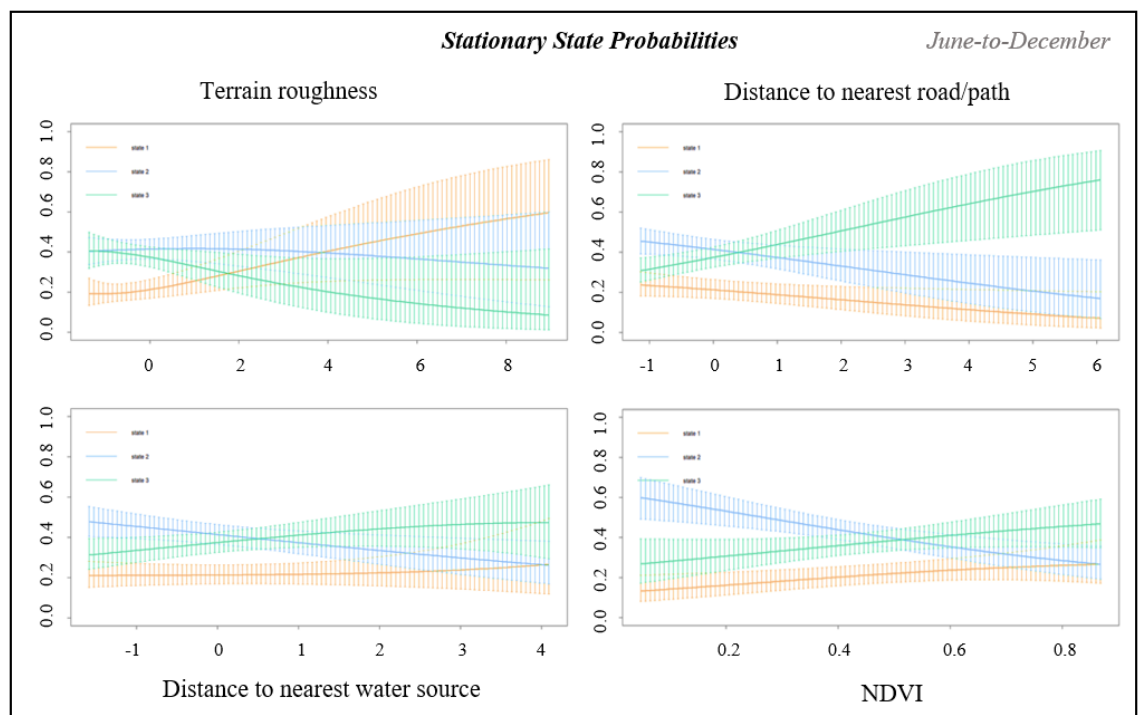


**Figure 74.** Graph showing stationary state probabilities for each covariate combining all the months.

## 4 DISCUSSION

Although elephant movements are complex and season-dependent (Young *et al.*, 2009a; Young *et al.*, 2009b; de Beer and van Aarde, 2008; Leggett, 2006; Cushman *et al.*, 2005; Douglas-Hamilton *et al.*, 2005), this study succeeded in delineating the movement patterns of two matriarchs within the SGR, a fenced reserve in South Africa. Furthermore, it demonstrated how external variables -namely in this study terrain roughness, distance to nearest road/path, distance to nearest water source, and NDVI- exerted a significant influence on movement patterns, as well as on the prediction of movements. Indeed, consistent results were found for each predictor variable throughout the analysed period, on a monthly scale and between different individuals.

From the analysis of the seven months combined, the step length mean for each state of the two matriarchs was consistent between the two individuals. Additionally, consistency was also found with a previous study, which analysed 155 elephants over 21 years (Berti *et al.*, 2023). This concordance with the latter indicated a great accuracy of the model used to study matriarchs' movements, denoting how well the chosen parameters fit the data. Nonetheless, on a monthly scale, the second matriarch, Jean, showed a longer average step length of 30.5%, 76% and 37% in states 1, 2 and 3, respectively, compared to the step length mean of the first matriarch, Elza. A valid hypothesis to explain this difference, which was particularly pronounced only in certain months, could be the presence of more calves in Elza's herd than in Jean's during the evaluated period. This theory could explain why Elza's pace was found to be slower than Jean's. It was verified that during the aerial census of September 2022, four calves under one year old were found in different herds. However, it could not be determined whether one of these herds was Elza's. Nonetheless, studying the influence of calves on herd's pace, Taylor *et al.* (2022) concluded that adult elephants may not need to adapt their speed because of the presence of calves. However, it should be noted that this research was the first on this topic, thus further analyses may be necessary to confirm or refute these results. Evaluating overall rather than on a monthly scale, the difference between the average step length of the two matriarchs has narrowed considerably; therefore, it is conceivable that as the months passed, the calves grew up and influenced the rhythm of the herds less.

A prevalence of time spent in state 1 was found, especially for Elza, during the wet months included in this study (i.e., November and December). The analysis revealed that Jean commenced to increase its time spent in state 1 from October onwards. This slight discrepancy between the two individuals can be explained by the fact that October is generally classified as a transition month between the two seasons, it is therefore plausible that different matriarchs change their movement behaviour with a gap of few weeks. In contrast, during the months belonging to the dry season analysed in this study (i.e., from June to September-October), both individuals spent more time mainly in states 2 and 3, with a peak in August. This may reflect the need to move more within the reserve when resource availability decreased, in order to reach areas with still available forage sources. On the contrary, with the transition to the wet season, they exhibited an important shift to short steps. This shift likely occurred because the flourishing of food availability, after months of scarcity, led them to dedicate more time foraging and feeding than before. These results are in contrast to some previous papers (Vogel *et al.*, 2020; Birkett *et al.*, 2012; Loarie *et al.*, 2009), which found a lower movement velocity during the dry season and an increase in speed during the wet season. However, it is essential to note that the matriarchs' movements analysed in this study were constrained by fences. In contrast, the previously mentioned studies encompassed open systems of vast extent, such as KNP (Birkett *et al.*, 2012), the Okavango Delta (Vogel *et al.*, 2020), and transboundary areas spanning different countries (Loarie *et al.*, 2009). Therefore, the seemingly contrasting results must be contextualised within the difference in available space for elephants. In light of this, the findings may be plausible and consistent with the extent of the fenced reserve considered, in which these matriarchs have lived for several years, and of which they have developed a great knowledge of where each resource is available and at what time of year. As the dry season reached its peak, there was an observable increase in the time spent in states 2 and 3 by the matriarchs. Their movements during this period appeared to be direct and precise, suggesting their intent to reach specific areas of the reserve. These areas were likely chosen based on their past experiences with the presence of foraging resources during that time of year. Furthermore, the main constraint that justified the results of the cited articles was the low availability of water during the dry season in such open systems, which forced the elephants to a smaller home range than during the wet season (Vogel *et al.*, 2020; Birkett *et al.*, 2012; Loarie *et al.*, 2009). This major limitation may have been overcome within the SGR due to the large number of artificial water points operating throughout the dry season. Therefore, not having such constraint in a relatively small closed system, conceivably

matriarchs decided to move more during the dry season in order to exploit areas with more availability of food supply. Likewise, having limited possibilities for large migrations, they probably decided to settle for longer periods in highly productive areas during the wet season.

#### **4.1 Terrain roughness**

In previous studies on elephant movements, changes in elevation or energy landscapes were included as a covariate for large areas (Berti *et al.*, 2023; Evans *et al.*, 2020; Songhrust *et al.*, 2016; Bohrer *et al.*, 2014). Williams *et al.* (2018) also included terrain roughness as a covariate to assess the correlation with movement pattern, within a 40,000 km<sup>2</sup> corridor area in south-eastern Kenya. However, they stated that no major influence of terrain roughness on elephant movement was found, whereas elevation played a key role in elephant movement. Notwithstanding, within the SGR, a fenced reserve of 258 km<sup>2</sup>, relatively small compared with the areas considered in such studies, the elevation seemed to not play a notable role, due to the geographical and topographical characteristics of the reserve itself. The latter, instead, comprises a great diversity in terrain roughness, due to mixed soil composition, and topography. Therefore, it seemed more logical to include it as covariate, since hills, valleys, drainages, changes in soil composition, slope, and ruggedness may have been important drivers on movement patterns. Therefore, Elza and Jean movements were analysed under the influence of the terrain roughness as a predictor variable. At the lowest values of roughness, Elza showed a higher probability of being in state 2, whereas Jean an equal probability of occurring in state 2 or 3. At the highest values of roughness, both Elza and Jean showed a higher probability of occurrence in state 1, generally. While Jean showed the exact same results across each month, Elza, instead, exhibited a weaker influence of such covariate on its movements as closer to the wet period. Overall, a strong occurrence in state 1 as the terrain became rougher was found in both matriarchs when combining the seven months together. These results indicated that when Elza's and Jean's herds had to travel long distances (i.e., they persisted in state 3), they preferred flatter areas to facilitate their movements. Furthermore, they switched to state 1 whenever they crossed areas with high roughness values because rough terrain can present obstacles that the elephants must circumvent. Steep slopes or drainages, for example, may limit their speed and movement in certain directions, forcing them to slow down and, hence, to switch to state 1. In particular, seasonal drainages can be classified as

rough terrain not only when they are full, but also when they are empty, as they often present irregular and rough terrain characteristics. These features may include rocky surfaces, debris, uneven terrain and even small cliffs or embankments. These terrain variations can make the elephants' movement more challenging. Hence, this phenomenon may elucidate why, when matriarchs selected a path necessitating the crossing of one of these soil types, they displayed a tendency to transition to state 1 upon approaching that particular soil type. Consequently, they remained in that state for as long as the soil roughness value remained elevated.

#### **4.2 Distance to nearest road/path**

The influence of distance to the nearest road/path was estimated using the road/path network of the reserve as a covariate. Previous research has estimated the most likely route of elephants based on their movements (Duffy *et al.*, 2011; Cushman and Huettmann 2010; Shannon *et al.*, 2009). In contrast, this study aimed to assess the influence of the existing road/path network within the reserve, which is also regularly used by rangers' and ecotourism guides' vehicles. In particular, the aim was to assess whether elephants used such paths as corridors or game path, and in what way. The findings regarding the influence of this predictor variable were consistent between the two matriarchs Elza and Jean. Combining the results of the transition probabilities and stationary state probabilities, it is worth noting that both matriarchs exhibited a limited influence of the nearest road or path on a particular state between June and August. In general, during this period, they displayed a stronger tendency to persist in states 1 and 2 when located farther away from the road. However, when in proximity to the closest road, they displayed a preference for transitioning to state 2-3. On the contrary, between September and December, persistence in state 2-3 was consistently found further away from the road, whereas at the nearest distance from it, occurrence in state 1 was the most likely. The period between June and August corresponded to the driest months of that year, when the vegetation was rapidly drying up. Thus, the results may explain the matriarchs' need to move more rapidly within the reserve in order to reach areas where food was still available as soon as possible. Consequently, the persistence of medium-to-long steps when on roads/paths may represent their use of these roads as corridors. This explanation is consistent with the study conducted by Vogel *et al.* (2020), which discovered that elephants use corridors when they

want to move quickly and directionally through vegetation and the environment. Additionally, the study conducted by Tsalyuk *et al.* (2019) discovered that when elephants needed to traverse the landscape, they exhibited a preference for utilizing roads, as these pathways enabled them to lower their energy consumption.

The period of the year between September and December was characterised by the end of the dry season, a slow transition to the wet season and the first part of the wet season proper. In the light of this, the results outlined in these months may represent the likelihood of a greater exploitation of roadside and pathway vegetation, which was easier to access due to its proximity to roads. This interpretation is in agreement with what has been empirically observed by reserve managers in recent years, who have noticed a greater impact of elephants on vegetation on both sides of the reserve's road network. Moreover, this tendency to more easily and frequently impact vegetation on the edges of paths is also well documented in the literature (Russo *et al.*, 2023; Blanché, 2021; Brodie *et al.*, 2015; Porensky *et al.*, 2013; Fernando and Leimgruber, 2011; Vanak *et al.*, 2010; Young *et al.*, 1995). In addition, Berger (2007), and Trombulak and Frissell (2000) pointed out that elephants may prefer roads during the wet season due to the greater availability of greener vegetation on the sides of the paths, as a result of the increased exposure to sunlight. Therefore, the fact that roads and paths provided easier travel routes for elephants may have led to an increased utilization of vegetation along their edges during the wet season. Additionally, these pathways likely facilitated more efficient navigation through the reserve during the dry season.

### **4.3 Distance to nearest water source**

It is well known that elephant movements are driven by access to vital resources (Vogel *et al.*, 2020), with water being the most important for their survival. As evidence, several papers have portrayed water points as the most impactful environmental factor in the ecology of elephant movements, both for the direct use (MacFadyen *et al.*, 2019; de Knegt *et al.*, 2011; de Beer and van Aarde, 2008; Chamaillé-Jammes *et al.*, 2007) and indirect use, for example for thermoregulation, shade, and mud bathing (Henley and Cook, 2019; Marshal *et al.*, 2011; Smit *et al.*, 2007; Stokke and du Toit, 2002). In this context, several authors have recognised the water as a driver for elephant choices and preferences (Chibeya *et al.*, 2021; Sach *et al.*, 2019; Taher *et al.*, 2021; Talukdar *et al.*, 2020; Wall *et*

*al.*, 2013). Therefore, this study aimed to evaluate the influence of water sources on the movement patterns of the two matriarchs, using the distance to the nearest water source as a predictor variable. Considering mainly the results of the stationary state probabilities plots, they showed consistency between the two matriarchs in terms of persistence in certain states near the water source. Indeed, both Elza and Jean were in states 1 or 2 when closer to the water. However, although Elza was almost equally likely to be in state 1 and 2 during the months considered, Jean showed a strong prevalence of being only in state 2 when near water points during December. This latter peculiarity can be explained by what was discovered by Bastille-Rousseau *et al.* (2020), according to whom elephants did not show a marked interest in necessarily staying close to water during the wet season, a preference instead pronounced during the dry season. Overall, the same probability of lying in states 1 and 2 when in the vicinity of water may be the consequence of an elevated number of water points throughout the reserve. Although some of these are seasonal, thus empty during the dry season, the amount of artificial and semi-artificial water sources remains high in relation to the size of the reserve. Therefore, it is plausible that the herds of the two matriarchs alternated between prolonged and brief stops whenever they were near a water point, preferring, however, more short stops. In support of this, previous research has found that elephants' movements to access water are generally frequent but of short duration (Polansky *et al.*, 2015; Chamaillé-Jammes *et al.*, 2013). Another hypothesis that may explain the high probability of being in state 2 in the proximity of the water may be that the matriarch briefly accelerated as it approached the water points, and then spent time in state 1 in close proximity to the water. Although the differences in speed between the different states were not calculated in this study, it is evident that the step length means of state 2 was greater than that one of state 1, therefore it can consequently be assumed that the average speed was higher in state 2. Furthermore, Chamaillé-Jammes *et al.* (2013) found out that elephants increased their speed when moving closer to water points, hence the previous assumption may be valid.

In contrast, at the greatest distance from the water, Elza and Jean showed two different movement patterns. Particularly, Elza was always found in state 3, with an extremely high probability from September onwards. In contrast, Jean predominantly occupied state 2 when farthest from the water in most months, except for September and October when state 1 at maximum distance from the water prevailed, albeit without a significant dominance over the other two states. Nonetheless, combining the seven months into a single analysis, Elza remained consistent with the results on a monthly scale, while



Jean showed a prevalence of state 3 away from water, again consistent with the other matriarch. The disparity in Jean's results could be attributed to the impact of two months, July and November, within the combined analysis of seven months. However, it's important to note that the individual analysis of these specific months was not conducted, leading to a gap in our understanding of how these months may have influenced the overall assessment of movement patterns in relation to this covariate. Since water is a major determinant of elephant movement patterns, it is conceivable that the two matriarchs were in state 3 for most months when they were away from water, while they tended to stay as close to water as possible when in the other two states. It is therefore likely that they moved quickly from one water source to the other in order to spend as little time as possible at maximum distance from the water and reach another water source as quickly as possible. In support of this, previous articles have highlighted how water-orientated elephant movements can commence from tens of km away (Polansky *et al.*, 2015).

#### **4.4 NDVI**

The importance of NDVI as a mean for comprehending the ecology of elephants has already been documented by several authors (Loarie *et al.*, 2009; Wittemyer *et al.*, 2007; Chamaillé-Jammes *et al.*, 2007). The exceptional temporal precision of NDVI proved invaluable for examining elephant movements, as it enabled the correlation of vegetation productivity data with the simultaneous tracking of individual locations (Pettorelli *et al.*, 2011). On a monthly scale, both Elza and Jean showed the same relationship between NDVI and their movements. Particularly, not only the transition probabilities, but also the stationary state probabilities, indicated a constant and persistent presence in state 1 at the highest NDVI values, and in state 3 at the lowest values. This trend was highly consistent between the two matriarchs and across all the months considered. It is therefore clear that the movements of the matriarchs were strongly influenced by the presence or absence of high vegetation availability. The strong correlation observed between high NDVI values and presence in state 1 throughout the analysed period suggested that Elza and Jean exhibited a preference for consistently foraging in the most productive areas of the reserve. This preference may be attributed to the greater diversity in vegetation types and nutrient concentrations in the chosen area, which differ between different times of the year. Loarie *et al.* (2009) drew similar conclusions because in all seasons of their study, elephants

showed a constant selection of the greenest vegetation, taking advantage of phenologically diverse vegetation. Thus, the elephants purposely chose the areas in which to feed, denoting a high knowledge of the places where they could find the most qualitative available food, not only in the wet season but also and especially in the dry season. Consequently, these two matriarchs showed a preference for quality over quantity even in the dry season, an uncommon behaviour in open systems, where quantity is generally chosen over quality in the dry season (Tsalyuk *et al.*, 2019; Young *et al.*, 2009a). Nevertheless, Young *et al.* (2009a) found a high presence of elephants in grid-cells with elevated NDVI values during the dry season, which is in agreement with what was found in this study.

In several months, particularly during the dry season, the transition probability values showed a higher probability of moving from state 3 to state 1 rather than from state 2 to state 1 as the NDVI value increased. This peculiarity may be further evidence of the matriarchs' great knowledge of the reserve itself and where they could find the most productive patches throughout the reserve. Therefore, their movements were fast, direct and precise (state 3) towards a specific spot that, once reached, represented the final destination for feeding and foraging (state 1). In support of this, Boettiger *et al.* (2011) and Loarie *et al.* (2009) pointed out that elephants' optimal foraging strategies involved actively seeking out regions with high NDVI values. Furthermore, Wittemeyer *et al.* (2008) indicated that non-random movements are generally associated with feeding strategies, particularly when food and water supplies are scarce or heterogeneously distributed.

## 5 CONCLUSION AND RECOMMENDATIONS

This research explored elephant movements under the influence of four different probable drivers (i.e., terrain roughness, distance to nearest road/path, distance to nearest water source, NDVI) in a fenced reserve in South Africa, to better understand movement patterns of such megaherbivores limited by fences. Particularly, it showed that movement states derived from step length and turning angle from hourly GPS positions of elephants with HMMs can be extremely effective in the analysis of elephant movement patterns per se and under the influence of different predictor variables. The findings of this study emphasised the importance of including terrain roughness, distance to nearest road/path, distance to nearest water source, and NDVI as a key driver of elephant movement patterns.

In summary, using terrain roughness as a covariant contributed to the assessment that increased roughness led to a change in the movement pattern, resulting in elephants slowing down. Such results aided to evaluate whether elephants showed preferences for certain types of terrain, how terrain influences their movements, and how they navigate the landscape to meet their ecological needs. Moreover, understanding which roads or paths were frequently used by elephants can inform resource management decisions. Elephants showed to use the road network to navigate the landscape faster during the dry season, and to exploit roadside vegetation during the wet season. Therefore, managers could focus vegetation restoration efforts or water source maintenance along these routes to ensure. Therefore, managers could concentrate their efforts on restoring vegetation or maintaining water sources along these routes to ensure that the needs of elephants and other wild animals are met. Additionally, persistence in state 3, the farthest from water sources, was found with direct and accurate movement patterns. Hence, the knowledge that elephants' movements are driven by water points with specific movement patterns has profound implications for conservation management within a fenced reserve. For instance, conservation manager can use this information to plan a rotation on water points available in order to avoid a repeated impact on the same patches of vegetation near water sources, giving vegetation time to recover. Finally, matriarchs consistently occurred in state 1, when NDVI values were highest, and in state 3, when NDVI values were lowest. Such strong correlation between elephant movements and high NDVI values can have several important conservation management implications within a fenced reserve: conservation managers can focus their habitat management efforts on areas with high NDVI values, as

these areas are likely critical for elephant foraging and nutrition. This may involve protecting and restoring key habitats that contribute to high NDVI values. All these strategies therefore have the common goal of promoting the conservation and welfare of elephants, maintaining an ecosystem balance that indirectly benefits the rest of the wildlife in the reserve.

In terrestrial ecosystems where megaherbivores such as elephants serve as critical ecosystem engineers (Vanak *et al.*, 2012; Shannon *et al.*, 2011; Owen-Smith *et al.*, 2006), it becomes imperative to not only understand the spatial distribution of individuals but also to discern the timing of behavioural changes and identify the pivotal factors driving these shifts (Birkett *et al.*, 2012). Such understanding enables the development of more efficient conservation management strategies for the preservation of the species. Hence, future research could investigate elephant movement patterns across various temporal scales, including finer scales like daily or weekly observations, as well as broader scales such as seasonal or annual trends. This approach can aim to gain a comprehensive understanding of the underlying mechanisms and influences guiding their choices and preferences. Ultimately, these insights can inform initiatives aimed at enhancing conservation management plans for elephants.

In conclusion, delving into the spatial ecology of elephants provides information that is of significant and, especially in the context of fenced reserves, even critical importance for the successful and efficient management and conservation not only of this species' habitat but also of the species itself (Chui, 2021).

## 6 REFERENCES

- Anadón, J. D., Wiegand, T., and Giménez, A. (2012) 'Individual-based movement models reveals sex-biased effects of landscape fragmentation on animal movement.', *Ecosphere*, 3(7), pp. 1-32. Available at: <https://doi.org/10.1890/ES11-00237.1> (Accessed: 21 August 2023).
- Apps, C. D., McLellan, B. N., Kinley, T. A., and Flaa, J. P. (2001) 'Scale-Dependent Habitat Selection by Mountain Caribou, Columbia Mountains.', *British Columbia on JSTOR*, 65, pp.65-77. Available at: <https://doi.org/3803278> (Accessed: 18 August 2023).
- Archie, E. A., Morrison, T. A., Foley, C. A., Moss, C. J., and Alberts, S. C. (2006a) 'Dominance rank relationships among wild female African elephants, *Loxodonta africana*.', *Animal Behaviour*, 71(1), pp. 117-127. Available at: <https://doi.org/10.1016/j.anbehav.2005.03.023> (Accessed: 27 August 2023).
- Archie, E. A., Moss, C. J., and Alberts, S. C. (2006b) 'The ties that bind: Genetic relatedness predicts the fission and fusion of social groups in wild African elephants.', *Proceedings of the Royal Society B: Biological Sciences*, 273(1586), pp. 513-522. Available at: <https://doi.org/10.1098/rspb.2005.3361> (Accessed: 27 August 2023).
- Asner, G. P., Vaughn, N., Smit, I. P. J., and Levick, S. (2016) 'Ecosystem-scale effects of megafauna in African savannas.', *Ecography*, 39(2), pp. 240-252. Available at: <https://doi.org/10.1111/ecog.01640> (Accessed: 13 August 2023).
- Augustine, D. J., and McNaughton, S. J. (2004) 'Regulation of shrub dynamics by native browsing ungulates on East African rangeland.', *Journal of Applied Ecology*, 41(1), pp. 45-58. Available at: <https://doi.org/10.1111/j.1365-2664.2004.00864.x> (Accessed: 25 August 2023).

Bagniewska, J. M., Hart, T., Harrington, L. A., and Macdonald, D. W. (2013) 'Hidden Markov analysis describes dive patterns in semiaquatic animals.', *Behavioral Ecology*, 24(3), pp. 659-667. Available at: <https://doi.org/10.1093/beheco/ars217> (Accessed: 21 August 2023).

Bastille-Rousseau, G., Wall, J., Douglas-Hamilton, I., Lesowapir, B., Loloju, B., Mwangi, N., and Wittemyer, G. (2020) 'Landscape-scale habitat response of African elephants shows strong selection for foraging opportunities in a human dominated ecosystem.', *Ecography*, 43(1), pp. 149-160. Available at: <https://doi.org/10.1111/ecog.04240> (Accessed: 10 September 2023).

Baxter, P. W. J., and Getz, W. M. (2005) 'A Model-Framed Evaluation of Elephant Effects On Tree And Fire Dynamics In African Savannas.', *Ecological Applications*, 15(4), pp. 1331-1341. Available at: <https://doi.org/10.1890/02-5382> (Accessed: 25 August 2023).

Baxter, P. W. J., and Getz, W. M. (2008) 'Development and Parameterization of a Rain- and Fire-driven Model for Exploring Elephant Effects in African Savannas.', *Environmental Modeling and Assessment*, 13, pp. 221-242. Available at: <https://doi.org/10.1007/s10666-007-9091-9> (Accessed: 25 August 2023).

Beirne, C., Houslay, T. M., Morkel, P., Clark, C. J., Fay, M., Okouyi, J., White, L. J., and Poulsen, J. R. (2021) 'African forest elephant movements depend on time scale and individual behavior.', *Scientific Reports*, 11(1), pp. 1-11. Available at: <https://doi.org/10.1038/s41598-021-91627-z> (Accessed: 20 August 2023).

Berger, J. (2004) 'The Last Mile: How to Sustain Long-Distance Migration in Mammals.', *Conservation Biology*, 18(2), pp. 320-331. Available at: <https://doi.org/10.1111/j.1523-1739.2004.00548.x> (Accessed: 22 August 2023).

Berger, J. (2007) 'Fear, human shields and the redistribution of prey and predators in protected areas.', *Biology letters*, 3(6), pp. 620-623. Available at: <https://doi.org/10.1098/rsbl.2007.0415> (Accessed: 10 September 2023).

Berti, E., Davoli, M., Buitenwerf, R., Dyer, A., Hansen, O. L. P., Hirt, M., Svenning, J.-C., Terlau, J. F., Brose, U., and Vollrath, F. (2022) ‘The r package enerscape: A general energy landscape framework for terrestrial movement ecology.’, *Methods in Ecology and Evolution*, 13(1), pp. 60-67. Available at: <https://doi.org/10.1111/2041-210X.13734> (Accessed: 13 August 2023).

Berti, E., Rosenbaum, B., Brose, U., and Vollrath, F. (2023) ‘Energy landscapes direct the movement preferences of elephants.’, *Authorea*, pre-print version, pp. 1-23. Available at: DOI: 10.22541/au.168373276.62196439/v1 (Accessed: 13 June 2023).

Birkett, P. J., Vanak, A. T., R. Muggeo, V. M., Ferreira, S. M., and Slotow, R. (2012) ‘Animal Perception of Seasonal Thresholds: Changes in Elephant Movement in Relation to Rainfall Patterns.’, *PLOS ONE*, 7(6), pp. e38363. Available at: <https://doi.org/10.1371/journal.pone.0038363> (Accessed: 18 August 2023).

Blackwell, P. G. (2003) ‘Bayesian inference for Markov processes with diffusion and discrete components.’, *Biometrika*, 90(3), pp. 613-627. Available at: <https://doi.org/10.1093/biomet/90.3.613> (Accessed: 22 August 2023).

Blanc, J.J., Barnes, R.F.W., Craig, G.C., Dublin, H.T., Thouless, C.R., Douglas-Hamilton, I., and Hart, J.A. (2007) ‘African elephant status report 2007: an update from the African elephant database.’, *Occasional Papers Series of the IUCN Species Survival Commission*, No 33. IUCN/SSC African elephant Specialist Group. IUCN, Gland, Switzerland, pp. 1-284. Available at: [bit.ly/3sR6Cbf](http://bit.ly/3sR6Cbf) (Accessed: 24 August 2023).

Blanché, L. A. (2021) *Displacement of Wildlife Due to Anthropogenic-Induced Edge Effects in Small Game Reserves* (Doctoral dissertation, Texas Christian University). Available at: <https://bit.ly/3LHq3tn> (Accessed: 08 September 2023).

Boettiger, A. N., Wittemyer, G., Starfield, R., Vollrath, F., Douglas-Hamilton, I., and Getz, W. M. (2011) ‘Inferring ecological and behavioral drivers of African elephant movement using a linear filtering approach.’, *Ecology*, 92(8), pp. 1648-1657. Available at: <https://doi.org/10.1890/10-0106.1> (Accessed: 11 September 2023).

Bohrer, G., Beck, P. S., Ngene, S. M., Skidmore, A. K., and Douglas-Hamilton, I. (2014) 'Elephant movement closely tracks precipitation-driven vegetation dynamics in a Kenyan forest-savanna landscape.', *Movement Ecology*, 2(2), pp. 1-15. Available at: <https://doi.org/10.1186/2051-3933-2-2> (Accessed: 30 August 2023).

Bolger, D. T., Newmark, W. D., Morrison, T. A., and Doak, D. F. (2008) 'The need for integrative approaches to understand and conserve migratory ungulates.', *Ecology Letters*, 11(1), pp. 63-77. Available at: <https://doi.org/10.1111/j.1461-0248.2007.01109.x> (Accessed: 22 August 2023).

Boundja, R. P., and Midgley, J. J. (2010) 'Patterns of elephant impact on woody plants in the Hluhluwe-Imfolozi park, Kwazulu-Natal, South Africa.', *African Journal of Ecology*, 48(1), pp. 206-214. Available at: <https://doi.org/10.1111/j.1365-2028.2009.01104.x> (Accessed: 27 August 2023).

Bowler, D. E., Benton, T. G., Bowler, D. E., and Benton, T. G. (2005) 'Causes and consequences of animal dispersal strategies: Relating individual behaviour to spatial dynamics.', *Biological Reviews of the Cambridge Philosophical Society*, 80, pp. 205–225. Available at: <https://doi.org/10.1017/S1464793104006645> (Accessed: 23 August 2023).

Brodie, J. F., Giordano, A. J., Ambu, L. (2015) 'Differential responses of large mammals to logging and edge effects.', *Mammalian Biology - Zeitschrift für Säugetierkunde*, 80(1), pp. 7–13. Available at: [doi:10.1016/j.mambio.2014.06.001](https://doi.org/10.1016/j.mambio.2014.06.001) (Accessed: 08 September 2023).

Brown, J. L. (2014) 'Comparative reproductive biology of elephants.', In *Reproductive Sciences in Animal Conservation: Progress and Prospects*; Holt, W.V., Brown, J.L., Comizzoli, P., Eds.; Advances in Experimental Medicine and Biology, vol 753. Springer: New York, NY, USA, 2014, pp. 135–169. Available at: [https://doi.org/10.1007/978-1-4939-0820-2\\_8](https://doi.org/10.1007/978-1-4939-0820-2_8) (Accessed: 28 August 2023).



Cagnacci, F., Boitani, L., Powell, R. A., and Boyce, M. S. (2010) 'Animal ecology meets gps - based radiotelemetry: A perfect storm of opportunities and challenges.', *Philosophical transactions of the Royal Society of London. Series B, Biological sciences*, 365, pp. 2157-2162. Available at: <https://doi.org/10.1098/rstb.2010.0107> (Accessed: 21 August 2023).

Campos-Arceiz, A., and Blake, S. (2011) 'Megagardeners of the forest – the role of elephants in seed dispersal.', *Acta Oecologica*, 37(6), pp. 542-553. Available at: <https://doi.org/10.1016/j.actao.2011.01.014> (Accessed: 24 August 2023).

Chamaillé-Jammes, S., Valeix, M., and Fritz, H. (2007) 'Managing heterogeneity in elephant distribution: Interactions between elephant population density and surface-water availability.' *Journal of Applied Ecology*, 44(3), pp. 625-633. Available at: <https://doi.org/10.1111/j.1365-2664.2007.01300.x> (Accessed: 10 September 2023).

Chamaillé-Jammes, S., Mtare, G., Makuwe, E., and Fritz, H. (2013) 'African Elephants Adjust Speed in Response to Surface-Water Constraint on Foraging during the Dry-Season.', *PLOS ONE*, 8(3), pp. e59164. Available at: <https://doi.org/10.1371/journal.pone.0059164> (Accessed: 11 September 2023).

Chase, M. J., Schlossberg, S., Griffin, C. R., Bouché, P. J. C., Djene, S. W., Elkan, P. W., Ferreira, S., Grossman, F., Kohi, E. M., Landen, K., Omondi, P., Peltier, A., Selier, S. A. J., Sutcliffe, R. (2016) 'Continent-wide survey reveals massive decline in African savannah elephants.', *PeerJ*, 4, pp. e2354. Available at: <https://doi.org/10.7717/peerj.2354> (Accessed: 30 August 2023).

Chibeya, D., Wood, H., Cousins, S., Carter, K., Nyirenda, M. A., and Maseka, H. (2021) 'How do African elephants utilize the landscape during wet season? A habitat connectivity analysis for Sioma Ngwezi landscape in Zambia.', *Ecology and Evolution*, 11(21), pp. 14916-14931. Available at: <https://doi.org/10.1002/ece3.8177> (Accessed: 13 August 2023).

Chiyo, P. I., Archie, E. A., Hollister-Smith, J. A., Lee, P. C., Poole, J. H., Moss, C. J., and Alberts, S. C. (2011) 'Association patterns of African elephants in all-male groups: The role of age and genetic relatedness.', *Animal Behaviour*, 81(6), pp. 1093-1099. Available at: <https://doi.org/10.1016/j.anbehav.2011.02.013> (Accessed: 28 August 2023).

Chiyo, P. I., Moss, C. J., and Alberts, S. C. (2012) 'The influence of life history milestones and association networks on crop-raiding behavior in male African elephants.', *PLoS ONE*, 7(2), pp. e31382. Available at: <https://doi.org/10.1371/journal.pone.0031382> (Accessed: 28 August 2023).

Chiyo, P. I., Wilson, J. W., Archie, E. A., Lee, P. C., Moss, C. J., and Alberts, S. C. (2014). The influence of forage, protected areas, and mating prospects on grouping patterns of male elephants. *Behavioral Ecology*, 25(6), pp. 1494-1504. Available at: <https://doi.org/10.1093/beheco/aru152> (Accessed: 27 August 2023).

Chui, Y. S. [崔驛選]. (2021) 'Socio-behavioural and spatial ecology of African elephants (*Loxodonta africana*).', (Thesis). University of Hong Kong, Pokfulam, Hong Kong SAR, pp. 1-376. Available at: <https://hub.hku.hk/handle/10722/325812> (Accessed: 25 August 2023).

Codron, J., Codron, D., Sponheimer, M., Kirkman, K., Duffy, K. J., Raubenheimer, E. J., Mélice, J.-L., Grant, R., Clauss, M., and Lee-Thorp, J. A. (2012) 'Stable isotope series from elephant ivory reveal lifetime histories of a true dietary generalist.', *Proceedings of the Royal Society B: Biological Sciences*, 279(1737), pp. 2433-2441. Available at: <https://doi.org/10.1098/rspb.2011.2472> (Accessed: 27 August 2023).

Comley, J. (2019). *Carnivore intra-guild competition in Selati Game Reserve, Limpopo Province, South Africa* (Doctoral dissertation, PhD thesis, Rhodes University). Available at: [bit.ly/47DZ9vQ](https://bit.ly/47DZ9vQ) (Accessed: 14 August 2023).

Cook, R. M., and Henley, M. D. (2019) 'The management dilemma: Removing elephants to save large trees.', *Koedoe: African Protected Area Conservation and Science*, 61(1), pp. 1-12. Available at: <https://hdl.handle.net/10520/EJC-1dbc10e923> (Accessed: 26 August 2023).

Coverdale, T. C., Kartzinel, T. R., Grabowski, K. L., Shriver, R. K., Hassan, A. A., Goheen, J. R., Palmer, T. M., and Pringle, R. M. (2016) 'Elephants in the understory: Opposing direct and indirect effects of consumption and ecosystem engineering by megaherbivores.', *Ecology*, 97(11), pp. 3219-3230. Available at: <https://doi.org/10.1002/ecy.1557> (Accessed: 24 August 2023).

Cumming, D. H., Fenton, M. B., Rautenbach, I. L., Taylor, R. D., Cumming, G. S., Cumming, M. S., and Portfors, C. V. (1997) 'Elephants, woodlands and biodiversity in southern Africa.', *South African Journal of Science*, 93(5), pp. 231-236. Available at: [bit.ly/3RjrgLk](https://doi.org/10.1111/j.0030-1299.2005.13538.x) (Accessed: 26 August 2023).

Cushman, S. A., Chase, M., and Griffin, C. (2005) 'Elephants in space and time.' *Oikos*, 109(2), pp. 331-341. Available at: <https://doi.org/10.1111/j.0030-1299.2005.13538.x> (Accessed: 22 August 2023).

Cushman, S. A., and Huettmann, F. (2010). *Spatial Complexity, Informatics, and Wildlife Conservation || Mapping Landscape Resistance to Identify Corridors and Barriers for Elephant Movement in Southern Africa.*, 10.1007/978-4-431-87771-4(Chapter 19), pp. 349–367. Available at: [doi:10.1007/978-4-431-87771-4\\_19](https://doi.org/10.1007/978-4-431-87771-4_19) (Accessed: 08 September 2023).

de Beer, Y., Kilian, W., Versfeld, W., and Van Aarde, R. (2006) 'Elephants and low rainfall alter woody vegetation in Etosha National Park, Namibia.', *Journal of Arid Environments*, 64(3), pp. 412-421. Available at: <https://doi.org/10.1016/j.jaridenv.2005.06.015> (Accessed: 24 August 2023).

de Beer, Y., and Van Aarde, R. (2008) 'Do landscape heterogeneity and water distribution explain aspects of elephant home range in southern Africa's arid savannas?', *Journal of Arid Environments*, 72(11), pp. 2017-2025. Available at: <https://doi.org/10.1016/j.jaridenv.2008.07.002> (Accessed: 29 August 2023).

de Boer, W., Van Oort, J., Grover, M., and Peel, M. (2015) 'Elephant-mediated habitat modifications and changes in herbivore species assemblages in Sabi Sand.', *South Africa. European Journal of Wildlife Research*, 61(4), pp. 491-503. Available at: <https://doi.org/10.1007/s10344-015-0919-3> (Accessed: 31 August 2023).

de Knegt, H. J., Hengeveld, G. M., Van Langevelde, F., De Boer, W. F., and Kirkman, K. P. (2007) 'Patch density determines movement patterns and foraging efficiency of large herbivores.', *Behavioral Ecology*, 18(6), pp. 1065-1072. Available at: <https://doi.org/10.1093/beheco/arm080> (Accessed: 19 August 2023).

de Knegt, H. J., van Langevelde, F., Skidmore, A. K., Delsink, A., Slotow, R., Henley, S., Bucini, G., de Boer, W. F., Coughenour, M. B., Grant, C. C., Heitkönig, I. M. A., Henley, M. D., Knox, N. M., Kohi, E. M., Mwakiwa, E., Page, B. R., Peel, M., Pretorius, Y., van Wieren, S. E., and Prins, H. H. T. (2011) 'The spatial scaling of habitat selection by African elephants.', *Journal of Animal Ecology*, 80(1), pp. 270-281. Available at: <https://doi.org/10.1111/j.1365-2656.2010.01764.x> (Accessed: 10 September 2023).

de Silva, S., and Wittemyer, G. A. (2012) 'Comparison of Social Organization in Asian Elephants and African Savannah Elephants.', *International Journal of Primatology*, 33, pp. 1125–1141. Available at: <https://doi.org/10.1007/s10764-011-9564-1> (Accessed: 28 August 2023).

Demarchi, M. W. (2003) 'Migratory Patterns and Home Range Size of Moose in the Central Nass Valley, British Columbia.', *Northwestern Naturalist*, 84(3), pp. 135–141. Available at: <https://doi.org/10.2307/3536539> (Accessed: 22 August 2023).

Dingemanse, N. J., Kazem, A. J. N., Réale, D., and Wright, J. (2010) 'Behavioural reaction norms: Animal personality meets individual plasticity.', *Trends in Ecology & Evolution*, 25(2), pp. 81-89. Available at: <https://doi.org/10.1016/j.tree.2009.07.013> (Accessed: 27 August 2023).

Doughty, C. E., Wolf, A., and Malhi, Y. (2013) 'The legacy of the Pleistocene megafauna extinctions on nutrient availability in Amazonia.', *Nature Geoscience*, 6(9), pp. 761-764. Available at: <https://doi.org/10.1038/ngeo1895> (Accessed: 19 August 2023).

Douglas-Hamilton, I., Krink, T., and Vollrath, F. (2005) 'Movements and corridors of African elephants in relation to protected areas.', *Naturwissenschaften*, 92, pp. 158-163. Available at: <https://doi.org/10.1007/s00114-004-0606-9> (Accessed: 29 August 2023).

Dublin, H. T. (2003). *IUCN/SSC AfESG Guidelines for the in situ Translocation of the African Elephant for Conservation Purposes*. IUCN.

Dudley, J. P. (2000) 'Seed Dispersal by Elephants in Semiarid Woodland Habitats of Hwange National Park, Zimbabwe.', *Biotropica*, 32(3), pp. 556–561. Available at: <http://www.jstor.org/stable/2663889> (Accessed: 24 August 2023).

Duffy, K. J., Dai, X., Shannon, G., Slotow, R., and Page, B. (2011) 'Movement patterns of African elephants (*Loxodonta africana*) in different habitat types.', *South African Journal of Wildlife Research-24-month delayed open access*, 41(1), pp. 21-28. Available at: <https://hdl.handle.net/10520/EJC117366> (Accessed: 08 September 2023).

Dunkin, R. C., Wilson, D., Way, N., Johnson, K., and Williams, T. M., (2013) 'Climate influences thermal balance and water use in African and Asian elephants: physiology can predict drivers of elephant distribution.', *Journal of Experimental Biology*, 216(15), pp. 2939-2952. Available at: <https://doi.org/10.1242/jeb.080218> (Accessed: 30 August 2023).

Earl, J. E., and Zollner, P. A. (2017) 'Advancing research on animal-transported subsidies by integrating animal movement and ecosystem modelling.', *Journal of Animal Ecology*, 86(5), pp. 987-997. Available at: <https://doi.org/10.1111/1365-2656.12711> (Accessed: 21 August 2023).

Eckhardt, H. C., van Wilgen, B. V., and Biggs, H. C. (2001) 'Trends in woody vegetation cover in the Kruger National Park, South Africa, between 1940 and 1998.', *African Journal of Ecology*, 38(2), pp. 108-115. Available at: <https://doi.org/10.1046/j.1365-2028.2000.00217.x> (Accessed: 25 August 2023).

Estes, J. A., Terborgh, J., Brashares, J. S., Power, M. E., Berger, J., Bond, W. J., Carpenter, S. R., Essington, T. E., Holt, R. D., C. Jackson, J. B., Marquis, R. J., Oksanen, L., Oksanen, T., Paine, R. T., Pikitch, E. K., Ripple, W. J., Sandin, S. A., Scheffer, M., Schoener, T. W., and Wardle, D. A. (2011) 'Trophic Downgrading of Planet Earth.', *Science*, 333(6040), pp. 301-306. Available at: <https://doi.org/1205106> (Accessed: 24 August 2023).

Evans, K. E., and Harris, S. (2008) 'Adolescence in male African elephants, *Loxodonta africana*, and the importance of sociality.', *Animal Behaviour*, 76(3), pp. 779-787. Available at: <https://doi.org/10.1016/j.anbehav.2008.03.019> (Accessed: 28 August 2023).

Evans, L. J., Goossens, B., Davies, A. B., Reynolds, G., and Asner, G. P. (2020) 'Natural and anthropogenic drivers of Bornean elephant movement strategies.' *Global Ecology and Conservation*, 22, pp. e00906. Available at: <https://doi.org/10.1016/j.gecco.2020.e00906> (Accessed: 08 September 2023).

Fahrig, L. (2007) 'Non-optimal animal movement in human-altered landscapes.', *Functional Ecology*, 21(6), pp. 1003-1015. Available at: <https://doi.org/10.1111/j.1365-2435.2007.01326.x> (Accessed: 20 August 2023).

Fernando, P., and Leimgruber, P. (2011) 'Asian elephants and seasonally dry forests.', *Ecology and conservation of seasonally dry forests in Asia*, pp. 151-163. Available at: <https://bit.ly/3PXobiF> (Accessed: 08 September 2023).

Fishlock, V., and Lee, P. C. (2013) 'Forest elephants: Fission–fusion and social arenas.' *Animal Behaviour*, 85(2), pp. 357-363. Available at: <https://doi.org/10.1016/j.anbehav.2012.11.004> (Accessed: 28 August 2023).

Forester, J. D., Ives, A. R., Turner, M. G., Anderson, D. P., Fortin, D., Beyer, H. L., Smith, D. W., and Boyce, M. S. (2007) 'State–Space Models Link Elk Movement Patterns to Landscape Characteristics in Yellowstone National Park.', *Ecological Monographs*, 77(2), pp. 285-299. Available at: <https://doi.org/10.1890/06-0534> (Accessed: 21 August 2023).

Freeman, E. W., Whyte, I., and Brown, J. L. (2009) 'Reproductive evaluation of elephants culled in Kruger National Park, South Africa between 1975 and 1995.', *African Journal of Ecology*, 47(2), pp. 192-201. Available at: <https://doi.org/10.1111/j.1365-2028.2008.00957.x> (Accessed: 28 August 2023).

Franke, A., Caelli, T., and Hudson, R. J. (2004) 'Analysis of movements and behavior of caribou (*Rangifer tarandus*) using hidden Markov models.', *Ecological Modelling*, 173(2-3), pp. 259-270. Available at: <https://doi.org/10.1016/j.ecolmodel.2003.06.004> (Accessed: 21 August 2023).

Fritz, H. (2017) 'Long-term field studies of elephants: Understanding the ecology and conservation of a long-lived ecosystem engineer.', *Journal of Mammalogy*, 98(3), pp. 603-611. Available at: <https://doi.org/10.1093/jmammal/gyx023> (Accessed: 25 August 2023).

Fryxell, J. M., Hazell, M., Borger, L., Dalziel, B. D., Haydon, D. T., Morales, J. M., and Rosatte, R. C. (2008) 'Multiple movement modes by large herbivores at multiple spatiotemporal scales.', *Proceedings of the National Academy of Sciences of the United States of America*, 105, pp. 19114-19119. Available at: <https://doi.org/10.1073/pnas.0801737105> (Accessed: 18 August 2023).

Gerhardt-Weber, K. E. M. (2011). *Elephant movements and humanelephant conflict in a transfrontier conservation area*. Stellenbosch: University of Stellenbosch.

Goldenberg, S. Z., De Silva, S., Rasmussen, H. B., Douglas-Hamilton, I., and Wittemyer, G. (2014) 'Controlling for behavioural state reveals social dynamics among male African elephants, *Loxodonta africana*.', *Animal Behaviour*, 95, pp. 111-119. Available at: <https://doi.org/10.1016/j.anbehav.2014.07.002> (Accessed: 28 August 2023).

Goldenberg, S. Z., Douglas-Hamilton, I., and Wittemyer, G. (2018) 'Inter-generational change in African elephant range use is associated with poaching risk, primary productivity and adult mortality.' *Proceedings of the Royal Society B: Biological Sciences*, 285(1879), pp. 20180286. Available at: <https://doi.org/10.1098/rspb.2018.0286> (Accessed: 29 August 2023).

Grant, C. C., Bengis, R., Balfour, D., Peel, M., Davies-Mostert, H., Killian, H., Little, R., Smit, I., Garai, M., Henley, M., Anthony, B., and Hartley, P. (2008) 'Controlling the distribution of elephants.' *Assessment of South African Elephant Management*. (eds. R.J. Scholes & K.G. Mennell), pp 329–369. Witwatersrand University Press, Johannesburg. Available at: <https://philpapers.org/rec/GRACTD-2> (Accessed: 30 August 2023).

Gravel, D., Massol, F., and Leibold, M. A. (2016) 'Stability and complexity in model meta-ecosystems.', *Nature Communications*, 7(1), pp. 1-8. Available at: <https://doi.org/10.1038/ncomms12457> (Accessed: 20 August 2023).

Gross, R. B., and Heinsohn, R. (2023) 'Elephants Not in the Room: Systematic Review Shows Major Geographic Publication Bias in African Elephant Ecological Research.', *Diversity*, 15(3), pp. 451-463. Available at: <https://doi.org/10.3390/d15030451> (Accessed: 24 August 2023).

Grubb, P., Groves, C. P., Dudley, J. P., and Shoshani, J. (2000) 'Living African elephants belong to two species: *Loxodonta africana* (Blumenbach, 1797) and *Loxodonta cyclotis* (Matschie, 1900).', *Elephant*, 2(4), pp. 1-4. Available at: [10.22237/elephant/1521732169](https://doi.org/10.22237/elephant/1521732169) (Accessed: 20 August 2023).

Guerbois, C., Chapanda, E., and Fritz, H. (2012) 'Combining multi-scale socio-ecological approaches to understand the susceptibility of subsistence farmers to elephant crop raiding on the edge of a protected area.' *Journal of Applied Ecology*, 49, pp. 1149-1158. Available at: <https://doi.org/10.1111/j.1365-2664.2012.02192.x> (Accessed: 30 August 2023).

Guimaraes, R. G., Galetti, M., and Jordano, P. (2008) 'Seed Dispersal Anachronisms: Rethinking the Fruits Extinct Megafauna Ate.', *PLOS ONE*, 3(3), pp. e1745. Available at: <https://doi.org/10.1371/journal.pone.0001745> (Accessed: 19 August 2023).

Guldmond, R., and Van Aarde, R. (2007) 'The impact of elephants on plants and their community variables in South Africa's Maputaland.', *African Journal of Ecology*, 45(3), pp. 327-335. Available at: [bit.ly/3sQ1rs2](https://bit.ly/3sQ1rs2) (Accessed: 26 August 2023).



Guldemon, R., and Van Aarde, R. (2008) 'A meta-analysis of the impact of African elephants on savanna vegetation.' *The Journal of Wildlife Management*, 72(4), pp. 892-899. Available at: <https://doi.org/10.2193/2007-072> (Accessed: 31 August 2023).

Guldemon, R. A., Purdon, A., and van Aarde, R. J. (2017) 'A systematic review of elephant impact across Africa.', *PLOS ONE*, 12(6), pp. e0178935. Available at: <https://doi.org/10.1371/journal.pone.0178935> (Accessed: 25 August 2023).

Gusset, M., Ryan, S. J., Hofmeyr, M., Davies-Mostert, H. T., Graf, J. A., Owen, C., Szykman, M., Macdonald, D. W., Monfort, S. L., Wildt, D. E., Maddock, A. H., L. Mills, M. G., Slotow, R., and Somers, M. J. (2008) 'Efforts Going to the Dogs? Evaluating Attempts to Re-Introduce Endangered Wild Dogs in South Africa.', *Journal of Applied Ecology*, 45(1) pp. 100-108. Available at: <https://doi.org/20143956> (Accessed: 30 August 2023).

Hanks, J. (1972) 'Growth of the African elephant (*Loxodonta africana*).', *African Journal of Ecology*, 10(4), pp. 251-272. Available at: <https://doi.org/10.1111/j.1365-2028.1972.tb00870.x> (Accessed: 24 August 2023).

Harris, G., Thirgood, S., Hopcraft, J. G. C., Cromsigt, J. P., and Berger, J. (2009) 'Global decline in aggregated migrations of large terrestrial mammals.', *Endangered Species Research*, 7(1), pp. 55-76. Available at: DOI: <https://doi.org/10.3354/esr00173> (Accessed: 20 August 2023).

Haynes, G. (2012) 'Elephants (and extinct relatives) as earth-movers and ecosystem engineers.', *Geomorphology*, 157-158, pp. 99-107. Available at: <https://doi.org/10.1016/j.geomorph.2011.04.045> (Accessed: 24 August 2023).

Hayward, M. W., Adendorff, J., O'Brien, J., Sholto-Douglas, A., Bissett, C., Moolman, L. C., Bean, P., Fogarty, A., Howarth, D., Slater R. and Kerley G. I. H. (2007) 'Practical considerations for the reintroduction of large, terrestrial, mammalian predators based on reintroductions to South Africa's Eastern Cape Province.', *The Open Conservation Biology Journal*, 1, pp. 1-11. Available at: [doi:10.2174/1874-8392/07](https://doi.org/10.2174/1874-8392/07) (Accessed: 30 August 2023).

Henley, M. D., and Cook, R. (2019) ‘The management dilemma: Removing elephants to save large trees.’, *Koedoe*, 61(1), pp. 1-12. Available at: <https://hdl.handle.net/10520/EJC-1dbc10e923> (Accessed: 10 September 2023).

Hertel, A. G., Niemelä, P. T., Dingemanse, N. J., and Mueller, T. (2020) ‘A guide for studying among-individual behavioral variation from movement data in the wild.’, *Movement Ecology*, 8(1), pp. 30-43. Available at: <https://doi.org/10.1186/s40462-020-00216-8> (Accessed: 27 August 2023).

Hijmans, R. J., Bivand, R., Pebesma, E., Sumner, M. D. (2023) ‘terra: Spatial Data Analysis’ (1.7-46). Available at: <https://rspatial.org/>

Hoare, R. (1999) ‘Determinants of human-elephant conflict in a land-use mosaic.’, *Journal of Applied Ecology*, 36(5), pp. 689-700. Available at: <https://doi.org/10.1046/j.1365-2664.1999.00437.x> (Accessed: 31 August 2023).

Holdo, R. M. (2003) ‘Woody plant damage by African elephants in relation to leaf nutrients in western Zimbabwe’, *Journal of Tropical Ecology*, Cambridge University Press, 19(2), pp. 189–196. Available at: doi: 10.1017/S0266467403003213. (Accessed: 27 August 2023).

Hollister, J., Shah, T., Nowosad, J., Robitaille, A. L., Beck, M. W., Johnson, M. (2023) ‘elevatr: Access Elevation Data from Various APIs’ (0.99.0). Available at: <https://github.com/jhollist/elevatr/>

Holzmann, H., Munk, A., Suster, M., Zucchini, W. (2006) ‘Hidden Markov models for circular and linear-circular time series.’, *Environmental and Ecological Statistics*, 13, pp. 325–347. Available at: <https://doi.org/10.1007/s10651-006-0015-7> (Accessed: 23 August 2023).

Hooten, M. B., Johnson, D. S., McClintock, B. T., and Morales, J. M. (2017). *Animal movement: statistical models for telemetry data*. CRC press.

Howes, B., Doughty, L. S. and Thompson, S. (2020) 'African elephant feeding preferences in a small South African fenced game reserve.' *Journal for Nature Conservation*, 53, pp. 1-9. Available at: <https://doi.org/10.1016/j.jnc.2019.03.001> (Accessed: 25 August 2023).

Ihwagi, F. W., Chira, R. M., Kironchi, G., Vollrath, F., and Douglas-Hamilton, I. (2012) 'Rainfall pattern and nutrient content influences on African elephants' debarking behaviour in Samburu and Buffalo Springs National Reserves, Kenya.', *African Journal of Ecology*, 50(2), pp. 152-159. Available at: <https://doi.org/10.1111/j.1365-2028.2011.01305.x> (Accessed: 27 August 2023).

Jacobs, O. S., and Biggs, R. (2002) 'The impact of the African elephant on marula trees in the Kruger National Park.', *African Journal of Wildlife Research*, 32(1), pp. 13-22. Available at: <https://hdl.handle.net/10520/EJC117144> (Accessed: 25 August 2023).

Jachowski, D. S., Slotow, R., and Millspaugh, J. J. (2013) 'Corridor use and streaking behavior by African elephants in relation to physiological state.', *Biological Conservation*, 167, pp. 276-282. Available at: <https://doi.org/10.1016/j.biocon.2013.08.005> (Accessed: 30 August 2023).

Jarman, P. J. (1972) 'Seasonal Distribution of Large Mammal Populations in the Unflooded Middle Zambezi Valley.', *Journal of Applied Ecology*, 9(1), pp. 283-299. Available at: <https://doi.org/10.2307/2402062> (Accessed: 26 August 2023).

Jiang, F., Song, P., Zhang, J., Cai, Z., Chi, X., Gao, H., Qin, W., Li, S., and Zhang, T. (2020) 'Assessing the impact of climate change on the spatio-temporal distribution of foot-and-mouth disease risk for elephants.', *Global Ecology and Conservation*, 23, pp. e01176. <https://doi.org/10.1016/j.gecco.2020.e01176> (Accessed: 24 August 2023).

Johnson, M. B., Clifford, S. L., Goossens, B., Nyakaana, S., Curran, B., White, L. J. T., Wickings, E. J., Bruford, M. W. (2007) 'Complex phylogeographic history of central African forest elephants and its implications for taxonomy.', *BMC Evolutionary Biology*, 7, pp. 244. Available at: <https://doi.org/10.1186/1471-2148-7-244> (Accessed: 23 August 2023).

Jonsen, I. D., Flemming, J. M., and Myers, R. A. (2005) 'Robust State-Space Modeling of Animal Movement Data.', *Ecology*, 86(11), pp. 2874-2880. Available at: <https://doi.org/10.1890/04-1852> (Accessed: 13 August 2023).

Jonsen, I., Basson, M., Bestley, S., Bravington, M., Patterson, T., Pedersen, M., Thomson, R., Thygesen, U., and Wotherspoon, S. (2013) 'State-space models for bio-loggers: A methodological road map.', *Deep Sea Research Part II: Topical Studies in Oceanography*, 88-89, pp. 34-46. Available at: <https://doi.org/10.1016/j.dsr2.2012.07.008> (Accessed: 23 August 2023).

Karels, D. L., McCown, J. W., Scheick, B. K., Bolker, B. M., and Oli, M. K. (2017) 'Effects of environmental factors and landscape features on movement patterns of Florida black bears.', *Journal of Mammalogy*, 98(5), pp. 1463-1478. Available at: <https://doi.org/10.1093/jmammal/gyx066> (Accessed: 20 August 2023).

Kays, R., Crofoot, M. C., Jetz, W., and Wikelski, M. (2015) 'Terrestrial animal tracking as an eye on life and planet.' *Science*, 348(6240), pp. 2478- 2489. Available at: <https://doi.org/aaa2478> (Accessed: 20 August 2023).

Kohi, E. M., S. Peel, M. J., Slotow, R., A. Heitkönig, I. M., Skidmore, A., and T. Prins, H. H. (2011) 'African Elephants *Loxodonta africana* Amplify Browse Heterogeneity in African Savanna.', *Biotropica*, 43(6), pp. 711-721. Available at: <https://doi.org/10.1111/j.1744-7429.2010.00724.x> (Accessed: 24 August 2023).

Kos, M., Hoetmer, A. J., Pretorius, Y., de Boer, W. F., de Kragt, H., Grant, C. C., Kohi, E., Page, B., Peel, M., Slotow, R., van der Waal, C., van Wieren, S. E., Prins, H. H. T., and van Langevelde, F. (2012) 'Seasonal diet changes in elephant and impala in mopane woodland.', *European Journal of Wildlife Research*, 58(1), pp. 279-287. Available at: <https://doi.org/10.1007/s10344-011-0575-1> (Accessed: 26 August 2023).

Kottek, M., Grieser, J., Beck, C., Rudolf, B. and Rubel, F. (2006) 'World map of the Köppen-Geiger climate classification updated.', *Meteorologische Zeitschrift* 15, pp. 259–263. Available at: [bit.ly/3P2O8Mr](http://bit.ly/3P2O8Mr) (Accessed: 14 August 2023).

Landman, M., and Kerley, G. I. (2014) 'Elephant both Increase and Decrease Availability of Browse Resources for Black Rhinoceros.', *Biotropica*, 46(1), pp. 42-49. Available at: <https://doi.org/10.1111/btp.12066> (Accessed: 26 August 2023).

Langrock, R., King, R., Matthiopoulos, J., Thomas, L., Fortin, D., and Morales, J. M. (2012) 'Flexible and practical modeling of animal telemetry data: Hidden Markov models and extensions.', *Ecology*, 93(11), pp. 2336-2342. Available at: <https://doi.org/10.1890/11-2241.1> (Accessed: 13 August 2023).

Langrock, R., C. Hopcraft, J. G., Blackwell, P. G., Goodall, V., King, R., Niu, M., Patterson, T. A., Pedersen, M. W., Skarin, A., and Schick, R. S. (2014) 'Modelling group dynamic animal movement.', *Methods in Ecology and Evolution*, 5(2), pp. 190-199. Available at: <https://doi.org/10.1111/2041-210X.12155> (Accessed: 22 August 2023).

Laursen, L., and Bekoff, M. (1978) *Loxodonta africana*. *Mammalian Species* (92), 1-8. Oxford University Press.

Laws, R. M. (1970) 'Biology of African elephants.' *Science Progress (1933- )*, 58(230), pp. 251–262. Available at: <http://www.jstor.org/stable/43419958> (Accessed: 26 August 2023).

Lee, P. C., Poole, J. H., Njiraini, N., Sayialel, C. N., and Moss, C. J. (2011) 'Male social dynamics: Independence and beyond.', In C. J. Moss, H. Croze & P. C. Lee (Eds.), *The Amboseli elephants: A long-term perspective on a long-lived mammal*. Chicago: University of Chicago Press. Chapter 17, pp. 260-271. Available at: <https://doi.org/10.7208/chicago/9780226542263.003.0017> (Accessed: 27 August 2023).

Leggett, K. E. A. (2006) 'Home Range and Seasonal Movement of Elephants in the Kunene Region, Northwestern Namibia.', *African Zoology*, 41(1), pp. 17-36. Available at: <https://doi.org/10.1080/15627020.2006.11407332> (Accessed: 29 August 2023).

Lindeque, M., and Lindeque, P. M. (1991) 'Satellite tracking of elephants in northwestern Namibia.' *African Journal of Ecology*, 29(3), pp. 196-206. Available at: <https://doi.org/10.1111/j.1365-2028.1991.tb01002.x> (Accessed: 26 August 2023).

Loarie, S. R., Aarde, R. J. V., and Pimm, S. L. (2009) 'Fences and artificial water affect African savannah elephant movement patterns.', *Biological Conservation*, 142(12), pp. 3086-3098. Available at: <https://doi.org/10.1016/j.biocon.2009.08.008> (Accessed: 29 August 2023).

Lombard, A. T., Johnson, C. F., Cowling, R. M., and Pressey, R. L. (2001) 'Protecting plants from elephants: Botanical reserve scenarios within the Addo Elephant National Park, South Africa.', *Biological Conservation*, 102(2), pp. 191-203. Available at: [https://doi.org/10.1016/S0006-3207\(01\)00056-8](https://doi.org/10.1016/S0006-3207(01)00056-8) (Accessed: 25 August 2023).

Lusseau, D. (2003) 'Effects of Tour Boats on the Behavior of Bottlenose Dolphins: Using Markov Chains to Model Anthropogenic Impacts.', *Conservation Biology*, 17(6), pp. 1785-1793. Available at: <https://doi.org/10.1111/j.1523-1739.2003.00054.x> (Accessed: 21 August 2023).

Mabille, G., Dussault, C., Ouellet, J. P., and Laurian, C. (2012) 'Linking trade-offs in habitat selection with the occurrence of functional responses for moose living in two nearby study areas.', *Oecologia*, 170, pp. 965–977. Available at: <https://doi.org/10.1007/s00442-012-2382-0> (Accessed: 27 August 2023).

MacFadyen, S., Hui, C., Verburg, P. H., and Van Teeffelen, A. J. A. (2019) 'Spatiotemporal distribution dynamics of elephants in response to density, rainfall, rivers and fire in Kruger National Park, South Africa.' *Diversity and Distributions*, 25(6), pp. 880-894. Available at: <https://doi.org/10.1111/ddi.12907> (Accessed: 10 September 2023).

Mackey, R., Page, B., Duffy, K., and Slotow, R. (2006) 'Modelling elephant population growth in small, fenced, South African reserves.' *South African Journal of Wildlife Research*, 36(1), pp. 33-43. Available at: <https://hdl.handle.net/10520/EJC117230> (Accessed: 31 August 2023).

Marshall, J. P., Rajah, A., Parrini, F., Henley, M. D., Henley, S. R., and Erasmus, B. N. (2011) 'Scale-dependent selection of greenness by African elephants in the Kruger-private reserve transboundary region, South Africa.', *European Journal of Wildlife Research*, 57(3), pp. 537-548. Available at: <https://doi.org/10.1007/s10344-010-0462-1> (Accessed: 10 September 2023).

McClintock, B. T., Langrock, R., Gimenez, O., Cam, E., Borchers, D. L., Glennie, R., and Patterson, T. A. (2020) 'Uncovering ecological state dynamics with hidden Markov models. *Ecology Letters*, 23(12), pp. 1878-1903. Available at: <https://doi.org/10.1111/ele.13610> (Accessed: 13 August 2023).

McKellar, A. E., Langrock, R., Walters, J. R., and Kesler, D. C. (2015) 'Using mixed hidden Markov models to examine behavioral states in a cooperatively breeding bird.', *Behavioral Ecology*, 26(1), pp. 148-157. Available at: <https://doi.org/10.1093/beheco/aru171> (Accessed: 18 August 2023).

Meenakshi, B., Haariharan, N. C., Krishnakanth, L., and Abishek, J. (2022) 'Animal Intrusion Detection and Ranging system using YOLOv4 and LoRa.', In *2022 International Conference on Power, Energy, Control and Transmission Systems (ICPECTS)* (pp. 1-6). IEEE. Available at: doi: 10.1109/ICPECTS56089.2022.10047729 (Accessed: 18 August 2023).

Michelot, T., Langrock, R., and Patterson, T. A. (2016) 'moveHMM: An R package for the statistical modelling of animal movement data using hidden Markov models.', *Methods in Ecology and Evolution*, 7(11), pp. 1308-1315. Available at: <https://doi.org/10.1111/2041-210X.12578> (Accessed: 16 June 2023).

Michelot, T., Langrock, R., and Patterson, T. (2023) 'moveHMM: An R package for the analysis of animal movement data.' *ArXiv Preprint*, pp. 1-24. Available at: [bit.ly/3KNH4BI](https://bit.ly/3KNH4BI) (Accessed: 13 June 2023).

Mole, M. A., Rodrigues DÁraujo, S., Van Aarde, R. J., Mitchell, D., and Fuller, A. (2016) ‘Coping with heat: Behavioural and physiological responses of savanna elephants in their natural habitat.’, *Conservation Physiology*, 4(1). Available at: <https://doi.org/10.1093/conphys/cow044> (Accessed: 30 August 2023).

Morales, J. M., Haydon, D. T., Frair, J., Holsinger, K. E., and Fryxell, J. M. (2004) ‘Extracting more out of relocation data: building movement models as mixtures of random walks.’, *Ecology*, 85(9), pp. 2436-2445. Available at: <https://doi.org/10.1890/03-0269> (Accessed: 21 August 2023).

Morales, J. M., Moorcroft, P. R., Matthiopoulos, J., Frair, J. L., Kie, J. G., Powell, R. A., and Haydon, D. T. (2010) ‘Building the bridge between animal movement and population dynamics.’, *Philosophical Transactions of the Royal Society B: Biological Sciences*, 365(1550), pp. 2289-2301. Available at: <https://doi.org/10.1098/rstb.2010.0082> (Accessed: 20 August 2023).

Moss, C. J., and Poole, J. H. (1983) ‘Relationships and social structure of African elephants.’ In *Primate Social Relationships: An Integrated Approach*; Hinde, R.A., Ed.; Blackwell Scientific: Oxford, UK, 1983; pp. 315–325. Available at: [bit.ly/45MeOIp](https://bit.ly/45MeOIp) (Accessed: 28 August 2023).

Moss, C. J. (2001) ‘The demography of an African elephant (*Loxodonta africana*) population in Amboseli, Kenya.’, *Journal of Zoology*. Cambridge University Press, 255(2), pp. 145–156. Available at: doi: 10.1017/S0952836901001212. (Accessed: 24 August 2023).

Moss, C. J., and Lee, P. C. (2011) ‘Female reproductive strategies: Individual life histories.’ In *The Amboseli Elephants: A Long-Term Perspective on a Long-Lived Mammal*; Moss, C.J., Croze, H., Lee, P.C., Eds.; The University of Chicago Press: Chicago, IL, USA, 2011; pp. 187–204. Available at: <https://doi.org/10.1644/11-MAMM-R-329.1> (Accessed: 28 August 2023).



Mramba, R. P., Andreassen, H. P., Mlingi, V., and Skarpe, C. (2019) 'Activity patterns of African elephants in nutrient-rich and nutrient-poor savannas.', *Mammalian Biology*, 94, pp. 18-24. Available at: <https://doi.org/10.1016/j.mambio.2018.12.001> (Accessed: 29 August 2023).

Mucina, L., and Rutherford, M. C. (2006). *The vegetation of South Africa, Lesotho and Swaziland*. South African National Biodiversity Institute.

Murphy, D., Mumby, H. S., and Henley, M. D. (2020) 'Age differences in the temporal stability of a male African elephant (*Loxodonta africana*) social network.', *Behavioral Ecology*, 31(1), pp. 21-31. Available at: <https://doi.org/10.1093/beheco/arz152> (Accessed: 28 August 2023).

Mwalyosi, R. B. (1987) 'Decline of *Acacia tortilis* in Lake Manyara National Park, Tanzania.', *African Journal of Ecology*, 25(1), pp. 51-53. Available at: <https://doi.org/10.1111/j.1365-2028.1987.tb01090.x> (Accessed: 26 August 2023).

Nasseri, N. A., McBrayer, L. D., and Schulte, B. A. (2011) 'The impact of tree modification by African elephant (*Loxodonta africana*) on herpetofaunal species richness in northern Tanzania.' *African Journal of Ecology*, 49(2), pp. 133-140. Available at: <https://doi.org/10.1111/j.1365-2028.2010.01238.x> (Accessed: 26 August 2023).

Nathan, R., Getz, W. M., Revilla, E., Holyoak, M., Kadmon, R., Saltz, D., and Smouse, P. E. (2008) 'A movement ecology paradigm for unifying organismal movement research.', *Proceedings of the National Academy of Sciences of the United States of America*, 105, pp. 19052-19059. Available at: <https://doi.org/10.1073/pnas.0800375105> (Accessed: 19 August 2023).

Ngene, S. M., Skidmore, A. K., Van Gils, H., Douglas-Hamilton, I., and Omondi, P. (2009) 'Elephant distribution around a volcanic shield dominated by a mosaic of forest and savanna (Marsabit, Kenya).', *African Journal of Ecology*, 47(2), pp. 234-245. Available at: <https://doi.org/10.1111/j.1365-2028.2008.01018.x> (Accessed: 13 August 2023).

Norton-Griffiths, M. (1975) 'The numbers and distribution of large mammals in Ruaha National Park, Tanzania.', *African Journal of Ecology*, 13(2), pp. 121-140. Available at: <https://doi.org/10.1111/j.1365-2028.1975.tb00127.x> (Accessed: 26 August 2023).

O'Connell-Rodwell, C. E., Wood, J. D., Kinzley, C., Rodwell, T. C., Alarcon, C., Wasser, S. K., and Sapolsky, R. (2011) 'Male African elephants (*Loxodonta africana*) queue when the stakes are high.', *Ethology Ecology & Evolution*, 23(4), pp. 388-397. Available at: <https://doi.org/10.1080/03949370.2011.598569> (Accessed: 28 August 2023).

Ottichilo, W. K. (1986) 'Population estimates and distribution patterns of elephants in the Tsavo ecosystem, Kenya, in 1980.', *African Journal of Ecology*, 24(1), pp. 53-57. Available at: <https://doi.org/10.1111/j.1365-2028.1986.tb00342.x> (Accessed: 26 August 2023).

Owen-Smith, R. N. (1988). *Megaherbivores: the influence of very large body size on ecology*. Cambridge university press.

Owen-Smith, R. N. (2002). *Adaptive herbivore ecology: from resources to populations in variable environments*. Cambridge University Press.

Owen-Smith, N. G. I. H., Kerley, G. I. H., Page, B., Slotow, R., and Van Aarde, R. J. (2006) 'A scientific perspective on the management of elephants in the Kruger National Park and elsewhere: elephant conservation.', *South African journal of science*, 102(9), pp. 389-394. Available at: <https://hdl.handle.net/10520/EJC96609> (Accessed: 12 September 2023).

Owen-Smith, N., Fryxell, J. M., and Merrill, E. H. (2010) 'Foraging theory upscaled: the behavioural ecology of herbivore movement.', *Philosophical Transactions of the Royal Society B: Biological Sciences*, 365(1550), pp. 2267-2278. Available at: <https://doi.org/10.1098/rstb.2010.0095> (Accessed: 20 August 2023).

Patterson, T. A., Basson, M., Bravington, M. V., and Gunn, J. S. (2009) 'Classifying movement behaviour in relation to environmental conditions using hidden Markov models.', *Journal of Animal Ecology*, 78(6), pp. 1113-1123. Available at: <https://doi.org/10.1111/j.1365-2656.2009.01583.x> (Accessed: 22 August 2023).

Patterson, T. A., Thomas, L., Wilcox, C., Ovaskainen, O., and Matthiopoulos, J. (2008) 'State-space models of individual animal movement.', *Trends in ecology & evolution*, 23(2), pp. 87-94. Available at: <https://doi.org/10.1016/j.tree.2007.10.009> (Accessed: 23 August 2023).

Patterson, T. A., Parton, A., Langrock, R., Blackwell, P. G., Thomas, L., and King, R. (2017) 'Statistical modelling of individual animal movement: an overview of key methods and a discussion of practical challenges.', *AStA Advances in Statistical Analysis*, 101, pp. 399-438. Available at: <https://doi.org/10.1007/s10182-017-0302-7> (Accessed: 13 August 2023).

Peel, M. J. S., and Martindale, G. J. (2020) *Selati Game Reserve Management Plan. Version 1.0*. Selati Game Reserve, pp. 1-161. Available at: [bit.ly/3qD08f9](http://bit.ly/3qD08f9) (Accessed: 15 August 2023).

Pettorelli, N., Ryan, S., Mueller, T., Bunnefeld, N., Jedrzejewska, B., Lima, M., and Kausrud, K. (2011) 'The Normalized Difference Vegetation Index (NDVI): unforeseen successes in animal ecology.', *Clim Res*, 46, pp. 15-27. Available at: <https://doi.org/10.3354/cr00936> (Accessed: 11 September 2023).

Polansky, L., Kilian, W., and Wittemyer, G. (2015) 'Elucidating the significance of spatial memory on movement decisions by African savannah elephants using state-space models.', *Proceedings of the Royal Society B: Biological Sciences*, 282(1805), pp. 20143042. Available at: <https://doi.org/10.1098/rspb.2014.3042> (Accessed: 27 August 2023).

Pomerleau, C., Patterson, T. A., Luque, S., Lesage, V., Heide-Jørgensen, M. P., Dueck, L. L., and Ferguson, S. H. (2011) 'Bowhead whale *Balaena mysticetus* diving and movement patterns in the eastern Canadian Arctic: implications for foraging ecology.', *Endangered Species Research*, 15, pp. 167-177. Available at: <https://doi.org/10.3354/esr00373> (Accessed: 21 August 2023).

Poole, J. H., Kasman, L. H., Ramsay, E. C., and Lasley, B. L. (1984) 'Musth and urinary testosterone concentrations in the African elephant (*Loxodonta africana*).', *J. Reprod. Fertil.*, 70(1), pp. 255–260. Available at: <https://doi.org/10.1530/jrf.0.0700255> (Accessed: 28 August 2023).

Poole, J. H. (1987) 'Rutting Behavior in African Elephants: the Phenomenon of Musth.', *Behaviour* 102(3-4), pp. 283-316. Available at: Brill <https://doi.org/10.1163/156853986X00171> (Accessed: 28 August 2023).

Poole, J. H., Lee, P. C., Njiraini, N., and Moss, C. J. (2011) 'Longevity, Competition, and Musth: A Long-term Perspective on Male Reproductive Strategies.', *Oxford Academic*, 18, pp. 272-288. Available at: <https://doi.org/10.7208/chicago/9780226542263.003.0018> (Accessed: 24 August 2023).

Porensky, L. M., Bucher, S. F., Veblen, K. E., Treydte, A. C., and Young, T. P. (2013) 'Megaherbivores and cattle alter edge effects around ecosystem hotspots in an African savanna.', *Journal of Arid Environments*, 96, pp. 55-63. Available at: <https://doi.org/10.1016/j.jaridenv.2013.04.003> (Accessed: 08 September 2023).

Purdon, A., and Van Aarde, R. (2017) 'Water provisioning in Kruger National Park alters elephant spatial utilisation patterns.', *Journal of Arid Environments*, 141, pp. 45-51. Available at: <https://doi.org/10.1016/j.jaridenv.2017.01.014> (Accessed: 30 August 2023).

Rasmussen, L. E. L., Hall-Martin, A. J., and Hess, D. L. (1996) 'Chemical profiles of male African elephants, *Loxodonta africana*: Physiological and ecological implications.', *Journal of Mammalogy*, 77(2), pp. 422-439. Available at: <https://doi.org/10.2307/1382819> (Accessed: 28 August 2023).

Ripple, W. J., Newsome, T. M., Wolf, C., Dirzo, R., Everatt, K. T., Galetti, M., Hayward, M. W., H. Kerley, G. I., Levi, T., Lindsey, P. A., Macdonald, D. W., Malhi, Y., Painter, L. E., Sandom, C. J., Terborgh, J., and Valkenburgh, B. V. (2015) 'Collapse of the world's largest herbivores.', *Science Advances*, 1(4), pp. 1-11. Available at: <https://doi.org/1400103> (Accessed: 24 August 2023).

Russo, N. J., Davies, A. B., Blakey, R. V., Ordway, E. M., and Smith, T. B. (2023) 'Feedback loops between 3D vegetation structure and ecological functions of animals.', *Ecology Letters*, 26(9), pp. 1597-1613. Available at: <https://doi.org/10.1111/ele.14272> (Accessed: 08 September 2023).

Rutherford, M. C., Mucina, L., and Powrie, L. W. (2006) 'Biomes and bioregions of southern Africa.', *The vegetation of South Africa, Lesotho and Swaziland*, 19, pp. 30-51. Available at: [bit.ly/3QNMwIK](http://bit.ly/3QNMwIK) (Accessed: 15 August 2023).

Sach, F., Dierenfeld, E. S., Langley-Evans, S. C., Watts, M. J., and Yon, L. (2019) 'African savanna elephants (*Loxodonta africana*) as an example of a herbivore making movement choices based on nutritional needs.', *PeerJ*, 7, pp. e6260. Available at: <https://doi.org/10.7717/peerj.6260> (Accessed: 10 September 2023).

Schick, R. S., Loarie, S. R., Colchero, F., Best, B. D., Boustany, A., Conde, D. A., Halpin, P. N., Joppa, L. N., McClellan, C. M., and Clark, J. S. (2008) 'Understanding movement data and movement processes: Current and emerging directions.', *Ecology Letters*, 11(12), pp. 1338-1350. Available at: <https://doi.org/10.1111/j.1461-0248.2008.01249.x> (Accessed: 22 August 2023).

Schulte, B. A., and LaDue, C. A. (2021) 'The Chemical Ecology of Elephants: 21st Century Additions to Our Understanding and Future Outlooks.', *Animals*, 11(2860), pp. 1-18. Available at: <https://doi.org/10.3390/ani11102860> (Accessed: 28 August 2023).

Schuttler, S. G., Philbrick, J. A., Jeffery, K. J., and Eggert, L. S. (2014) 'Fine-Scale Genetic Structure and Cryptic Associations Reveal Evidence of Kin-Based Sociality in the African Forest Elephant.', *PLOS ONE*, 9(2), pp. e88074. Available at: <https://doi.org/10.1371/journal.pone.0088074> (Accessed: 28 August 2023).

Seager, S. (2023) *Personal Communication*. Selati Game Reserve, South Africa, 2-29 June 2023. Steve Seager, Wildlife Manager of the Selati Game Reserve.

Selati Game Reserve (2017). *Our Research – Selati Game Reserve*. Available at: <http://selatigamereserve.co.za/our-research/> (Accessed: 14 August 2023).

Selier, S. A. J., Slotow, R. and Balfour, D. (2018) 'Management of African elephant populations in small fenced areas: Current practices, constraints and recommendations.', *Bothalia*, 48(2), pp. a2414. Available at: <https://doi.org/10.4102/abc.v48i2.2414> (Accessed: 31 August 2023).

Senft, R. L., Coughenour, M. B., Bailey, D. W., Rittenhouse, L. R., Sala, O. E., and Swift, D. M. (1987) 'Large Herbivore Foraging and Ecological Hierarchies.', *BioScience*, 37(11), pp. 789–799. Available at: <https://doi.org/10.2307/1310545> (Accessed: 20 August 2023).

Shaffer, L. J., Khadka, K. K., and Naithani, K. J. (2019) 'Human-Elephant Conflict: A Review of Current Management Strategies and Future Directions.', *Frontiers in Ecology and Evolution*, 6, pp. 1-12. Available at: <https://doi.org/10.3389/fevo.2018.00235> (Accessed: 23 August 2023).

Shannon, G., Page, B., Slotow, R. and Duffy, K. (2006) 'African elephant home range and habitat selection in Pongola Game Reserve, South Africa', *African Zoology*, 41(1), pp. 37-44. Available at: <http://dx.doi.org/10.1080/15627020.2006.11407333> (Accessed: 26 August 2023).

Shannon, G., Page, B. R., Mackey, R. L., Duffy, K. J., and Slotow, R. (2008) 'Activity Budgets and Sexual Segregation in African Elephants (*Loxodonta africana*).', *Journal of Mammalogy*, 89(2), pp. 467-476. Available at: <https://doi.org/10.1644/07-MAMM-A-132R.1> (Accessed: 29 August 2023).

Shannon, G., Matthews, W. S., Page, B. R., Parker, G. E., and Smith, R. J. (2009) 'The effects of artificial water availability on large herbivore ranging patterns in savanna habitats: A new approach based on modelling elephant path distributions.', *Diversity and Distributions*, 15(5), pp. 776-783. Available at: <https://doi.org/10.1111/j.1472-4642.2009.00581.x> (Accessed: 08 September 2023).

Shannon, G., Page, B. R., Duffy, K. J., and Slotow, R. (2010) 'The ranging behaviour of a large sexually dimorphic herbivore in response to seasonal and annual environmental variation.', *Austral Ecology*, 35(7), pp. 731-742. Available at: <https://doi.org/10.1111/j.1442-9993.2009.02080.x> (Accessed: 29 August 2023).

Shannon, G., Thaker, M., Vanak, A. T., Page, B. R., Grant, R., and Slotow, R. (2011) 'Relative impacts of elephant and fire on large trees in a savanna ecosystem.', *Ecosystems*, 14, pp. 1372-1381. Available at: <https://doi.org/10.1007/s10021-011-9485-z> (Accessed: 12 September 2023).

Sheil, D., and Salim, A. (2006) 'Forest Tree Persistence, Elephants, and Stem Scars.' *Biotropica*, 36(4), pp. 505-521. Available at: <https://doi.org/10.1111/j.1744-7429.2004.tb00346.x> (Accessed: 27 August 2023).

Shoshani, J., Sanders, W. J., and Tassy, P. (2001) 'Elephants and other proboscideans: a summary of recent findings and new taxonomic suggestions.' In *La terra degli Elefanti—The world of Elephants, Proceedings of the 1st International Congress*, pp. 676-679. Available at: [bit.ly/3PynagP](http://bit.ly/3PynagP) (Accessed: 24 August 2023).

Shoshani, J., and Tassy, P. (2004) 'Advances in proboscidean taxonomy & classification, anatomy & physiology, and ecology & behavior.', *Quaternary International*, 126-128, pp. 5-20. Available at: <https://doi.org/10.1016/j.quaint.2004.04.011> (Accessed: 24 August 2023).

Siegel, M. (2023) *Personal Communication*. Selati Game Reserve, South Africa, 2-29 June 2023. Madeline Siegel, Research Coordinator of the Selati Game Reserve

Slotow, R., Van Dyk, G., Poole, J., Page, B., and Klocke, A. (2000) 'Older bull elephants control young males.', *Nature*, 408(6811), pp. 425-426. Available at: <https://doi.org/10.1038/35044191> (Accessed: 24 August 2023).

Slotow, R., Garai, M. E., Reilly, B., Page, B., and Carr, R. D. (2005) 'Population dynamics of elephants re-introduced to small fenced reserves in South Africa.', *South African Journal of Wildlife Research-24-month delayed open access*, 35(1), pp. 23-32. Available at: <https://hdl.handle.net/10520/EJC117208> (Accessed: 31 August 2023).

Slotow, R. (2012) 'Fencing for Purpose: A Case Study of Elephants in South Africa.' In: Somers, M., Hayward, M. (eds) *Fencing for Conservation*. Springer, New York, NY. Available at: [https://doi.org/10.1007/978-1-4614-0902-1\\_6](https://doi.org/10.1007/978-1-4614-0902-1_6) (Accessed: 31 August 2023).

Smit, I. P., Grant, C. C., and Devereux, B. J. (2007) 'Do artificial waterholes influence the way herbivores use the landscape? Herbivore distribution patterns around rivers and artificial surface water sources in a large African savanna park.', *Biological Conservation*, 136(1), pp. 85-99. Available at: <https://doi.org/10.1016/j.biocon.2006.11.009> (Accessed: 10 September 2023).

Songhurst, A., McCulloch, G., and Coulson, T. (2016) 'Finding pathways to human - Elephant coexistence: A risky business.' *Oryx*, 50, pp. 713-720. Available at: <https://doi.org/10.1017/S0030605315000344> (Accessed: 30 August 2023).

Spiegel, O., Leu, S. T., Bull, C. M., and Sih, A. (2017) 'What's your move? Movement as a link between personality and spatial dynamics in animal populations.', *Ecology Letters*, 20(1), pp. 3-18. Available at: <https://doi.org/10.1111/ele.12708> (Accessed: 20 August 2023).

Ssali, F., Sheil, D., and Nkurunungi, J. B. (2013) 'How selective are elephants as agents of forest tree damage in Bwindi Impenetrable National Park, Uganda?', *African Journal of Ecology*, 51(1), pp. 55-65. Available at: <https://doi.org/10.1111/aje.12006> (Accessed: 27 August 2023).

Stevens, N., Erasmus, B. F. N., Archibald, S., and Bond, W. J. (2016) 'Woody encroachment over 70 years in South African savannahs: overgrazing, global change or extinction aftershock?.', *Philosophical Transactions of the Royal Society B: Biological Sciences*, 371(1703), pp. 20150437. Available at: <https://doi.org/10.1098/rstb.2015.0437> (Accessed: 26 August 2023).

Stillfried, M., Gras, P., Börner, K., Göritz, F., Painer, J., Röllig, K., Wenzler, M., Hofer, H., and Ortmann, S. (2017) 'Secrets of Success in a Landscape of Fear: Urban Wild Boar Adjust Risk Perception and Tolerate Disturbance.', *Frontiers in Ecology and Evolution*, 5, pp. 310590. Available at: <https://doi.org/10.3389/fevo.2017.00157> (Accessed: 21 August 2023).



Stokke, S., and Du Toit, J. T. (2002) 'Sexual segregation in habitat use by elephants in Chobe National Park, Botswana.', *African Journal of Ecology*, 40(4), pp. 360-371. Available at: <https://doi.org/10.1046/j.1365-2028.2002.00395.x> (Accessed: 30 August 2023).

Taher, T. M., Lihan, T., Arifin, N. A. T., Khodri, N. F., Mustapha, M. A., Patah, P. A., Razali, S. H. A., and Nor, S. M. (2021) 'Characteristic of habitat suitability for the Asian elephant in the fragmented Ulu Jelai Forest Reserve, Peninsular Malaysia.', *Tropical Ecology*, 62(3), pp. 347-358. Available at: <https://doi.org/10.1007/s42965-021-00154-5> (Accessed: 13 August 2023).

Talukdar, N. R., Choudhury, P., Ahmad, F., Ahmed, R., Ahmad, F., and Al-Razi, H. (2020) 'Habitat suitability of the Asiatic elephant in the trans-boundary Patharia Hills Reserve Forest, northeast India.', *Modeling Earth Systems and Environment*, 6(3), pp. 1951-1961. Available at: <https://doi.org/10.1007/s40808-020-00805-x> (Accessed: 13 August 2023).

Taylor, L. A., Vollrath, F., Lambert, B., Lunn, D., Douglas - Hamilton, I., and Wittemyer, G. (2020) 'Movement reveals reproductive tactics in male elephants.', *Journal of Animal Ecology*, 89(1), pp. 57-67. Available at: <https://doi.org/10.1111/1365-2656.13035> (Accessed: 14 August 2023).

Taylor, L. A., Wittemyer, G., Lambert, B., Douglas-Hamilton, I., and Vollrath, F. (2022) 'Movement behaviour after birth demonstrates precocial abilities of African savannah elephant, *Loxodonta africana*, calves.', *Animal Behaviour*, 187, pp. 331-353. Available at: <https://doi.org/10.1016/j.anbehav.2022.03.002> (Accessed: 13 September 2023).

Teren, G., Owen-Smith, N., and N. Erasmus, B. F. (2018) 'Elephant-mediated compositional changes in riparian canopy trees over more than two decades in northern Botswana.', *Journal of Vegetation Science*, 29(4), pp. 585-595. Available at: <https://doi.org/10.1111/jvs.12638> (Accessed: 25 August 2023).

Thirgood, S., Mosser, A., Tham, S., Hopcraft, G., Mwangomo, E., Mlengeya, T., Kilewo, M., Fryxell, J., E. Sinclair, A. R., and Borner, M. (2004) 'Can parks protect migratory ungulates? The case of the Serengeti wildebeest.', *Animal Conservation*, 7(2), pp. 113-120. Available at: <https://doi.org/10.1017/S1367943004001404> (Accessed: 22 August 2023).

Thompson, K. E., Ford, A., Esteban, G., Poupard, A., Zoon, K. and Pettoirelli, N. (2022) 'Impacts of African savannah elephants (*Loxodonta africana*) on tall trees and their recovery within a small, fenced reserve in South Africa.', *African Journal of Ecology*, 60(3), pp. 357– 366. Available at: <https://doi.org/10.1111/aje.12963> (Accessed: 25 August 2023).

Thouless, C., Dublin, H. T., Blanc, J., Skinner, D. P., Daniel, T. E., Taylor, R., and Bouché, P. (2016) 'African elephant status report 2016.', *Occasional paper series of the IUCN Species Survival Commission*, 60, pp. 309-319. Available at: [bit.ly/44LGrl](http://bit.ly/44LGrl) (Accessed: 23 August 2023).

Towner, A. V., Leos-Barajas, V., Langrock, R., Schick, R. S., Smale, M. J., Kaschke, T., D. Jewell, O. J., and Papastamatiou, Y. P. (2016) 'Sex-specific and individual preferences for hunting strategies in white sharks.' *Functional Ecology*, 30(8), pp. 1397-1407. Available at: <https://doi.org/10.1111/1365-2435.12613> (Accessed: 23 August 2023).

Trombulak, S. C., and Frissell, C. A. (2000) 'Review of Ecological Effects of Roads on Terrestrial and Aquatic Communities.', *Conservation Biology*, 14(1), pp. 18-30. Available at: <https://doi.org/10.1046/j.1523-1739.2000.99084.x> (Accessed: 10 September 2023).

Tsalyuk, M., Kilian, W., Reineking, B., and Getz, W. M. (2019) 'Temporal variation in resource selection of African elephants follows long-term variability in resource availability.', *Ecological Monographs*, 89(2), pp. e01348. Available at: <https://doi.org/10.1002/ecm.1348> (Accessed: 27 August 2023).

Valeix, M., Fritz, H., Sabatier, R., Murindagomo, F., Cumming, D., and Duncan, P. (2011) 'Elephant-induced structural changes in the vegetation and habitat selection by large herbivores in an African savanna.' *Biological Conservation*, 144(2), pp. 902-912. Available at: <https://doi.org/10.1016/j.biocon.2010.10.029> (Accessed: 26 August 2023).

van de Kerk, M., Onorato, D. P., Criffield, M. A., Bolker, B. M., Augustine, B. C., McKinley, S. A., and Oli, M. K. (2015) 'Hidden semi-Markov models reveal multiphasic movement of the endangered Florida panther.', *Journal of Animal Ecology*, 84(2), pp. 576-585. Available at: <https://doi.org/10.1111/1365-2656.12290> (Accessed: 23 August 2023).

Vanak, A., Thaker, M., and Slotow, R. (2010) 'Do fences create an edge-effect on the movement patterns of a highly mobile mega-herbivore?', *Biological Conservation*, 143(11), pp. 2631-2637. Available at: <https://doi.org/10.1016/j.biocon.2010.07.005> (Accessed: 31 August 2023).

Vanak, A. T., Shannon, G., Thaker, M., Page, B., Grant, R., and Slotow, R. (2012) 'Biocomplexity in large tree mortality: Interactions between elephant, fire and landscape in an African savanna.', *Ecography*, 35(4), pp. 315-321. Available at: <https://doi.org/10.1111/j.1600-0587.2011.07213.x> (Accessed: 12 September 2023).

Venter, J. A., Prins, H. H. T., Mashanova, A., de Boer, W. F., and Slotow, R. (2015) 'Intrinsic and extrinsic factors influencing large African herbivore movements.', *Ecological Informatics*, 30, pp. 257-262. Available at: <https://doi.org/10.1016/j.ecoinf.2015.05.006> (Accessed: 20 August 2023).

Vogel, S. M., Lambert, B., Songhurst, A. C., McCulloch, G. P., Stronza, A. L., and Coulson, T. (2020) 'Exploring movement decisions: Can Bayesian movement-state models explain crop consumption behaviour in elephants (*Loxodonta africana*)?', *Journal of Animal Ecology*, 89(4), pp. 1055-1068. Available at: <https://doi.org/10.1111/1365-2656.13177> (Accessed: 21 August 2023).

Von Gerhardt, K., Van Niekerk, A., Kidd, M., Samways, M., and Hanks, J. (2014) 'The role of elephant *Loxodonta africana* pathways as a spatial variable in crop-raiding location.', *Oryx*, 48(3), pp. 436-444. Available at: <https://doi.org/10.1017/S003060531200138X> (Accessed: 30 August 2023).

Wall, J., Wittemyer, G., Klinkenberg, B., LeMay, V., and Douglas-Hamilton, I. (2013) 'Characterizing properties and drivers of long distance movements by elephants (*Loxodonta africana*) in the Gourma, Mali.', *Biological Conservation*, 157, pp. 60-68. Available at: <https://doi.org/10.1016/j.biocon.2012.07.019> (Accessed: 31 August 2023).

Wang, Y., Smith, J. A., and Wilmers, C. C. (2017) 'Residential development alters behavior, movement, and energetics in an apex predator, the puma.', *PLOS ONE*, 12(10), pp. e0184687. Available at: <https://doi.org/10.1371/journal.pone.0184687> (Accessed: 20 August 2023).

Webber, Q. M., and Vander Wal, E. (2017) 'An evolutionary framework outlining the integration of individual social and spatial ecology.', *Journal of Animal Ecology*, 87(1), pp. 113-127. Available at: <https://doi.org/10.1111/1365-2656.12773> (Accessed: 27 August 2023).

Western, D. (1989) 'The ecological role of elephants in Africa.', *Pachyderm*, 12, pp. 1-49. Available at: [bit.ly/44OyYA9](http://bit.ly/44OyYA9) (Accessed: 24 August 2023).

Whoriskey, K., Auger-Méthé, M., Albertsen, C. M., Whoriskey, F. G., Binder, T. R., Krueger, C. C., and Flemming, J. M. (2017) 'A hidden Markov movement model for rapidly identifying behavioral states from animal tracks.', *Ecology and Evolution*, 7(7), pp. 2112-2121. Available at: <https://doi.org/10.1002/ece3.2795> (Accessed: 21 August 2023).

Whyte, I. J., Biggs, H. C., Gaylard, A. and Braack, L. E. O. (1999) 'A new policy for the management of the Kruger National Park's elephant population.', *Koedoe*, 42(1), pp. 111–132. Available at: <https://doi.org/10.4102/koedoe.v42i1.228> (Accessed: 30 August 2023).

Whyte, I. (2001). *Headaches and heartaches: The elephant management dilemma*. In D. Schmidtz, & E. Willot (Eds.). *Environmental ethics: Introductory readings* (pp. 293–305). New York: Oxford University Press.

William, G., Sonia, S., Christophe, B., Atle, M., Nicolas, M., Maryline, P., and Clément, C. (2018) 'Same habitat types but different use: Evidence of context-dependent habitat selection in roe deer across populations.', *Scientific Reports*, 8(1), pp. 1-13. Available at: <https://doi.org/10.1038/s41598-018-23111-0> (Accessed: 27 August 2023).

Williams, H. F., Bartholomew, D. C., Amakobe, B., and Githiru, M. (2018) 'Environmental factors affecting the distribution of African elephants in the Kasigau wildlife corridor, SE Kenya.', *African Journal of Ecology*, 56(2), pp. 244-253. Available at: <https://doi.org/10.1111/aje.12442> (Accessed: 08 September 2023).

Wittemyer, G., Douglas-Hamilton, I., and Getz, W. (2005) 'The socioecology of elephants: Analysis of the processes creating multitiered social structures.', *Animal Behaviour*, 69(6), pp. 1357-1371. Available at: <https://doi.org/10.1016/j.anbehav.2004.08.018> (Accessed: 27 August 2023).

Wittemyer, G., and Getz, W. (2007) 'Hierarchical dominance structure and social organization in African elephants, *Loxodonta africana*.', *Animal Behaviour*, 73(4), pp. 671-681. Available at: <https://doi.org/10.1016/j.anbehav.2006.10.008> (Accessed: 28 August 2023).

Wittemyer, G., Getz, W.M., Vollrath, F., and Douglas-Hamilton, I. (2007) 'Social dominance, seasonal movements, and spatial segregation in African elephants: a contribution to conservation behavior.', *Behavioral Ecology and Sociobiology*, 61, pp. 1919–1931. Available at: <https://doi.org/10.1007/s00265-007-0432-0> (Accessed: 27 August 2023).

Wittemyer, G., Polansky, L., and Getz, W. M. (2008) 'Disentangling the effects of forage, social rank, and risk on movement autocorrelation of elephants using Fourier and wavelet analyses.', *Proceedings of the National Academy of Sciences*, 105(49), pp. 19108-19113. Available at: <https://doi.org/10.1073/pnas.0801744105> (Accessed: 22 August 2023).

Wittemyer, G., Daballen, D., and Douglas-Hamilton, I. (2013) 'Comparative Demography of an At-Risk African Elephant Population.' *PLOS ONE*, 8(1), pp. e53726. Available at: <https://doi.org/10.1371/journal.pone.0053726> (Accessed: 26 August 2023).

Wittemyer, G., Keating, L. M., Vollrath, F., and Douglas-Hamilton, I. (2017) 'Graph theory illustrates spatial and temporal features that structure elephant rest locations and reflect risk perception.', *Ecography*, 40(5), pp. 598-605. Available at: <https://doi.org/10.1111/ecog.02379> (Accessed: 29 August 2023).

Woodroffe, R., Hedges, S., and Durant, S. M. (2014) 'To Fence or Not to Fence.', *Science*, 344(6149), pp. 46-48. Available at: <https://doi.org/1246251> (Accessed: 30 August 2023).

Young, T. P., Patridge, N., and Macrae, A. (1995) 'Long-Term Glades in Acacia Bushland and Their Edge Effects in Laikipia, Kenya.', *Ecological Applications*, 5(1), pp. 97–108. Available at: [doi:10.2307/1942055](https://doi.org/10.2307/1942055) (Accessed: 08 September 2023).

Young, K. D., Ferreira, S. M., and Van Aarde, R. J. (2009a) 'Elephant spatial use in wet and dry savannas of southern Africa.', *Journal of Zoology*, 278(3), pp. 189-205. Available at: <https://doi.org/10.1111/j.1469-7998.2009.00568.x> (Accessed: 26 August 2023).

Young, K. D., Ferreira, S. M., and Van Aarde, R. J. (2009b) 'The influence of increasing population size and vegetation productivity on elephant distribution in the Kruger National Park.', *Austral Ecology*, 34(3), pp. 329-342. Available at: <https://doi.org/10.1111/j.1442-9993.2009.01934.x> (Accessed: 29 August 2023).

## 7 APPENDIX I

This appendix shows some photographs of the two matriarchs studied in this paper: Elza (Fig. 1-7) and Jean (Fig.8-10).



**Figure 1.** Close-up of Elza in Selati Game Reserve (Provided by: Selati Game Reserve).





**Figure 2.** Photography shot by a camera trap. Date and time are shown in the photo (Provided by Selati Game Reserve).



**Figure 3.** Photography shot by a camera trap. Date and time are shown in the photo (Provided by Selati Game Reserve).





**Figure 4.** Elza with other elephants of its herd (Provided by Selati Game Reserve).



**Figure 5.** Elza walking with its herd (Provided by Selati Game Reserve).





**Figure 6.** Elza walking with its herd (Provided by Selati Game Reserve).



**Figure 7.** Elza walking with its herd (Provided by Selati Game Reserve).





**Figure 8.** Close-up of Jean (Provided by Selati Game Reserve).





**Figure 9.** Jean (Provided by Selati Game Reserve).



**Figure 10.** Jean eating mopane leaves (Provided by Selati Game Reserve).

## 8 APPENDIX II

This Appendix contains all the relevant maps about the covariates used in this study. Particularly, the road network (Fig.1), the distribution of water points, divided into natural and artificial, as well as into perennial and seasonal (Fig.2), and the graphical outputs of NDVI calculation for each month (Fig. 3-9).

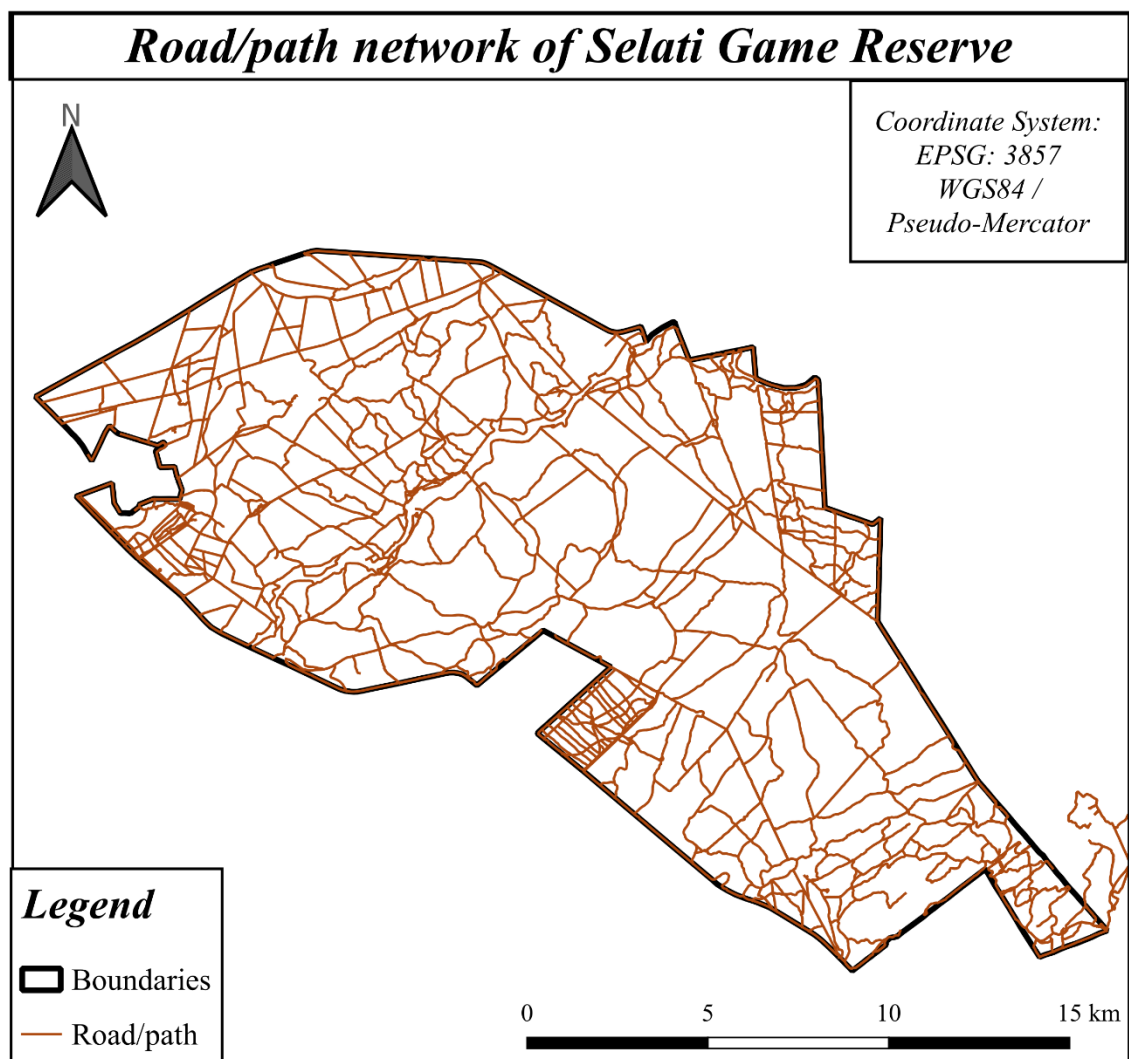


**Figure 1.** Road/path network of Selati Game Reserve (Created with QGIS Desktop by Zelia Romano).

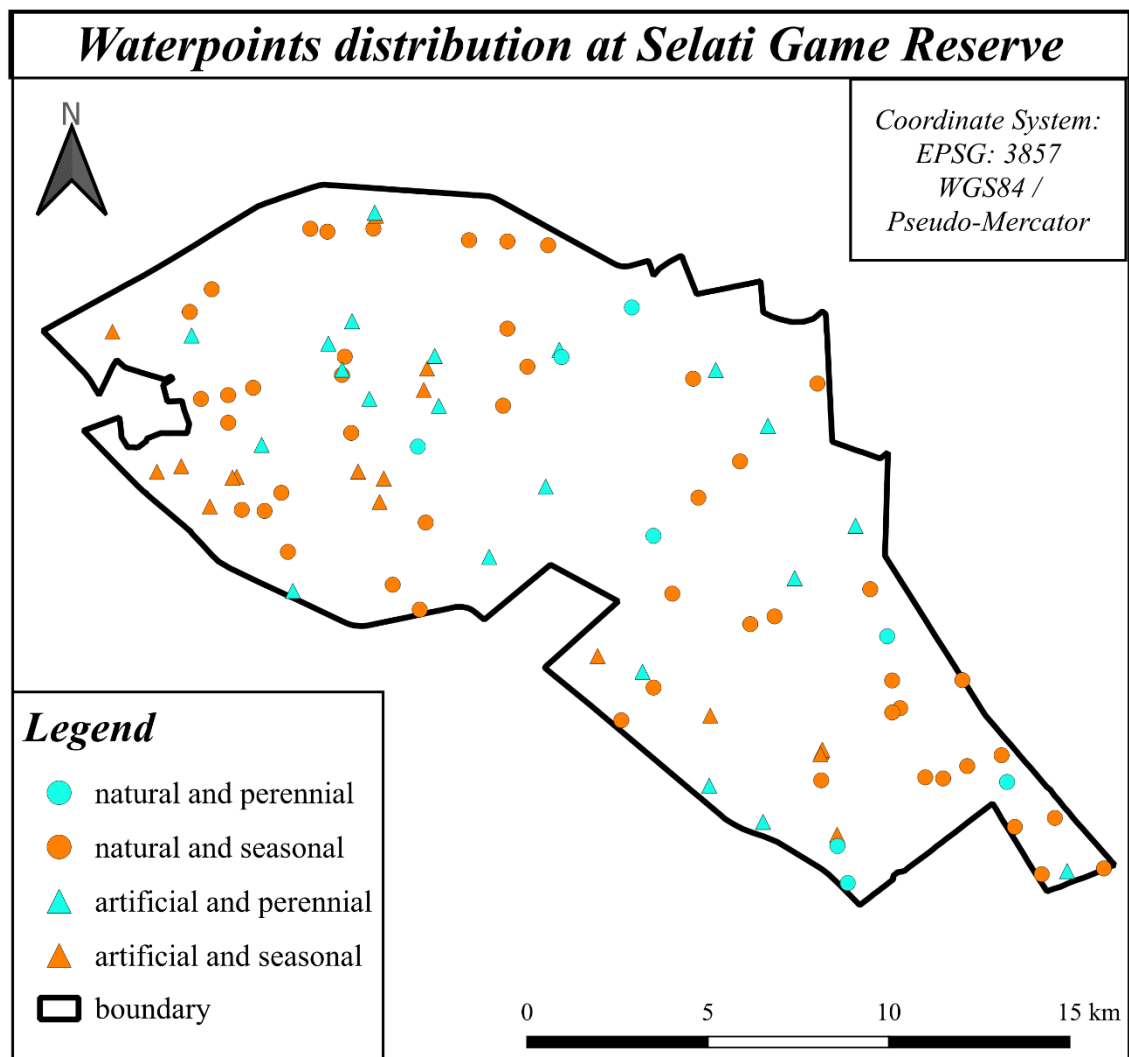


**Figure 2.** Distribution of all water points present at Selati Game Reserve (Created with QGIS Desktop by Zelia Romano).



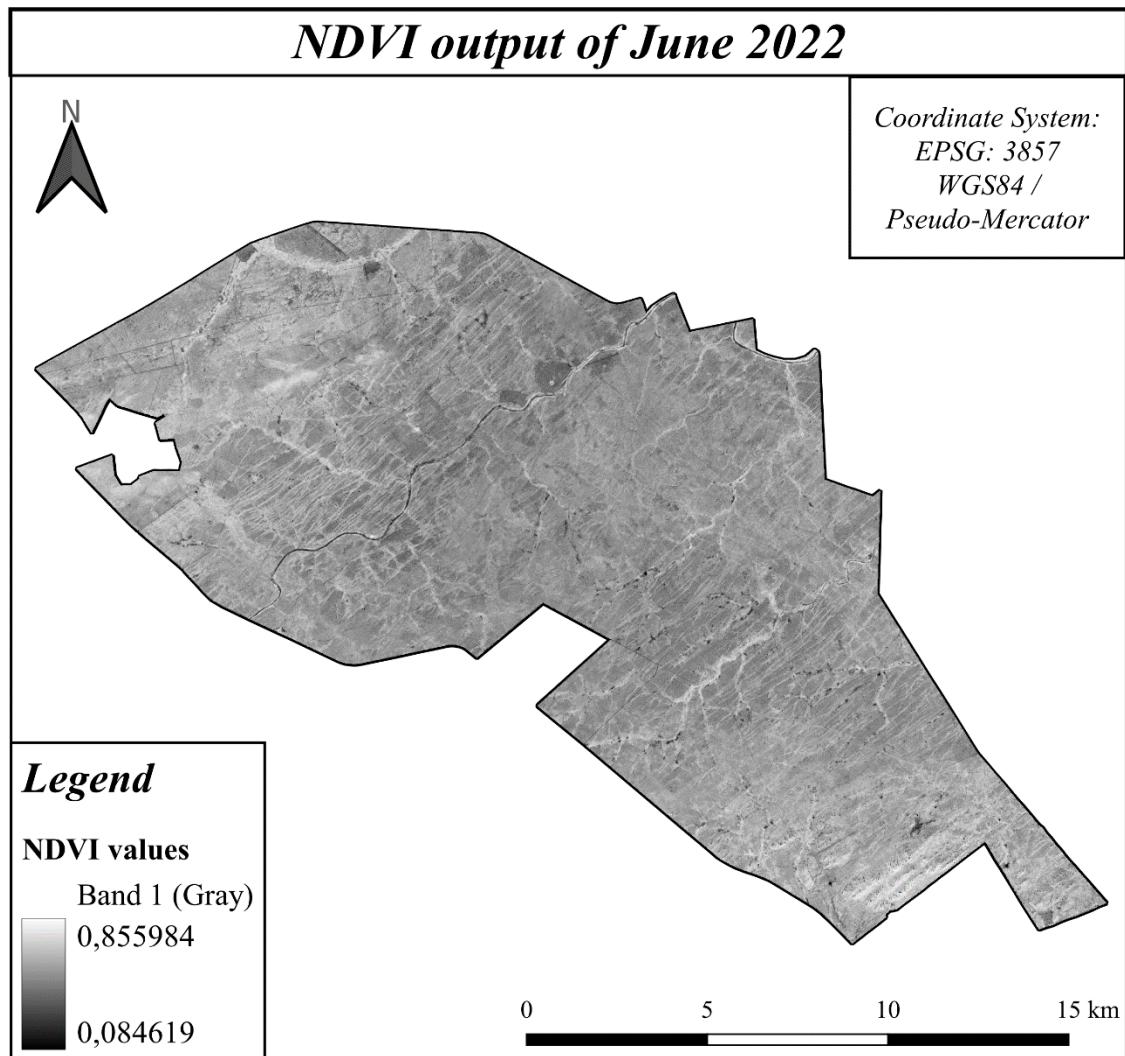


**Figure 3.** NDVI output for the month of June 2022 (Created with QGIS Desktop by Zelia Romano).

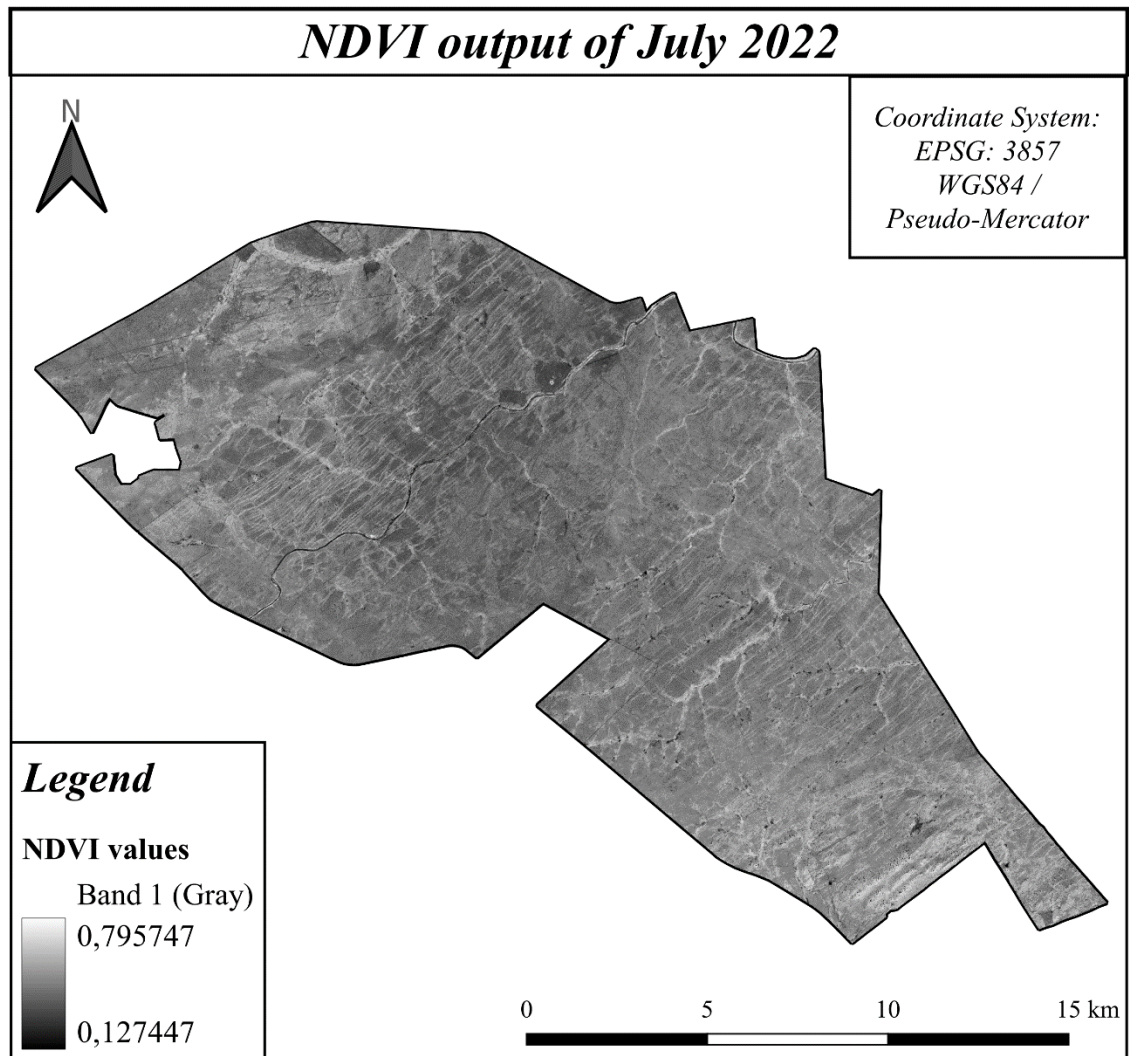


**Figure 4.** NDVI output for the month of July 2022 (Created with QGIS Desktop by Zelia Romano).



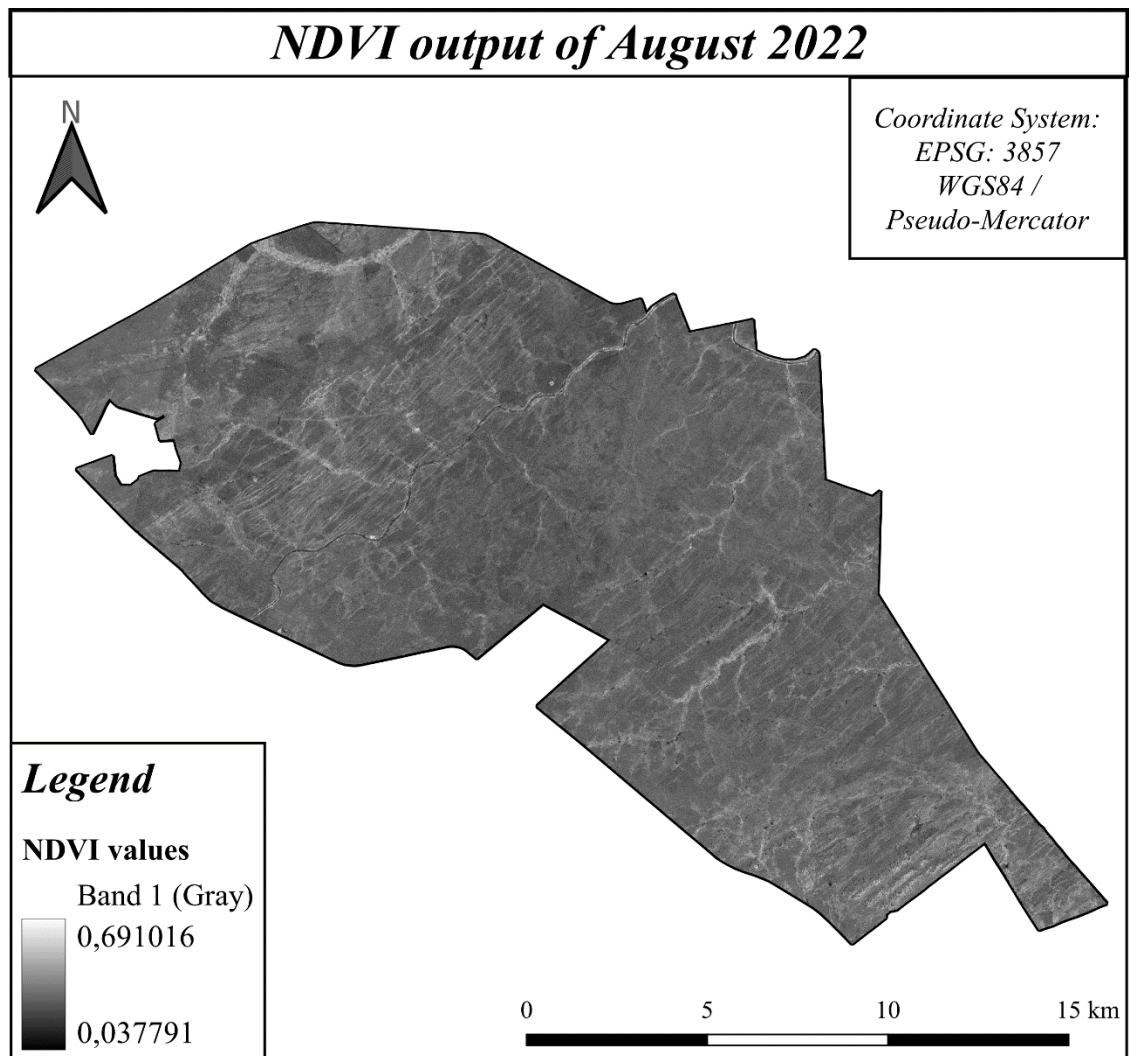


**Figure 5.** NDVI output for the month of August 2022 (Created with QGIS Desktop by Zelia Romano).

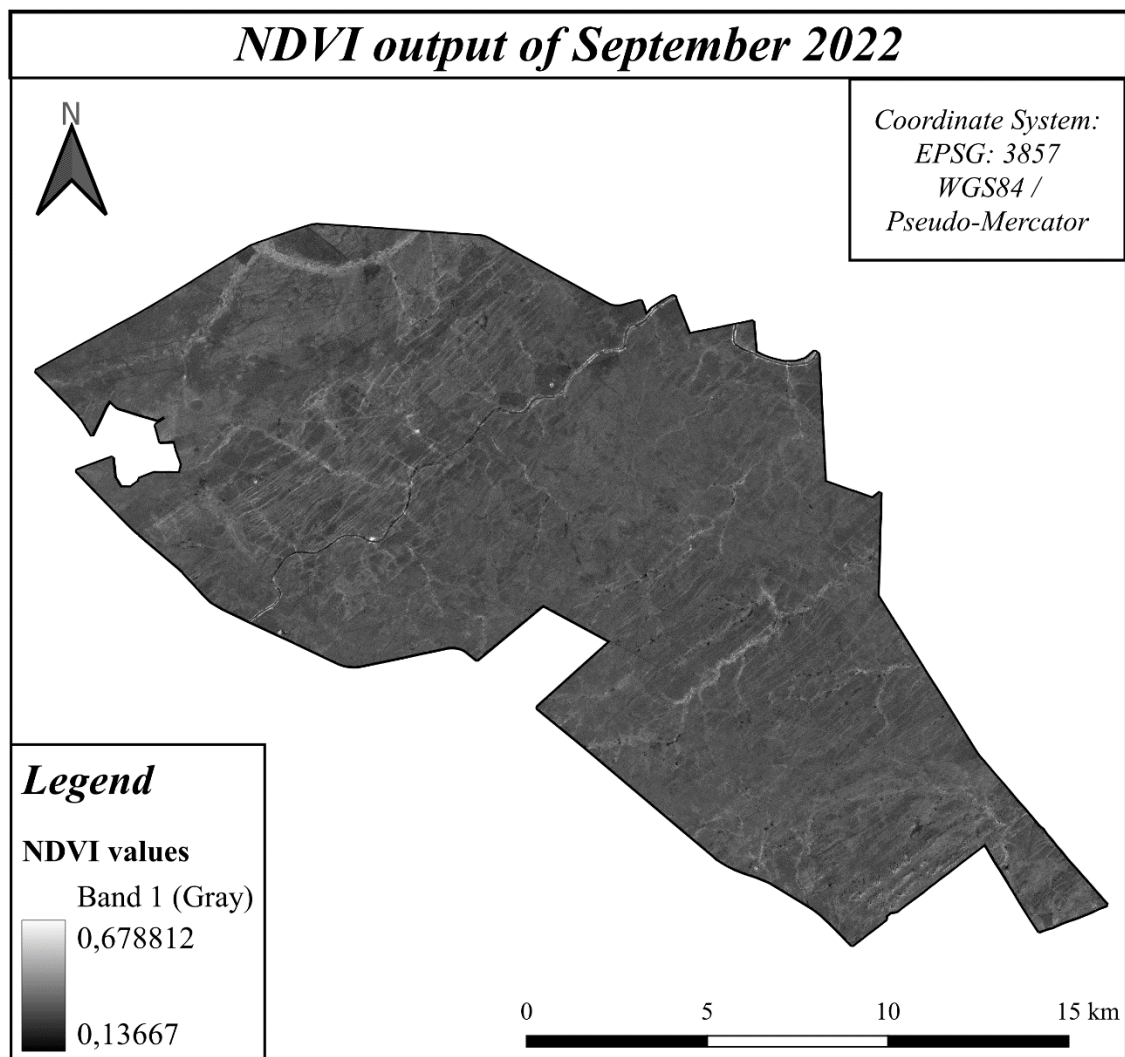


**Figure 6.** NDVI output for the month of September 2022 (Created with QGIS Desktop by Zelia Romano).

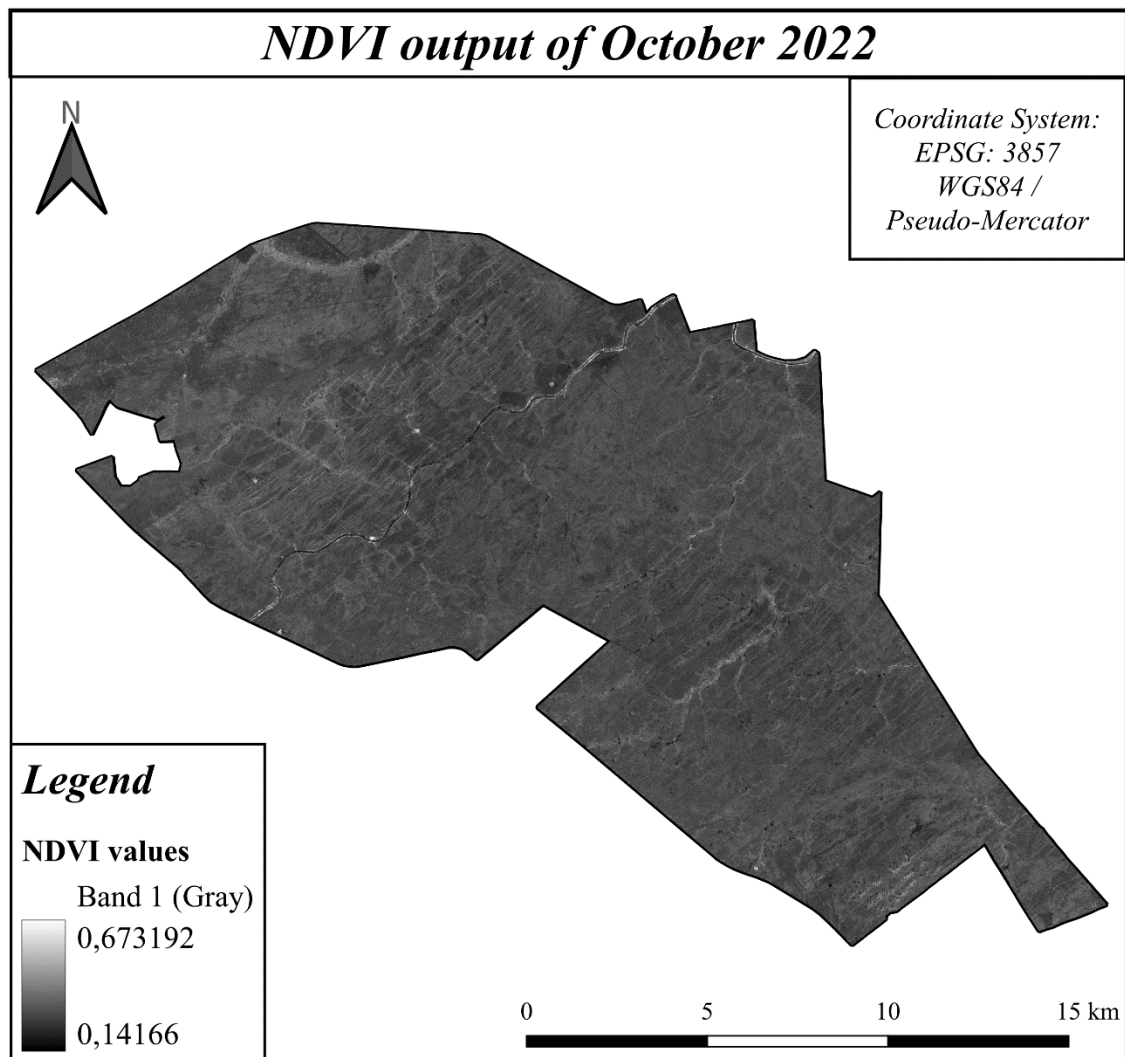


**Figure 7.** NDVI output for the month of October 2022 (Created with QGIS Desktop by Zelia Romano).

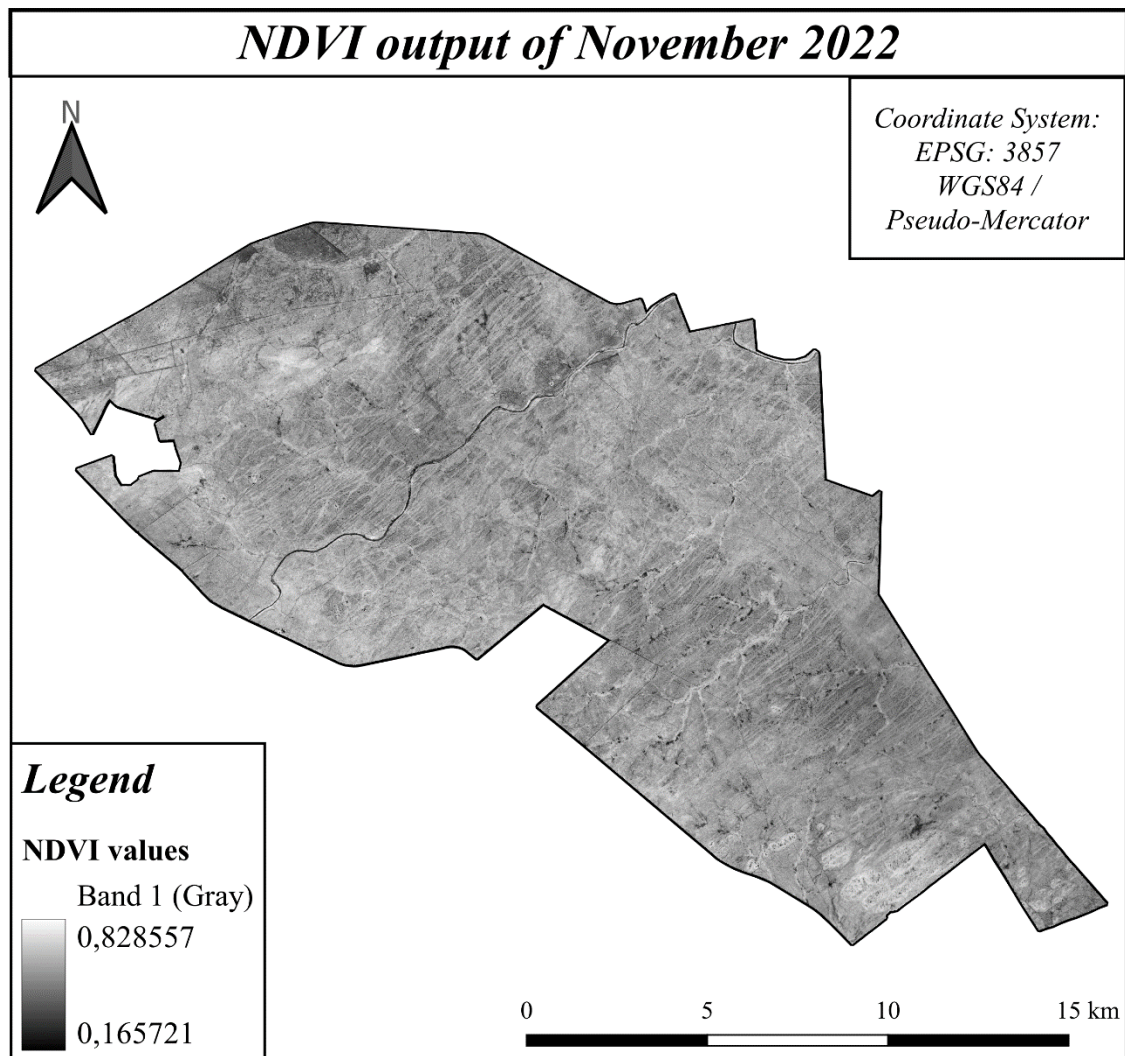


**Figure 8.** NDVI output for the month of November 2022 (Created with QGIS Desktop by Zelia Romano).

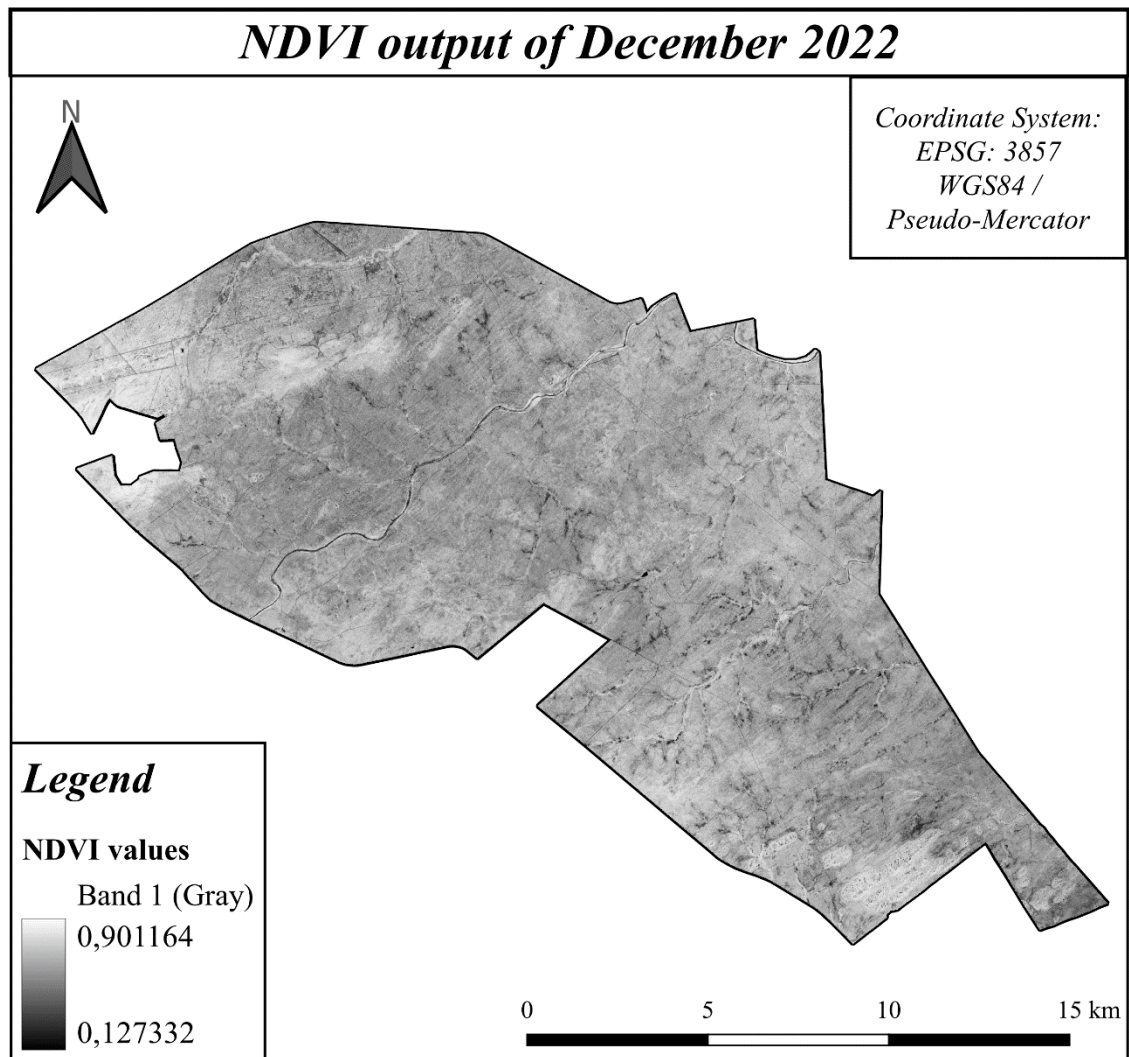


**Figure 9.** NDVI output for the month of December 2022 (Created with QGIS Desktop by Zelia Romano).



## 9 APPENDIX III

Here are reported the details of all the satellite images used for performing the NDVI calculation.

**Table 1.** ID (i.e., tile number), acquisition date, and acquisition time (in UTC) of the satellite images used in this study are reported for each month.

	<b>ID</b>	<b>Acquisition date</b> <b>dd-mm-yyyy</b>	<b>Acquisition time</b> <b>hh:mm:ss</b>
June	3227b58e-eb8f-4390- 9d70-f5baf7b3ec5b	17-06-2022	07:43:37 / 07:43:39 07:43:41 / 07:43:43
July	c79f6424-73a3-4685- 87a7-39b489900769	14-07-2022	07:26:46 / 07:26:48 07:57:54 / 07:57:56
August	58a06dbb-319c-494d- b3e0-89d86c94a969	18-08-2022	07:11:43 / 07:11:46 07:57:05 / 07:57:07
September	347489d1-722f-42c5- 9b0c-708a7675dca9	16-09-2022	07:42:16 / 07:42:19 07:42:21 / 07:43:59 07:44:01
October	e0e2792a-4ec3-4458- b881-245886b2f102	04-10-2022	07:07:26 / 07:07:28 07:30:08 / 07:30:10 07:52:39 / 07:52:41 07:52:43
November	e03daeaf-eeda-461a- 8a95-e99f8bfac69b	17-11-2022	07:09:17 / 07:09:19 07:11:52 / 07:11:54 07:40:45 / 07:40:47
December	e2fbc078-3e0d-4ec1- a031-acd44302ddb2	24-12-2022	07:08:29 / 07:08:31 07:09:32 / 07:41:27 07:41:29

**Table 2.** Satellite ID, Satellite orbit number, Product level, Product type, Asset type are showed for each month in this table.

	Satellite ID	Satellite orbit number	Product level	Product type	Asset type
June	248f 2484	34, 65 37	3B	Analytic MS	ortho_analytic_4b_sr ortho_analytic_4b_xml ortho_udm2
July	2262 240c	45, 73 09, 38	3B	Analytic MS	ortho_analytic_4b_sr ortho_analytic_4b_xml ortho_udm2
August	2432 240a	83, 13 29, 50	3B	Analytic MS	ortho_analytic_4b_sr ortho_analytic_4b_xml ortho_udm2
September	249a 2483	88, 16, 44 50, 79	3B	Analytic MS	ortho_analytic_4b_sr ortho_analytic_4b_xml ortho_udm2
October	2447 2251 2424	42, 70 07, 35 17, 46, 75	3B	Analytic MS	ortho_analytic_4b_sr ortho_analytic_4b_xml ortho_udm2
November	245c 241f 2461	47, 62 48, 81 09, 44	3B	Analytic MS	ortho_analytic_4b_sr ortho_analytic_4b_xml ortho_udm2
December	2451 241e 2480	30, 62 24 27, 41	3B	Analytic MS	ortho_analytic_4b_sr ortho_analytic_4b_xml ortho_udm2

## 10 APPENDIX IV

Maps of Elza's (Fig. 1-8) and Jean's (Fig. 9-14) tracks are showed below, each map referring to a different month.

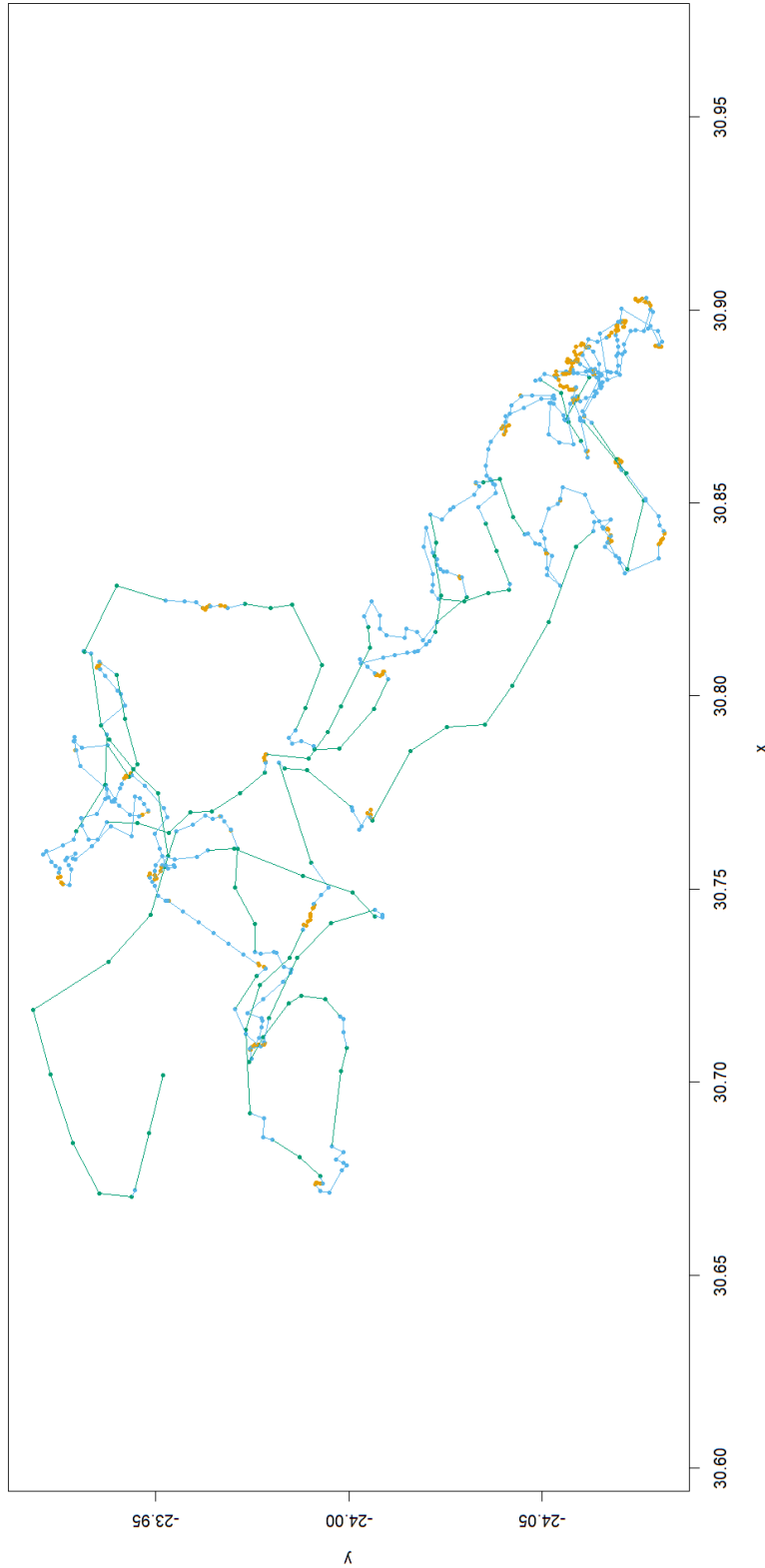


**Figure 1.** Elza's tracks in June 2022. State 1 = orange; state 2= blue; state 3= green.



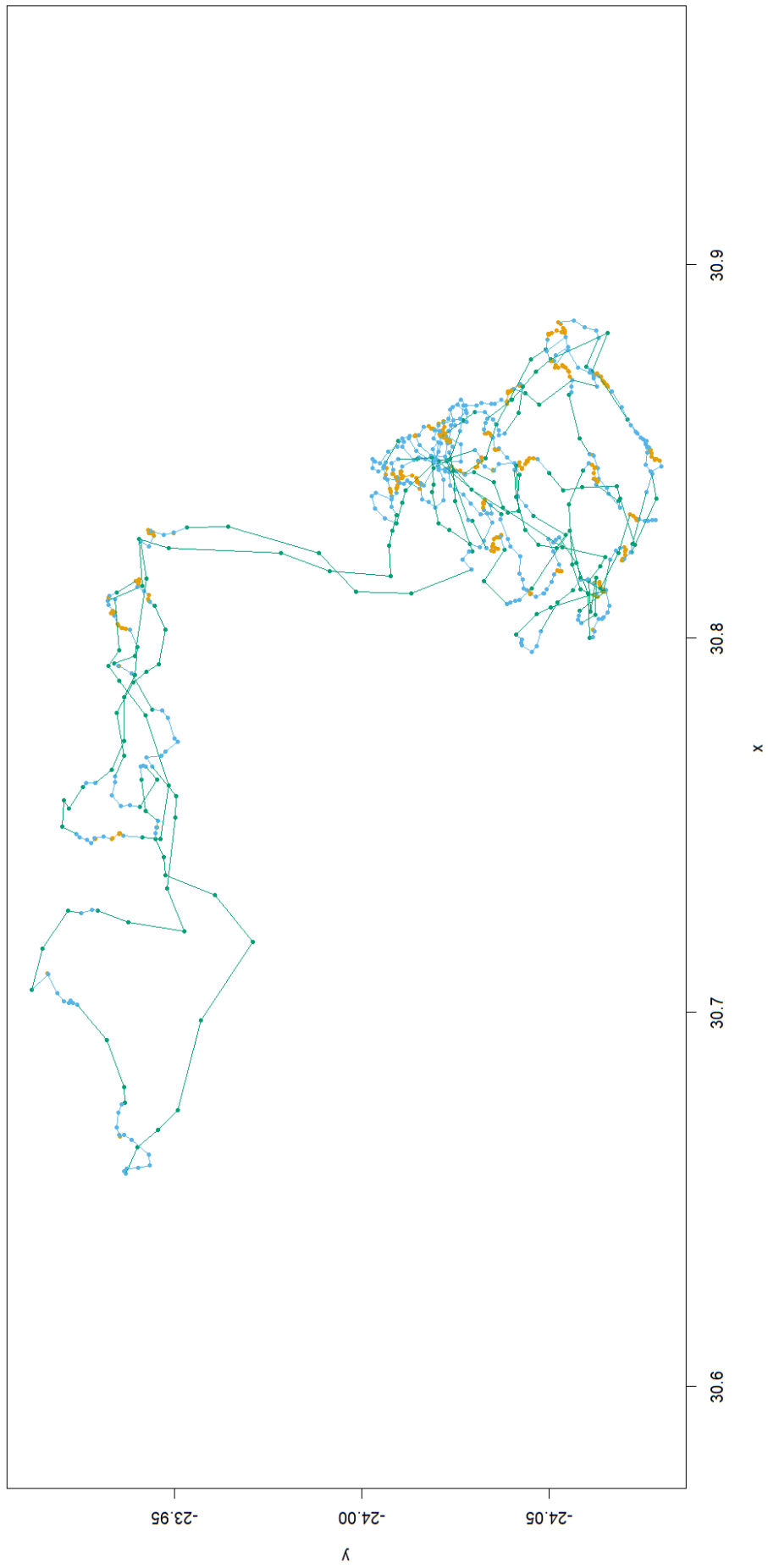


**Figure 2.** Elza's tracks in July 2022. State 1 = orange; state 2= blue; state 3= green.

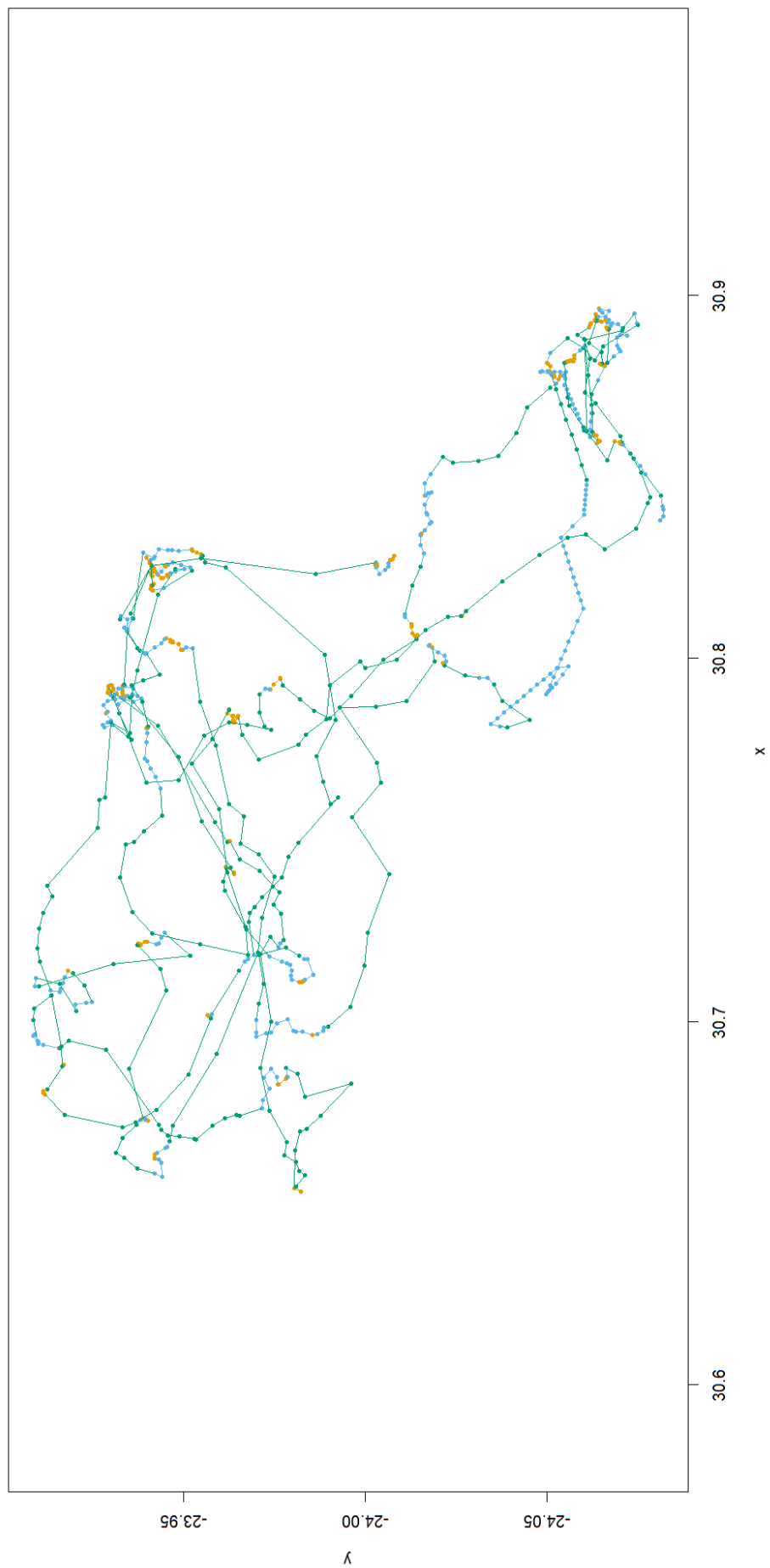


**Figure 3.** Elza's tracks in August 2022. State 1 = orange; state 2= blue; state 3= green.

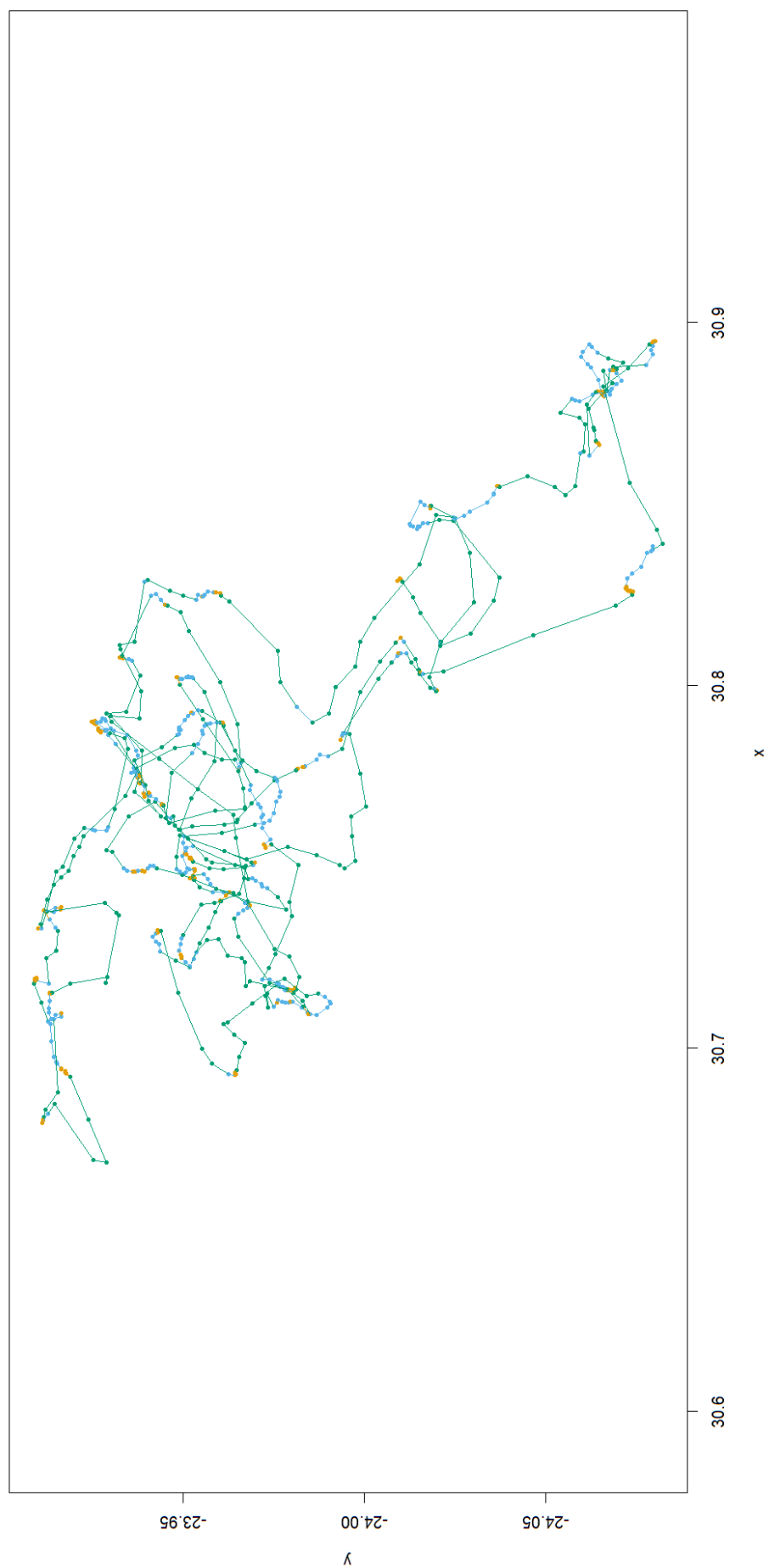


**Figure 4.** Elza's tracks in September 2022. State 1 = orange; state 2= blue; state 3= green.

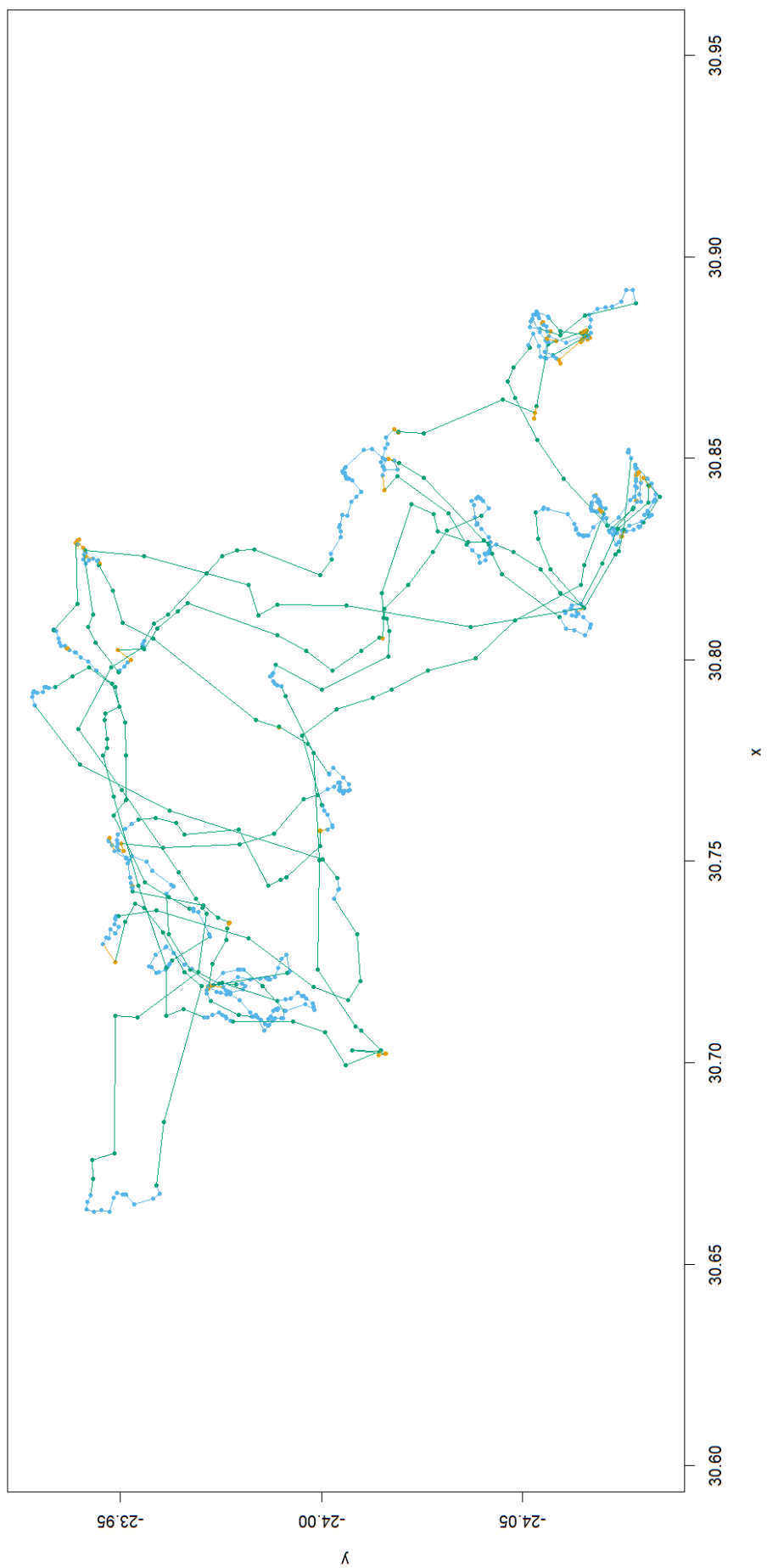


**Figure 5.** Elza's tracks in October 2022. State 1 = orange; state 2= blue; state 3= green.

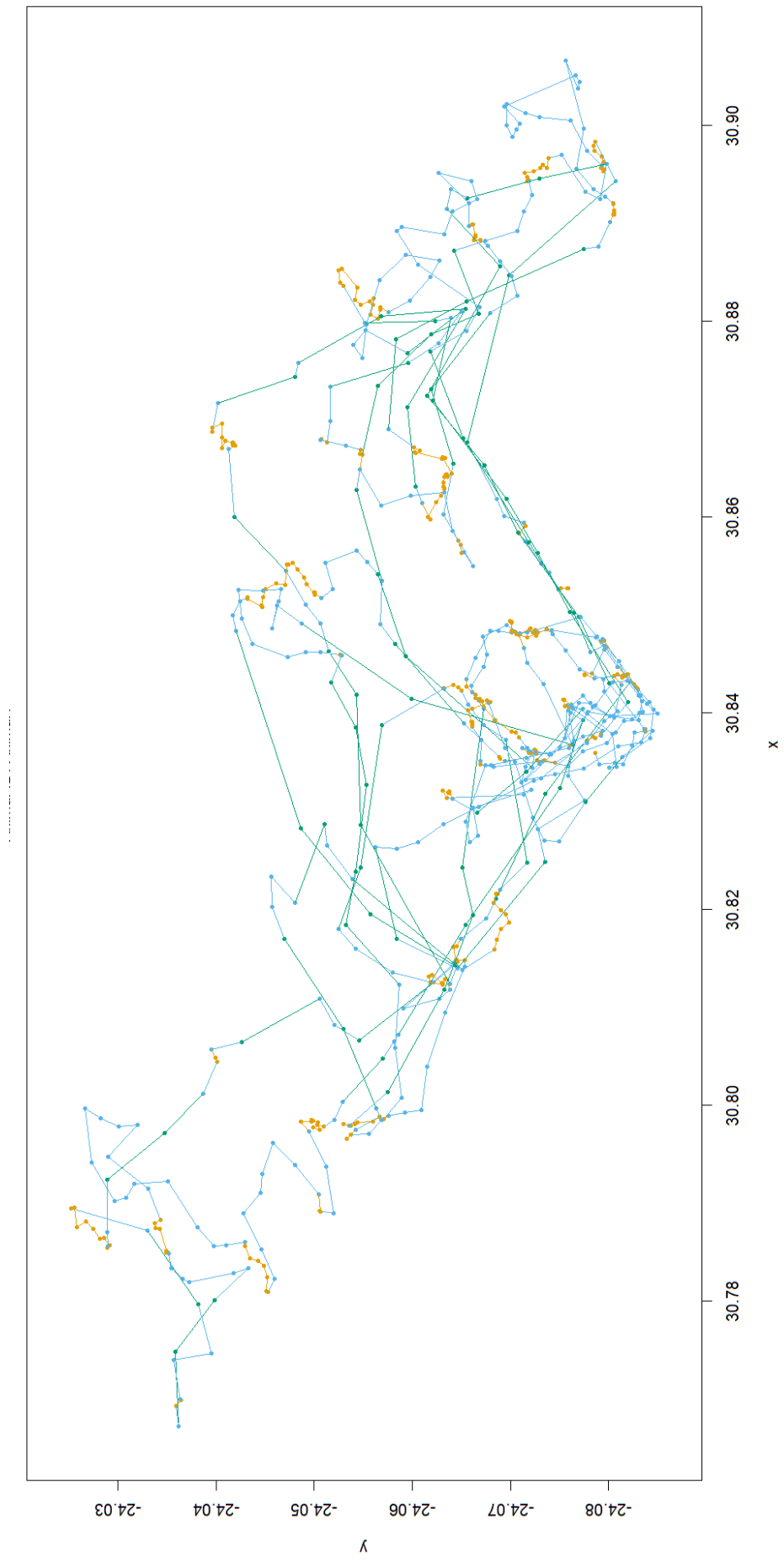


**Figure 6.** Elza's tracks in November 2022. State 1 = orange; state 2= blue; state 3= green.

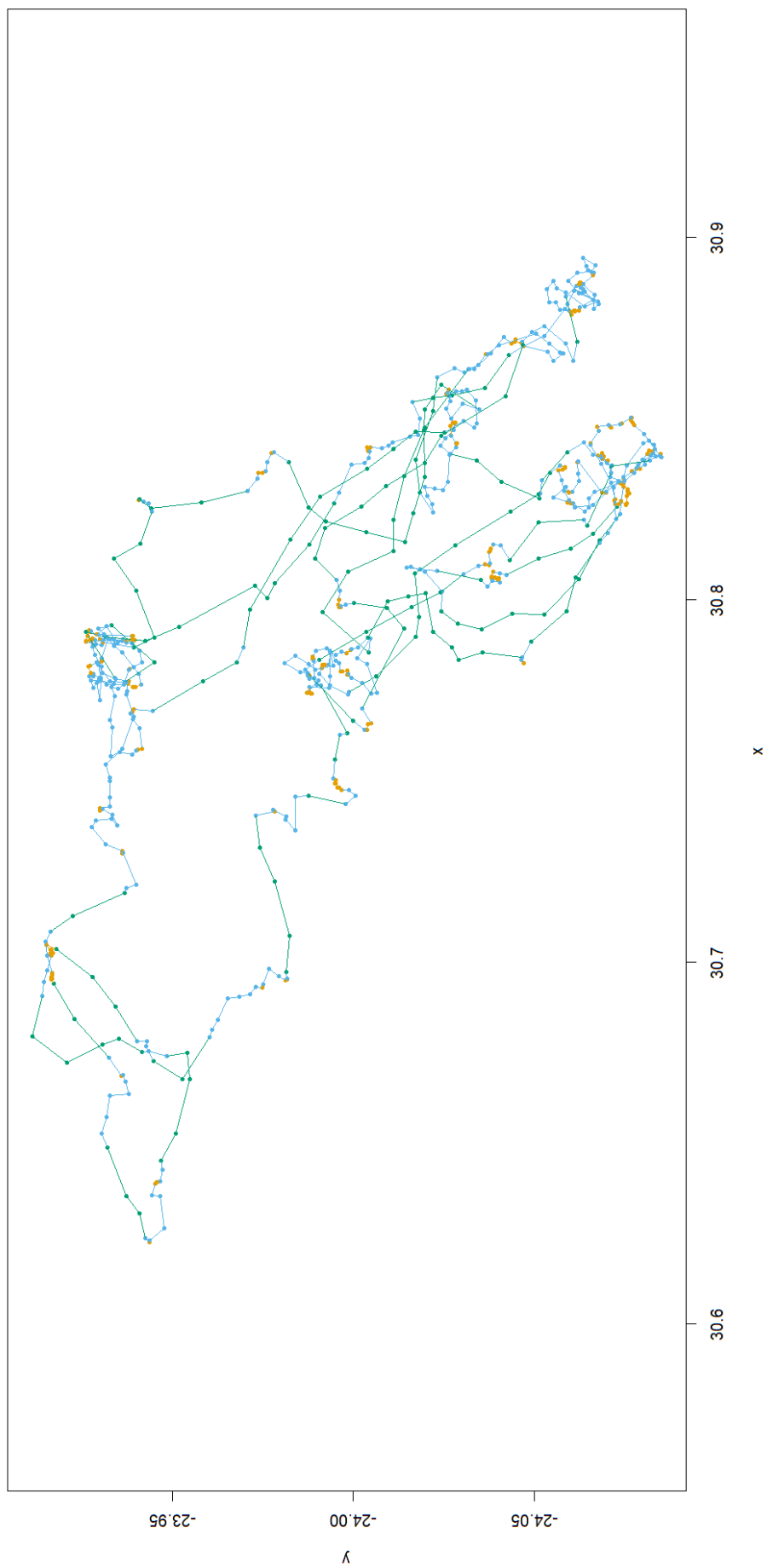


**Figure 7.** Elza's tracks in December 2022. State 1 = orange; state 2= blue; state 3= green.

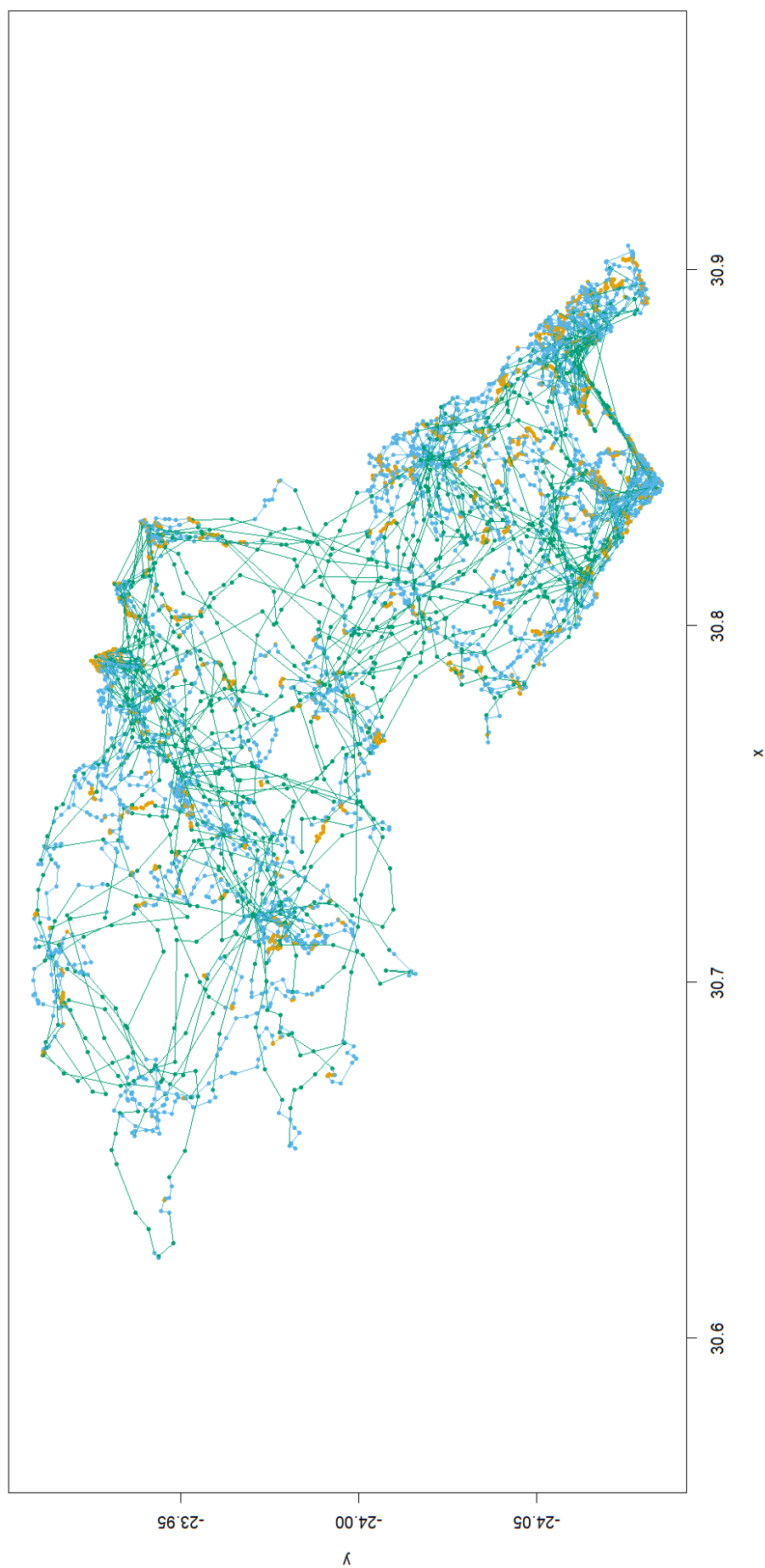


**Figure 8.** Elza's tracks from the 1<sup>st</sup> of June to the 31<sup>st</sup> of December 2022. State 1 = orange; state 2= blue; state 3= green.

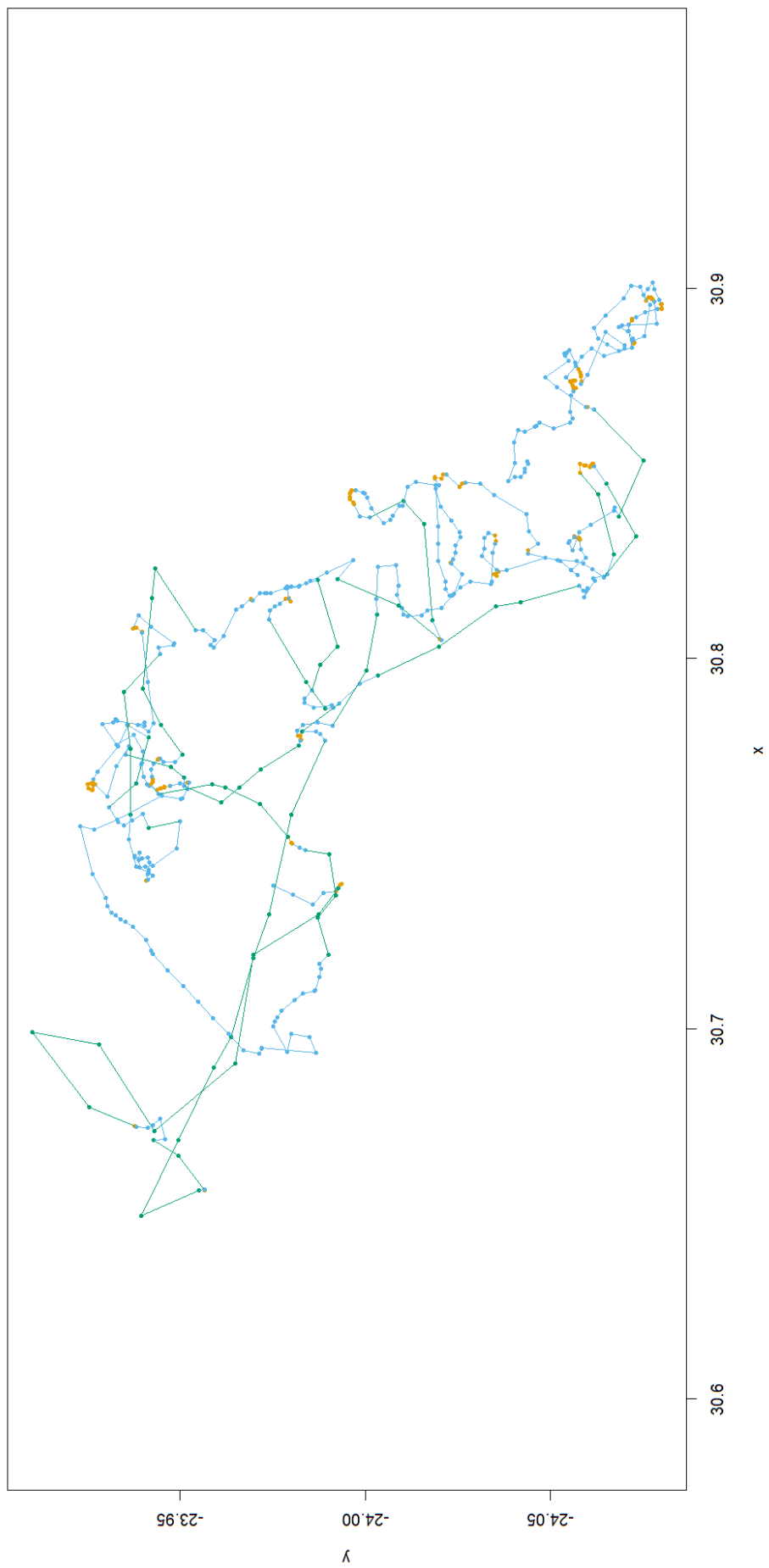


**Figure 9.** Jean's tracks in June 2022. State 1 = orange; state 2= blue; state 3= green.



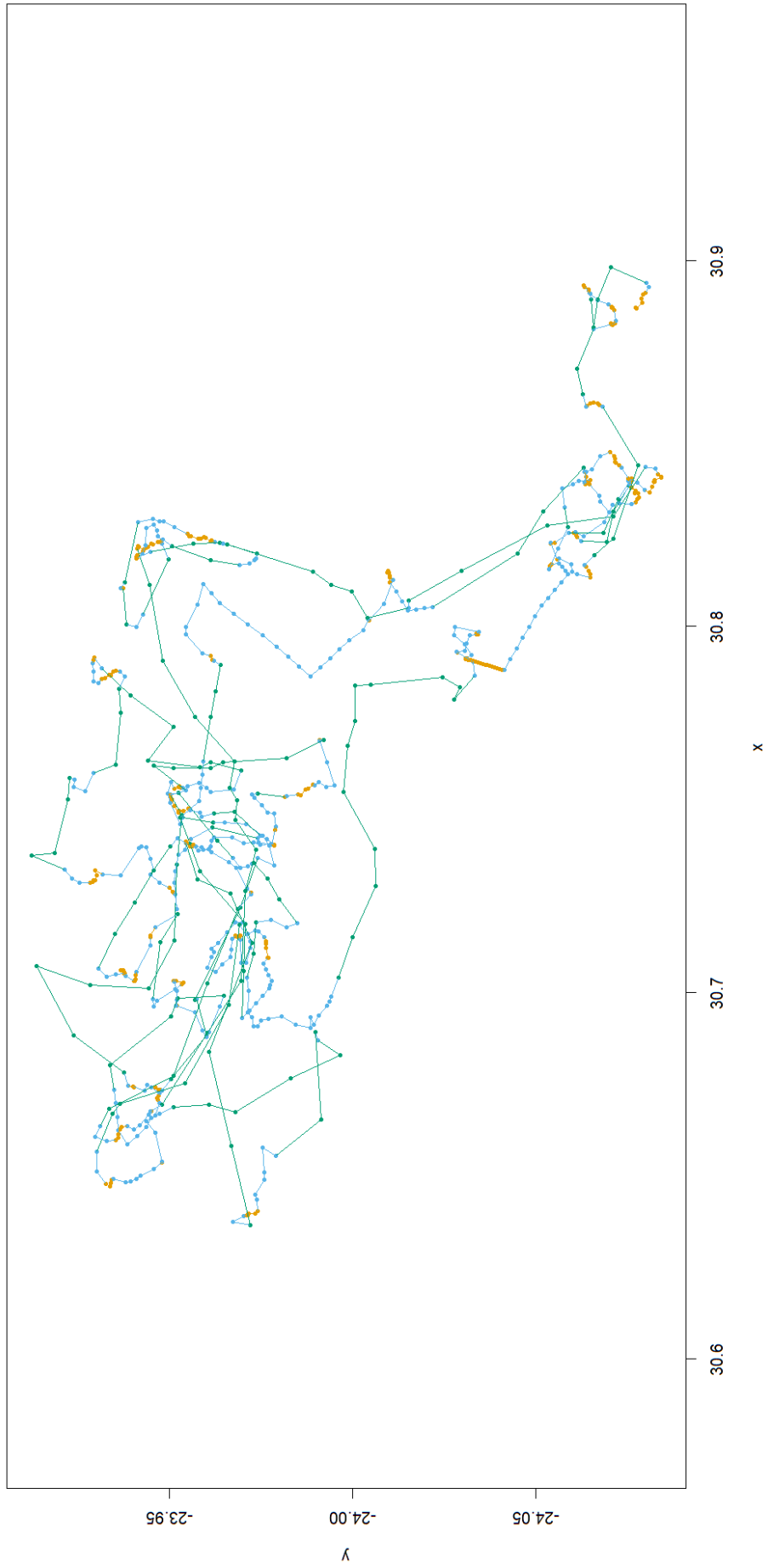


**Figure 10.** Jean's tracks in August 2022. State 1 = orange; state 2= blue; state 3= green.

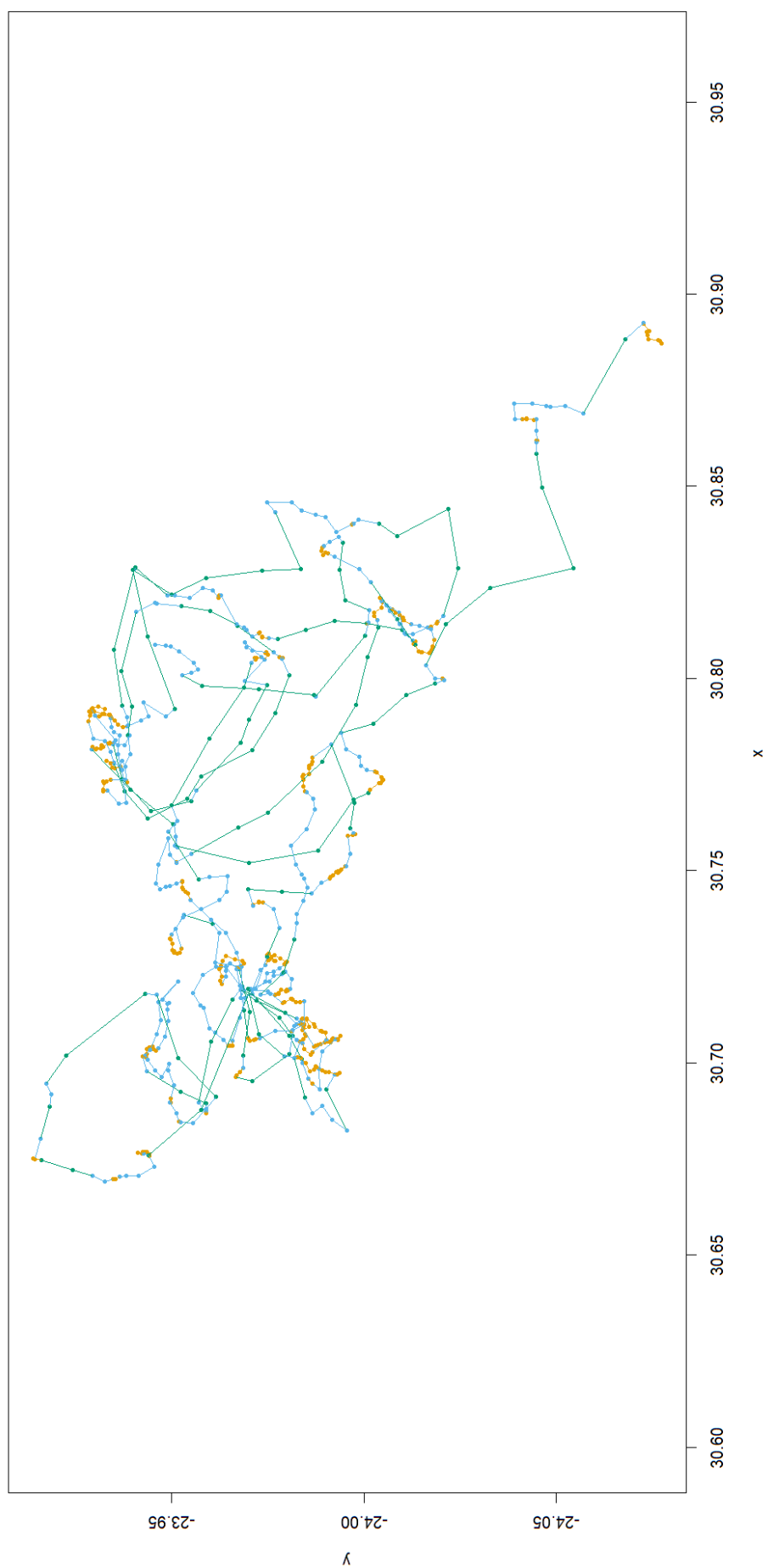


**Figure 11.** Jean's tracks in September 2022. State 1 = orange; state 2= blue; state 3= green.

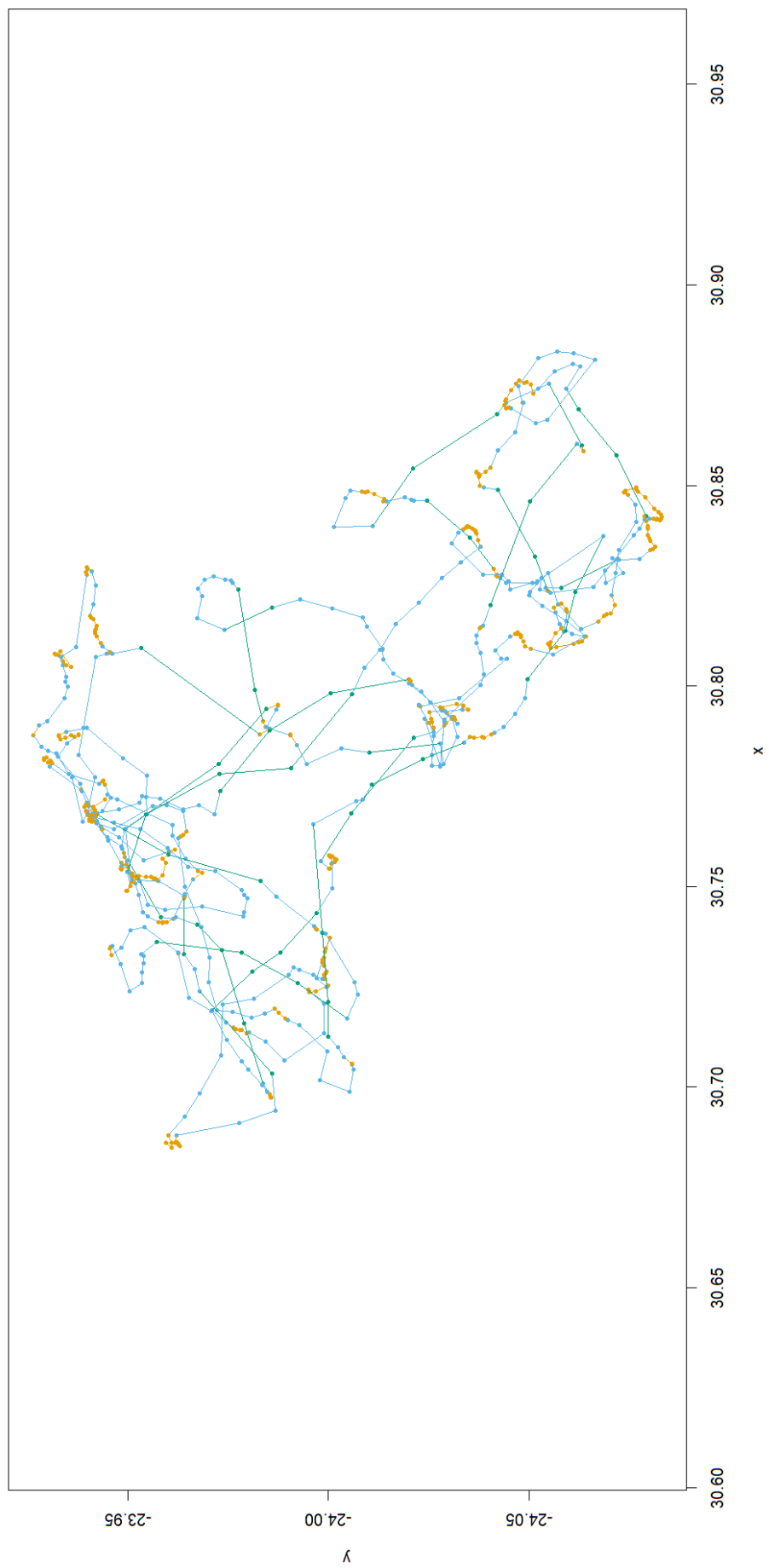


**Figure 12.** Jean's tracks in October 2022. State 1 = orange; state 2= blue; state 3= green.

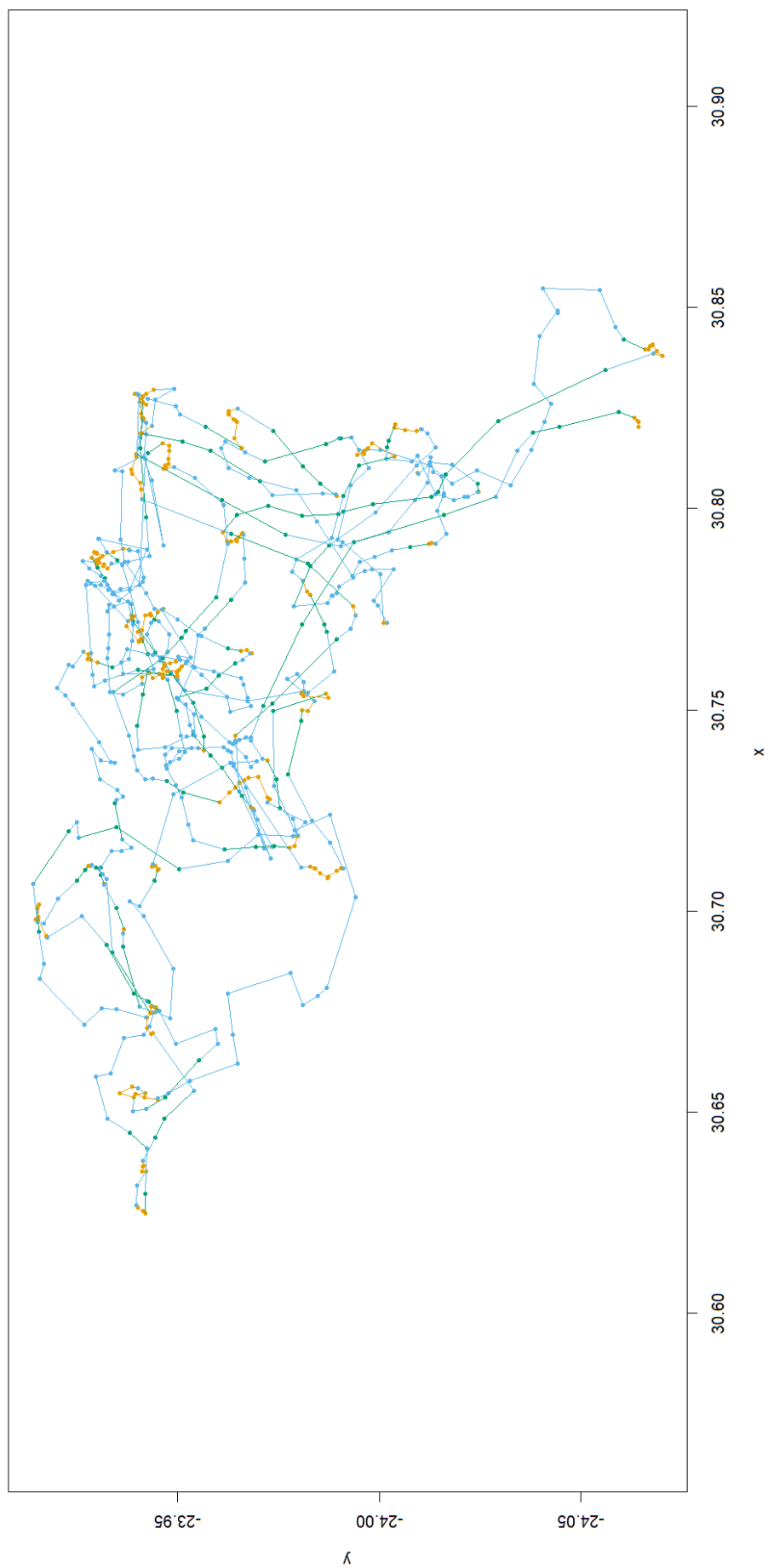


**Figure 13.** Jean's tracks in December 2022. State 1 = orange; state 2= blue; state 3= green.

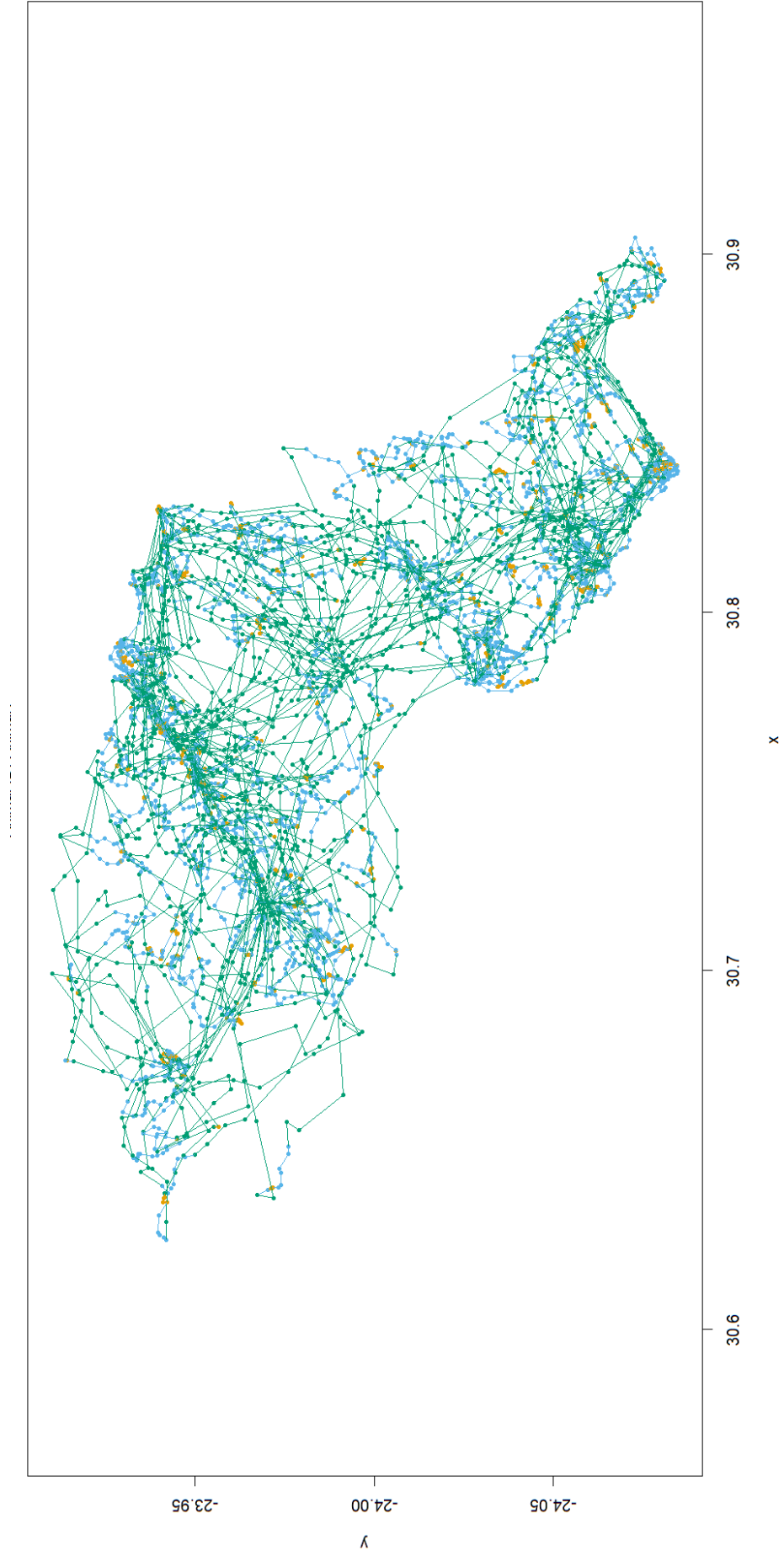


**Figure 14.** Jean's tracks from the 8<sup>th</sup> of June to the 31<sup>st</sup> of December 2022. State 1 = orange; state 2= blue; state 3= green.